Lagrangian and Eulerian Descriptions in Solid Mechanics and Their Numerical Solutions in hpk Framework

by

Salahi Basaran

B.S. (Mechanical Engineering), University of Kansas, 2000

M.S. (Mechanical Engineering), Virginia Polytechnic University, 2002

Submitted to the Department of Mechanical Engineering and the Faculty of the Graduate School of the University of Kansas in partial fulfillment of the requirements for the Degree of Doctor of Philosophy

---

Dr. Karan S. Surana (Advisor), Chair

Dr. Peter W. TenPas

Dr. Ray Taghavi

Dr. Albert Romkes

Dr. Bedru Yimer

Date Defended

The Thesis committee for Salahi Basaran certifies that this is the approved version of the following thesis:

Lagrangian and Eulerian Descriptions in Solid Mechanics and Their Numerical Solutions in hpk Framework

Committee:

Dr. Karan S. Surana (Advisor), Chair

Dr. Peter W. TenPas

Dr. Ray Taghavi

Dr. Albert Romkes

Dr. Bedru Yimer

Date approved

This thesis is dedicated to my beloved parents and to my brother who is also my best friend

Acknowledgments

I would like to extend my sincerest gratitude to my advisor Dr. Karan S. Surana (Deane E. Ackers Distinguished Professor). I would like to extend my thanks to him for his enthusiasm and constantly pushing me to be better. I thank Dr. Surana not only for providing me financial support during my dissertation but also for granting access to the Computational Mechanics Laboratory at the University of Kansas.

The financial support provided by DEPSCoR/AFOSR through grant numbers F49620-03-01-0298 to the University of Kansas, Department of Mechanical Engineering and through grant number F49620-03-01-0201 to Texas A&M University is gratefully acknowledged. The seed grant provided by ARO through grant number FED46680 to the University of Kansas, Department of Mechanical Engineering is also acknowledged. The financial support from the Department of Mechanical Engineering of the University of Kansas to support this work is much appreciated. Computing facilities provided by Computational Mechanics Laboratory (CML) of the Mechanical Engineering Department have been instrumental in conducting the numerical studies.

I would also like to thank Dr. Peter W. TenPas, Dr. Ray Taghavi, Dr. Albert Romkes and Dr. Bedru Yimer for taking time to serve on my thesis committee. Furthermore, I would like to thank Dr. TenPas for helping me to appreciate fluid mechanics and thermodynamics. Similarly, I extend my gratitude to Dr. Yimer for making heat transfer fun for me.

I am grateful to the Mechanical Engineering staff, Carol Gonce and Lucas Jacobsen deserve special mention, for helping me in many different ways.

I am indebted to many colleagues for providing emotional support and comradery throughout my time in Lawrence. I am thankful to all my best friends scattered around the world for providing me with their continuous encouragements.

Most importantly, I wish to thank my parents, Baykan Basaran and Osman Basaran and my dear brother, Halil Basaran. They raised me, supported me, and loved me unconditionally. To them I dedicate this thesis.

Abstract

In this thesis mathematical models for a deforming solid medium are derived using conservation laws in Lagrangian as well as Eulerian descriptions. First, most general forms of the mathematical models permitting compressibility of the matter are considered which are then specialized for incompressible medium. Development of constitutive equations central to the validity of the mathematical models is considered and specific forms of the constitutive models are derived. Numerical solution of these mathematical models are obtained using finite element method based on h, p, k mathematical and computational framework in which the integral forms are variationally consistent and hence the resulting computational processes are unconditionally stable.

The Lagrangian descriptions using second Piola-Kirchhoff stress and Green's strain (with displacement as dependent variables) permitting large motion and large strain remain the most widely used strategy for developing mathematical models for solids. In this approach the governing differential equations resulting from conservation laws present no problems but the constitutive equations relating the second Piola-Kirchhoff stress to Green's strain (or any other conjugate pairs of stresses and strains) must be given careful consideration to ensure that they are derivable from a potential. The second major issue of concern is that while using these mathematical models, increasing mesh distortion with progressively increasing deformation eventually leads to highly distorted finite element meshes for which either the computed solution become grossly in error or the computations cease altogether. This situation is often salvaged by rediscretization and mapping of solution from the existing discretization onto the new discretization. Many unresolved problems associated with this approach adversely effect accuracy of the computations.

In Eulerian descriptions, we do not follow motions of material particles. Hence, in this approach the discretization remain fixed and the material particles flow through it. The mathematical models based on conservation laws consists of : continuity equation, momentum equations, and the energy equation employing velocities, Cauchy stresses, temperature and heat fluxes as dependent variables. One can use Fourier law of heat conduction to express heat flux in terms

of material conductivities and temperature gradients. The other constitutive equations relating Cauchy stresses to strain-rate tensor are required. These constitutive equations are known as rate constitutive equations. In the published work Jaumann, Truesdell, upper Convected, and lower Convected etc. rate constitutive equations have been used and hence will be considered in the present work. It is well known that for a given set of material constants all rate constitutive equations do not produce the same response. This is another area of investigation. Since Eulerian descriptions do not monitor motions of material particles, moving interfaces, boundaries, and fronts are relatively difficult to track during deformation process.

Thus, in the Lagrangian descriptions, mesh distortion, rediscretization, solution mappings, and validity and development of constitutive equations are areas of potential research and concern. While in the Eulerian descriptions, rate constitutive equations, their development and non-unique response based on the choice, tracking of moving fronts, boundaries and interfaces remain areas of research. In this thesis, we consider investigations of both Lagrangian and Eulerian descriptions for solid mechanics. Mathematical models are established based on conservation laws. Details of the constitutive equations in both Lagrangian and Eulerian descriptions are presented. Limitations of the constitutive models are presented and also illustrated numerically. A variety of model problems are chosen for numerical studies. The wave propagation model problems are considered for numerical studies. Mathematical developments and numerical studies are aimed at investigating the two approaches of constructing mathematical models: (i) Behaviors and limitations of constitutive models in both descriptions (ii) Overall benefits and drawbacks of Lagrangian and Eulerian descriptions.

Contents

List of Figures

Chapter 1

Introduction, literature review and scope of work

1.1 Introduction

For over four decades, the finite element method has been widely applied to a variety of problems in linear elasticity and non-linear solid mechanics such as metal forming, large deformation of plates, shells and beams. In constructing finite element formulation in solid mechanics two approaches are commonly employed. In the first approach mathematical models are constructed using conservation laws and constitutive equations and then used in the development of the finite element processes using methods of approximation, generally Galerkin method with weak form. In the development of the mathematical models Lagrangian descriptions with second Piola-Kirchhoff stresses and Green's strains are used almost exclusively. The resulting governing differential equations (GDEs) are a system of nonlinear partial differential equations. In the second approach, principle of virtual work [1] is utilized directly in constructing the finite element processes without first deriving the mathematical models using conservation laws. Incremental equations of equilibrium are derived and solved iteratively. In this approach also the formulations are constructed using Lagrangian descriptions with second Piola-Kirchhoff stresses and Green's strains.

While the first approach is more appealing from the point of view that a complete description of mathematical models (GDEs) permits one to investigate the viability of various methods of approximations in constructing finite element processes, the second approach remains the most dominant methodology in the published work. There have been other alternatives used and proposed in the published work some of which are discussed in the following sections. There are also some published works [2, 3] on the development of the mathematical models using Eulerian descriptions but this approach has not been as commonly adopted as the one based on the Lagrangian descriptions.

The finite element processes based on Lagrangian descriptions suffer from the mesh distortion problems with progressively increasing deformation. Thus, at some stage, the computations becomes erroneous or cease all together. This problem is seemingly overcome by periodic rediscretization during the deformation process. Rediscretization obviously requires a new mesh but more importantly necessitates mapping of the solution from an existing discretization onto the new discretization. This process is generally prone to significant errors and thus may lead to erroneous solutions in a process that requires repeated rediscretizations. Another significant problem is in the constitutive equations that express a relationship between second Piola-Kirchhoff stresses and Green's strains. This relationship is not always derivable based on a potential and hence, lacks a mathematical foundation from the continuum mechanics point of view. A major strength of the Lagrangian descriptions is that in this methodology motion of material particles is intrinsic in the mathematical models hence moving boundaries interfaces, and fronts can be tracked precisely.

The use of mathematical models for solid mechanics based on Eulerian descriptions is not very common but appears attractive to consider primarily for the following two reasons: (1) In this approach the mesh remains fixed and the material particles flow through it, thus there are no issues of mesh distortion and hence no rediscretization and associated problems of solution mapping. (2) In multi-physics and interaction problems such as fluid-solid interaction [4], the use of Eulerian descriptions for fluid necessitates Eulerian description for solids if the interaction of the fluid and solid is to be an integral and intrinsic part of the mathematical models. This

approach eliminates the constraint equations (used presently) at the interfaces between the solid and fluid used to describe their interaction and many approximations and problems associated with them. Just like Lagrangian descriptions, the Eulerian descriptions are not free of problems either. Since in Eulerian descriptions material particles are not followed, the simulations of moving boundaries, moving fronts, free boundaries, and interfaces become difficult. The Eulerian descriptions necessitate use of velocities in the mathematical models (as opposed to displacements in The Lagrangian descriptions) hence it becomes necessary to have constitutive equations in terms of strain rates. For this purpose rate equation are employed as constitutive equations. Many rate constitutive equations have been proposed in the published work. A rigorous mathematical formulation (based on continuum mechanics) for the rate equations is still subject of discussions and issue of controversy. It is well known that for the same material constants, different rate constitutive equations produce different response. This of course raises the question of the validity of rate equations as a constitutive equations framework for solid mechanics.

In regard to the finite element processes, the currently used methodologies are based on h and p utilizing local approximations of class C^0 in space and time. Surana et al. [5–7] have shown that order k of the approximation space defining global differentiability of order $(k-1)$ is an independent parameter in addition to h and p in all finite element processes. Thus the finite element processes must be based on h, p, and k as opposed to h and p used currently. The h, p, k mathematical and computational framework for finite element processes is highly meritorious over h, p framework [5–7].

1.2 Literature Review

A literature review of currently used methodologies and approaches for linear and nonlinear solid mechanics problems are presented in this section. The literature review is divided in four group: the total Lagrangian formulations, the updated Lagrangian formulations, formulations based on the Eulerian descriptions, and rate constitutive equations. Traditionally, the

Lagrangian (referential) descriptions gained prominence over the Eulerian (spatial) descriptions in solid mechanics problems. Truesdell's description [8] for Lagrangian and Eulerian frame of references is the following: (i) referential description: independent variables are the position $\bar{X}$ of a particle X in an arbitrary chosen reference configuration, and the time t (ii) spatial description: independent variables are the current position $\bar{x}$ of a particle X, and the time t. we note that the independent variables $\bar{x}$ is a function of $\bar{X}$ and the time t, i.e. $\bar{x} = \bar{x}(\bar{X}, t)$.

It is critical for mathematical models to describe the actual behavior of a physical systems or processes with a high degree of accuracy. In addition to this, the usage of correct constitutive models is important as well as their objectivity i.e. frame invariant. Furthermore, one must utilize energetically conjugate pair of stresses and strains in their development [9, 10]. The total Lagrangian formulation uses the initial configuration as the reference configuration. Incremental-iterative Newton-Raphson solution procedure [1, 9] is generally employed for solving nonlinear algebraic equations. In this approach, second Piola-Kirchhoff stress tensor and Green-Lagrange strain tensor are generally used as a conjugate pairs. Oden [11] presented finite element method to analyze 3-D elastic bodies that are subjected to large deformation and finite strains. Main focus of this paper is the development of non-linear stiffness relations for finite deformation of elastic bodies. Oden [11] and Hibbitt et al. [12] are the first one to use fully nonlinear kinematic relations where they focused on the development of non-linear stiffness relations for elastic bodies that are subjected to large deformation and finite strains. Nemat-Nasser et al. [13] used similar approach based on absolute minimum principle (absolute minimum of potential energy). Incremental approach was used to solve large deformation problems with both material and geometric nonlinearities. Authors provided explicit results for both compressible and incompressible elastic materials where formulations in the Lagrangian and the Eulerian frame of reference are provided and compared. Wood et al. [14] developed equilibrium equations for the deforming body using virtual work principle with Newton-Raphson method is used for solving nonlinear algebraic equilibrium equations. The total Lagrangian approach is used and there were no restrictions on the magnitude of displacements and rotations.

The updated Lagrangian formulation uses the last equilibrium position as the reference

configuration. This is a source of error because it implies that reference configuration itself is being approximated [15]. Cauchy stress tensor and Almansi strain tensor are generally used as a conjugate pair in this approach for constitutive equations. Horrigmoe and Bergan [16] presented their work on incremental variational principles of solid mechanics where they used incremental form of the principle of stationary potential energy. Their goal was to develop a consistent form of incremental variational principle so that these formulations can be applied to analyze large displacement nonlinear problems. The updated Lagrangian formulation was used where authors noted that similar formulation based on the total Lagrangian can be derived in the same manner. Heyliger et al. [17] presented a mixed variational finite element method using the updated Lagrangian formulation in which the displacements and stresses appear as dependent variables. Cauchy stresses and Almansi strains are used in the constitutive equations. Numerical computations of displacements are shown to be in good agreement with displacement based formulations. Authors reported that stresses in their formulation are more accurate compared to displacements based approaches.

In the published literature, the updated Lagrangian formulations and the Eulerian formulations are often used interchangeably especially in the context with finite element processes. Gadala et al. [2, 3] indicated that in the updated Lagrangian formulation, the independent variables are $\bar{x}$ and t, where $\bar{x}$ is the position occupied by the material X at time t. This is the reason why this formulation is referred as the updated Lagrangian formulation instead of the Eulerian formulation where $\bar{x}$ and t are dependent as in $\bar{x} = \bar{x}(\bar{X}, t)$. In the Eulerian approach, attention is focused on a given region of space instead of a given body of matter. A Literature survey of the problems with geometric and material nonlinearity problems is given by Gadala et al. [3]. Main focus of the survey is to distinguish differences between the updated Lagrangian and Eulerian formulations. In addition to this, an Eulerian formulation suitable for both static and dynamic problems is presented. Authors also discussed the development of the total Lagrangian formulations. However no numerical studies are presented for given formulations.

Key [18] used Cauchy stress in the formulation of large deformation dynamic response of solids. A fixed spatial coordinate system is used to describe the formulation. In this paper, ex-

plicit central difference time integration scheme with artificial viscosity is used. The numerical results are compared to experimental data or analytical solutions.

Swedlow [19] proposed a new formulation for Navier's equations in terms of displacement rates by using the material time derivative of the equilibrium equations in the Eulerian frame of reference. Author provided detailed derivations for torsion of prismatic bars, plane strain and plane stress problems. Swedlow show that the equilibrium equations derived using this technique are elliptic provided elastic/plastic moduli are bounded and non-negative. Osias [20] applied Swedlow's formulation to tensile necking processes in plane strain and plane strain problems. Finite deformation of elasto-plastic material was simulated by solving Jaumann rate equations incrementally. Governing differential equations and constitutive equations for finite elasto-plastic deformation were derived using the Eulerian frame of reference. The results of this investigation provided numerical solutions for tensile necking of metals in plane stress and plane strain; however, author acknowledged that mechanics of tensile testing data was not precise to validate the numerical results over the full range of the tensile testing data. In 1974, Osias et al. [21] used Galerkin method to validate numerical results for number of homogeneous finite deformation problems with analytical solutions.

For elasto-plastic problems, Lee et al. [22, 23] presented least squares finite element formulation. Lee [24] combined least squares formulation with GDEs developed by Swedlow [19] using Cauchy stress rate and velocities as dependent variables. The same computational algorithm was used for both elliptic and hyperbolic regions. The resulting matrices are always symmetric and positive definite due to least squares process. Siu et al. [25] extended formulation developed in [24] to describe three dimensional deformation analysis where the deformation is treated as a process instead of an event. Benson [26] has an extensive literature review on Lagrangian and Eulerian hydrocodes that are used to solve transient, large deformation solid mechanics problems. The paper provides detailed reviews on both finite element and finite difference codes. Benson [27] introduced an implicit multi-material Eulerian formulation in order to extend the applicability of explicit formulation to quasi-static problems. This approach has two issues that must be addressed: mixture theory for the multi-material elements and the trans-

port step where solutions from the deformed Lagrangian mesh are mapped onto Eulerian mesh. Benson noted that mixed elements containing a high percentage of void material will experience convergence difficulties. Furthermore, author concluded that Jaumann rate had adequate accuracy while requiring less storage than the Green-Naghdi rate.

A numerical method based on absolute minimum principle is developed by Nemat-Nasser et al. [13]. Incremental approach is used to solve large deformation problems with both material and geometric nonlinearities. Authors provided explicit results for both compressible and incompressible elastic materials where the Lagrangian and Eulerian formulations are used and compared. Atluri [28] reviewed the question of 'generalization' of finite strains in different theories such as infinitesimal strain theory of elasticity and elasto-plasticity with isotropic and kinematic hardening. Atluri presented different stress distributions for different objective stress rates in simple shear problems. The authors concluded that all stress rates are equivalent as long as the constitutive equation is properly posed. Prager [29] discussed the development of four different stress rates: Jaumann; Cotter and Rivlin; Truesdell; and Oldroyd. Prager stated that following condition is not sufficient for unique constitutive rate equations:

> If a stressed continuum performs a rigid body motion and the stress field is independent of time when referred to a coordinate system that participates in this motion, the stress rate vanishes.

Dienes [30] reviewed the literature on stress rates in deforming bodies that are experiencing large deformations. It was pointed out that constitutive laws must be formulated in such a way that they account for material rotations even in the absence of additional strain. In this paper, expression for the rate of material rotation was given as an explicit function of vorticity, rate of deformation, and stretch. This derivation includes the case when material axes become strongly skewed. Derived expression is similar to Green-McInnis but suitable for viscoelastic and elastic-plastic materials. Xiao et al. [31] proposed a new rate constitutive law rate based on logarithmic strains. They claimed that use of logarithmic strain is beneficial, since logarithmic strains can be identical to stretching and they form a work-conjugate pair with Cauchy stresses. Authors concluded in their analysis by stating that if stretching is used to measure the rate

of change of deformation, the logarithmic rate is the only choice. This formulation requires calculation of eigenvalues and eigenvectors which makes it hard to implement in finite element framework. Xiao et al. [32] applied logarithmic stress rate to the Kirchhoff stress in hypo-elasticity problems. Authors indicated that simple shear response of this model is stable where models based on Jaumann stress rate predicts unstable oscillatory shear. In 1999, Xiao et al. [32] studied existence and uniqueness of the integrable hypo-elastic equation of grade zero for different stress rates. Main goal of this study was to find a better criteria for choosing an objective stress rate other than its response to simple shear problem. Xiao et al. suggested that investigators in solid mechanics field should consider the following criteria: the hypo-elastic equation of grade zero must be exactly integrable to define an elastic relation.

1.3 Scope of Present Work

In this thesis, we present development of mathematical models and associated computational infrastructure in which all solid mechanics problems are treated with same rigor and accuracy. The mathematical models incorporate finite strain, finite strain rate, and large motion of the solid continuum as well as linear and non-linear material behavior. The mathematical framework utilized in the present work is based on h,p,k finite element framework and space-time variationally consistent integral forms. The order k of the approximation space permits higher order global differentiability in space and time. The space-time variationally consistent integral forms ensure unconditionally stable computational process during the entire evolution. Least squares finite element process enforces that the coefficient matrices are always symmetric and positive definite. In the following, summary of the work presented in this thesis is given:

(i) Development of mathematical models based on conservation laws

(ii) Constitutive equations, equations of state for an elastic deforming solid, stress-strain relationships for an elastic deforming solid

(iii) Mathematical and computational infrastructure: Space-time least squares processes (STLSP)

In chapter 2, mathematical models in Lagrangian and Eulerian descriptions for a deforming solid medium are presented. Governing differential equations (GDEs), continuity equation, momentum equations, and energy equation, are developed for conjugate pairs of stresses and strains. The development of constitutive equations are presented in chapter 3 for both Lagrangian and Eulerian descriptions where chapter 4 provides a closure for the mathematical models. Chapter 5 includes discussions on computational framework and details of the least squares finite element formulation for initial value problems (IVPs). Numerical studies for 1-D and 2-D elastic wave propagation as well as investigation of rate equilibrium equation are presented in chapter 6. Finally, chapter 7 includes summary and conclusions.

Chapter 2

Development of Mathematical Models Based on Conservation Laws

In this chapter we consider development of mathematical models for a deforming solid medium using Lagrangian as well as Eulerian descriptions. We utilize conservation of mass, Newton's second law for a volume of matter (rate of change of linear momentum must equilibrate with the forces acting on the volume) and conservation of energy to derive: continuity equation, momentum equations, and energy equation. In the development of the governing differential equations (GDEs) resulting from these mathematical models we choose appropriate measures of stresses, strains and heat flux without regard to the constitutive equations that relate stresses to strains and heat fluxes to the temperature gradients. That is we do not consider the constitution of the matter. Thus the mathematical models presented in this chapter do not have closure. In other words, we have more dependent variables than the number of equations. The development of the constitutive equations are presented in chapter 3 for Lagrangian and Eulerian descriptions. These constitutive equations together with GDEs from conservation laws provides a system of partial differential equations (PDEs) that have closure. The mathematical models based on continuum approach using conservation laws without regard to material constitution are relatively straightforward to establish for desired physics. However, the constitutive equations are still an area of research even for simple material behaviors. It is for this reason that developments

related to the material constitution are not presented in this chapter but are considered in chapter 3.

2.1 Preliminaries, Notations, Definitions and Fundamental Relations

Consider a body B in the undeformed state (time $t = 0$). Let P be a point in the body with coordinates x_1, x_2, x_3 with respect a fixed frame of reference x_1, x_2, x_3. Upon deformation the body B occupies $\bar{B}$ at time t. The point $P(x_1, x_2, x_3)$ is now $\bar{P}(\bar{x}_1, \bar{x}_2, \bar{x}_3)$ (figure 2.1).
Clearly,

$$\begin{aligned} \bar{x}_1 &= \bar{x}_1(x_1, x_2, x_3, t) \\ \bar{x}_2 &= \bar{x}_2(x_1, x_2, x_3, t) \\ \bar{x}_3 &= \bar{x}_3(x_1, x_2, x_3, t) \end{aligned} \tag{2.1}$$

Let u_1, u_2, u_3 be the displacements of point $P(x_1, x_2, x_3)$, then the following holds

$$\begin{aligned} \bar{x}_1 &= x_1 + u_1(x_1, x_2, x_3, t) \\ \bar{x}_2 &= x_2 + u_2(x_1, x_2, x_3, t) \\ \bar{x}_3 &= x_3 + u_3(x_1, x_2, x_3, t) \end{aligned} \tag{2.2}$$

Inverse of (2.2) can be given as,

$$x_j = \bar{x}_j - \bar{u}_j(\bar{x}_i, t) \quad i, j = 1, 2, 3 \tag{2.3}$$

(2.1) - (2.3) are fundamental in the study of deformable matter. In what follows, we adopt two different notation strategies. The first one consists that of matrix and vector notations. In the second case we use Einstein's index notation. Obviously one is derivable from the other. We utilize both these notations based on convenience. Thus if f is a scalar field than its differentiation

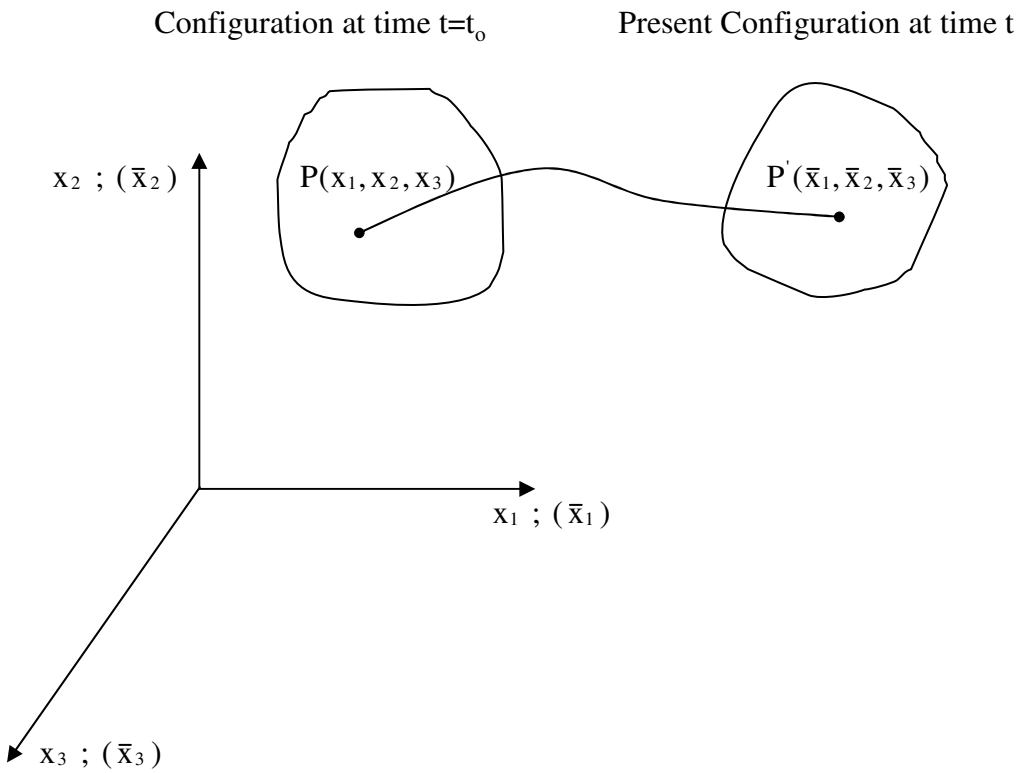

Figure 2.1: Configuration of a Body at Two Different Times

with a vector field $\{x\} = [x_1, x_2, x_3]^t$ is represented as a row vector,

$$\frac{\partial f}{\partial \{x\}} = \left[\frac{\partial f}{\partial x_1}, \frac{\partial f}{\partial x_2}, \frac{\partial f}{\partial x_3}\right] = \{b\}^t \tag{2.4}$$

The differentiation of a vector field say $\{\bar{x}\}$ with respect to another vector field say $\{x\}$ gives a Jacobian matrix,

$$[J(t)] = \frac{\partial \{\bar{x}\}}{\partial \{x\}} = \left[\frac{\bar{x}_1, \bar{x}_2, \bar{x}_3}{x_1, x_2, x_3}\right] = \begin{bmatrix} \frac{\partial \bar{x}_1}{\partial x_1} & \frac{\partial \bar{x}_1}{\partial x_2} & \frac{\partial \bar{x}_1}{\partial x_3} \\ \frac{\partial \bar{x}_2}{\partial x_1} & \frac{\partial \bar{x}_2}{\partial x_2} & \frac{\partial \bar{x}_2}{\partial x_3} \\ \frac{\partial \bar{x}_3}{\partial x_1} & \frac{\partial \bar{x}_3}{\partial x_2} & \frac{\partial \bar{x}_3}{\partial x_3} \end{bmatrix} \tag{2.5}$$

$|J| > 0$ is essential for $[J(t)]$ to be invertible. Inverse of $[J(t)]$ is given by

$$[\bar{J}] = [J]^{-1} = \frac{\partial \{x\}}{\partial \{\bar{x}\}} = \left[\frac{x_1, x_2, x_3}{\bar{x}_1, \bar{x}_2, \bar{x}_3}\right] \tag{2.6}$$

$|\bar{J}| > 0$ is also essential for $[\bar{J}]$ to be invertible. Using (2.2) - (2.3) and (2.5) - (2.6) we can write the following.

$$[J] = [I] + \left[\frac{u_1, u_2, u_3}{x_1, x_2, x_3}\right] = [I] + [\dot{J}] \tag{2.7}$$

and

$$[\bar{J}] = [I] + \left[\frac{u_1, u_2, u_3}{\bar{x}_1, \bar{x}_2, \bar{x}_3}\right] = [I] + [\dot{\bar{J}}] \tag{2.8}$$

If x_i and t are independent variables in the development of the mathematical models then such mathematical models are called Lagrangian descriptions. On the other hand if $\bar{x}_i$ and t are independent variables in the development of the mathematical models then the resulting mathematical models are called Eulerian descriptions. As a general notation, the quantities without the over bar are Lagrangian descriptions, whereas those with over bar are Eulerian descriptions.

2.1.1 Measures of Strains:

For a solid matter undergoing large motion and large deformation one could use various measures of strain [33, 34]. In Lagrangian descriptions we generally consider Cauchy strain, Finger strain and Green's strain denoted by $[C]$, $[F]$, and $[\varepsilon]$ and are given by

$$[C] = [J]^t[J] = [I] + [\dot{J}]^t + [\dot{J}] + [\dot{J}]^t[\dot{J}] \tag{2.9}$$

$$[F] = [C]^{-1} = [\bar{J}][\bar{J}]^t = [I] - [\bar{\dot{J}}]^t - [\bar{\dot{J}}] + [\bar{\dot{J}}][\bar{\dot{J}}]^t \tag{2.10}$$

$$[\varepsilon] = \frac{1}{2}\left[[J]^t[J] - [I]\right] = \frac{1}{2}\left[[\dot{J}]^t + [\dot{J}] + [\dot{J}]^t[\dot{J}]\right] \tag{2.11}$$

In Eulerian descriptions we consider Cauchy, Finger and Almansi strains [33, 34] denoted by $[\bar{C}]$, $[\bar{F}]$, and $[\bar{\varepsilon}]$ and are given by

$$[\bar{C}] = [\bar{J}]^t[\bar{J}] = [I] - [\bar{\dot{J}}]^t - [\bar{\dot{J}}] + [\bar{\dot{J}}][\bar{\dot{J}}]^t \tag{2.12}$$

$$[\bar{F}] = [\bar{C}]^{-1} = [J][J]^t = [I] + [\dot{J}] + [\dot{J}]^t + [\dot{J}][\dot{J}]^t \tag{2.13}$$

$$[\bar{\varepsilon}] = \frac{1}{2}\left[[I] - [\bar{J}]^t[\bar{J}]\right] = \frac{1}{2}\left[[\bar{\dot{J}}]^t + [\bar{\dot{J}}] - [\bar{\dot{J}}]^t[\bar{\dot{J}}]\right] \tag{2.14}$$

2.1.2 Measures of Stresses:

The concept of stress is based on force and area. Thus deformed object with deformed area is a natural way to define stress. We define a stress matrix $[\bar{\sigma}]$ related to the equilibrium of the deformed object. $[\bar{\sigma}]$ is called Eulerian stress matrix or Cauchy stress matrix. It can be shown that [33] $[\bar{\sigma}]$ is symmetric and is a tensor of rank two. Thus $[\bar{\sigma}]$ is a natural measure of stress in Eulerian descriptions.

In Lagrangian descriptions there is no concept of stress. Thus a measure of stress in such descriptions is established through a correspondence rule [35]. Two such measures commonly used in the literature are considered here. The first measure is called Lagrange stress (first Piola-Kirchhoff stress) $[\sigma^*]$ and the second measure is called second Piola-Kirchhoff stress $[\sigma]$.

These two measures are obviously related to $[\bar{\sigma}]$ through $[J]$ or $[\bar{J}]$. We have the following relationships [35],

$$[\sigma^*] = |J|[J]^{-1}[\bar{\sigma}] \neq [\sigma^*]^t \tag{2.15}$$

$$[\sigma] = |J|[J]^{-1}[\bar{\sigma}][J^t]^{-1} = [\sigma]^t \tag{2.16}$$

Clearly $[\sigma^*]$ is non-symmetric whereas $[\sigma]$ is symmetric. Some other useful relations are,

$$[\bar{\sigma}] = |J|^{-1}[J][\sigma][J]^t \tag{2.17}$$

$$[\sigma] = [J]^{-1}[\sigma^*]^t = [\sigma^*][J^t]^{-1} \tag{2.18}$$

$$[\sigma^*] = [\sigma][J]^t \tag{2.19}$$

Second Piola-Kirchhoff stress is commonly used in Lagrangian descriptions involving large motions and finite strain. For infinitesimal deformation $|J| = 1$, $[J] = [I]$, and hence $[\bar{\sigma}] = [\sigma]$.

2.2 Mathematical Models for a Deforming Solid Continuum Using Lagrangian Description

We consider a deforming solid to be compressible and experiencing large motion and finite strain. In Lagrangian descriptions all quantities are expressed in terms of undeformed position coordinates x_i and time t. Let $\vec{v} = [v_1, v_2, v_3]^t$ or v_i ; $i = 1, 2, 3$ to be velocities of a point $P(x_i)$, $\vec{F}^b = [F_1^b, F_2^b, F_3^b]^t$ or F_i^b ; $i = 1, 2, 3$ to be the body forces per unit mass and $\vec{q} = [q_1, q_2, q_3]^t$ or q_i ; $i = 1, 2, 3$ be the heat fluxes in the coordinate directions x_1, x_2, x_3.

We consider a volume V with boundary ∂V that deforms into volume $\bar{V}$ with boundary $\partial\bar{V}$. Conservation of mass yields continuity equation. Application of Newton's second law to the deforming volume i.e. rate of change of linear momentum must equilibrate with the forces acting on the deforming volume yields momentum equations. Application of the first law of

thermodynamics i.e. rate of work done and rate of heat added to the deforming volume must result in the rate of change of internal energy, yields energy equation. Refer to [35] for details of the derivations. If we utilize second Piola-Kirchhoff stress measure, then we have the following system of equations.

Continuity Equation:

$$\rho = \bar{\rho}|J| \tag{2.20}$$

Momentum Equations:

$$\rho\frac{\partial \vec{v}}{\partial t} - \left(|J|^{-1}[J][\sigma]^t[J]^t\right)\{\nabla\}|J| - \vec{F}^b\rho = 0 \tag{2.21}$$

Energy Equation:

$$\rho\frac{\partial e}{\partial t} + |J|\left(\{\nabla\}^t[J]^{-1}\right)\left([J^t]^{-1}\{q\}\right) - [J][\sigma]\left[\frac{\partial \vec{v}}{\partial\{x\}}\right]^t = 0 \tag{2.22}$$

where ρ and $\bar{\rho}$ are densities in undeformed and deformed configurations, e is specific internal energy, $[\sigma]$ are second Piola-Kirchhoff stresses and $\{\nabla\} = \left[\frac{\partial}{\partial x_1}, \frac{\partial}{\partial x_2}, \frac{\partial}{\partial x_3}\right]^t$. These are system of five partial differential equations in density $\bar{\rho}$, velocities $\vec{v}$, stresses σ_{ij}, fluxes q_i, and specific internal energy e. These equations do not have a closure i.e. there are more unknowns than the number of equations. This is not surprising due to the fact that the constitution of the matter was never considered in deriving these equations. Constitutive equations (derived in chapter 3) relate stresses to strains, heat fluxes to temperature and specific internal energy to density, temperature and pressure and provide closure to the GDEs resulting from conservation laws. We consider some specific causes of deformations in the following.

2.2.1 Incompressible Solid Matter: Large Motion, Finite Strain

We consider finite strain large deformation but assume matter to be incompressible. In this case $|J| = 1$ and $|J|^{-1}$ and hence $\rho = \bar{\rho}$ i.e. continuity is satisfied identically and hence is no longer part of the mathematical model. Momentum and energy equations reduce to,

$$\rho \frac{\partial \vec{v}}{\partial t} - \left[[J][\sigma]^t [J]^t \right] \{\nabla\} - \vec{F}^b \rho = 0 \tag{2.23}$$

$$\rho \frac{\partial e}{\partial t} + (\{\nabla\}^t [J]^{-1})([J^t]^{-1}\{q\}) - [J][\sigma] \left[\frac{\partial \vec{v}}{\partial \{x\}} \right]^t = 0 \tag{2.24}$$

2.2.2 Incompressible Solid Matter: Small Deformation Small Strain

If we consider the deformation to be infinitesimal and the motion to be infinitesimal then, $|J| = 1$ (due to incompressibility) and $[J] = [I]$ (due to $x_i = \bar{x}_i$) and hence the GDEs reduce to

$$\rho \frac{\partial \vec{v}}{\partial t} - [\sigma]\{\nabla\} - \vec{F}^b \rho = 0 \tag{2.25}$$

$$\rho \frac{\partial e}{\partial t} + \{\nabla\}^t \{q\} - \sigma_{ij} \frac{\partial v_i}{\partial x_j} = 0 \tag{2.26}$$

If the deformation is independent of time then, we have

$$[\sigma]\{\nabla\} - \vec{F}^b \rho = 0 \tag{2.27}$$

$$\rho \frac{\partial e}{\partial t} + \{\nabla\}^t \{q\} - \sigma_{ij} \frac{\partial v_i}{\partial x_j} = 0 \tag{2.28}$$

or in index notation,

$$\frac{\partial \sigma_{ij}}{\partial x_j} + F_i^b \rho = 0 \tag{2.29}$$

$$\rho \frac{\partial e}{\partial t} + \frac{\partial q_i}{\partial x_i} - \sigma_{ij} \frac{\partial v_i}{\partial x_j} = 0 \tag{2.30}$$

The specific internal energy term in the energy equation must be retained at this stage. It needs to be expanded further in terms of $\rho, \vec{v}$, and p (pressure).

Remarks

(1) The mathematical details presented above for various cases of deformation need constitutive equations and details of specific internal energy in order to have closure.

(2) All quantities are functions of initial position coordinate in the undeformed configuration and time except that (2.27) and (2.28) are invariant of time.

2.3 Mathematical Models for Deforming Solid Continuum Using Eulerian Description

In Eulerian descriptions all quantities of interest are function of deformed coordinates $\bar{x}_i$ and time t.

Considering volumes of the matter V and $\bar{V}$ with boundaries ∂V and $\partial \bar{V}$ and applying same conservation laws as in the case of Lagrangian descriptions, we obtain the following system of governing differential equations (in index notation) for a compressible solid undergoing large motion and finite strains [35]. Noting that the quantities with over bars refer to deformed configuration.

Continuity Equation:

$$\frac{\partial \bar{\rho}}{\partial t} + \frac{\partial}{\partial \bar{x}_i}(\bar{\rho} v_i) = 0 \tag{2.31}$$

Momentum Equations:

$$\bar{\rho}\frac{\partial v_i}{\partial t} + \bar{\rho}\frac{\partial v_i}{\partial \bar{x}_j} v_j - \frac{\partial \bar{\sigma}_{ij}}{\partial \bar{x}_j} - F_i^b \bar{\rho} = 0 \quad ; \quad i = 1, 2, 3 \tag{2.32}$$

Energy Equation:

$$\bar{\rho}\frac{De}{Dt} + \frac{\partial \bar{q}_i}{\partial \bar{x}_i} - \bar{\sigma}_{ij}\frac{\partial v_i}{\partial \bar{x}_j} = 0 \tag{2.33}$$

where $\bar{\sigma}_{ij}$ are components of Cauchy stress tensor and $\frac{D}{Dt}$ is the material time derivative (expanded form is given in chapter 3). In this case also, just like in case of Lagrangian descriptions, these equations do not have closure. That is we have more variables than the equations. The constitutive equations and equations of state described in chapter 3 provide closure to these systems of GDEs.

2.3.1 Incompressible Solid Matter: Large Motion, Finite Strain

If the matter is incompressible, then $\rho = \bar{\rho}$ i.e. deformation is volume preserving or isochoric in which case (2.31) to (2.33) can be written as,

Continuity Equation:

$$\rho\frac{\partial v_i}{\partial \bar{x}_i} = 0 \tag{2.34}$$

Momentum Equations:

$$\rho\frac{\partial v_i}{\partial t} + \rho\frac{\partial v_i}{\partial \bar{x}_j}v_j - \frac{\partial \bar{\sigma}_{ij}}{\partial \bar{x}_j} - F_i^b\rho = 0 \quad ; \quad i = 1, 2, 3 \tag{2.35}$$

Energy Equation:

$$\rho\frac{De}{Dt} + \frac{\partial \bar{q}_i}{\partial \bar{x}_i} - \bar{\sigma}_{ij}\frac{\partial v_i}{\partial \bar{x}_j} = 0 \tag{2.36}$$

Remarks:

(1) There is no need to reduce these further to small motion small deformation case due to the fact that the incentive to use Eulerian descriptions is warranted by large motion of the material particles.

(2) The small motion small deformation behavior is obviously intrinsic in (2.34) - (2.36).

(3) $\frac{De}{Dt}$ need to be further expanded using specific form of 'e'.

(4) Obviously, we need constitutive equations and equations of state (if the matter is compressible).

2.4 Summary

In this chapter, mathematical models for solid matter are derived based on conservation laws using both Lagrangian and Eulerian descriptions. In addition, fundamental deformation relations, mappings relationships from Lagrangian to Eulerian, and measures of strains and stresses are presented. The most general form of governing differential equations (GDEs) are described for large motion, finite strain compressible matter in Lagrangian descriptions, however, it is straightforward to get simplified forms of GDEs for incompressible solid matter for large motion, finite strain case as well as small deformation, small strain cases. These various forms of GDEs are also presented in this chapter. Similarly, for Eulerian descriptions, GDEs for large motion and finite strain for both compressible and incompressible solid matter are given. The constitution of the matter is not considered in this chapter, hence, the mathematical models presented here do not have closure. The constitutive equations providing closure to these mathematical models are given in chapter 3.

Chapter 3

Constitutive Equations, Equations of State and Other Relations for an Elastic Deforming Solid

In the developments of the mathematical models for continuum (chapter 2), we employed conservation laws and utilized stresses, fluxes and internal energy per unit mass as dependent variables in addition to density and velocities. These developments did not consider the constitution of the medium and hence are applicable to any or all continua. We know that bodies of same shape and size when subjected to identical disturbances and constraints respond differently. Thus, we need to incorporate the constitution of the material or matter into the mathematical models (derived in chapter 2). We shall see that the stresses, fluxes and internal energy can be expressed in terms of displacements, velocities, temperature, and the constitution of the matter i.e. the appropriate properties of the matter. We generally refer to these relations as constitutive equations. Thus, the constitutive equations are in essence mathematical models of the behavior of material. These mathematical models are generally derived based on experimental observations and must be calibrated (i.e. determination of unknown parameters) and validated using experiments. Once, the mathematical models for constitutive behavior are established, then the difference between the predictions using these models and experiments is generally attributed

to the inaccuracies in the representation of the constitutive behavior in the mathematical models or the constitutive equations. A material for which the constitutive behavior is only a function of the current state of deformation is called elastic material. In the following we consider constitutive equations in Lagrangian as well as Eulerian descriptions.

3.1 Stress-Strain Relationship for Elastic Matter: Lagrangian Description

The general stress-strain relations for elastic matter have been considered by Truesdell and Eringen. We use some of these in the following. What follows is applicable for large motion, finite strain case as long as the material is elastic. An ideal elastic body is characterized by its natural state in which the stresses depend upon the state of deformation only and when the external loads are removed or released, the body or matter resumes the natural state again. Thus, the work done by the external forces acting on the body is stored in the body as elastic energy (internal energy) which is fully recovered upon removing the loads. Hence, the constitutive relation for such bodies must be derivable from an internal energy function. On this basis, Green (1839-41) assumed that internal energy is a function of strain. An alternate approach, due to Cauchy (1823, 1828, 1829), is based on the assumption that in an ideally elastic body the stress is a function of strain. For infinitesimal strain, both of these methods yield the same results but for finite strain Green's method leads to a more definite theory in spite of the fact that Cauchy's method is more general but requires additional assumption to obtain more definitive form.

Let W be the strain energy per unit volume. Then for homogeneous isotropic material one could show [35] that

$$W = W([J]) \tag{3.1}$$

Since $[C] = [J]^t[J]$; Cauchy strain tensor, (3.1) can also be written as,

$$W = W([C]) \tag{3.2}$$

objectivity of W i.e. frame invariance requires that,

$$W = W(I_c, II_c, III_c) \tag{3.3}$$

in which I_c, II_c, III_c are the invariants of the strain tensor $[C]$. Note that we also have other measures of strains such as $[\varepsilon]$, $[F]$, $[\bar{C}]$, $[\bar{F}]$, and $[\bar{\varepsilon}]$ all of which naturally have invariants and they are all related to each other through $[J]$. W can be expressed as a function of the three invariants of a desired strain tensor. In the work presented here, we choose Green's strain with invariants $I_\varepsilon, II_\varepsilon, III_\varepsilon$. Thus,

$$W = W(I_\varepsilon, II_\varepsilon, III_\varepsilon) \tag{3.4}$$

becomes our starting point for deriving constitutive equations for an elastic matter undergoing large motion and finite strain. In addition to choosing Green's strain $[\varepsilon]$ as strain measure, we also need an energetically [35] conjugate choice of stress which is second Piola-Kirchhoff stress $[\sigma]$ for Green's strain. Thus in the following we seek a relationship between $[\sigma]$ and $[\varepsilon]$. When $[\sigma]$ and $[\varepsilon]$ are energetically conjugate pairs, one could show [35] using virtual work consideration that,

$$\{\sigma\}^t = \frac{\partial W}{\partial \{\varepsilon\}} \tag{3.5}$$

in which

$$\{\sigma\} = [\sigma_{x_1x_1}, \sigma_{x_2x_2}, \sigma_{x_3x_3}, \sigma_{x_2x_3}, \sigma_{x_3x_1}, \sigma_{x_1x_2}]^t \tag{3.6}$$

and

$$\{\varepsilon\} = [\varepsilon_{x_1x_1}, \varepsilon_{x_2x_2}, \varepsilon_{x_3x_3}, \gamma_{x_2x_3}, \gamma_{x_3x_1}, \gamma_{x_1x_2}]^t \tag{3.7}$$

Thus, $\{\sigma\}$ as a function of $\{\varepsilon\}$ admits W as a potential. This form was derived by Cosserat (1896).

We can also write (3.5) in index notation,

$$\sigma_{ij} = \frac{\partial W}{\partial \varepsilon_{ij}} \tag{3.8}$$

We note that

$$\gamma_{x_2x_3} = 2\varepsilon_{x_2x_3} \quad , \quad \gamma_{x_3x_1} = 2\varepsilon_{x_3x_1} \quad \text{and} \quad \gamma_{x_1x_2} = 2\varepsilon_{x_1x_2} \tag{3.9}$$

Thus, we see that determination of the constitutive equations depends upon existence of W. In the following we present two derivation of the constitutive relations. The first derivation is more general and is applicable to large motion finite strain case whereas the second derivation is specifically for small deformation small strain case but applicable to non-linear elastic materials as well as linear elastic materials.

3.1.1 Case(a): Large Deformation Finite Strain: General Theory

If we use $[\sigma]$ and $[\varepsilon]$ as energetically conjugate pairs then we have,

$$\{\sigma\}^t = \frac{\partial W}{\partial \{\varepsilon\}} \quad ; \quad W = W(I_\varepsilon, II_\varepsilon, III_\varepsilon) \tag{3.10}$$

Applying chain rule of differentiation to (3.10), we obtain

$$\frac{\partial W}{\partial \{\varepsilon\}} = \frac{\partial W}{\partial I_\varepsilon}\frac{\partial I_\varepsilon}{\partial \{\varepsilon\}} + \frac{\partial W}{\partial II_\varepsilon}\frac{\partial II_\varepsilon}{\partial \{\varepsilon\}} + \frac{\partial W}{\partial III_\varepsilon}\frac{\partial III_\varepsilon}{\partial \{\varepsilon\}} \tag{3.11}$$

where

$$I_\varepsilon = \varepsilon_{x_1x_1} + \varepsilon_{x_2x_2} + \varepsilon_{x_3x_3} \tag{3.12}$$

$$II_\varepsilon = \varepsilon_{x_1x_1}\varepsilon_{x_2x_2} + \varepsilon_{x_2x_2}\varepsilon_{x_3x_3} + \varepsilon_{x_3x_3}\varepsilon_{x_1x_1} - \frac{1}{4}(\gamma^2_{x_2x_3} + \gamma^2_{x_3x_1} + \gamma^2_{x_1x_2}) \tag{3.13}$$

$$III_\varepsilon = \varepsilon_{x_1x_1}\varepsilon_{x_2x_2}\varepsilon_{x_3x_3} + \frac{1}{4}(\gamma_{x_1x_2}\gamma_{x_2x_3}\gamma_{x_3x_1} - \varepsilon_{x_1x_1}\gamma^2_{x_2x_3} - \varepsilon_{x_2x_2}\gamma^2_{x_3x_1} - \varepsilon_{x_3x_3}\gamma^2_{x_1x_2}) \tag{3.14}$$

Thus,

$$\frac{\partial I_\varepsilon}{\partial\{\varepsilon\}} = \{a_1\}^t = [1, 1, 1, 0, 0, 0] \tag{3.15}$$

$$\frac{\partial II_\varepsilon}{\partial\{\varepsilon\}} = \{a_2\}^t = [(\varepsilon_{x_2x_2} + \varepsilon_{x_3x_3}), (\varepsilon_{x_3x_3} + \varepsilon_{x_1x_1}), (\varepsilon_{x_1x_1} + \varepsilon_{x_2x_2}), -\frac{1}{2}\gamma_{x_2x_3}, -\frac{1}{2}\gamma_{x_3x_1}, -\frac{1}{2}\gamma_{x_1x_2}]$$

or

$$\frac{\partial II_\varepsilon}{\partial\{\varepsilon\}} = \{a_2\}^t = I_\varepsilon\{a_1\}^t - \{\varepsilon\}^t \tag{3.16}$$

and

$$\frac{\partial III_\varepsilon}{\partial\{\varepsilon\}} = \{a_3\}^t = [(\varepsilon_{x_2x_2}\varepsilon_{x_3x_3} - \frac{1}{2}\gamma^2_{x_2x_3}), (\varepsilon_{x_1x_1}\varepsilon_{x_3x_3} - \frac{1}{2}\gamma^2_{x_1x_3}), (\varepsilon_{x_1x_1}\varepsilon_{x_2x_2} - \frac{1}{2}\gamma^2_{x_1x_2}), \frac{1}{4}(\gamma_{x_1x_2}\gamma_{x_1x_3} - 2\varepsilon_{x_1x_1}\gamma_{x_2x_3}), \frac{1}{4}(\gamma_{x_2x_3}\gamma_{x_1x_2} - 2\varepsilon_{x_2x_2}\gamma_{x_3x_1}), \frac{1}{4}(\gamma_{x_2x_3}\gamma_{x_3x_1} - 2\varepsilon_{x_3x_3}\gamma_{x_1x_2})] \tag{3.17}$$

If we let,

$$\frac{\partial W}{\partial I_\varepsilon} = \beta_1 \quad , \quad \frac{\partial W}{\partial II_\varepsilon} = \beta_2 \quad , \quad \frac{\partial W}{\partial III_\varepsilon} = \beta_3 \tag{3.18}$$

Then we have,

$$\{\sigma\}^t = \frac{\partial W}{\partial \{\varepsilon\}} = \beta_1\{a_1\} + \beta_2\{a_2\} + \beta_3\{a_3\} \tag{3.19}$$

Knowing explicit form of W, we can now establish $\{\sigma\}^t$ as a function of $\{\varepsilon\}$, the desired constitutive relations between second Piola-Kirchhoff stress and Green's strain. Thus the key element in establishing the constitutive equations are:

(a) Choice of energetically conjugate pairs of stresses and strains (We have used $[\sigma]$ and $[\varepsilon]$).

(b) Determination of W as a function of the invariants of $[\varepsilon]$. This obviously depends upon the type of deformation, strain and motion and hence choice of the $[\sigma]$ and $[\varepsilon]$.

(c) In later section, we consider second order elasticity to establish specific form of W and then derive explicit relationship between $[\sigma]$ and $[\varepsilon]$.

3.1.2 Case(b): Small Deformation, Small Strain: Linear or Non-linear Elastic Material

Obviously, the constitutive equations for this case can be derived using what has been presented in case(a). However, the approach presented in this section is more appealing for the specific case of small deformation, small strain. For this particular case of deformation x_i and $\bar{x}_i$ are same hence if the material is homogeneous and isotropic we can express W as a function of ε_{ij} and there is no need to express W as a function of invariants of the $[\varepsilon]$. This permits a different approach of deriving the constitutive equations. Details are given in the reference [35]. Materials for which the following constitutive laws apply are also referred to as hyper-elastic materials. Let W be the strain energy density function for elastic material with initial

strain $[\varepsilon^0] \neq [0]$ and initial stress $[\sigma^0]$ such that,

$$\{\sigma\}^t = \frac{\partial W}{\partial \{\varepsilon\}} \qquad or \qquad \sigma_{ij} = \frac{\partial W}{\partial \varepsilon_{ij}} \tag{3.20}$$

Expand $W([\varepsilon])$ in Taylor series about $[\varepsilon^0]$. Symbolically, we write,

$$W = W|_{[\varepsilon^0]} + \left.\frac{\partial W}{\partial \{\varepsilon\}}\right|_{[\varepsilon^0]} (\{\varepsilon\} - \{\varepsilon^0\}) + \frac{1}{2!} \left.\frac{\partial^2 W}{\partial \{\varepsilon\}^2}\right|_{[\varepsilon^0]} (\{\varepsilon\} - \{\varepsilon^0\})^2 + \frac{1}{3!} \left.\frac{\partial^3 W}{\partial \{\varepsilon\}^3}\right|_{[\varepsilon^0]} (\{\varepsilon\} - \{\varepsilon^0\})^3 + \dots \tag{3.21}$$

More precisely, using index notation, we can write the above equation as,

$$W = C_0 + C_{ij}(\varepsilon_{ij} - \varepsilon^0_{ij}) + \frac{1}{2!}\hat{C}_{ijkl}(\varepsilon_{ij} - \varepsilon^0_{ij})(\varepsilon_{kl} - \varepsilon^0_{kl}) + \frac{1}{3!}\tilde{C}_{ijklmn}(\varepsilon_{ij} - \varepsilon^0_{ij})(\varepsilon_{kl} - \varepsilon^0_{kl})(\varepsilon_{mn} - \varepsilon^0_{mn}) + \dots \tag{3.22}$$

This expression for W is the most general case for the small deformation, small strain case that permits linear as well as non-linear elastic behavior.

Remarks:

(i) For non-linear elastic materials, W is a cubic or higher order function of strains

(ii) For linear elastic materials, W is a quadratic function of strains

Generalized Hooke's Law; Linear Elastic Material:

Based on remark (ii),W is a quadratic function of strains and we can write,

$$W = C_0 + C_{ij}(\varepsilon_{ij} - \varepsilon^0_{ij}) + \frac{1}{2!}\hat{C}_{ijkl}(\varepsilon_{ij} - \varepsilon^0_{ij})(\varepsilon_{kl} - \varepsilon^0_{kl}) \tag{3.23}$$

$$\sigma_{mn} = \frac{\partial W}{\partial \varepsilon_{mn}} = C_{mn} + C_{ij}\delta_{im}\delta_{jn} + \frac{1}{2!}\hat{C}_{ijkl}\delta_{im}\delta_{jn}(\varepsilon_{kl} - \varepsilon^0_{kl}) + \frac{1}{2!}\hat{C}_{ijkl}(\varepsilon_{ij} - \varepsilon^0_{ij})\delta_{km}\delta_{ln} \quad (3.24)$$

where

$$\delta_{ij} = \begin{cases} 1 & \text{when} \quad i = j \\ 0 & \text{when} \quad i \neq j \end{cases}$$

Therefore we can rewrite (3.24) as,

$$\sigma_{mn} = \frac{\partial W}{\partial \varepsilon_{mn}} = C_{mn} + \frac{1}{2!}(\hat{C}_{mnkl}\varepsilon_{kl} - \hat{C}_{mnkl}\varepsilon^0_{kl} + \hat{C}_{ijmn}\varepsilon_{ij} - \hat{C}_{ijmn}\varepsilon^0_{ij}) \quad (3.25)$$

or

$$\sigma_{mn} = \frac{\partial W}{\partial \varepsilon_{mn}} = C_{mn} + \frac{1}{2}(\hat{C}_{mnkl}\varepsilon_{kl} + \hat{C}_{ijmn}\varepsilon_{ij}) - \frac{1}{2}(\hat{C}_{mnkl}\varepsilon^0_{kl} + \hat{C}_{ijmn}\varepsilon^0_{ij}) \quad (3.26)$$

Note that,

$$\hat{C}_{mnij} = \frac{\partial}{\partial \varepsilon_{ij}}\left(\frac{\partial W}{\partial \varepsilon_{mn}}\right)\Big|_{[\varepsilon^0]} \quad (3.27)$$

$$\hat{C}_{ijmn} = \frac{\partial}{\partial \varepsilon_{mn}}\left(\frac{\partial W}{\partial \varepsilon_{ij}}\right)\Big|_{[\varepsilon^0]} \quad (3.28)$$

and

$$C_{mn} = \frac{\partial W}{\partial \varepsilon_{mn}}\Big|_{[\varepsilon^0]} \quad (3.29)$$

From (3.27) and (3.28), we have

$$\hat{C}_{mnij} = \hat{C}_{ijmn} \quad (3.30)$$

Hence

$$\frac{1}{2}\hat{C}_{mnij}\varepsilon_{ij} + \frac{1}{2}\hat{C}_{ijmn}\varepsilon_{ij} = \hat{C}_{mnij}\varepsilon_{ij} \tag{3.31}$$

Hence (3.25) can be written as,

$$\sigma_{mn} = \frac{\partial W}{\partial \varepsilon_{mn}} = C_{mn} + C_{mnij}\varepsilon_{ij} - C_{mnij}\varepsilon^0_{ij} \tag{3.32}$$

In which, C_{mn} are initial stresses σ^0_{ij} or $[\sigma^0]$ and ε^0_{ij} are initial strains. (3.32) is the desired generalized Hooke's law for linear isotropic elastic material with small strain and small motion. C_{mnij} are called material stiffness coefficients which are strictly deterministic. When $[\sigma^0] = [0]$ and $[\varepsilon^0] = [0]$, (3.32) reduces to

$$\sigma_{mn} = C_{mnij}\varepsilon_{ij} \tag{3.33}$$

Let (3.33) hold in x-frame and let $x^{'}$-frame be obtained from x-frame by an orthogonal rotation matrix $[R]$ then, σ_{mn} and ε_{ij} transform into $\sigma^{'}_{mn}$ and $\varepsilon^{'}_{ij}$ as a second rank tensors and we obtain,

$$\sigma^{'}_{mn} = C^{'}_{mnij}\varepsilon^{'}_{ij} \tag{3.34}$$

One can show [35] that $C^{'}_{mnij}$ can be obtained using C_{mnij} and $[R]$ using fourth order tensor transformation. Hence C_{mnij} and $C^{'}_{mnij}$ are fourth order tensor in x-frame and $x^{'}$-frame respectively. The tensor C_{mnij} contains 81 constants. One can show that for orthotropic materials these constants reduce to nine. Explicits determination of these constants is more convenient if one writes (3.33) in vector and matrix notation.

We begin with (3.33), by virtue of (3.27) and (3.28) and the fact that $[\sigma]$ and $[\varepsilon]$ are sym-

metric tensors, we can write (3.33) in the following form,

$$\begin{Bmatrix} \sigma_{x_1x_1} \\ \sigma_{x_2x_2} \\ \sigma_{x_3x_3} \\ \sigma_{x_2x_3} \\ \sigma_{x_3x_1} \\ \sigma_{x_1x_2} \end{Bmatrix} = \begin{bmatrix} C_{1111} & C_{1122} & C_{1133} & C_{1123} & C_{1113} & C_{1112} \\ & C_{2222} & C_{2233} & C_{2223} & C_{2213} & C_{2212} \\ & & C_{3333} & C_{3323} & C_{3313} & C_{3312} \\ & \text{symm.} & & C_{2323} & C_{2313} & C_{2312} \\ & & & & C_{1313} & C_{1312} \\ & & & & & C_{1212} \end{bmatrix} \begin{Bmatrix} \varepsilon_{x_1x_1} \\ \varepsilon_{x_2x_2} \\ \varepsilon_{x_3x_3} \\ \varepsilon_{x_2x_3} \\ \varepsilon_{x_3x_1} \\ \varepsilon_{x_1x_2} \end{Bmatrix} \tag{3.35}$$

Introducing new notation for C_{ijkl}

$$11 \rightarrow 1 \quad , \quad 22 \rightarrow 2 \quad , \quad 33 \rightarrow 3,$$
$$23 \rightarrow 4 \quad , \quad 13 \rightarrow 5 \quad , \quad 12 \rightarrow 6$$

We can write C_{ijkl} or $[C]$ as follows:

$$[C] = \begin{bmatrix} C_{11} & C_{12} & C_{13} & C_{14} & C_{15} & C_{16} \\ & C_{22} & C_{23} & C_{24} & C_{25} & C_{26} \\ & & C_{33} & C_{34} & C_{35} & C_{36} \\ & \text{symm.} & & C_{44} & C_{45} & C_{46} \\ & & & & C_{55} & C_{56} \\ & & & & & C_{66} \end{bmatrix} \tag{3.36}$$

Thus we can write the following,

$$\{\sigma\} = [C]\{\varepsilon\} \tag{3.37}$$

and we assume that $[C]$ is invertible, then we can write the following relationship

$$\{\varepsilon\} = [S]\{\sigma\} \tag{3.38}$$

where $[S] = [C]^{-1}$ and $[C] = [S]^{-1}$

For orthotropic material one could show [35] that $[C]$ in (3.36) reduces to the following,

$$[C] = \begin{bmatrix} C_{11} & C_{12} & C_{13} & 0 & 0 & 0 \\ C_{12} & C_{22} & C_{23} & 0 & 0 & 0 \\ C_{13} & C_{23} & C_{33} & 0 & 0 & 0 \\ 0 & 0 & 0 & C_{44} & 0 & 0 \\ 0 & 0 & 0 & 0 & C_{55} & 0 \\ 0 & 0 & 0 & 0 & 0 & C_{66} \end{bmatrix} \tag{3.39}$$

From elementary strength of materials consideration, one could directly obtain components of $[S]$ (a derivation based on W is given in the next section

$$\begin{Bmatrix} \varepsilon_{x_1x_1} \\ \varepsilon_{x_2x_2} \\ \varepsilon_{x_3x_3} \\ \varepsilon_{x_2x_3} \\ \varepsilon_{x_3x_1} \\ \varepsilon_{x_1x_2} \end{Bmatrix} = \begin{bmatrix} \frac{1}{E_{x_1x_1}} & -\frac{\nu_{x_2x_1}}{E_{x_2x_2}} & -\frac{\nu_{x_3x_1}}{E_{x_3x_3}} & 0 & 0 & 0 \\ -\frac{\nu_{x_1x_2}}{E_{x_1x_1}} & \frac{1}{E_{x_2x_2}} & -\frac{\nu_{x_3x_2}}{E_{x_3x_3}} & 0 & 0 & 0 \\ -\frac{\nu_{x_1x_3}}{E_{x_1x_1}} & -\frac{\nu_{x_2x_3}}{E_{x_2x_2}} & \frac{1}{E_{x_3x_3}} & 0 & 0 & 0 \\ 0 & 0 & 0 & \frac{1}{2G_{x_2x_3}} & 0 & 0 \\ 0 & 0 & 0 & & \frac{1}{2G_{x_3x_1}} & 0 \\ 0 & 0 & 0 & 0 & 0 & \frac{1}{2G_{x_1x_2}} \end{bmatrix} \begin{Bmatrix} \sigma_{x_1x_1} \\ \sigma_{x_2x_2} \\ \sigma_{x_3x_3} \\ \sigma_{x_2x_3} \\ \sigma_{x_3x_1} \\ \sigma_{x_1x_2} \end{Bmatrix} \tag{3.40}$$

or

$$\{\varepsilon\} = [S]\{\sigma\} \tag{3.41}$$

In which E, ν, and G are Young's moduli, Poisson's ratios and shear moduli respectively.

or

$$\{\varepsilon\} = \begin{bmatrix} S_{11} & S_{12} & S_{13} & 0 & 0 & 0 \\ & S_{22} & S_{23} & 0 & 0 & 0 \\ & & S_{33} & 0 & 0 & 0 \\ & \text{symm.} & & S_{44} & 0 & 0 \\ & & & & S_{55} & 0 \\ & & & & & S_{66} \end{bmatrix} \{\sigma\} = [S]\{\sigma\} \tag{3.42}$$

Inverse of $[S]$ gives $[C]$ and we have, $\{\sigma\} = [C]\{\varepsilon\}$ where $[C] = [S]^{-1}$

$$[C] = \begin{bmatrix} C_{11} & C_{12} & C_{13} & 0 & 0 & 0 \\ & C_{22} & C_{23} & 0 & 0 & 0 \\ & & C_{33} & 0 & 0 & 0 \\ & \text{symm.} & & C_{44} & 0 & 0 \\ & & & & C_{55} & 0 \\ & & & & & C_{66} \end{bmatrix}$$

3.1.3 Case(c): Second Order Elasticity: W for Finite Strain, Large Deformation and Large Motion

In section 3.1.1 we presented general theory of deriving constitutive equation using W for elastic material, however in this development specific form of W was never considered. We consider this here for second order elasticity. The strain energy density function for an elastic material subjected to finite deformation can be expressed in terms of three invariants of the strain (in this case I_ε, II_ε, III_ε of $[\varepsilon]$; Green's strain). For incompressible material W can be expressed as a function of I_ε and II_ε due to the fact that III_ε is related to change in volume which does not occur in incompressible matter. This fact permits specific forms of W. A clear understanding of second order elasticity is essential. We note that if we designate elements of $[\varepsilon]$ as infinitesimals then I_ε is an infinitesimal of order one (contains only first powers of the

elements of $[\varepsilon]$), II_ε is an infinitesimal of (at least) order two, and III_ε is an infinitesimal of (at least) order three. In the following we express W as a power series in terms I_ε, II_ε, and III_ε but separate infinitesimals of various orders. In the second order elasticity we choose to neglect the infinitesimals of order higher than three. Thus in second order elasticity, we write,

$$W = W_0 + W_1 + W_2 + W_3 + \dots \tag{3.43}$$

We choose

$$W_1 = \alpha_\varepsilon I_\varepsilon \tag{3.44}$$

$$W_2 = \frac{1}{2}(\lambda_\varepsilon + 2\mu_\varepsilon) I_\varepsilon^2 - 2\mu_\varepsilon II_\varepsilon \tag{3.45}$$

$$W_3 = l_\varepsilon I_\varepsilon^3 + m_\varepsilon I_\varepsilon II_\varepsilon + n_\varepsilon III_\varepsilon \tag{3.46}$$

Choice of W_0 is of no consequence if it is constant as it drops out upon differentiating with respect to I_ε, II_ε, and III_ε. In (3.44) - (3.46) α_ε, λ_ε, μ_ε, l_ε, m_ε, and n_ε are material constants. Recall the development in section 3.1.1, we need partial derivatives of W with respect to I_ε, II_ε, and III_ε i.e.

$$\frac{\partial W}{\partial I_\varepsilon} = \frac{\partial W_1}{\partial I_\varepsilon} + \frac{\partial W_2}{\partial I_\varepsilon} + \frac{\partial W_3}{\partial I_\varepsilon} \tag{3.47}$$

$$\frac{\partial W}{\partial II_\varepsilon} = \frac{\partial W_1}{\partial II_\varepsilon} + \frac{\partial W_2}{\partial II_\varepsilon} + \frac{\partial W_3}{\partial II_\varepsilon} \tag{3.48}$$

$$\frac{\partial W}{\partial III_\varepsilon} = \frac{\partial W_1}{\partial III_\varepsilon} + \frac{\partial W_2}{\partial III_\varepsilon} + \frac{\partial W_3}{\partial III_\varepsilon} \tag{3.49}$$

In which

$$\frac{\partial W_1}{\partial I_\varepsilon} = \alpha_\varepsilon \quad , \quad \frac{\partial W_1}{\partial II_\varepsilon} = 0 \quad , \quad \frac{\partial W_1}{\partial III_\varepsilon} = 0 \tag{3.50}$$

$$\frac{\partial W_2}{\partial I_\varepsilon} = (\lambda_\varepsilon + 2\mu_\varepsilon) I_\varepsilon \quad , \quad \frac{\partial W_2}{\partial II_\varepsilon} = -2\mu_\varepsilon \quad , \quad \frac{\partial W_2}{\partial III_\varepsilon} = 0 \tag{3.51}$$

$$\frac{\partial W_3}{\partial I_\varepsilon} = 3l_\varepsilon I_\varepsilon^2 + m_\varepsilon II_\varepsilon \quad , \quad \frac{\partial W_3}{\partial II_\varepsilon} = m_\varepsilon I_\varepsilon \quad , \quad \frac{\partial W_3}{\partial III_\varepsilon} = n_\varepsilon \tag{3.52}$$

Putting these together, we obtain,

$$\frac{\partial W}{\partial I_\varepsilon} = \alpha_\varepsilon + (\lambda_\varepsilon + 2\mu_\varepsilon)I_\varepsilon + 3l_\varepsilon I_\varepsilon^2 + m_\varepsilon II_\varepsilon = \beta_1 \tag{3.53}$$

$$\frac{\partial W}{\partial II_\varepsilon} = -2\mu_\varepsilon + m_\varepsilon I_\varepsilon = \beta_2 \tag{3.54}$$

$$\frac{\partial W}{\partial III_\varepsilon} = n_\varepsilon = \beta_3 \tag{3.55}$$

Recall that

$$\{\sigma\}^t = \frac{\partial W}{\partial \{\varepsilon\}} = \frac{\partial W}{\partial I_\varepsilon}\frac{\partial I_\varepsilon}{\partial \{\varepsilon\}} + \frac{\partial W}{\partial II_\varepsilon}\frac{\partial II_\varepsilon}{\partial \{\varepsilon\}} + \frac{\partial W}{\partial III_\varepsilon}\frac{\partial III_\varepsilon}{\partial \{\varepsilon\}} \tag{3.56}$$

where $\frac{\partial I_\varepsilon}{\partial \{\varepsilon\}} = \{a_1\}^t$, $\frac{\partial II_\varepsilon}{\partial \{\varepsilon\}} = \{a_2\}^t$, and $\frac{\partial III_\varepsilon}{\partial \{\varepsilon\}} = \{a_3\}^t$

The partial derivatives of I_ε, II_ε, and III_ε with respect to $\{\varepsilon\}$ are given by (3.15) - (3.17) and thus we have

$$\{\sigma\} = \beta_1\{a_1\} + \beta_2\{a_2\} + \beta_3\{a_3\} \tag{3.57}$$

or in matrix form,

$$\{\sigma\} = [D_s([\varepsilon])]\{\varepsilon\} + \alpha_\varepsilon \begin{Bmatrix} 1 \\ 1 \\ 1 \\ 0 \\ 0 \\ 0 \end{Bmatrix} \tag{3.58}$$

This is the desired constitutive equation for the second order elasticity.

Remarks:

(i) The constitutive equation derived above are for second order elasticity and thus can accommodate up to third order infinitesimals and hence, can be used for large deformation finite strain.

(ii) The constitutive equations contain constants: α_ε, λ_ε, μ_ε, l_ε, m_ε, and n_ε. Choice of these

is critical for specific materials.

(iii) The choices l_ε, m_ε, and n_ε for W_3 may vary. For example we may choose,

$$W_3 = \left(\frac{l_\varepsilon + 2m_\varepsilon}{3}\right) I_\varepsilon^3 - 2m_\varepsilon I_\varepsilon II_\varepsilon + n_\varepsilon III_\varepsilon \tag{3.59}$$

in this case meanings of l_ε, m_ε change but the development remains unaffected.

(iv) Explicit form of $[D_s([\varepsilon])]$ in (3.58) can be derived and is given in the appendix A (using l_ε, m_ε, and n_ε).

Special Case: Linear Elasticity: Infinitesimal Deformation

This implies infinitesimal of order 2 in the expression W i.e. W becomes

$$W = W_0 + W_1 + W_2 \tag{3.60}$$

where

$$W_1 = \alpha_\varepsilon I_\varepsilon \tag{3.61}$$

$$W_2 = \frac{1}{2}(\lambda_\varepsilon + 2\mu_\varepsilon) I_\varepsilon^2 - 2\mu_\varepsilon II_\varepsilon \tag{3.62}$$

$$W_3 = 0 \tag{3.63}$$

We can choose $W_0 = 0$ without loss of generality.

Thus,

$$\beta_1 = \alpha_\varepsilon + (\lambda_\varepsilon + 2\mu_\varepsilon) I_\varepsilon \tag{3.64}$$

$$\beta_2 = -2\mu_\varepsilon \tag{3.65}$$

$$\beta_3 = 0 \tag{3.66}$$

and we have

$$\{\sigma\} = \beta_1\{a_1\} + \beta_2\{a_2\} \tag{3.67}$$

or in matrix form

$$\{\sigma\} = [D_s]\{\varepsilon\} + \alpha_\varepsilon \begin{Bmatrix} 1 \\ 1 \\ 1 \\ 0 \\ 0 \\ 0 \end{Bmatrix}$$

Note that $[D_s]$ is not a function of $[\varepsilon]$. Explicit form of $[D_s]$ is given in the following

$$[D_s] = \begin{bmatrix} (\lambda_\varepsilon + 2\mu_\varepsilon) & \lambda_\varepsilon & \lambda_\varepsilon & 0 & 0 & 0 \\ \lambda_\varepsilon & (\lambda_\varepsilon + 2\mu_\varepsilon) & \lambda_\varepsilon & 0 & 0 & 0 \\ \lambda_\varepsilon & \lambda_\varepsilon & (\lambda_\varepsilon + 2\mu_\varepsilon) & 0 & 0 & 0 \\ 0 & 0 & 0 & 2\mu_\varepsilon & 0 & 0 \\ 0 & 0 & 0 & 0 & 2\mu_\varepsilon & 0 \\ 0 & 0 & 0 & 0 & 0 & 2\mu_\varepsilon \end{bmatrix} \tag{3.68}$$

3.2 Stress-Strain Relations for Elastic Matter: Eulerian Descriptions

From the descriptions of the mathematical models for a deforming elastic solid in Eulerian frame, we note that the equations resulting from the conservation laws are in terms of velocities. In case of Lagrangian descriptions it is possible to substitute velocities in terms of derivatives of displacements and thereby eliminating velocities all together from the GDEs. This however, is not possible in the mathematical models resulting from Eulerian descriptions. Thus, when using the GDEs for solids in Eulerian descriptions it becomes essential to derive constitutive equations in terms of velocity gradients or strain rates. We proceed as follows. From Eulerian descriptions for fluids, we have the following.

Let v_i or $\vec{v}$ be the velocities and $\{\bar{\nabla}\} = [\frac{\partial}{\partial \bar{x}_1}, \frac{\partial}{\partial \bar{x}_2}, \frac{\partial}{\partial \bar{x}_3}]^t$ be the differential operator. Then, we

define,

$$D_{ij} = \frac{1}{2}\left(\frac{\partial v_i}{\partial \bar{x}_j} + \frac{\partial v_j}{\partial \bar{x}_i}\right) = D_{ji} \tag{3.69}$$

$$w_{ij} = \frac{1}{2}\left(\frac{\partial v_i}{\partial \bar{x}_j} - \frac{\partial v_j}{\partial \bar{x}_i}\right) \neq w_{ji} \tag{3.70}$$

the symmetric and anti-symmetric parts of the velocity gradient tensor $[\bar{\nabla}\vec{v}]$ respectively. w_{ij} are responsible for pure rotation and hence referred to as components of the spin tensor $[w]$. D_{ij} on the other hand are called components of the strain rate tensor $[D]$, responsible for the stresses (or stress rates). Thus the constitutive equation must be derived in terms of D_{ij}. One can show that $[D]$ is a second order tensor and hence transform according to a second order tensor due to rotation of coordinate frame. Thus $[D]$ is objective, a strict requirement to be admissible in the development of the constitutive equations. To look for conjugate stress pair, the choice in the Eulerian descriptions is obviously Cauchy stress $[\bar{\sigma}]$ or $\bar{\sigma}_{ij}$ (as used in the development of GDEs from the conservation laws). Since $[D]$ is a tensor of strain rates, the conjugate stress has to be stress rate (unlike fluids). In Eulerian descriptions, the most straight forward way to obtain rate of $[\bar{\sigma}]$ is to take its material time derivative. However, we find that $\frac{D[\bar{\sigma}]}{Dt}$ is not objective or frame invariant [35]. Thus we can not relate $[D]$ to $\frac{D[\bar{\sigma}]}{Dt}$ through material constitution.
Let $\frac{\mathfrak{D}}{\mathfrak{D}t}$ be a material time derivative operator such that $\frac{\mathfrak{D}[\bar{\sigma}]}{\mathfrak{D}t}$ is objective, then we can write the following, relating $[\bar{\sigma}]$ and $[D]$.

$$\frac{\mathfrak{D}[\bar{\sigma}]}{\mathfrak{D}t} = \mathbb{D} : \mathbf{D} \tag{3.71}$$

Since $[\bar{\sigma}]$ and $[D]$ are both tensors of rank two, it follows [35] that $\mathbb{D}$ is a material tensor of rank four. Thus, (3.71) becomes the fundamental starting point in the development of the constitutive equations for the solid elastic matter in Eulerian descriptions. Specific forms of $\frac{\mathfrak{D}}{\mathfrak{D}t}$ and $\mathbb{D}$ need to be established. The constitutive equation of the form (3.71) are referred to as rate constitutive equations due to the fact these relate stress rates to strain rates.

One can show that convected derivatives of [35] tensor $[\bar{\sigma}]$ are objective. The convected

derivative can be obtained in more than one way i.e. upper Convected (Co-deformational), lower Convected, Jaumann, Truesdell etc. [35]. We define these in the following but omit their derivations.

Let us define the conjugate pairs of $\frac{\mathfrak{D}}{\mathfrak{D}t}$ and $\mathbb{D}$

$$\frac{^{C}\mathfrak{D}}{\mathfrak{D}t} \quad , \quad {}^{C}\mathbb{D} \quad ; \quad \frac{^{LC}\mathfrak{D}}{\mathfrak{D}t} \quad , \quad {}^{LC}\mathbb{D} \quad ; \quad \frac{^{J}\mathfrak{D}}{\mathfrak{D}t} \quad , \quad {}^{J}\mathbb{D} \quad ; \quad \frac{^{T}\mathfrak{D}}{\mathfrak{D}t} \quad , \quad {}^{T}\mathbb{D} \tag{3.72}$$

In which C, LC, J, and T stand for convected (upper convected), lower convected, Jaumann, and Truesdell. Using (3.71) and (3.72),we can write convected, lower convected, Jaumann, and Truesdell rate constitutive equation respectively as follows:

$$\frac{^{C}\mathfrak{D}[\bar{\sigma}]}{\mathfrak{D}t} = {}^{C}\mathbb{D} : D \tag{3.73}$$

$$\frac{^{LC}\mathfrak{D}[\bar{\sigma}]}{\mathfrak{D}t} = {}^{LC}\mathbb{D} : D \tag{3.74}$$

$$\frac{^{J}\mathfrak{D}[\bar{\sigma}]}{\mathfrak{D}t} = {}^{J}\mathbb{D} : D \tag{3.75}$$

$$\frac{^{T}\mathfrak{D}[\bar{\sigma}]}{\mathfrak{D}t} = {}^{T}\mathbb{D} : D \tag{3.76}$$

Explicit forms of $\frac{\mathfrak{D}[\bar{\sigma}]}{\mathfrak{D}t}$ for various rate equations are given in the following,

$$\frac{^{C}\mathfrak{D}[\bar{\sigma}]}{\mathfrak{D}t} = \frac{D[\bar{\sigma}]}{Dt} - \left[([\bar{\sigma}] \cdot [\bar{\nabla}\vec{v}])^{t} + [\bar{\sigma}] \cdot [\bar{\nabla}\vec{v}])\right] \tag{3.77}$$

$$\frac{^{LC}\mathfrak{D}[\bar{\sigma}]}{\mathfrak{D}t} = \frac{D[\bar{\sigma}]}{Dt} + \left[([\bar{\sigma}] \cdot [\bar{\nabla}\vec{v}])^{t} + [\bar{\sigma}] \cdot [\bar{\nabla}\vec{v}])\right] \tag{3.78}$$

$$\frac{^{J}\mathfrak{D}[\bar{\sigma}]}{\mathfrak{D}t} = \frac{D[\bar{\sigma}]}{Dt} + [w] \cdot [\bar{\sigma}] - [\bar{\sigma}] \cdot [w] \tag{3.79}$$

$$\frac{^{T}\mathfrak{D}[\bar{\sigma}]}{\mathfrak{D}t} = \frac{D[\bar{\sigma}]}{Dt} + \mathit{div}\,\vec{v}[\bar{\sigma}] - [\bar{\nabla}\vec{v}] \cdot [\bar{\sigma}] - [\bar{\sigma}] \cdot [\bar{\nabla}\vec{v}] \tag{3.80}$$

where

$$\frac{D[\bar{\sigma}]}{Dt} = \frac{\partial[\bar{\sigma}]}{\partial t} + \vec{v} \cdot \bar{\nabla}[\bar{\sigma}] \tag{3.81}$$

Thus everything is defined in the four different descriptions of the constitutive equation except material tensor $\mathbb{D}$.

Remarks:

(1) It is obvious that the four rate equations are a set of partial differential equations in $[\bar{\sigma}]$, strain rates and the constitution of the matter (contained in $\mathbb{D}$).

(2) For the same $[D]$ i.e. for a given strain rate tensor, all four constitutive equations will yield the same response only if constants of $\mathbb{D}$ were different for each rate equation.

(3) For the same $[D]$ and $\mathbb{D}$ in each rate equation, the response would be different for each rate equation.

3.3 Heat Flux Equation

If we use Fourier law of heat conduction, the heat fluxes q_i or $\bar{q}_i$ can be expressed in terms of the conductivities of the solid matter and temperature gradients and we can write,

Lagrangian descriptions:

$$q_i = -k_{ij}\frac{\partial T}{\partial x_j} \tag{3.82}$$

Eulerian descriptions:

$$\bar{q}_i = -k_{ij}\frac{\partial T}{\partial \bar{x}_j} \tag{3.83}$$

3.4 Equation of State: Eulerian Description

If the solid matter is compressible, then compression causes change in volume and hence change in density which in turn results in change in temperature and thermodynamic pressure. Thus, in dealing with compressible solid matter thermodynamic pressure $p = p(\bar{\rho}, T)$ must be introduced in the mathematical models. Definition of $p = p(\bar{\rho}, T)$ is called the equation of state.

For solid matter compressibility is only significant for very high pressures which might occur in specific applications such as blast.

Similar to fluid, here also we introduce Stokes hypothesis,

$$\bar{\sigma}_{ij} = -p\delta_{ij} + \bar{\tau}_{ij} \tag{3.84}$$

where p is positive when compressive, $\bar{\sigma}_{ij}$ are usual Cauchy stresses and $\bar{\tau}_{ij}$ are Cauchy stress deviations.

(3.84) must be introduced in GDEs derived from the conservation laws as well as in the constitutive equations. Now we can define $p = p(\bar{\rho}, T)$ as equation of state. At present this symbolic form suffices for the mathematical developments. However, specific form of the equation of state must be considered depending upon the application.

3.5 Specific Internal Energy $'e'$

Recall that in the energy equation the term $\frac{De}{Dt}$ was present, we need to pay closer attention to this term. We note that specific internal energy e is a function of p, $\bar{\rho}$, and T. But $p = p(\bar{\rho}, T)$ and hence we can write,

$$e = e(\rho, T) \tag{3.85}$$

Lagrangian descriptions:

$$\rho\frac{De}{Dt} = \rho\frac{\partial e}{\partial t} = \rho\left(\frac{\partial e}{\partial \rho}\frac{\partial \rho}{\partial t} + \frac{\partial e}{\partial T}\frac{\partial T}{\partial t}\right) \tag{3.86}$$

if specific form of e is known then $\frac{\partial e}{\partial \rho}$ and $\frac{\partial e}{\partial T}$ are strictly deterministic.

Eulerian descriptions:

In Eulerian descriptions one can show [35] that for compressible solid matter,

$$\bar{\rho}\frac{D\bar{e}}{Dt} = \bar{\rho}\frac{\partial \bar{e}}{\partial T}\left(\frac{\partial T}{\partial t} + v_i\frac{\partial T}{\partial \bar{x}_i}\right) - \bar{\rho}^2\frac{\partial \bar{e}}{\partial \bar{\rho}}\frac{\partial v_i}{\partial \bar{x}_i} \tag{3.87}$$

in which $\frac{\partial \bar{e}}{\partial T}$ and $\frac{\partial \bar{e}}{\partial \bar{\rho}}$ are strictly deterministic once we have explicit form of $\bar{e}$.

3.6 Variable Material Properties

In high temperature applications, the conductivities, Young's moduli, shear moduli, and specific heat may not be constant and may indeed depend upon temperature. In such cases, we can use appropriate analytical expression (from experimental data with curve fit or derived otherwise).

Thus, it suffices to say,

$$\begin{aligned} \text{Young's moduli:} \quad & E_{ij} = E_{ij}(T) \\ \text{Shear moduli:} \quad & G_{ij} = G_{ij}(T) \\ \text{Thermal conductivities:} \quad & k_{ij} = k_{ij}(T) \end{aligned} \tag{3.88}$$

3.7 Explicit Expression for $'e'$ and C_v (specific heat)

In this section, we present details of specific internal energy $e = e(p, \rho, T)$. Since $p = p(\rho, T)$ (equation of state), we have $e = e(\rho, T)$. For compressible matter with temperature dependent specific heat, we can write the following for specific internal energy e.

$$e = \int_{T_0}^{T} C_v dT - \int_{\rho_0}^{\rho} \frac{1}{\rho^2}\left(\left(T\frac{\partial p}{\partial T}\right)_\rho - p\right) d\rho \tag{3.89}$$

with $C_v = C_v(T)$, we have

$$C_v = C_v^* - T\int_{\rho_0}^{\rho} \frac{1}{\rho^2}\left(\frac{\partial^2 p}{\partial T^2}\right)_\rho d\rho \tag{3.90}$$

and

$$C_v^* = \sum_{j=0}^{m} C_j T^j \tag{3.91}$$

Remarks:

(i) Using $p = p(\rho, T)$ from equation of state, we can obtain explicit expression for C_v and then for $e = e(\rho, T)$ for any desired equation of state and hence, we have explicit expression for $\frac{\partial e}{\partial T}$ and $\frac{\partial e}{\partial \rho}$ needed in the energy equation.

(ii) Thus, $p = p(\rho, T)$ and $e = e(\rho, T)$ and their spatial derivatives are completely defined explicitly for any desired equation of state.

3.8 Summary

In this chapter, developments of constitutive equations for solid matter are presented. A general theory for deriving stress-strain relationships for elastic matter based on potential function is given in section 3.1. The specific forms of the constitutive equations for first order and second order elasticity are given. In addition, an alternate derivation for special case of Hooke's law for linear elastic materials is presented using Taylor series expansion of strain energy density function. In Lagrangian descriptions, it is possible to substitute velocities for displacements in constitutive equations. In Eulerian descriptions, GDEs are in terms of velocities therefore, it becomes essential to derive constitutive equations in terms of strain rate tensor. Additionally, objectivity is a strict requirement in the development of constitutive equations. Since material derivative of stress, $[\bar{\sigma}]$ is not objective, $[D]$ and $\frac{D[\bar{\sigma}]}{Dt}$ can not be related through material constitution. Four different objective rate constitutive equations are presented for Eulerian descriptions: upper Convected, lower Convected, Jaumann, and Truesdell which are commonly used in the literature. Heat flux equations, equation of state and specific internal energy details are given toward the end of the chapter.

Chapter 4

Complete Mathematical Models for a Deforming Solid in Lagrangian and Eulerian Descriptions

4.1 Introduction

In chapter 2, governing differential equations (GDEs) resulting from conservation laws are presented in Lagrangian as well as Eulerian descriptions. We noted that these systems of GDEs do not have closure due to the fact that the constitution of the matter was never considered in their derivations, thus these GDEs are valid for all matter within the assumptions used in their derivations. In chapter 3, we developed constitutive equations for a deforming solid in Lagrangian and Eulerian descriptions. In Lagrangian descriptions we choose second Piola-Kirchhoff stresses and Green's strains as conjugate pairs of choice in the development of constitutive equations for first order as well as second order elasticity. Eulerian descriptions due to choice of velocities as dependent variables (as opposed to displacements) require rate constitutive equations. A number of rate equations commonly reported in the published work were presented.

In this chapter we bring the GDEs from chapter 2 and the constitutive equations from chapter 3 together to present complete descriptions of mathematical models (in Lagrangian and Eu-

lerian descriptions) that have closure. Thus, these mathematical models are suitable for mathematical descriptions of boundary value problems (BVPs) and initial value problems (IVPs) describing behaviors of deforming solid matter. In the following we give a quick summary of the developments in this chapter.

Lagrangian descriptions:

(1) Large motion, finite strain, compressible matter

- First order elasticity
- Second order elasticity

(2) Large motion, finite strain, incompressible matter

- First order elasticity
- Second order elasticity

(3) Large motion, small strain, incompressible matter

- First order elasticity

(4) Small motion, small strain, incompressible matter

- First order elasticity

Eulerian descriptions:

Since Eulerian descriptions have no restriction on motion hence, we consider the following,

(1) Compressible matter

- Rate constitutive equations

(2) Incompressible matter

- Rate constitutive equations

We present details of the complete mathematical models in the following. The material presented in the following is from chapters 2 and 3, but integrated to present complete models. Flux equations in all models are substituted into the energy equation and thus, eliminated as a separate system of equations.

4.2 Lagrangian Descriptions

4.2.1 Large Motion, Finite Strain, Compressible Matter

We consider second Piola-Kirchhoff stress and Green's strains as energetically conjugate pairs and strokes hypothesis to replace σ_{ij} with

$$[\sigma] = -p[I] + [\tau] \tag{4.1}$$

in which τ are Cauchy stress deviations. This is necessitated due to equation of state $p = p(\rho, T)$.

$$\rho\frac{\partial^2\vec{u}}{\partial t^2} + (|J|^{-1}[J](-p[I] + [\tau])[J]^t)\{\nabla\} - \vec{F}^b\rho = 0 \tag{4.2}$$

$$\rho\frac{\partial e}{\partial t} - |J|(\{\nabla\}^t[J]^{-1})([J^t]^{-1}\{[K]\{\nabla T\}\} - [J](-p[I] + [\tau])\left[\frac{\partial\vec{u}}{\partial\{x\}}\right]^t = 0 \tag{4.3}$$

$$\{\tau\} = p\left\{\begin{matrix}1\\1\\1\\0\\0\\0\end{matrix}\right\} + [D_s([\varepsilon])\{\varepsilon\} \quad ; \quad \text{second order elasticity} \tag{4.4}$$

$$\{\tau\} = p\left\{\begin{matrix}1\\1\\1\\0\\0\\0\end{matrix}\right\} + [D_s]\{\varepsilon\} \quad ; \quad \text{first order elasticity} \tag{4.5}$$

$$\{\tau\}^t = [\tau_{11}, \tau_{22}, \tau_{33}, \tau_{23}, \tau_{31}, \tau_{12}] \tag{4.6}$$

$$\{\varepsilon\}^t = [\varepsilon_{11}, \varepsilon_{22}, \varepsilon_{33}, \frac{1}{2}\gamma_{23}, \frac{1}{2}\gamma_{31}, \frac{1}{2}\gamma_{12}] \tag{4.7}$$

$$\vec{u} = \frac{\partial(\vec{u})}{\partial t} \qquad \text{and} \qquad \frac{\partial e}{\partial t} = \frac{\partial e}{\partial\rho}\frac{\partial\rho}{\partial t} + \frac{\partial e}{\partial T}\frac{\partial T}{\partial t} \tag{4.8}$$

$p = p(\rho, T)$; equation of state and $e = e(\rho, T, p) = e(\rho, T)$ are known explicitly from the constitution of the matter.

Remarks:

(i) $[\varepsilon]$ is a nonlinear function of displacement gradients $[\dot{J}]$

(ii) $[D_s]$ for first order elasticity is only a function of material parameters λ_ε and μ_ε

(iii) $[D_s([\varepsilon])]$ for second order elasticity is a function of invariants I_ε, II_ε, III_ε of $[\varepsilon]$ as well as $[\varepsilon]$in addition to material parameters α_ε, λ_ε, μ_ε, l_ε, m_ε, n_ε.

(iv) We can express $[\varepsilon]$ in terms of components of $[\dot{J}]$, then substitute $[\varepsilon]$ in constitutive equations to express $[\tau]$ in terms of p and components of $[\dot{J}]$. This resulting expression for $[\tau]$ can be substituted in momentum and energy equation to eliminate $[\tau]$ and $[\varepsilon]$ all together from GDEs. The resulting model contains density, displacements and temperature as dependent variables due to the fact that pressure can be eliminated by equation of state. This gives us the final desired set of GDEs constituting the mathematical model.

4.2.2 Large Motion, Finite Strain, Incompressible Matter

For incompressible matter $|J| = 1$ and hence continuity is satisfied identically due to the fact that $\rho = \bar{\rho}$ i.e. no change in density. Furthermore for incompressible matter equation of state is not required, hence, Stokes hypothesis is not necessary i.e. we can maintain $[\sigma]$ in the model. Also for constant specific heat (C_v), $e = C_v T$ hence $\frac{\partial e}{\partial t} = C_v \frac{\partial T}{\partial t}$ in the energy equation. The resulting equations are as follows.

$$\rho \frac{\partial^2 \vec{u}}{\partial t^2} + ([J][\sigma]^t[J]^t)\{\nabla\} - \vec{F}^b \rho = 0 \tag{4.9}$$

$$\rho C_v \frac{\partial T}{\partial t} - (\{\nabla\}^t[J]^{-1})([J^t]^{-1}\{[K]\{\nabla T\}\} - [J][\sigma]\left[\frac{\partial \vec{u}}{\partial\{x\}}\right]^t = 0 \tag{4.10}$$

$$\{\sigma\} = [D_s([\varepsilon])]\{\varepsilon\} \qquad ; \qquad \text{second order elasticity} \tag{4.11}$$

$$\{\sigma\} = [D_s]\{\varepsilon\} \qquad ; \qquad \text{first order elasticity} \tag{4.12}$$

Remarks:

(i) $[\varepsilon]$ is a nonlinear function of displacements $[\dot{J}]$

(ii) $[D_s]$ for first order elasticity is only a function of material parameters λ_ε and μ_ε

(iii) $[D_s([\varepsilon])]$ for second order elasticity is a function of invariants I_ε, II_ε, III_ε of $[\varepsilon]$ as well as $[\varepsilon]$in addition to material parameters α_ε, λ_ε, μ_ε, l_ε, m_ε, n_ε.

(iv) We can express $[\varepsilon]$ in terms of components of $[\dot{J}]$, then substitute $[\varepsilon]$ in constitutive equations to express $[\sigma]$ in terms of components of $[\dot{J}]$. This resulting expression for $[\sigma]$ can be substituted in momentum and energy equation to eliminate $[\sigma]$ and $[\varepsilon]$ all together from the GDEs. The resulting system of GDEs in displacements and temperature are the desired system of PDEs.

4.2.3 Large Motion, Small Strain, Incompressible Matter

In this case also $|J| = 1$, $\rho = \bar{\rho}$ (no change in density) hence, there is no equation of state and $e = C_v T$ for constant C_v (as in 4.2.2)

$$\rho \frac{\partial^2 \vec{u}}{\partial t^2} + ([J][\sigma]^t[J]^t)\{\nabla\} - \vec{F}^b\rho = 0 \tag{4.13}$$

$$\rho C_v \frac{\partial T}{\partial t} - (\{\nabla\}^t[J]^{-1})([J^t]^{-1}\{[K]\{\nabla T\}\} - [J][\sigma]\left[\frac{\partial \vec{u}}{\partial\{x\}}\right]^t = 0 \tag{4.14}$$

$$\{\sigma\} = [D_s]\{\varepsilon\} \qquad ; \qquad \text{first order elasticity} \tag{4.15}$$

In this case the momentum and energy equations are same as in 4.2.2. but the constitutive equation only requires first order elasticity. $[\sigma]$ and $[\varepsilon]$ are second Piola-Kirchhoff stress and Green's strain due to large motion.

Remarks:

(i) $[\varepsilon]$ is a non-linear function of displacements $[\dot{J}]$

(ii) $[D_s]$ for first order elasticity is only a function of material parameters λ_ε and μ_ε

(iii) By substituting components of $[\dot{J}]$ in $[\varepsilon]$ in the constitutive equations and then substitution of $[\sigma]$ in momentum and energy equation permits us to obtain the desired system of PDEs in displacement and temperature.

4.2.4 Small Motion, Small Strain, Incompressible Matter

In this case, we have $|J| = 1$, $[J] = [I]$ and hence $[J]^{-1} = [I]$ (due to $x_i = \bar{x}_i$). There is no equation of state and $e = C_v T$ for constant C_v. Only first order elasticity is required in which $[\sigma]$ and $[\varepsilon]$ Cauchy stress (same as Piola-Kirchhoff stress) and linear part of the Green's strains (standard engineering strains). The GDEs in this case are simplified considerably and become familiar equations in linear elasticity.

$$\rho \frac{\partial^2 \vec{u}}{\partial t^2} + [\sigma]\{\nabla\} - \vec{F}^b \rho = 0 \tag{4.16}$$

$$\rho C_v \frac{\partial T}{\partial t} - \{\nabla\}^t (\{[K]\{\nabla T\}\} - \sigma_{ij} \frac{\partial \dot{u}_i}{\partial x_j} = 0 \tag{4.17}$$

$$\{\sigma\} = [D_s]\{\varepsilon\} \qquad ; \qquad [\varepsilon] = \frac{1}{2}[[\dot{J}] + [\dot{J}]^t] \tag{4.18}$$

Remarks:

(i) $[D_s]$ is the familiar matrix containing λ_ε and μ_ε or E and ν for homogeneous isotropic material

(ii) $\{\sigma\}$ can be expressed in terms of components of $[\dot{J}]$ by substituting for $\{\varepsilon\}$ in terms of $[\dot{J}]$ and then $[\sigma]$ can be substituted in the momentum and energy equation to eliminate $\{\sigma\}$ and $\{\varepsilon\}$ all together from the GDEs. The resulting mathematical model contains four PDEs in three displacements and temperature and hence has closure

4.3 Eulerian Description

4.3.1 Large Motion, Compressible Matter:

Here Cauchy stress deviations and strain rate tensors are the choices for conjugate pair.

$$\frac{\partial \bar{\rho}}{\partial t} + \frac{\partial}{\partial \bar{x}_i}(\bar{\rho} v_i) = 0 \tag{4.19}$$

$$\bar{\rho}\frac{\partial v_i}{\partial t} + \bar{\rho}\frac{\partial v_i}{\partial \bar{x}_j} v_j + \frac{\partial p}{\partial \bar{x}_i} - \frac{\partial \bar{\tau}_{ij}}{\partial \bar{x}_j} - \vec{F}^b \bar{\rho} = 0 \quad ; \quad i = 1, 2, 3 \tag{4.20}$$

$$\bar{\rho}\frac{\partial \bar{e}}{\partial T}\left(\frac{\partial T}{\partial t} + v_i \frac{\partial T}{\partial \bar{x}_i}\right) - \frac{\partial}{\partial \bar{x}_i}\left(K_{ij}\frac{\partial T}{\partial \bar{x}_j}\right) + \left(p(\bar{\rho}, T) - \bar{\rho}^2 \frac{\partial \bar{e}}{\partial \bar{\rho}}\right)\frac{\partial v_i}{\partial \bar{x}_i} - \bar{\tau}_{ij}\frac{\partial \bar{v}_i}{\partial \bar{x}_j} = 0 \tag{4.21}$$

$$\frac{\mathfrak{D}[-p[I] + [\bar{\tau}]]}{\mathfrak{D}t} = \mathbb{D} : \mathbf{D} \quad ; \quad \text{rate constitutive equations} \tag{4.22}$$

Remarks:

(i) $[D]$ is the strain rate tensor

(ii) $\frac{\mathfrak{D}}{\mathfrak{D}t}$ and $\mathbb{D}$ are conjugate choices depending upon the choice of rate equation (discussed in chapter 3).

(iii) Stokes hypothesis is essential to bring p in GDEs so that equation of state $p = p(\rho, T)$ can be used.

(iv) Equation of state defines $p = p(\rho, T)$ and $e = e(p, T, \rho) = e(\rho, T)$. Both p and e are known for a specific material constitution for constant as well as variable properties of the matter

(v) Since the constitutive rate equations are differential equations in $[\bar{\tau}]$ and strain rate tensor, components of $[\bar{\tau}]$ i.e $\bar{\tau}_{ij}$ must remain dependent variables in the mathematical model. Due to equation of state $p = p(\rho, T)$, p is no longer a dependent variable in the mathematical model.

(vi) The resulting mathematical model is a system of eleven PDEs in density $\bar{\rho}$, three velocities

$\vec{v}$, six stresses $\bar{\tau}_{ij}$ and temperature T and thus we have closure. This system of PDEs constitutes the final description of the mathematical model.

4.3.2 Large Motion, Incompressible Matter

Due to incompressibility, density is constant. There is no equation of state and $\bar{e} = C_v T$ for constant specific heat C_v. Due to absence of the equation of state, Stokes hypothesis is not required and hence, the mathematical model can be expressed using Cauchy stress $[\bar{\sigma}]$ and strain rate tensor $[D]$ and we have (noting that $\bar{\rho} = \rho$),

$$\rho \frac{\partial v_i}{\partial \bar{x}_i} = 0 \tag{4.23}$$

$$\rho \frac{\partial v_i}{\partial t} + \rho \frac{\partial v_i}{\partial \bar{x}_j} v_j + \frac{\partial \sigma_{ij}}{\partial \bar{x}_j} - \vec{F}^b \rho = 0 \quad ; \quad i = 1, 2, 3 \tag{4.24}$$

$$\rho C_v \left(\frac{\partial T}{\partial t} + v_i \frac{\partial T}{\partial \bar{x}_i} \right) - \frac{\partial}{\partial \bar{x}_i} \left(K_{ij} \frac{\partial T}{\partial \bar{x}_j} \right) - \bar{\sigma}_{ij} \frac{\partial v_i}{\partial \bar{x}_j} = 0 \tag{4.25}$$

$$\frac{\mathfrak{D}[\bar{\sigma}]}{\mathfrak{D}t} = \mathbb{D} : \mathbf{D} \quad ; \quad \text{rate constitutive equations} \tag{4.26}$$

Remarks:

(i) $\frac{\mathfrak{D}}{\mathfrak{D}t}$ and $\mathbb{D}$ are conjugate choices depending upon the choice of rate equation (discussed in chapter 3).

(ii) Since the constitutive equations are a system of PDEs in $\bar{\sigma}_{ij}$ and D_{ij}, $\bar{\sigma}_{ij}$ can not be eliminated from the GDEs and hence, must remain as dependent variables.

(iii) The mathematical model presented here contains eleven PDEs but only ten variables (three velocities, temperature and six stresses). Thus it does not have a closure. This situation can be corrected by either of the two ways.

(a) If $\bar{\sigma}_{ij}$ are variables then incompressibility requirements warrants that continuity to be eliminated due to the fact that here a control volume experiences motion but no change i.e. material particles in it remain intact.

(b) Use Stokes hypothesis, $\bar{\sigma}_{ij} = -p\delta_{ij} + \bar{\tau}_{ij}$ to substitute $\bar{\sigma}_{ij}$ and make pressure a dependent variable, now continuity equation is admissible even though statement in (a) hold.

4.4 Mathematical Model due to Swedlow, Osias, and Lee

In this section we present a mathematical model for a deforming solid that has been published and used by Swedlow, Osias, and Lee and others quite frequently [19–23, 25, 36, 37]. The motivation for this model is neither clear to us nor it has been stated in the publications. We only present this model here for two reasons: (i) for a time period of 5-10 years many papers have appeared on this model including numerical studies and we wonder about the validity of these (ii) to demonstrate that this mathematical model is in violation of basic principles even if we ignore the motivation for its development. In the subsequent chapter we present numerical studies to illustrate this point for a model problem utilizing this mathematical model as well as using another model problem (1-D convection-diffusion problem) for which the mathematical framework is constructed using the same principle used by the authors in references [19–23, 25, 36, 37]. Following references [19–23, 25, 36, 37], we present the development given by the authors. In the absence of body forces and inertial effects the equilibrium equations for a deforming solid are written as,

$$[\bar{\sigma}]\{\bar{\nabla}\} = 0 \tag{4.27}$$

By taking material time derivative of the above equations, the authors obtain what are referred to as rate equilibrium equations.

$$\frac{D}{Dt}([\bar{\sigma}]\{\bar{\nabla}\}) = 0 \tag{4.28}$$

or

$$\frac{\partial}{\partial t}([\bar{\sigma}]\{\bar{\nabla}\}) + \vec{v} \cdot \vec{\nabla}([\bar{\sigma}]\{\bar{\nabla}\}) = 0 \tag{4.29}$$

The rate constitutive equation used in references [19–23, 25, 36, 37] is due to Jaumann,

$$\frac{{}^{J}\mathfrak{D}[\bar{\sigma}]}{\mathfrak{D}t} = {}^{J}\mathbb{D} : \mathbf{D} \tag{4.30}$$

where

$$\frac{{}^{J}\mathfrak{D}[\bar{\sigma}]}{\mathfrak{D}t} = \frac{D[\bar{\sigma}]}{Dt} + ([w] \cdot [\bar{\sigma}] - [\bar{\sigma}] \cdot [w]) \tag{4.31}$$

$$[w] = \frac{1}{2}(\bar{\nabla}\vec{v} - (\bar{\nabla}\vec{v})^{t}) \quad , \quad \frac{D[\bar{\sigma}]}{Dt} = \frac{\partial[\bar{\sigma}]}{\partial t} + \vec{v} \cdot \vec{\nabla}[\bar{\sigma}] \tag{4.32}$$

$$\text{or} \qquad w_{ij} = \frac{1}{2}(D_{ij} - D_{ji}) \tag{4.33}$$

Thus the final mathematical model consists of

$$\frac{\partial}{\partial t}([\bar{\sigma}]\{\bar{\nabla}\}) + \vec{v} \cdot \vec{\nabla}([\bar{\sigma}]\{\bar{\nabla}\}) = 0 \tag{4.34}$$

and

$$\frac{\partial[\bar{\sigma}]}{\partial t} + \vec{v} \cdot \vec{\nabla}[\bar{\sigma}] + [[w] \cdot [\bar{\sigma}] - [\bar{\sigma}] \cdot [w]] = {}^{J}\mathbb{D} : \mathbf{D} \tag{4.35}$$

Remarks:

(1) This is a system of nine PDEs in three velocities and six Cauchy stresses, $\bar{\sigma}_{ij}$ and hence has closure.

(ii) The equilibrium equations in first order derivatives of Cauchy stresses are a system of first order PDEs in $\bar{\sigma}_{ij}$ and are based on Newton's second law applied to a volume of matter. Its material derivative is essentially differentiation of the conservation law yielding a higher order system of PDEs that are not derivable from the physics of deforming matter

(obvious from $[\bar{\sigma}]\{\bar{\nabla}\} = 0$ containing all of the essential physics).

(iii) Since these GDEs contain higher order derivatives of the dependent $(\bar{\sigma}_{ij})$ variables compared to the GDEs from the conservation laws, their unique solution will obviously require additional boundary conditions (BCs) and/or initial conditions (ICs) that may or may not be possible to ascertain from the physics of the process. Hence the solutions of the associated BVPs and IVPs may have serious issues of the uniqueness. Our numerical experiments with this mathematical model as well as for another model for which the mathematical model is constructed using this approach confirm this.

(iv) The essential points we wish to underline are:

(a) Differentiating the GDEs resulting from the conservation laws and then using them as part of the mathematical models in place of the original GDEs resulting from conservation laws is not permissible due to the fact that the resulting equations describe higher order physics compared to what is present in the process and is reflected the GDEs resulting from the conservation laws.

(b) However, it is permissible to use differentiated forms of the GDEs from the conservation laws for simplification purposes. For example for two dimensional compressible flow the continuity equation is,

$$\frac{\partial u}{\partial x} + \frac{\partial v}{\partial y} = 0$$

Thus when continuity holds, the following hold as well

$$\frac{\partial^2 u}{\partial x^2} + \frac{\partial^2 v}{\partial x \partial y} = 0$$

$$\frac{\partial^2 u}{\partial x \partial y} + \frac{\partial^2 v}{\partial y^2} = 0 \quad \ldots \text{etc}$$

and these can be used to simplify other equations in the system of GDEs. But the original continuity equation can not be replaced using any of these differentiated form. It is

rather obvious that these differentiated form of the continuity equation can not be derived directly using the principle of conservation of mass due to the fact that the principle of conservation of mass is first order physics in relation to the velocity field and not second order as in the differentiated forms.

4.5 Summary

In this chapter, material presented in chapter 2 (governing differential equations) and chapter 3 (constitutive equations) is integrated to present complete mathematical models. The mathematical models are given in Eulerian descriptions as well as Lagrangian descriptions and they are suitable for both boundary value problems (BVPs) and initial value problems (IVPs) for investigating wide variety of solid mechanics problems. The most general formulations for compressible elastic matter are given for large deformation, finite strain case. In addition, the formulations for incompressible elastic matter with small deformation, small strain assumption are also presented.

In section 4.4, equilibrium rate formulation is investigated which is based on the material time derivative of the equilibrium equations in the absence of inertial and body forces. Since the GDEs obtained from this contain higher order derivatives of the dependent variables compared to GDEs from conservation laws, there is a need for additional BCs and/or ICs. However, it is not always possible to determine these from the physics, hence uniqueness of the solution from these mathematical models is always a serious issue.

Chapter 5

Mathematical and Computational Infrastructure, Finite Element Formulations and Solution Method

5.1 Introduction

An examination of the complete mathematical models that have closure (Chapter 4) reveals that except for small motion small strain Lagrangian description all other mathematical models are a system of non-linear partial differential equations (PDEs) in space and time. The descriptions of the physical processes utilizing these mathematical models will naturally result in initial value problems. For such problems, the solution changes as time elapses. A comprehensive literature review of various finite element methodologies based on space-time decoupled and space-time coupled methods can be found in reference [38] and is not presented here for the sake of brevity. Based on Surana et al. [38], space-time coupled methods utilizing space-time strip or slab for an increment of time with time marching is highly meritorious for simulating the evolution and hence is adopted here. Space-time coupled finite element methodology obviously requires space-time integral forms for each space-time strip and hence each space-time element of the strip. Surana et al. [5–7, 38] introduced the concepts of variational consistency

(VC) and variational inconsistency (VIC) for boundary value problems (BVPs) by establishing a correspondence between the integral forms and the calculus of variations and showed that VC integral forms yield unconditionally stable and non degenerate computational processes. This cannot be ensured for the integral forms that are variationally inconsistent. The authors showed that when the differential operators in the BVPs are non-linear only least squares processes gives variationally consistent integral forms. These non-linear algebraic equations are solved using Newton's first order method with line search assuming the term containing the second variation of residual can be neglected in the second variation of the least squares functional [5–7, 38]. Thus, for non-linear GDEs the least squares finite element method is highly meritorious over all others.

These concepts for BVPs have been extended by Surana et al. for initial value problems (IVPs) [38] by introducing the concepts of space-time variationally consistent (STVC) and space-time variationally inconsistent (STVIC) for space-time integral forms. Authors showed that what holds for BVPs also holds for IVPs when the integral forms are space-time integral forms and thus, space-time least squares processes for a space-time strip with time marching become the preferred computational strategy for obtaining numerical solutions of IVPs and is utilized in the present work. In summary, except space-time least squares method all other methods of approximation are space-time VIC when the differential operators in the mathematical models of IVPs are non-linear PDEs.

It is well known that in finite element processes local approximations over an element is extremely crucial. Surana et al. [5–7, 38] have shown for BVPs that the order k of the approximation space defining global differentiability of order $(k-1)$ is an independent parameter in all finite element processes in addition to h, the characteristic length of discretization and p, the local approximation. Thus, the authors proposed h, p, k mathematical framework for BVPs as apposed to the h, p framework used currently in computational mathematics. The authors showed benefits of hpk framework in terms of accuracy, reduced degree of freedoms, better convergence and the most essential feature of being able to incorporate the desired physics through k in the design of the computational processes. This work for BVPs has been extended

by Surana et al. [38] for IVPs yielding hpk framework for IVPs in which the order of global differentiability in space and time can be controlled by k_1 and k_2 the orders of the approximation spaces in space and in time. In the present work we utilize higher order global differentiability approximation in space and time which is only possible in hpk framework.

Thus, in summary, we use space-time least squares processes in hpk framework for IVPs. In the following we present details of the space-time least squares process in hpk framework for IVPs as well as the solution method for time marching the evolution.

5.2 Space-time Least Squares Process for IVPs

In this section we present details of space-time least squares finite element process (STLSP). The material is presented in abstraction but one could easily make it problem specific using the specific forms of the differential operator and the dependent variables.

$$\begin{aligned} &\text{Let } B_j({}^i\varphi) \; - \; f_j \; = 0 \qquad \text{in} \qquad {}^n\Omega_{xt} = \Omega_x \times {}^n\Omega_t = \Omega_x \times (t_n, t_{n+1}) \\ &i = 1, \ldots m \qquad \text{and} \qquad j = 1, \ldots m \end{aligned} \tag{5.1}$$

be a system of non-linear partial differential equations in space and time in dependent variables ${}^i\varphi$ over a space-time domain ${}^n\Omega_{xt}$ of n^{th} space-time strip from time t_n to t_{n+1}.

$$\text{Let } {}^n\bar{\Omega}^T_{xt} = \bigcup_e^M {}^n\bar{\Omega}^e_{xt} \tag{5.2}$$

be a discretization of ${}^n\bar{\Omega}_{xt}$ in which ${}^n\bar{\Omega}^e_{xt}$ is a typical space-time element $'e'$. Let m^i_1 and m^i_2 ; $i = 1, \ldots m$ be the highest orders of the derivatives of the dependent variables ${}^i\varphi$ in space and time appearing in the PDEs (5.1). ${}^nI$ and ${}^nI^e$ be the least squares functionals for the n^{th} space-time strip and the space-time element $'e'$ respectively. Let ${}^i\varphi^e_h$ be the space-time local approximation for the dependent variables ${}^i\varphi$ over ${}^n\bar{\Omega}^e_{xt}$. We choose,

$${}^i\varphi^e_h \in {}^iV_h \; \subset H^{(k^i_1,k^i_2);(p^i_1,p^i_2)\,n}\bar{\Omega}^e_{xt} \tag{5.3}$$

in which $H^{(k_1^i,k_2^i);(p_1^i,p_2^i)\,n}\bar{\Omega}^e_{xt}$ is a scalar product space containing monomial basis functions of global differentiability of orders $(k_1^i - 1)$ and $(k_2^i - 1)$ and degrees of local approximations, p_1^i , p_2^i for variables ${}^i\varphi$ in space and time.

Let ${}^i\varphi_h$ be the global approximation of ${}^i\varphi$ over ${}^n\bar{\Omega}^T_{xt}$, then,

$$ {}^i\varphi_h = \bigcup_e^M {}^i\varphi_h^e \tag{5.4}$$

(5.3) and (5.4) ensure that ${}^i\varphi_h^e$ and ${}^i\varphi_h$ are of the same classes i.e. of same global differentiability in space and time. By substituting (5.3) in (5.1), we obtain residuals or residual equations for ${}^n\bar{\Omega}^e_{xt}$,

$$ B_j({}^i\varphi_h^e) \; - \; f_j \; = \; {}^nE_j^e({}^i\varphi_h^e) \quad \forall\, (\mathbf{x}, t) \in {}^n\bar{\Omega}^e_{xt} \tag{5.5}$$

Least squares functional ${}^nI$ is constructed using (5.5) for ${}^n\bar{\Omega}^T_{xt}$ as follows,

$$ {}^nI({}^i\varphi_h) = \sum_{j=1}^{m} ({}^nE_j, {}^nE_j) = \sum_{e=1}^{M} (\sum_{j=1}^{m} ({}^nE_j^e, {}^nE_j^e)) = \sum_{e=1}^{M} {}^nI^e({}^i\varphi_h^e) \tag{5.6}$$

${}^nI^e({}^i\varphi_h^e)$ is the least squares functional for ${}^n\bar{\Omega}^e_{xt}$, the space-time domain of a space-time element $'e'$. This establishes existence of the functional ${}^nI({}^i\varphi_h)$. In least squares method, we seek extrema (minimum in this case) of the functional ${}^nI({}^i\varphi_h)$. First variation of ${}^nI$ provides necessary conditions and the second variation ${}^nI$ must yield a unique extremum principle or sufficient condition.

$$ \delta({}^nI({}^i\varphi_h)) = \sum_{e=1}^{M} \sum_{j=1}^{M} ({}^nE_j^e, \delta({}^nE_j^e)) = g({}^i\varphi_h) = 0 \tag{5.7}$$

Based on the work presented by Surana et al. [5–7, 38]

$$ \delta^2({}^nI({}^i\varphi_h)) \cong \sum_{e=1}^{M} \sum_{j=1}^{M} (\delta({}^nE_j^e), \delta({}^nE_j^e)) > 0 \tag{5.8}$$

Hence, the integral form resulting from (5.7) is variationally consistent. We seek a solution ${}^{i}\varphi_h$ for ${}^{n}\bar{\Omega}^{T}_{xt}$ that satisfies (5.7) (necessary condition). Since the PDEs are nonlinear, $g({}^{i}\varphi_h)$ is a nonlinear function of ${}^{i}\varphi_h$, thus, we must find ${}^{i}\varphi_h$ that satisfies (5.7) iteratively. We proceed as follows.

Let $({}^{i}\varphi_h)_0$ be an assumed or starting solution, thus,

$$g(({}^{i}\varphi_h)_0) \neq 0 \tag{5.9}$$

Let $\Delta({}^{i}\varphi_h)$ be correction to $({}^{i}\varphi_h)_0$ such that,

$$g(({}^{i}\varphi_h)_0 + \Delta({}^{i}\varphi_h)) = 0 \tag{5.10}$$

Expand $g(({}^{i}\varphi_h)_0 + \Delta({}^{i}\varphi_h))$ in (5.10) in Taylor series about $({}^{i}\varphi_h)_0$ and retain only up to first order terms in $\Delta({}^{i}\varphi_h)$,

$$g(({}^{i}\varphi_h)_0 + \Delta({}^{i}\varphi_h)) \cong g(({}^{i}\varphi_h)_0) + \left.\frac{\partial g}{\partial({}^{i}\varphi_h)}\right|_{({}^{i}\varphi_h)_0} \Delta({}^{i}\varphi_h) = 0 \tag{5.11}$$

But, from (5.8),

$$\frac{\partial g}{\partial({}^{i}\varphi_h)} = \delta^2({}^{n}I({}^{i}\varphi_h)) \tag{5.12}$$

Hence, from (5.11) we obtain $\Delta({}^{i}\varphi_h)$,

$$\Delta({}^{i}\varphi_h) = -\left([\delta^2({}^{n}I({}^{i}\varphi_h)]^{-1}_{({}^{i}\varphi_h)_0}\right) g({}^{i}\varphi_h)\big|_{({}^{i}\varphi_h)_0} \tag{5.13}$$

The improved solution is then obtained using,

$${}^{i}\varphi_h = ({}^{i}\varphi_h)_0 + \alpha(\Delta({}^{i}\varphi_h)) \tag{5.14}$$

α is a scalar (generally $0 < \alpha < 2$) determined such that,

$$ {}^{n}I({}^{i}\varphi_h) \leq {}^{n}I(({}^{i}\varphi_h)_0) \tag{5.15} $$

This method is referred to as Newton's first order method with line search. The iterative solution procedure is considered converged when absolute value of each component of g in (5.7) is below a certain preset tolerance, generally $0(10^{-6})$ or lower.

Remarks

(1) Surana et al. [5–7, 38] have shown that approximation in (5.8) is essential to achieve space-time variational consistency of the integral form resulting from (5.7). Space-time variational consistency by (5.8) ensures that the coefficient matrix in (5.13) is unconditionally positive definite and hence, the computations are unconditionally stable.

(2) The approximation in (5.8) does not affect least squares process as it ends with (5.7). This approximation only influences the slope of the hyperplane to the hypersurface defined by $\delta({}^{n}I({}^{i}\varphi_h)) = 0$. In simple words it only influences the slope of the tangent at $({}^{i}\varphi_h)_0$ in Newton's linear method for solving the non-linear equations from (5.7). The benefits of this are obviously enormous (STVC) as it ensures unconditionally positive definite coefficient matrix in (5.13).

5.3 Computation of Evolution

The STLSP described in 5.2 is applied to the first space-time strip or slab (from $t = 0$ to t=Δt) using BCs and ICs and a solution ${}^{i}\varphi_h$ is computed. h, p and k are adjusted so that the solution for the first space time strip is converged that is we ensure that ${}^{n}I({}^{i}\varphi_h) \leq \Delta$ a predetermined value (generally $O(10^{-6})$ or lower). This ensures that (based on (5.6)) GDEs for each space-time element of ${}^{n}\bar{\Omega}^{T}_{xt}$ are satisfied accurately in the point-wise sense. Now we consider second space-time strip from $t = \Delta t$ to $t = 2\Delta t$. The initial conditions at $t = \Delta t$ for this space-time strip are obtained from the ${}^{i}\varphi_h$ for first space-time strip at $t = \Delta t$. Using these ICs and the

BCs, a solution is computed for the second space-time strip. During the computations for the second space-time strip we maintain same p_1^i ,p_2^i, k_1^i and k_2^i as in case of first space-time strip. Generally these suffice unless there is a new event in the process at later values of time. This process is continued until the desired value of time is reached.

We note that in this time marching approach it is essential to obtain a converged solution $({}^nI \leq \Delta)$ for the current space-time strip before time marching due to the fact that the solution from the current space-time strip serves as initial conditions for the next space-time strip. This is obviously easy to accomplish.

This approach ensures desired accuracy of the solution during evolution and for each space-time strip we only solve a very small problem compared to the approaches in which the entire space time domain is discretized using space-time elements.

5.4 Global Differentiability in Space and Time Choices k_1^i, k_2^i, p_1^i, p_2^i:

If we choose $k_1^i \geq m_1^i + 1$, $k_2^i \geq m_2^i + 1$; $p_1^i \geq 2k_1^i - 1$, $p_2^i \geq 2k_2^i - 1$, then we ensure that all space-time integrals in the entire process are Riemann. The equality for the choices of k_1^i and k_2^i corresponds to the minimally conforming spaces for the integrals to be Riemann.

We could also choose, k_1^i = m_1^i, k_2^i = m_2^i, in which case the integrals in the LSP will be Lebesgue. $k_1^i < m_1^i$ and $k_2^i < m_2^i$ are obviously not admissible in the LSP. Benefits of the choices of k_1^i and k_2^i that ensure integrals in Riemann sense in the entire LSP have been reported by Surana et al. [4].

5.5 Summary

It is shown by Surana et al. [38] that space-time least squares finite element processes (STLSP) are highly meritorious for initial value problems (IVPs) over all others. This is due to the fact that only space-time least squares processes produce space-time variationally consistent (STVC) integral forms regardless of the nature of the space-time differential operators whereas

all other methods of approximation are space-time variationally inconsistent (STVIC) regardless of the nature of differential operators. Variationally consistent integral forms yield unconditionally stable and non-degenerate computational processes. Numerical studies in chapter 6 are carried using hpk mathematical framework with the STVC integral forms. Based on Surana et al. [5–7, 38] hpk framework result in improved accuracy, reduced degree of freedoms, better convergence rate and ability to incorporate the desired physics of the problem through k in the design of the computational process. Newton's first order method with line search is used to solve the nonlinear equations where the iterative solution procedure is assumed converged when the $|g|$ is below a preset tolerance.

Chapter 6

Numerical Studies

6.1 Introduction

From the mathematical models one observes that there are many areas, specially rate equilibrium equations and constitutive equations, that require closer examination to decide their applicability based on assumptions under which they are derived. First, we present a short discussion on the main issues of concern in each section followed by numerical studies. In all numerical studies Eulerian descriptions in velocities and stresses are used unless stated otherwise (Hence over bar for Eulerian variables is omitted in this chapter). Periodically comparisons are made using results obtained from mathematical models derived using Lagrangian descriptions. The numerical studies are derived in the following sections,

(a) Investigation of the mathematical model based on rate equilibrium approach

(b) 1-D axial wave propagation model problem to investigate rate constitutive equations

(c) 2-D wave propagation under various loading with zero and non-zero Poisson's ratio using mathematical models based on velocities and stresses

(d) Some comparisons with numerical results obtained using Lagrangian descriptions in displacements, second Piola-Kirchhoff stresses and Green's strains.

6.2 Investigation of Mathematical Model Based on Rate Equilibrium Approach

The mathematical models based on rate equilibrium approach [20–25, 36] have been published and used. This approach is based on Eulerian description with material time derivative of the static equilibrium equations in Cauchy stresses to obtain what is referred to as a rate equilibrium equations in velocities and Cauchy stresses. The appearance of the velocities in Eulerian description obviously require rate constitutive equations. In all published works on this approach Jaumann rate constitutive equations are utilized.

Remarks

(i) Since the material time derivative of the static equilibrium equations are used, these mathematical models do not contain inertial effects and hence can not be used to study time dependent motion of solids.

(ii) Based on (i), these mathematical models are only valid for static case for which the rationale of material time derivative is not quite clear.

(iii) We note that the static equilibrium equations used here are a special case of momentum equations and that are obtained as a result of neglecting convective terms and inertial terms. Thus the static equilibrium equations are a result of conservation law based on Newton's second law applied to a volume of solid matter. These contain first order derivatives of the Cauchy stresses. That is derivation of these equations only recognize the gradients of stresses for specific physics. When one takes material derivative of the static equilibrium equations, we obtain a form that contain derivatives of the stresses of order higher than one. Additionally velocity field and time derivatives of the Cauchy stresses appear as well. It is quite obvious that this form could not have been derived using conservation law based on Newton's second law.

When using the rate equilibrium equation as part of the mathematical model two additional difficulties arise: (a) The appearance of higher order derivatives require higher order regularity

of the approximations which in accordance with static equilibrium equation is unnecessary. (b) Uniqueness of the solution with the rate equilibrium equations obviously requires additional boundary conditions and initial conditions which may not be possible to establish based on physics of the problem.

In summary, the rate equilibrium equations bring higher order physics in the mathematical models which is not present in the original equilibrium equations based on the conservation law. The higher order physics obviously necessitates additional boundary conditions for the uniqueness of the solution which may be absent in the description of the original problem. The most disturbing feature of these models is that they fail for time dependent motion and if the static response is the goal, then these models are not required in the first place. Jaumann rate constitutive equations appears to have limitations as well (discussed in next section).

6.2.1 Model Problem 1

In this section we present a numerical study using rate equilibrium equations approach with Jaumann constitutive equations using 1-D axial wave propagation as a model problem. We consider a rod of length L, fixed at one end $(x = 0)$ and subjected to an axial stress σ_{xx} at the other end $x = L$. σ_{xx} is a pulse of duration $2\Delta t$ and peak value of σ_{xx} (figure 6.1). The discretization consists of a space-time strip of ten element uniform mesh (space-time elements). Numerical solution for the evolution is computed for p-level of 9 (in both space and time) with space-time local approximations of class $C^{11}({}^n\bar{\Omega}^e_{xt})$. Dimensionless values of various quantities one shown in figure 6.1. We choose peak value of σ_{xx} to be -0.01. Figures 6.2 (a), (b) and (c) show that evolutions of Cauchy stress σ_{xx} and axial velocity u. At the end of first time step, $\sigma_{xx} = -0.01$ for all values of x is static response for $\sigma_{xx} = -0.01$. Since $\sigma_{xx} = 0$ at the end of the second time step and thereafter, we observe the same for time evolutions of σ_{xx} in figure 6.2 (a). Velocity evolutions in figure 6.2 (b) and (c) appear spurious for static response axial velocity should have been zero. Thus, it is not clear whether we have a static response or dynamic response in this study.

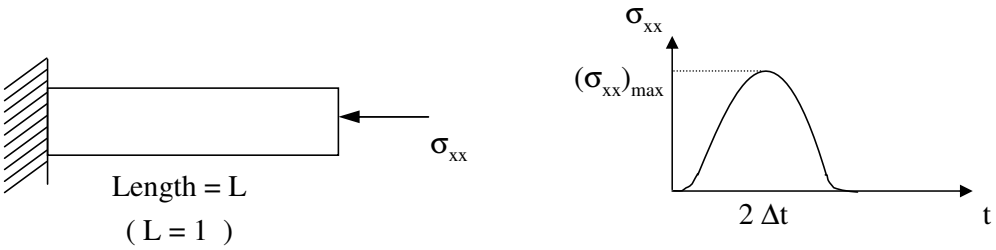

$E = 1\ ,\ \rho = 1\ ,\ A = 1$

$\Delta t = 0.1$

$p_\xi = p_\zeta = p = 9$

10 element uniform mesh

Solution of class C^{11} in space and time

Figure 6.1: 1-D Elastic Wave Propagation: Model Problem 1

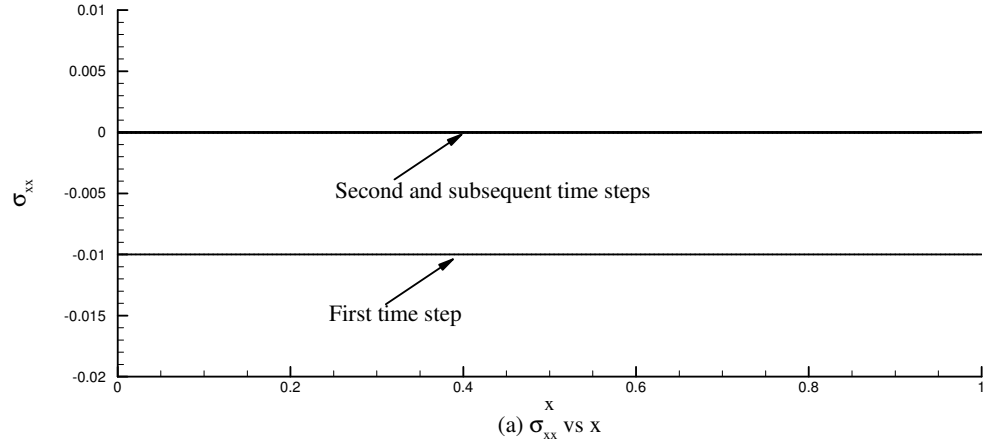

(a) σ_{xx} vs x

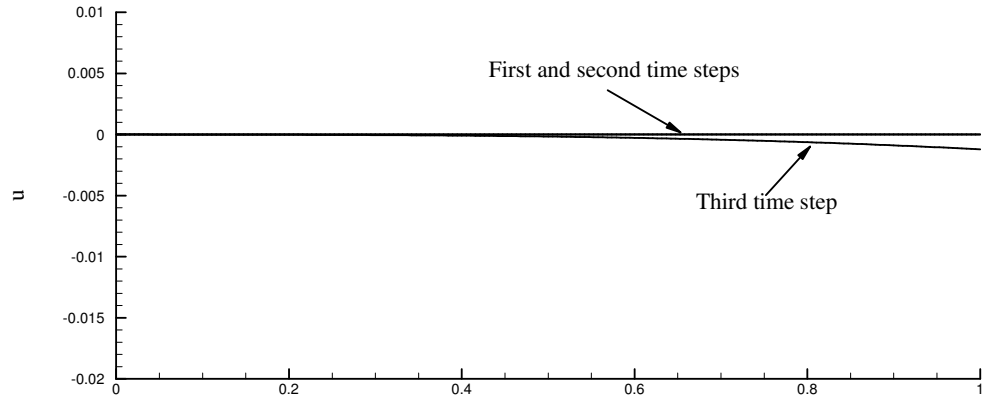

(b) u vs x

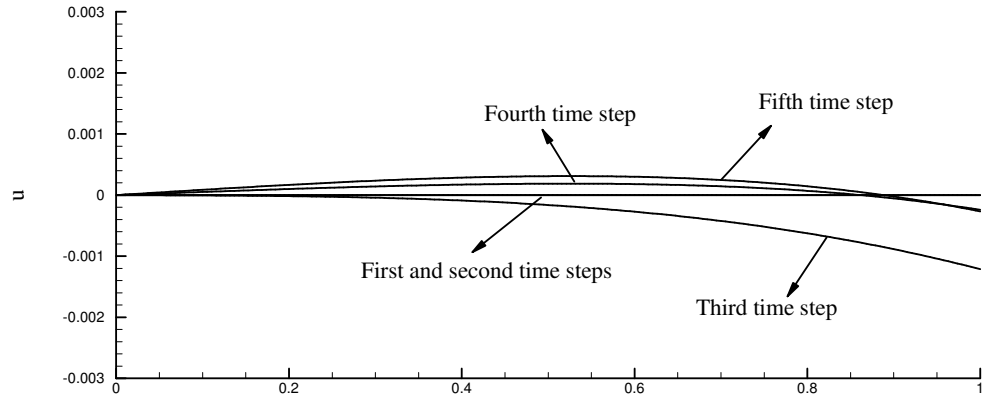

(c) u vs x

Figure 6.2: Solutions for Rate Equilibrium Equation for $\sigma_{xx} = -.01$, C^{11} and $p = 9$

6.2.2 Model Problem 2

This model problem is constructed using exactly the same principle as used in rate equilibrium equation models i.e. differentiation of a conservation law. The purpose of this study is to demonstrate clearly that mathematical models derived using differentiated forms of the GDEs resulting from the conservation laws: (i) have higher order physics that is not present in the GDEs resulting from the conservation laws (ii) require additional boundary conditions (due to higher order partial differential equations (PDEs) than those from the conservation laws) for the uniqueness of the solution. Description of these additional boundary conditions is obviously not possible from the physics of the original problem which is of lower order. Thus uniqueness of the solution from such models can not be ensured.

Consider 1-D steady state convection diffusion equation,

$$\frac{d\phi}{dx} - \frac{1}{Pe}\frac{d^2\phi}{dx^2} = 0 \qquad \forall x \quad \in \quad \Omega_x = (0,1) \tag{6.1}$$

with

$$\phi(0) = 1 \quad \text{and} \quad \phi(1) = 0 \tag{6.2}$$

Equation (6.1) is the one dimensional form of energy equation in the absence of viscous dissipation. Thus, it is derived from the principle of conservation of energy (second law of thermodynamics). Equation (6.1) is a second order ordinary differential equation with two boundary conditions (6.2) and hence has a unique solution. Peclet number Pe is a measure of diffusion or conductivity of the medium.

The analytical or theoretical solution of (6.1) and (6.2) is given by,

$$\phi(x) = \left(\frac{e^{xPe} - e^{Pe}}{1 - e^{Pe}}\right) \tag{6.3}$$

and

$$\frac{d^n\phi}{dx^n} = \left(\frac{(Pe)^n e^{xPe}}{1-Pe}\right) \tag{6.4}$$

A finite element formulation of equation (6.1) is constructed using least squares method. Numerical solutions are computed for a uniform discretization of 20 elements with solutions of class C^1 at p-levels of 7,9, and 11. Figures 6.3 (a) and 6.3 (b) show that plots of $\phi(x)$ versus x and $\frac{d\phi}{dx}$ versus x and a comparison with the theoretical solutions (figure 6.3). Excellent agreement is obtained between the two. Based on references [20–25, 36], we differentiate (6.1) with respect to x to obtain,

$$\frac{d^2\phi}{dx^2} - \frac{1}{Pe}\frac{d^3\phi}{dx^3} = 0 \quad \forall x \quad \in \quad \Omega = (0,1) \tag{6.5}$$

with

$$\phi(0) = 1 \quad \text{and} \quad \phi(1) = 0 \tag{6.6}$$

We now consider (6.5) instead of (6.1) but with the same two boundary conditions (6.6) (as in (6.2)). A solution of (6.5) and (6.6) is non-unique due to the fact that we have a third order differential equations but only two boundary conditions. The physics of the problem in (6.1) and (6.2) has no more information on ϕ at the boundaries then the state in (6.2). Thus an additional boundary condition is not possible (at least based on physics). We note that (6.1) is a conservation law with second order physics (meaning up to second order derivatives of ϕ) whereas (6.5) has third order physics that conservation laws do not recognize. Thus (6.5) is not a description of the 1-D energy equation in the absence of viscous dissipation. When (6.1) is satisfied i.e. for a ϕ that satisfies (6.1) $\forall x \in \Omega_x = (0,1)$, (6.5) also holds. That is a solution of (6.1) and (6.2) is also a solution of (6.5) and (6.6) but a solution of (6.5) (if obtainable) may or may not be a solution of (6.1) and (6.2).

We present numerical studies to further illustrate these points. A least squares formulation

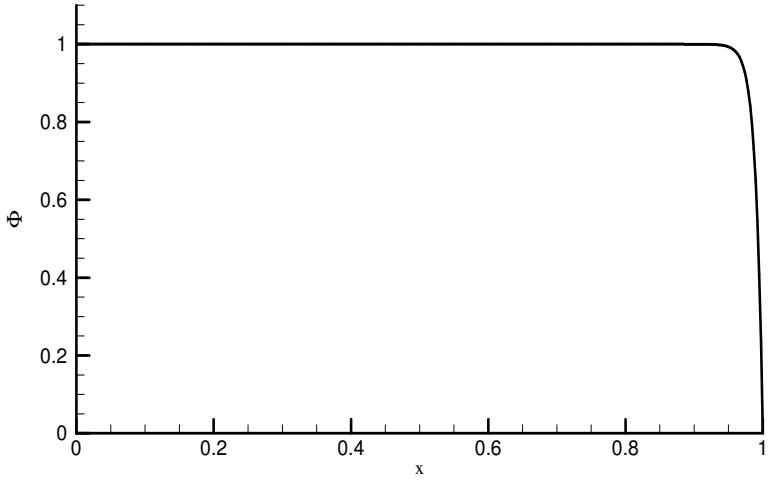

(a) Φ vs x for *p*=7,9,11 and theoretical solution

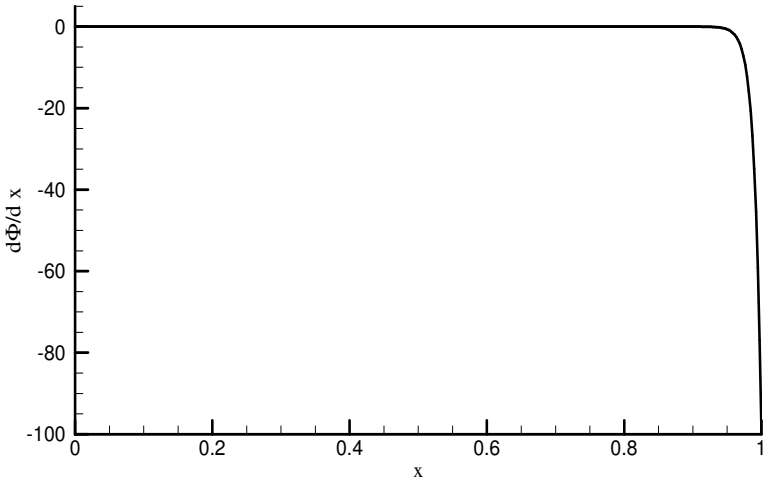

(b) dΦ/dx vs x for *p*=7,9,11 and theoretical solution

Figure 6.3: 1-D Convection-Diffusion Equation : $Pe = 100$: Comparison of Theoretical Solution and LSP Solution of Class C^1 for $p = 7, 9, 11$

of (6.5) is constructed. Numerical solutions are computed using a uniform discretization of 20 elements (same as used for (6.1) and (6.2)) with p-level of 9 and solution class C^1 for the following sets of boundary conditions.

$$\begin{aligned}
&\text{case (a):} \quad \phi(0) = 1 \quad ; \quad \phi(1) = 0 \\
&\text{case (b):} \quad \phi(0) = 1 \quad ; \quad \phi(1) = 0 \quad ; \quad \left.\frac{d\phi}{dx}\right|_{x=0} = 0 \qquad \text{additional BC} \\
&\text{case (c):} \quad \phi(0) = 1 \quad ; \quad \phi(1) = 0 \quad ; \quad \left.\frac{d\phi}{dx}\right|_{x=1} = -100 \qquad \text{additional BC}
\end{aligned}$$

The numerically computed solutions are shown in figures 6.4 and 6.5.

Remarks

(1) For all choices of boundary conditions, the numerically computed solutions are spurious.

(2) Additional boundary conditions used for cases (b) and (c) are obviously not based on physics and hence, are no help either.

(3) For such simple ordinary PDEs (based on a single conservation law) we clearly observe the lack of validity of the mathematical model utilizing differentiated form of the governing differential equation resulting from the conservation law. Non-uniqueness of the solution if such mathematical model is not surprising due to the fact that their derivation or development has no mathematical or physical basis.

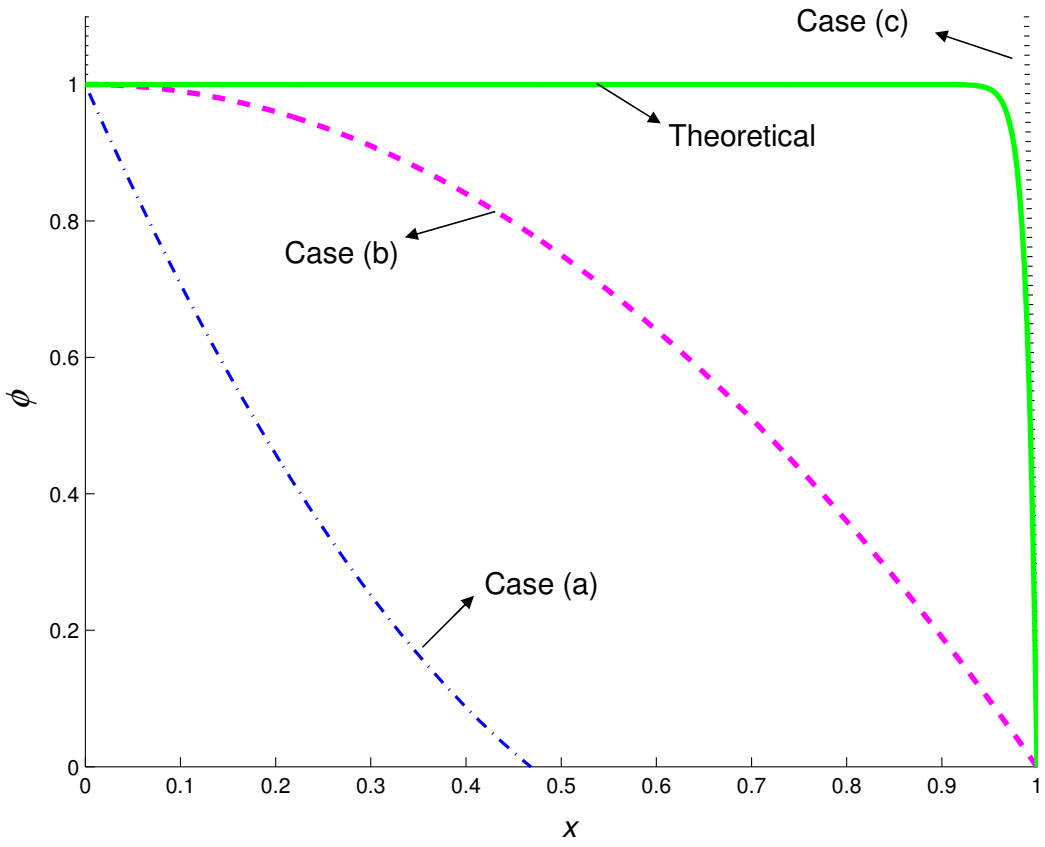

Figure 6.4: 1-D Convection-Diffusion expanded view, $Pe = 100$

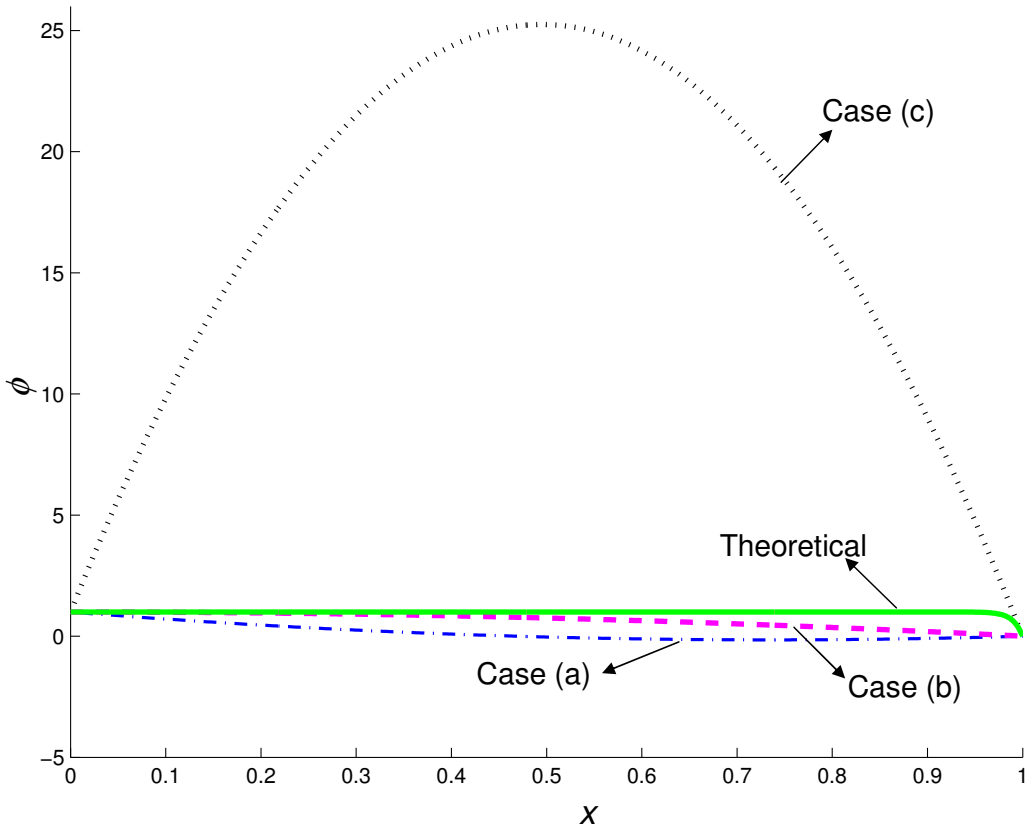

Figure 6.5: 1-D Convection-Diffusion full view, $Pe = 100$

6.3 Investigation of Rate Constitutive Equations: 1-D Axial Wave Propagation

In this section we consider 1-D axial stress wave propagation problem (model problem 3). The model problem consists of a rod of uniform cross-section and constant material properties. The length of the rod is L (figure 6.6). The rod is assumed completely fixed at left end $(x = 0)$ and the right end $(x = L)$ is subjected to a compressive axial stress pulse of duration $2\Delta t$ and maximum magnitude of σ_{xx} at $t = \Delta t$. A ten element uniform spatial discretization is considered giving a space-time strip of ten space-time elements. We consider $p_\xi = p_\eta = p = 9$ and local approximation of class $C^{11}({}^n\bar{\Omega}^e_{xt})$ in space and time.

Using this model problem, we investigate the behaviors of various rate constitutive equations. In the literature, Jaumann rate constitutive equations are dominantly used even though it is well known that these constitutive equations provide non-physical oscillatory response for simple shear problems [39, 40]. It is obvious that for a fixed $\mathbb{D}$ corresponding to same material properties, different rate constitutive equations will produce different response [28, 30, 31] that may be dependent on the magnitude of σ_{xx} as well. Atluri [28] suggested that by adding additional terms to the constitutive equations, one can get same behaviors. In the work considered here, we will not pursue this approach, instead we consider same material tensor $\mathbb{D}$ for all rate constitutive equations to study in 1-D elastic stress wave propagation problems for progressively increasing magnitude of σ_{xx} (figure 6.6). We consider upper Convected, lower Convected, Jaumann and Truesdell rate constitutive equations. For each rate constitutive model, time evolution is computed for the model problem shown in figure 6.6 using σ_{xx}, a pulse of duration $2\Delta t$ with maximum magnitudes of (say $(\sigma_{xx})_{\text{max}}$) -0.01,-0.1, and -0.3.

Figures 6.7 - 6.9 show time evolution of stress σ_{xx} and velocity u for the three different magnitudes of $(\sigma_{xx})_{\text{max}}$ using upper Convected rate constitutive model. In all cases wave propagation, reflection and propagation of the reflected waves are simulated free of oscillations. The wave shapes (magnitude and base) are preserved. From figures 6.7 (b) and 6.8 (b) we observe that maximum magnitudes of the reflected waves is $2(\sigma_{xx})_{\text{max}}$. For $(\sigma_{xx})_{\text{max}} = -0.01$ and

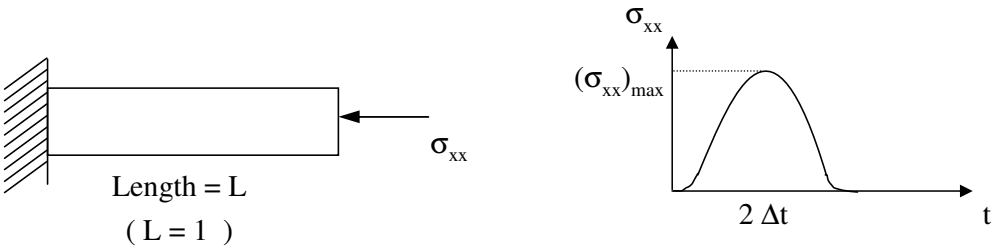

$E = 1\ ,\ \rho = 1\ ,\ A = 1$

$\Delta t = 0.1$

$p_\xi = p_\zeta = p = 9$

10 element uniform mesh

Solution of class C^{11} in space and time

Figure 6.6: 1-D Elastic Wave Propagation : Model Problem 3

$(\sigma_{xx})_{\text{max}} = -0.1$, the values of $|g|_{\text{max}}$ and least squares functional, ${}^{n}I$, are of the order of $O(10^{-7})$ and $O(10^{-8})$ respectively. This indicates good convergence of Newton's method with line search and accuracy of 1-D wave propagation simulations. In case of $(\sigma_{xx})_{\text{max}} = -0.3$, we note from figure 6.9 (b) that $2(\sigma_{xx})_{\text{max}}$ is not obtained. This is primarily due to the fact that increasing $(\sigma_{xx})_{\text{max}}$ with same Δt steepens the wave for which the discretization and p-level is not adequate to simulate the wave reflection process. However, upon further evolution the original wave shape is recovered. Furthermore, the values of $|g|_{\text{max}}$ and least square functional ${}^{n}I$ are of the order of $O(10^{-6})$ and $O(10^{-6})$ respectively for this case. Velocity pulse for all values of $(\sigma_{xx})_{\text{max}}$ maintains amplitude and base during the evolution. Upon reflection the velocity pulse changes sign as expected.

Similar results for lower Convected rate constitutive model are shown in figures 6.10 - 6.12. For $(\sigma_{xx})_{\text{max}} = -0.01$ (figure 6.10), we observe correct simulation of the 1-D elastic wave propagations for σ_{xx} and u. The values of $|g|_{\text{max}}$ and least square functional, ${}^{n}I$, are of the order of $O(10^{-7})$ and $O(10^{-8})$ respectively. However for $(\sigma_{xx})_{\text{max}} = -0.1$ and $(\sigma_{xx})_{\text{max}} = -0.3$ (figures 6.11 and 6.12), the pulse magnitude and base deteriorate upon evolution and result in failure of computations after a few time increments and $|g|_{\text{max}}$ and ${}^{n}I$ are of the order of $O(10^{-6})$ and $O(10^{-4})$ respectively.

Results shown in figures 6.13 - 6.15 for Jaumann rate constitutive equations and those in figures 6.16 - 6.18 for Truesdell rate constitutive equations show behaviors similar to lower Convected. For $(\sigma_{xx})_{\text{max}} = -0.01$, the evolution of σ_{xx} and u are good but result in total failure for $(\sigma_{xx})_{\text{max}} = -0.1$ and $(\sigma_{xx})_{\text{max}} = -0.3$.

From this simple study we note that only upper Convected rate constitutive equations preserve the wave during the evolution for progressively increasing $(\sigma_{xx})_{\text{max}}$ and the other three rate constitutive equation show breakdown for $(\sigma_{xx})_{\text{max}} = -0.1$ and $(\sigma_{xx})_{\text{max}} = -0.3$. Moreover, similar studies for model problem 3 (figure 6.6) are carried out in Lagrangian description using displacements, second Piola-Kirchhoff stress and Green's strain. Comparisons between Lagrangian description and Eulerian description using upper Convected rate constitutive equations for evolution of σ_{xx} and u are given in figure 6.19 and 6.20. From these studies, it is clear

that the results from Lagrangian as well as Eulerian descriptions for 1-D elastic wave propagation agree quite well. The relationship between second Piola-Kirchhoff stress and Cauchy stress is given in 2.17 and is utilized here to transform second Piola-Kirchhoff stress to Cauchy stress. Discrepancy between Eulerian and Lagrangian velocities is observed in figure 6.20 which is more apparent for higher magnitudes of stresses. This is due to the fact that the material particles are attached to the mesh in Lagrangian description, consequently the velocities represent the velocities of these material particles. However, in Eulerian description, material particles flow through the mesh so velocities are of those particles that occupy the specific grid points.

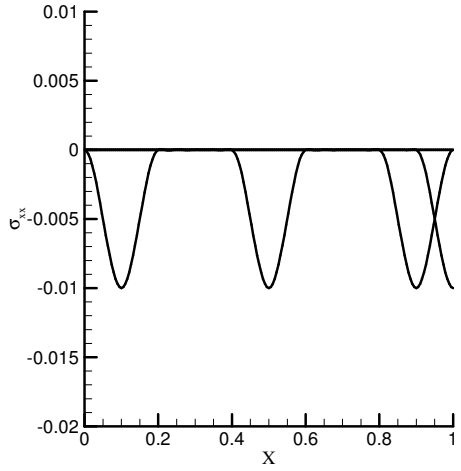

(a) Incident Stress Wave

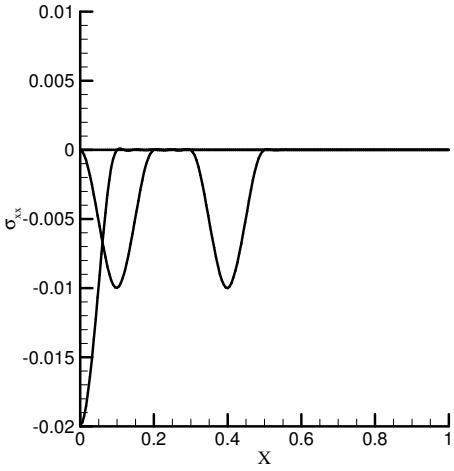

(b) Reflected Stress Wave

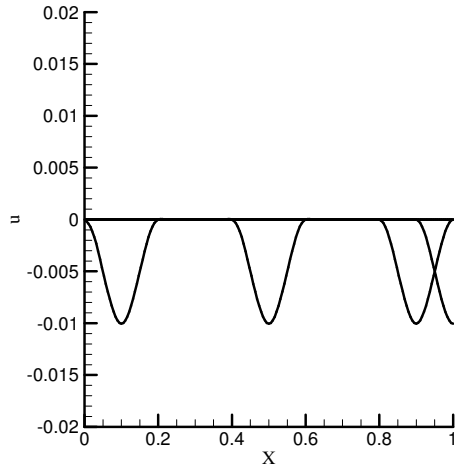

(c) Incident Velocity Wave

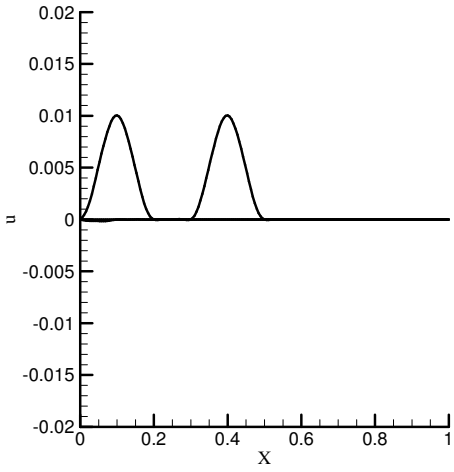

(d) Reflected Velocity Wave

Figure 6.7: 1-D Elastic Wave Propagation, Upper Convected ($\sigma_{xx} = -0.01$)

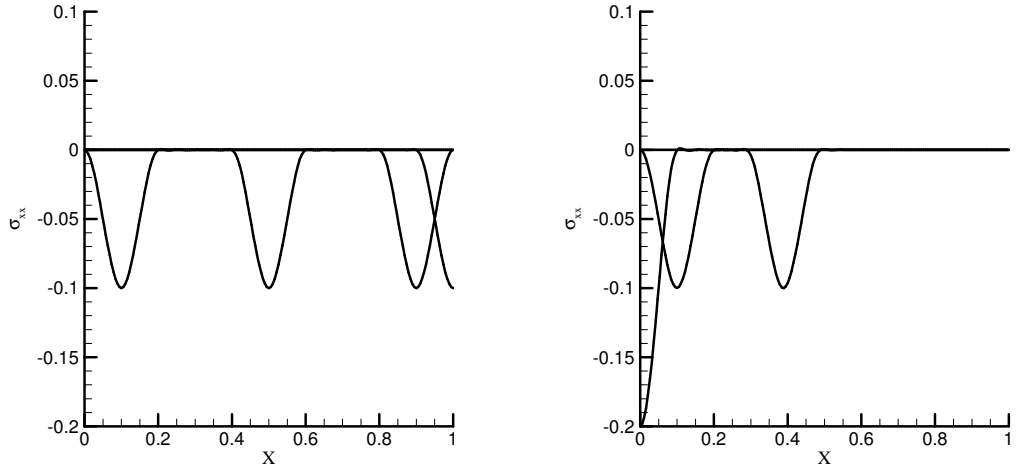

(a) Incident Stress Wave

(b) Reflected Stress Wave

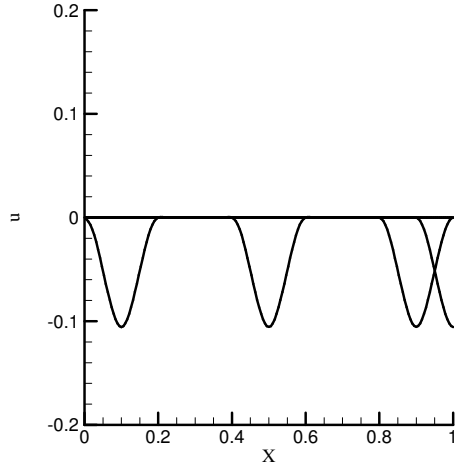

(c) Incident Velocity Wave

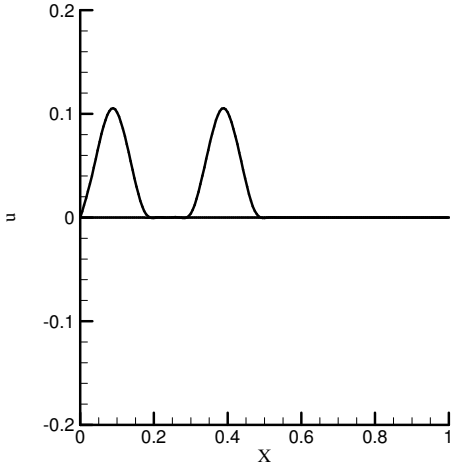

(d) Reflected Velocity Wave

Figure 6.8: 1-D Elastic Wave Propagation, Upper Convected ($\sigma_{xx} = -0.1$)

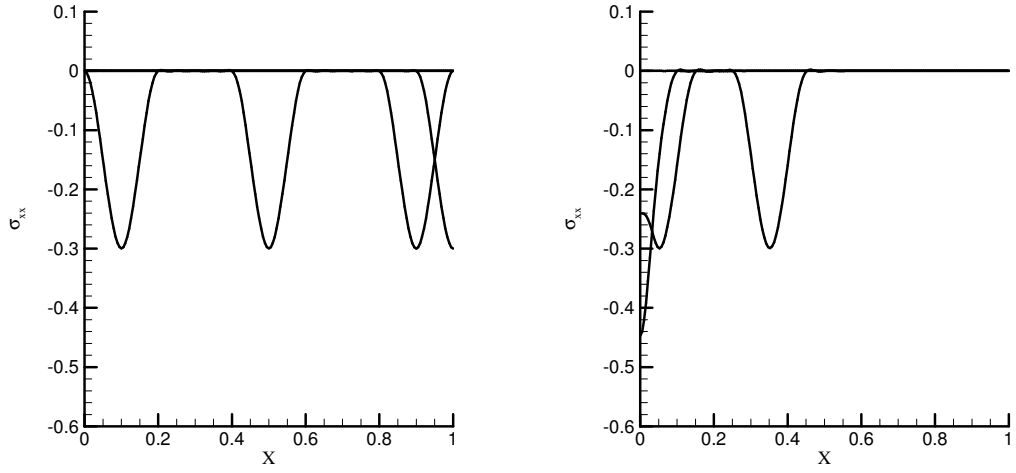

(a) Incident Stress Wave

(b) Reflected Stress Wave

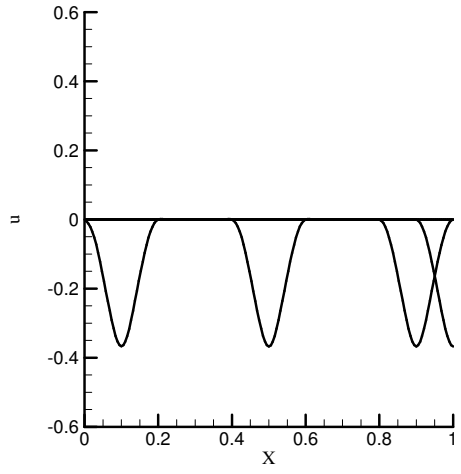

(c) Incident Velocity Wave

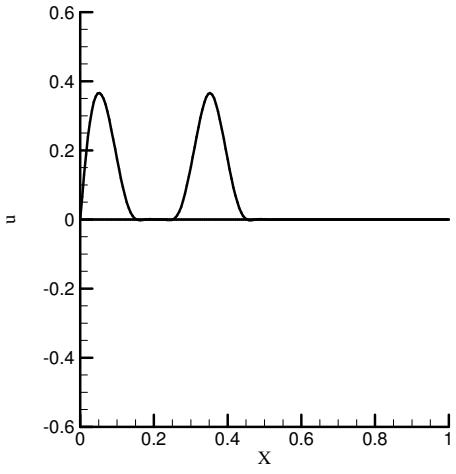

(d) Reflected Velocity Wave

Figure 6.9: 1-D Elastic Wave Propagation, Upper Convected ($\sigma_{xx} = -0.3$)

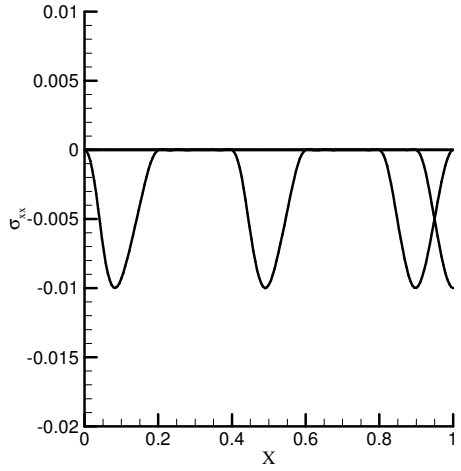

(a) Incident Stress Wave

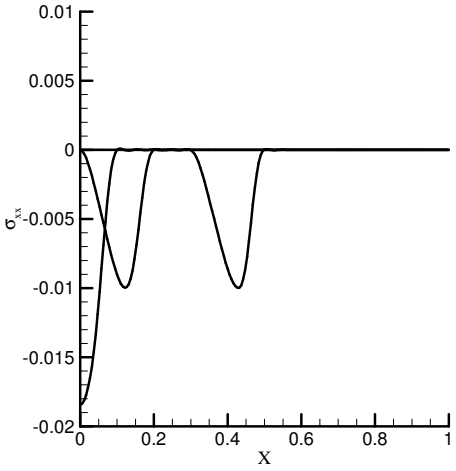

(b) Reflected Stress Wave

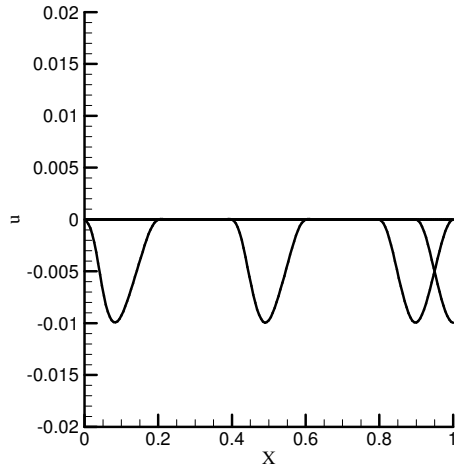

(c) Incident Velocity Wave

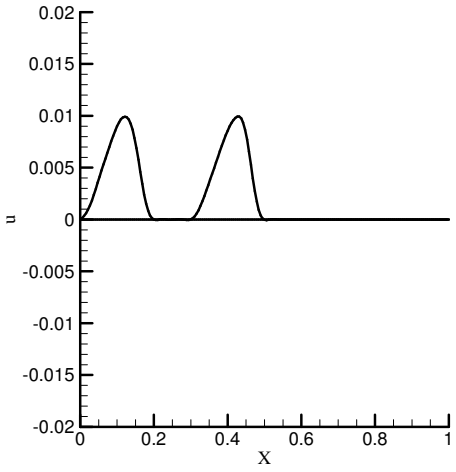

(d) Reflected Velocity Wave

Figure 6.10: 1-D Elastic Wave Propagation, Lower Convected ($\sigma_{xx} = -0.01$)

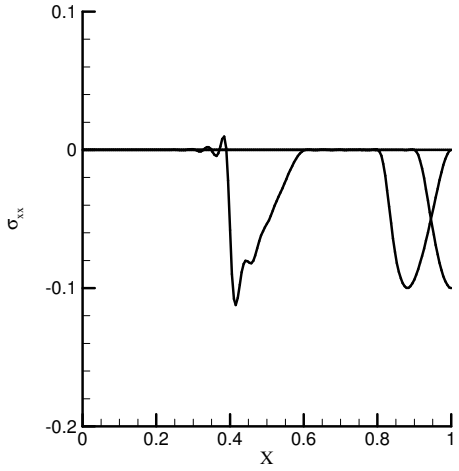

(a) Incident Stress Wave

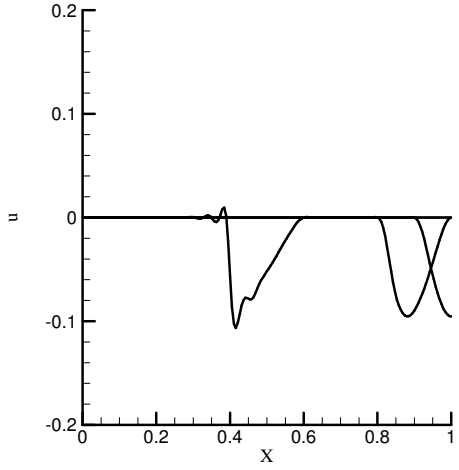

(b) Incident Velocity Wave

Figure 6.11: 1-D Elastic Wave Propagation, Lower Convected ($\sigma_{xx} = -0.1$)

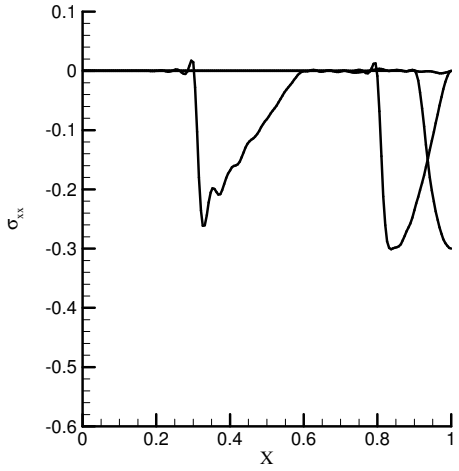

(a) Incident Stress Wave

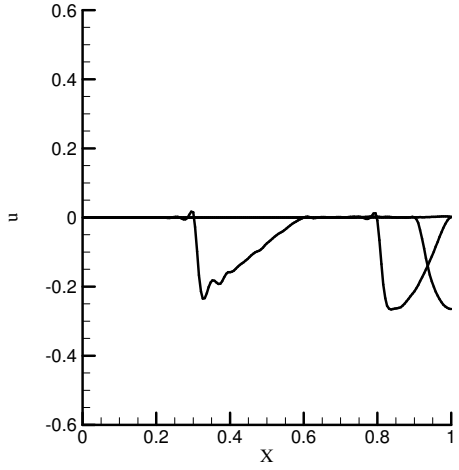

(b) Incident Velocity Wave

Figure 6.12: 1-D Elastic Wave Propagation, Lower Convected ($\sigma_{xx} = -0.3$)

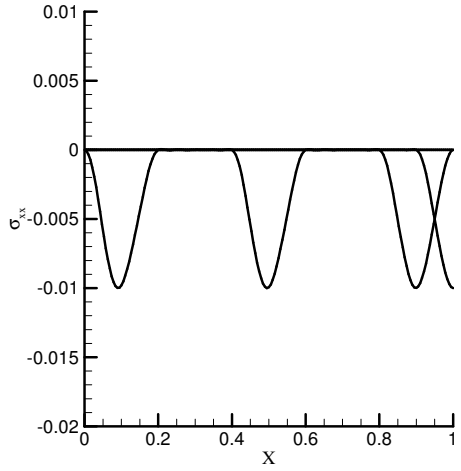

(a) Incident Stress Wave

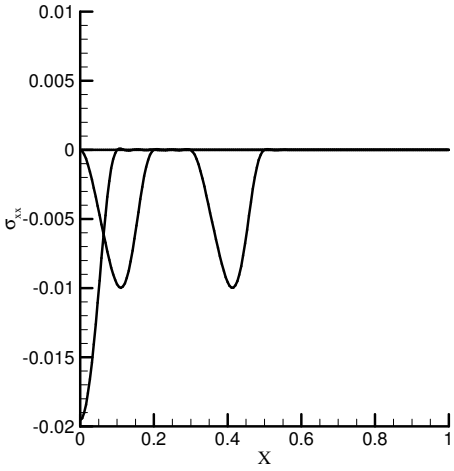

(b) Reflected Stress Wave

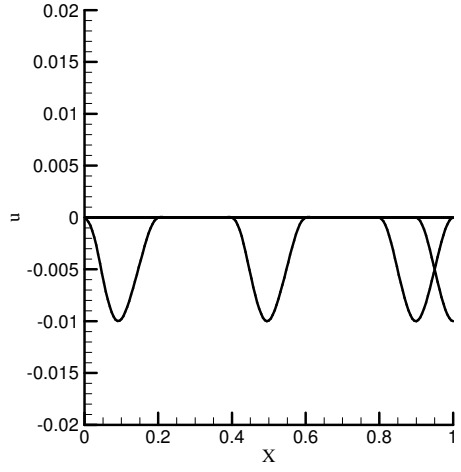

(c) Incident Velocity Wave

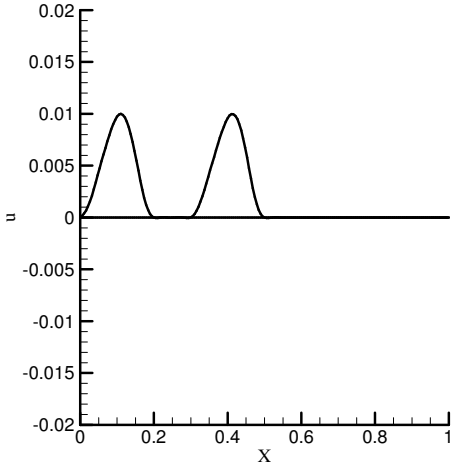

(d) Reflected Velocity Wave

Figure 6.13: 1-D Elastic Wave Propagation, Jaumann ($\sigma_{xx} = -0.01$)

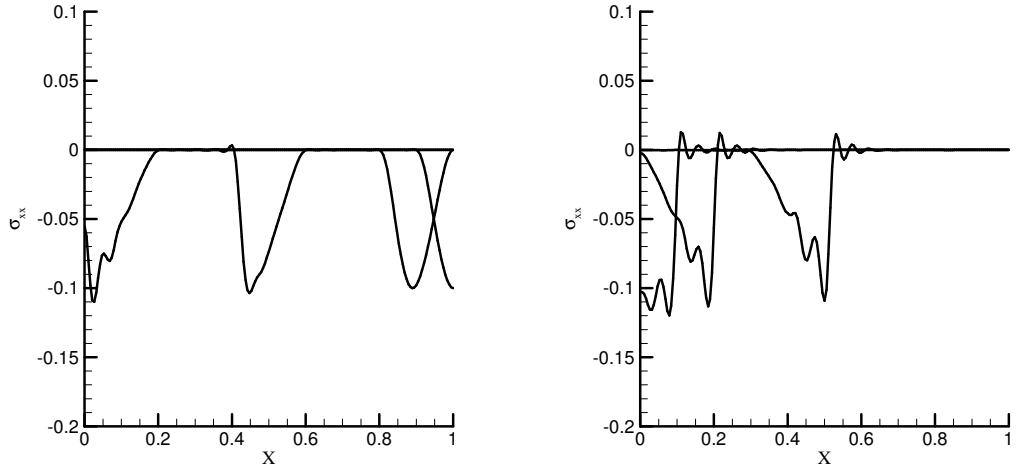

(a) Incident Stress Wave

(b) Reflected Stress Wave

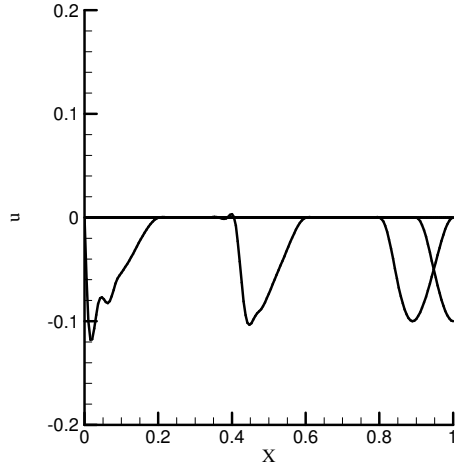

(c) Incident Velocity Wave

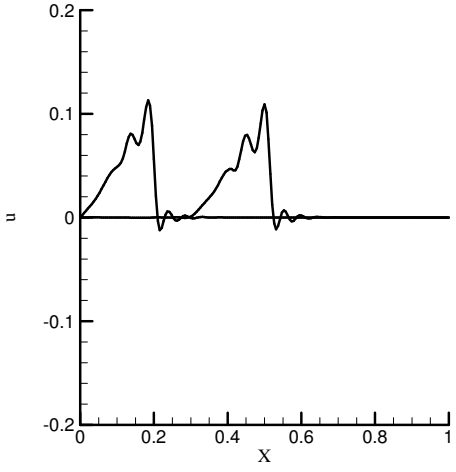

(d) Reflected Velocity Wave

Figure 6.14: 1-D Elastic Wave Propagation, Jaumann ($\sigma_{xx} = -0.1$)

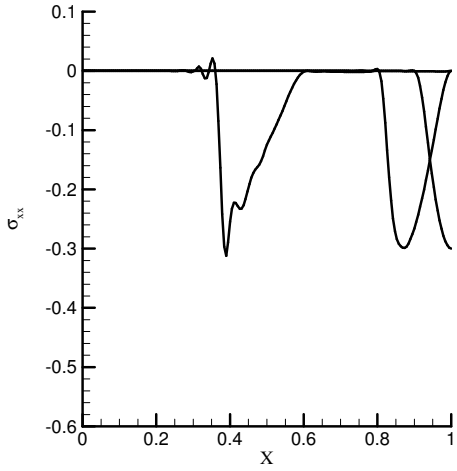

(a) Incident Stress Wave

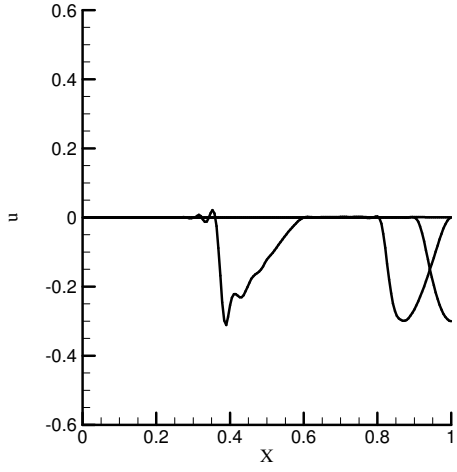

(b) Incident Velocity Wave

Figure 6.15: 1-D Elastic Wave Propagation, Jaumann ($\sigma_{xx} = -0.3$)

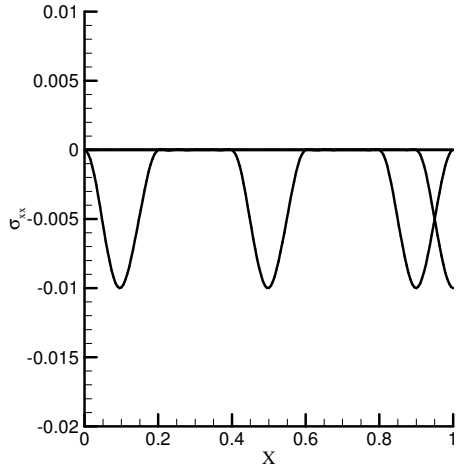

(a) Incident Stress Wave

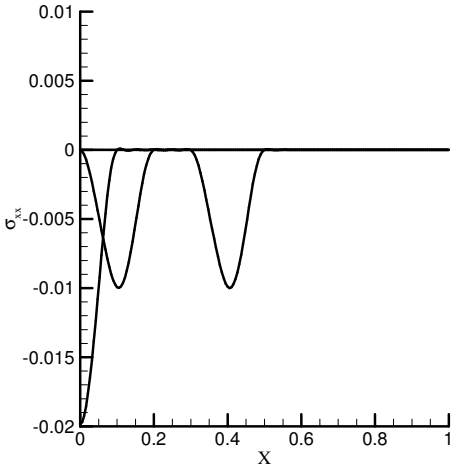

(b) Reflected Stress Wave

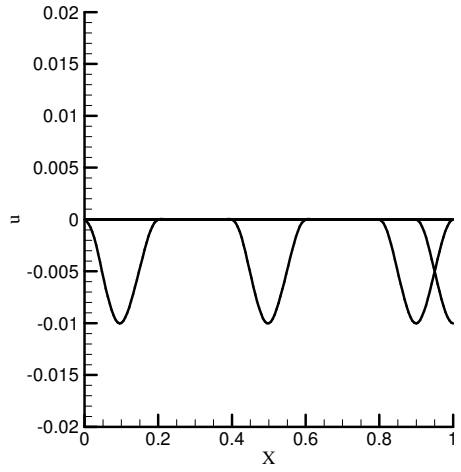

(c) Incident Velocity Wave

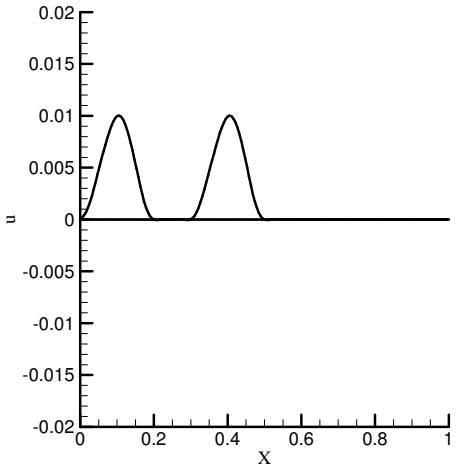

(d) Reflected Velocity Wave

Figure 6.16: 1-D Elastic Wave Propagation, Truesdell ($\sigma_{xx} = -0.01$)

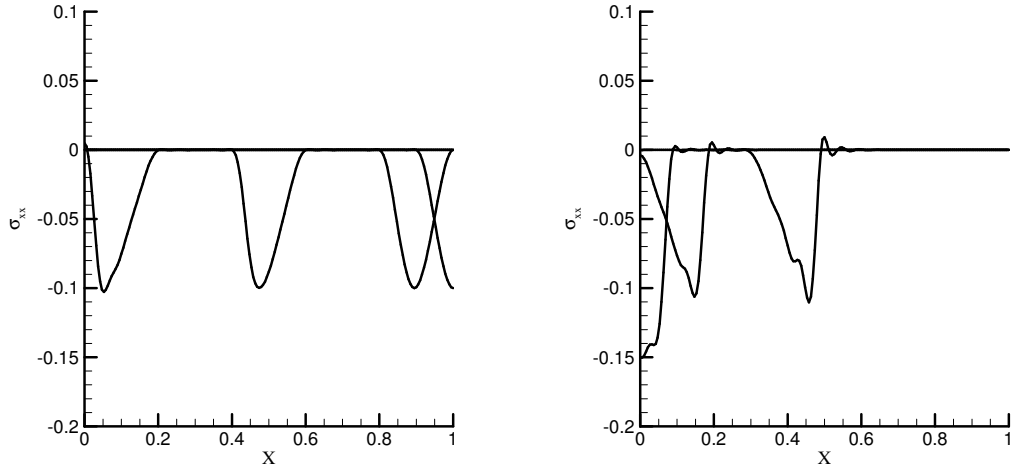

(a) Incident Stress Wave

(b) Reflected Stress Wave

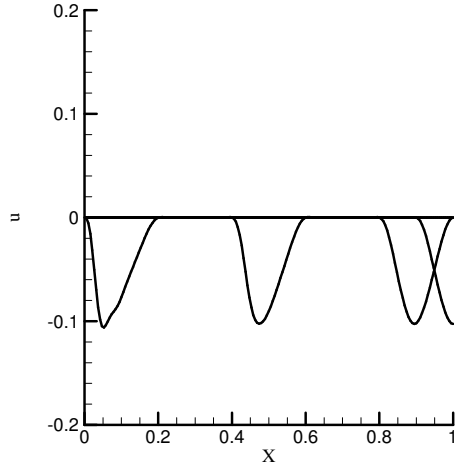

(c) Incident Velocity Wave

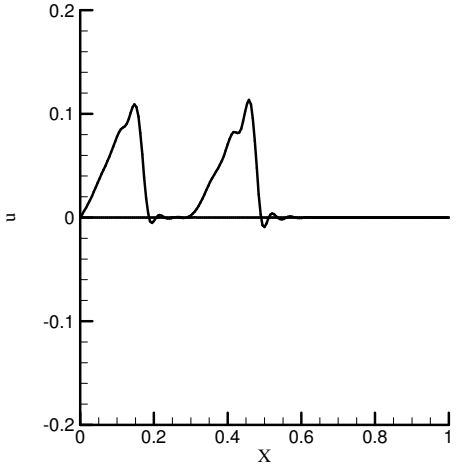

(d) Reflected Velocity Wave

Figure 6.17: 1-D Elastic Wave Propagation, Truesdell ($\sigma_{xx} = -0.1$)

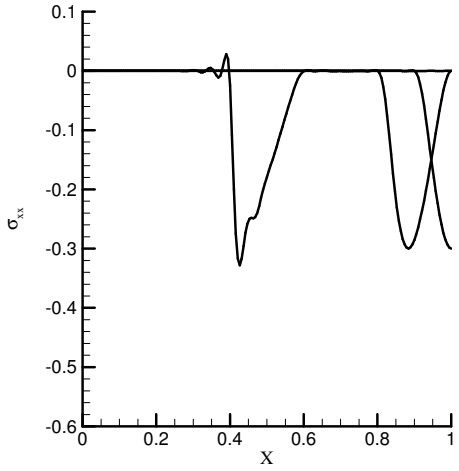

(a) Incident Stress Wave

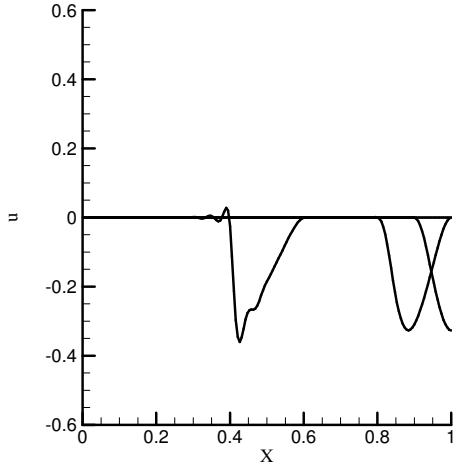

(b) Incident Velocity Wave

Figure 6.18: 1-D Elastic Wave Propagation, Truesdell ($\sigma_{xx} = -0.3$)

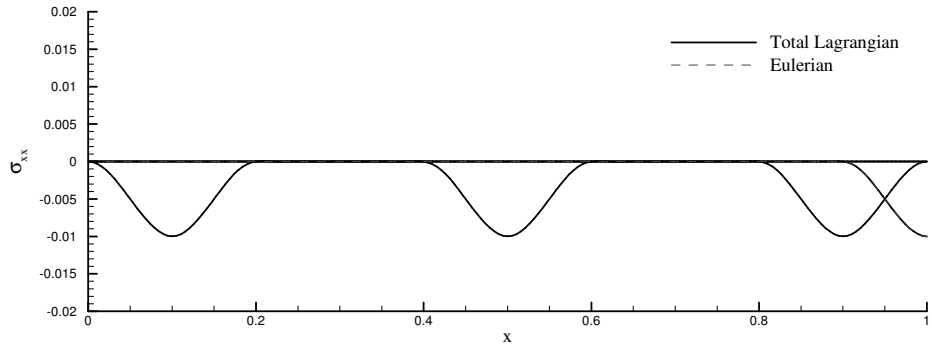

(a) (σ_{xx})= -0.01

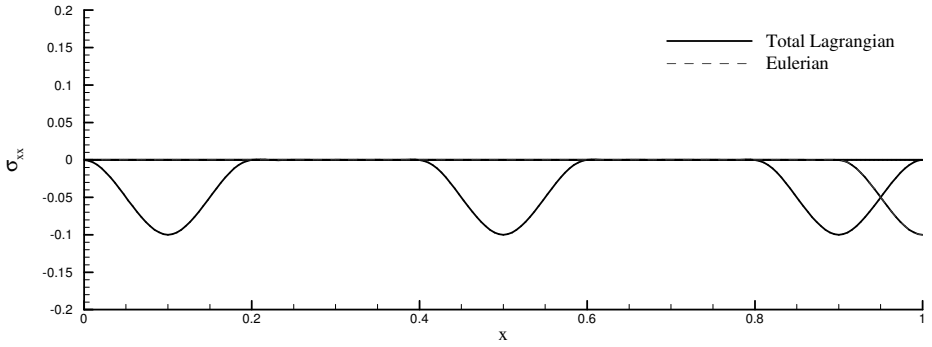

(b) (σ_{xx})= -0.1

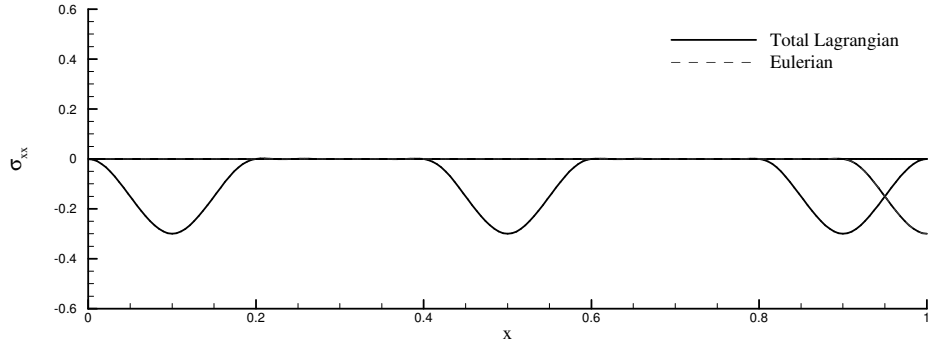

(c) (σ_{xx})= -0.3

Figure 6.19: Comparison of Evolution of σ_{xx} for Total Lagrangian vs Eulerian Description (Upper Convected)

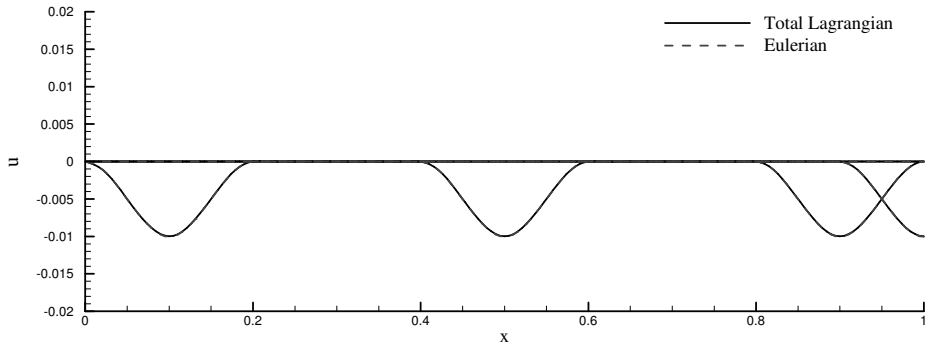

(a) (σ_{xx})= -0.01

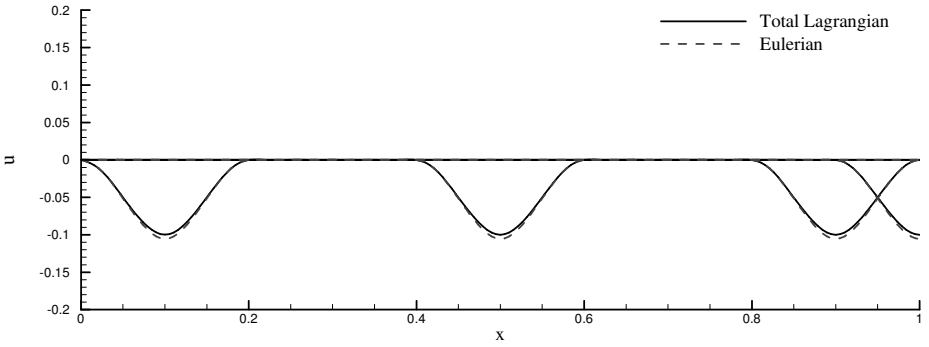

(b) (σ_{xx})= -0.1

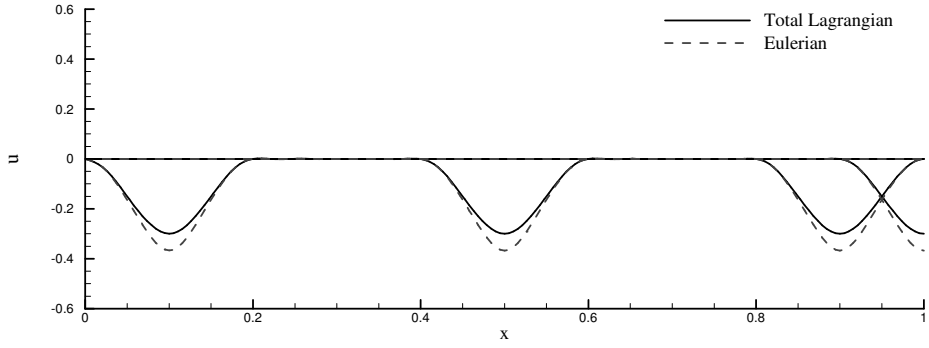

(c) (σ_{xx})= -0.3

Figure 6.20: Comparison of Evolution of u for Total Lagrangian vs Eulerian Description (Upper Convected)

6.4 Model Problem 4

We consider square panel (1×1) in plane strain subjected to uniform tension (figure 6.21). The material properties, choice of reference quantities and the dimensional properties as well as dimensionless parameters are shown in figure 6.21. For the first time step, initial conditions (ICs) are set to be zero for all the variables. The solutions for the current space-time strip will serve as initial conditions for the next time step. Similar to 1-D elastic wave propagation, here also we compare the performances of various rate constitutive equations. Choice of σ_{yy} is critical from 1-D elastic stress wave propagation studies presented in section 6.3. Since for low magnitudes of axial stress all rate constitutive equations yield roughly the same response, in case (a) we choose $\sigma_{yy} = 0.2$ with Poisson's ratio, ν of 0.0, large enough to evaluate the behaviors of different rate constitutive equations for two dimensional elasticity. (For reference, studies for magnitude of $\sigma_{yy} = 0.01$ and $\nu = 0.0$ is given in appendix B)

We consider a space-time slab with 10×10 uniform spatial discretization for an increment of time with p-levels of 3 in spatial directions as well as time and local approximations of class C^{11} in spatial directions and time. For this choice of local approximation, the approximation space is minimally conforming and hence all integrals are Riemann for the space-time slab. We consider two cases

case (a):	Poisson's ratio	$\nu = 0.0$	applied uniform tension	$\sigma_{yy} = 0.2$
case (b):	Poisson's ratio	$\nu = 0.3$	applied uniform tension	$\sigma_{yy} = 0.01$

For each space-time slab, time evolution is computed using $\Delta t = 0.1$. Using all four rate constitutive equations for both case (a) and case (b). The total σ_{yy} is applied in 4 increments of time in a continuous and differentiable manner.

6.4.1 Case (a): Poisson's ratio, $\nu = 0.0$, and applied uniform tension $\sigma_{yy} = 0.2$

In this case the behavior of the plate is purely axial in the y-direction and hence it serves as a good test of the accuracy and performance of the various rate constitutive equations. That is,

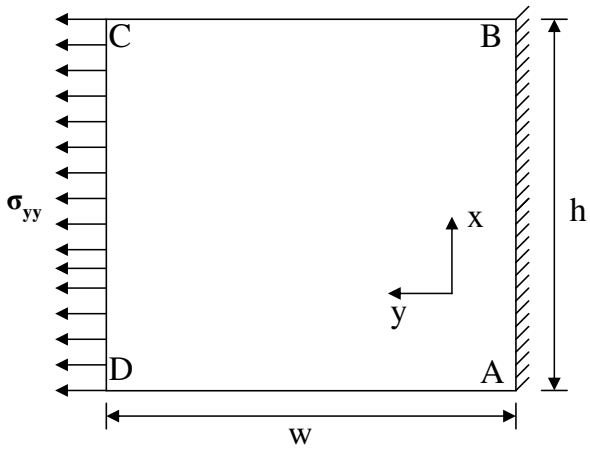

Boundary Conditions :

CD : σ_{yy}= 0.01 or 0.2 ; uniform stress

AD : σ_{xx}= 0 ; τ_{xy}= 0 ; free surface

BC : σ_{xx}= 0 ; τ_{xy} = 0 ; free surface

AB : u = 0 ; v = 0 ; τ_{xy}= 0 ; fix end

Material Properties :

$\hat{\rho} = 7860 \ \ \mathrm{kg/m^3}$

$\hat{E} = 2 \times 10^{11} \ \mathrm{Pa}$

Dimensionless Properties :

$h = 1 \quad ; \ w = 1 \quad ; \ \rho = 1$

$E = 1 \quad ; \ \nu = 0.0 \text{ or } 0.3$

Reference Properties :

$\rho_0 = 7860 \ \mathrm{kg/m^3}$

$E_0 = 2 \times 10^{11} \ \mathrm{Pa}$

$u_0 = 5044.3 \ \mathrm{m/s}$

$\tau_0 = 2 \times 10^{11} \ \mathrm{Pa}$

Figure 6.21: 2-D Elastic Wave Propagation, Model Problem 4 (uniform load) : C^{11} with p-levels of 3 ; 10×10 uniform mesh ; $\Delta t = 0.1$

except σ_{yy} and v all other stresses and u are zero.

(a_1) Upper Convected Rate Constitutive Equations

Figures 6.22 - 6.24 show evolution of stress σ_{yy}. Evolution of velocity v is shown in figures 6.25 - 6.27. The evolution of stress σ_{yy} and velocity v are oscillation free. Stress wave propagation and reflection are simulated correctly. At the reflection, the stress σ_{yy} doubles in magnitudes and upon further evolution regains its applied amplitude.

(a_2) Lower Convected Rate Constitutive Equations

Figures 6.28 - 6.30 and figures 6.31 and 6.33 show evolution of σ_{yy} and v for lower Convected rate constitutive equations. From 6.31 - 6.33, we clearly note that evolution and propagation of σ_{yy} is diffused. The reflection of the stress wave is non-physical. The evolution and propagation of velocity front is non-physical as well.

(a_3) Jaumann Rate Constitutive Equations

The evolutions of σ_{yy} and v shown in figures 6.34 - 6.36 and figures 6.37 - 6.39 show these to be better than those from the lower Convected rate constitutive equations, but as evolution proceeds, the stress fronts begin to diffuse. Highly diffused reflected stress waves are quite obvious in Figure 6.36. The velocity front evolution and propagation is much better than the stress wave before the reflection but it too becomes highly diffused upon reflection.

(a_4) Truesdell Rate Constitutive Equations

Figures 6.40 - 6.42 and figures 6.43 and 6.45 show evolutions and propagations of σ_{yy} and v for Truesdell rate constitutive equations. From Figures 6.40 - 6.42, we note that σ_{yy} fronts appear reasonable. Upon closer examination and a comparison with figures 6.22 - 6.24 and 6.25 - 6.27 (for upper Convected rate constitutive equations) shows that upon reflection the stress wave speed is lower in this case even though the profiles of the fronts are maintained reasonably well.

Except upper Convected rate constitutive equations, all others produce non-physical evolutions of σ_{yy} and v.

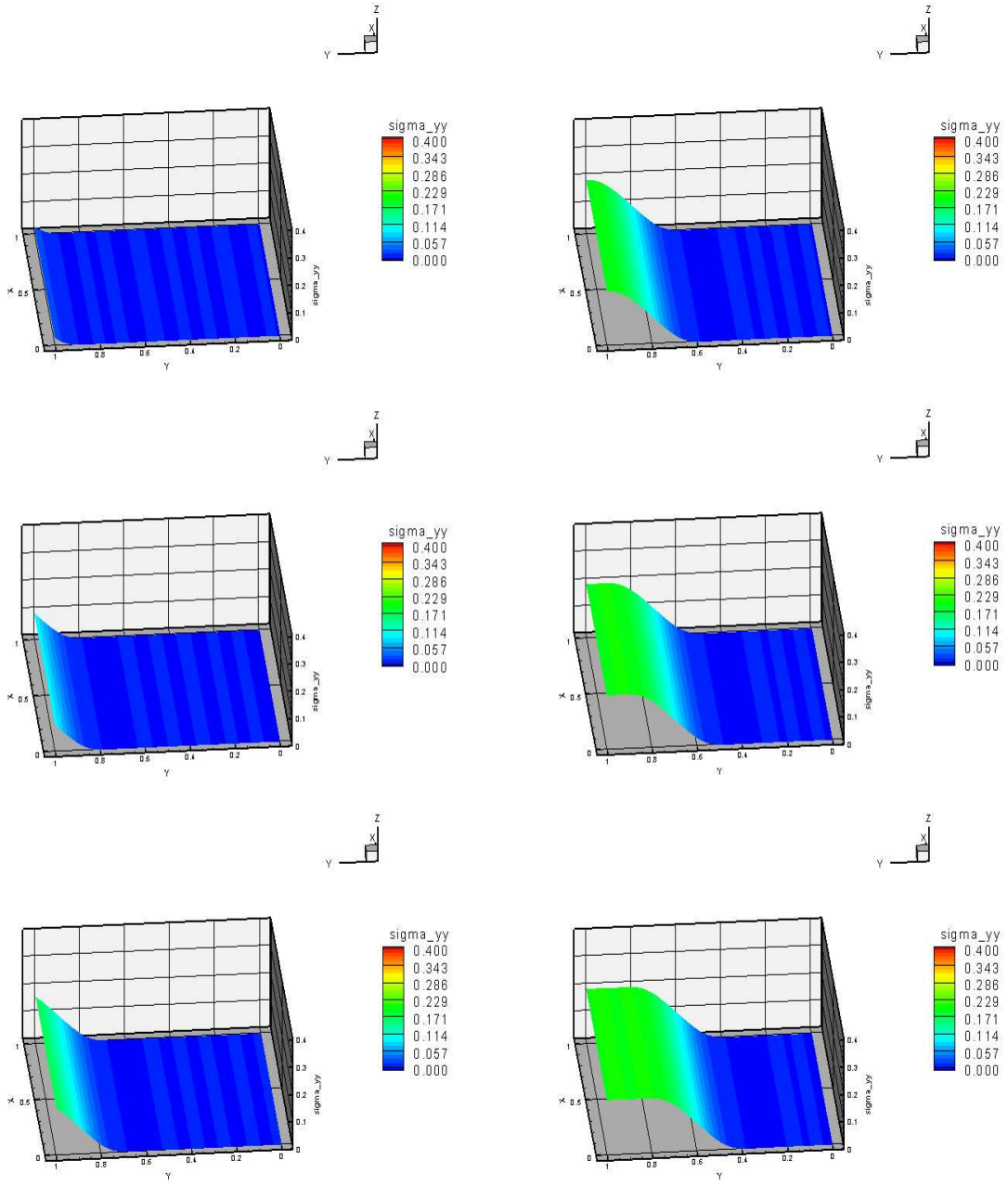

Figure 6.22: Model Problem 4, case (a_1) : $\nu = 0.0$ and $\sigma_{yy} = 0.2$: Evolution of σ_{yy} : Upper Convected Stress Rate - Time steps from 1^{st} to 6^{th}

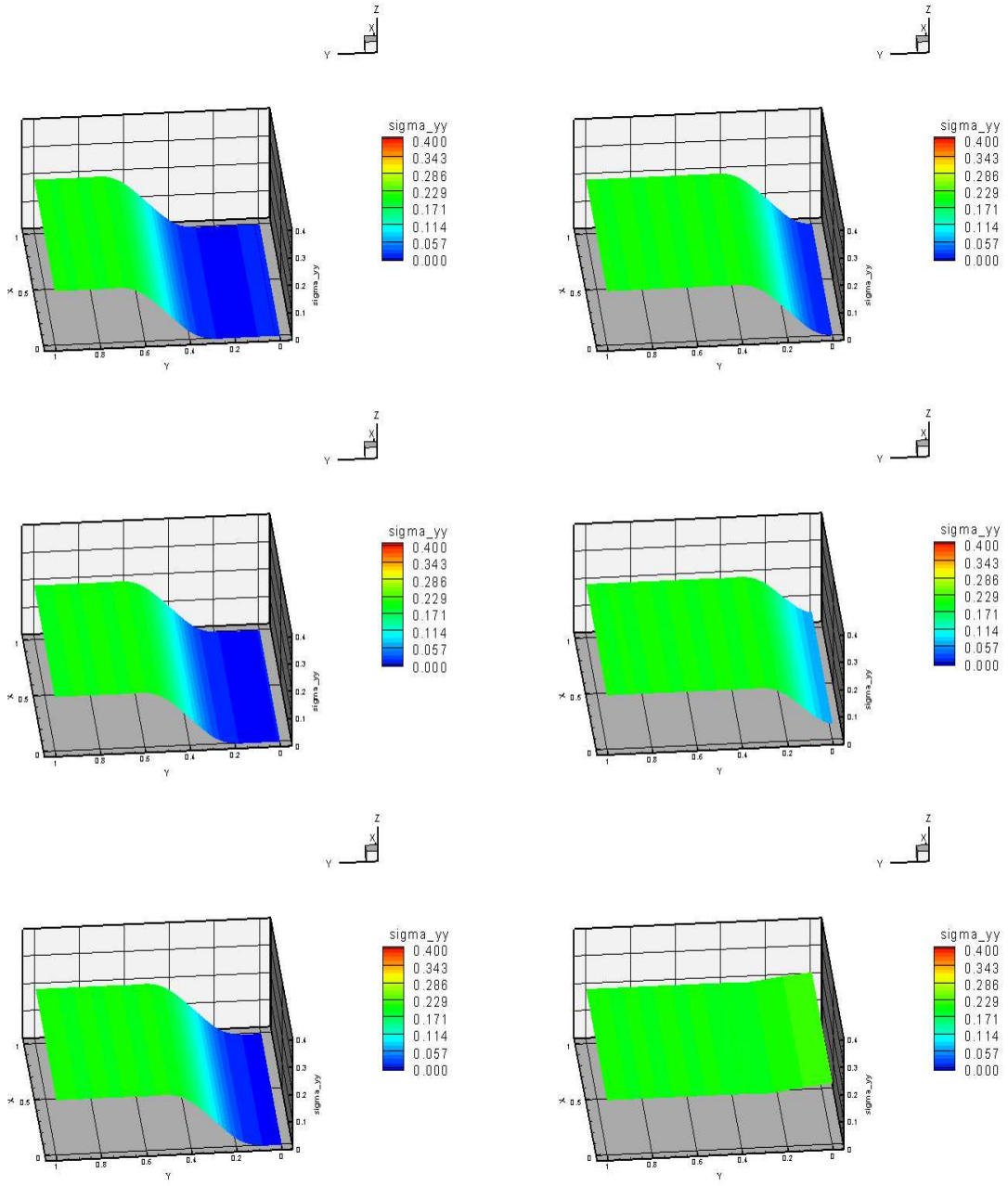

Figure 6.23: Model Problem 4, case (a_1) : $\nu = 0.0$ and $\sigma_{yy} = 0.2$: Evolution of σ_{yy} : Upper Convected Stress Rate - Time steps from 7^{th} to 12^{th}

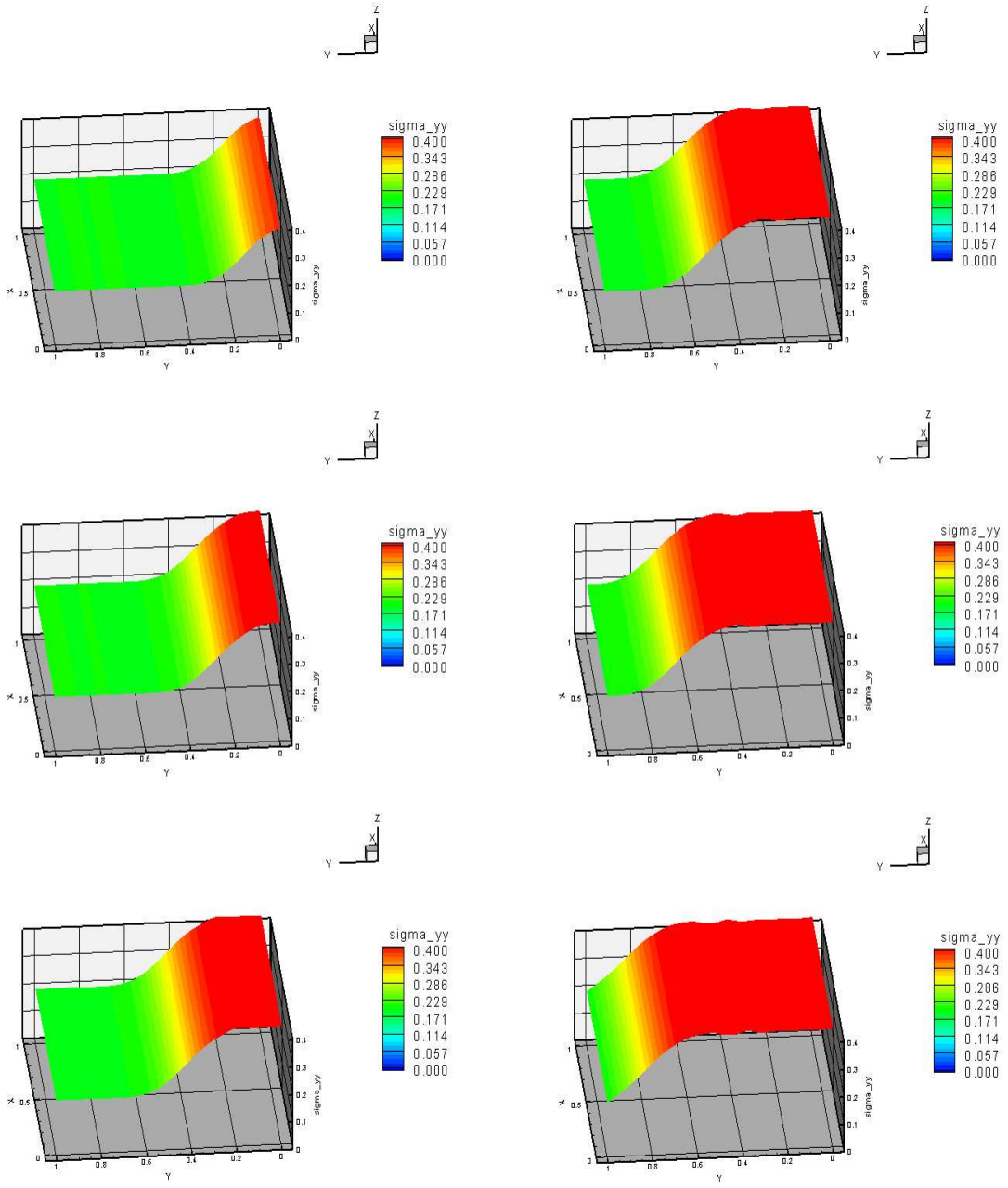

Figure 6.24: Model Problem 4, case (a_1) : $\nu = 0.0$ and $\sigma_{yy} = 0.2$: Evolution of σ_{yy} : Upper Convected Stress Rate - Time steps from 13^{th} to 18^{th}

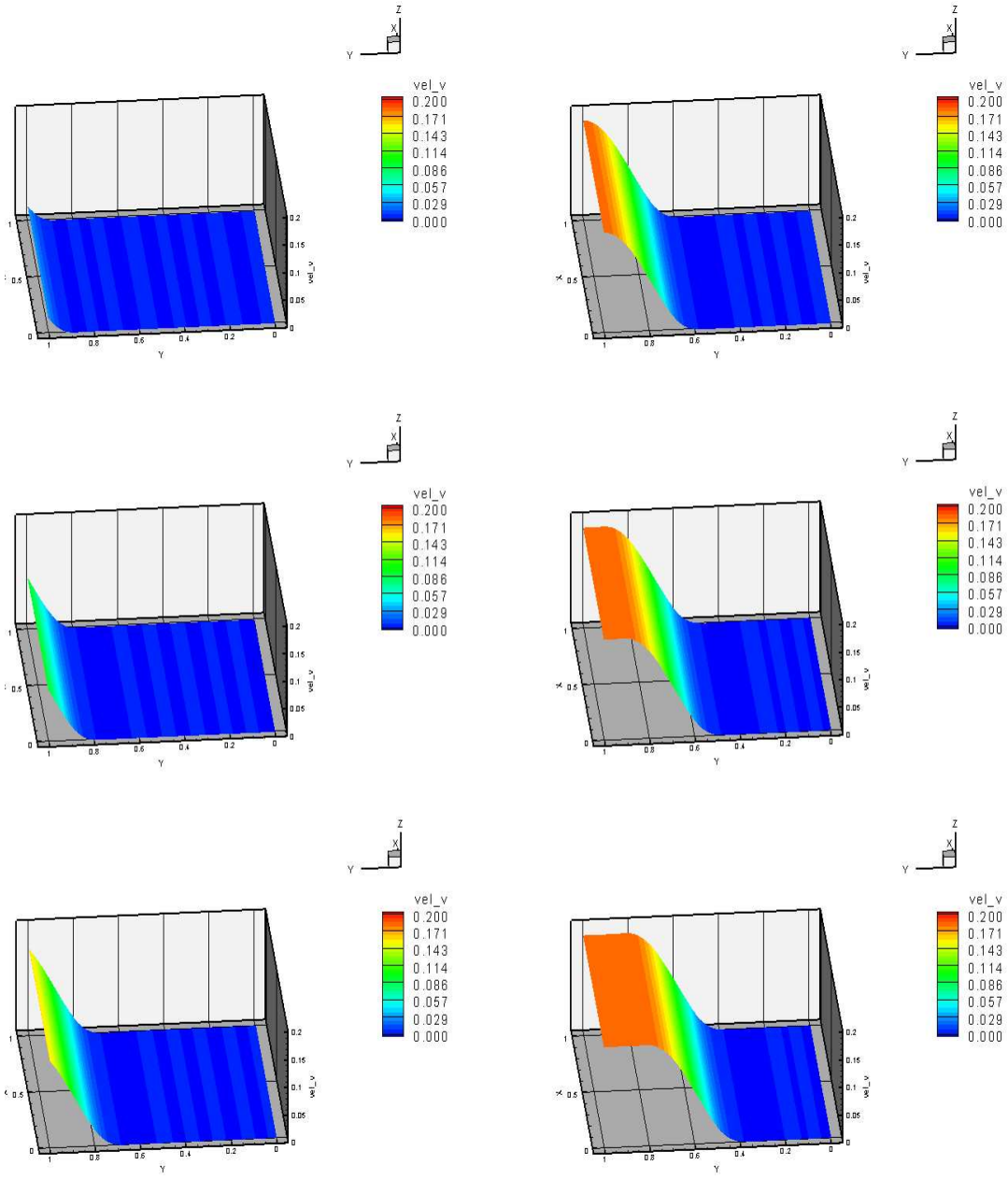

Figure 6.25: Model Problem 4, case (a_1) : $\nu = 0.0$ and $\sigma_{yy} = 0.2$: Evolution of v : Upper Convected Stress Rate - Time steps from 1^{st} to 6^{th}

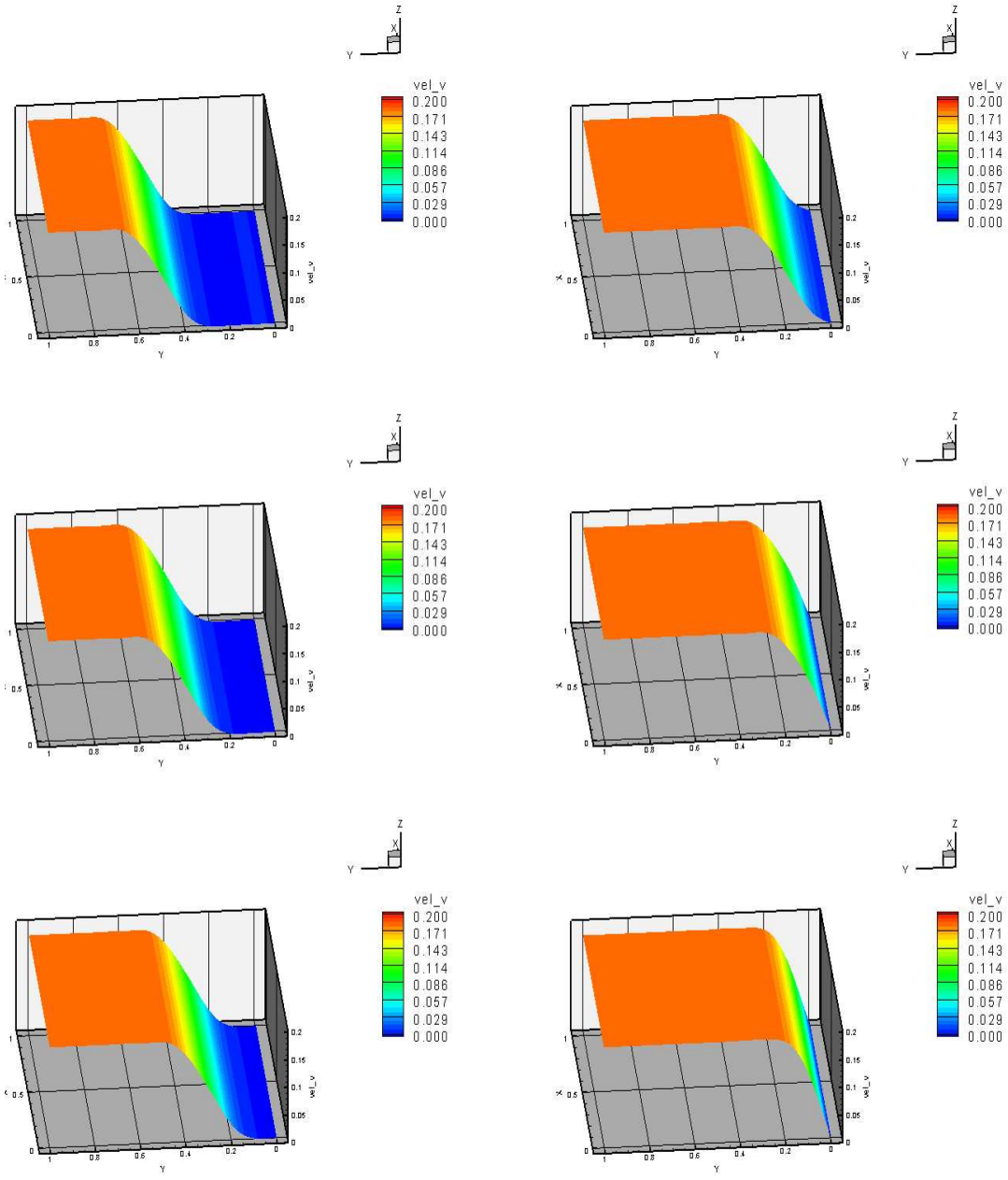

Figure 6.26: Model Problem 4, case (a_1) : $\nu = 0.0$ and $\sigma_{yy} = 0.2$: Evolution of v : Upper Convected Stress Rate - Time steps from 7^{th} to 12^{th}

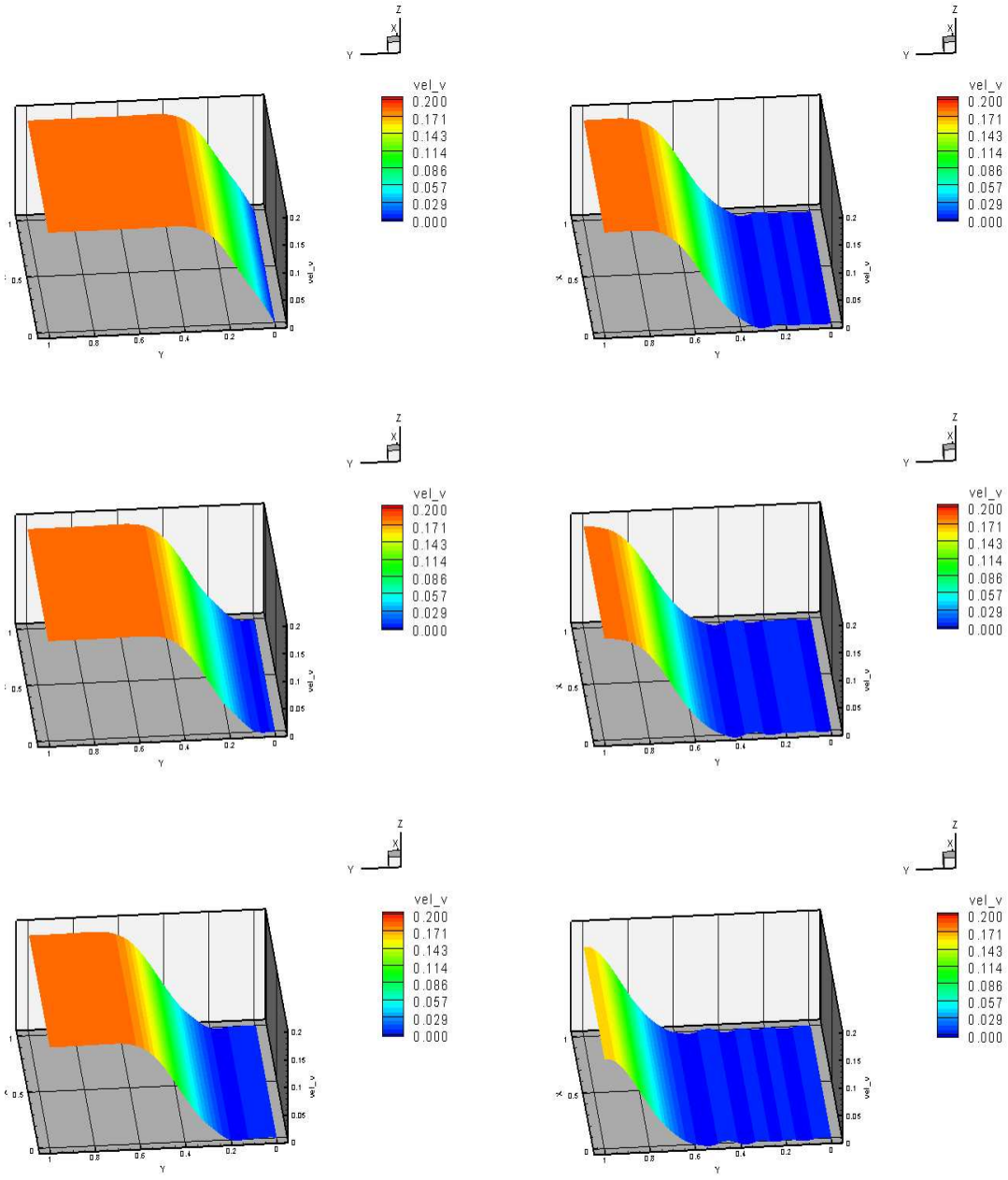

Figure 6.27: Model Problem 4, case (a_1) : $\nu = 0.0$ and $\sigma_{yy} = 0.2$: Evolution of v : Upper Convected Stress Rate - Time steps from 13^{th} to 18^{th}

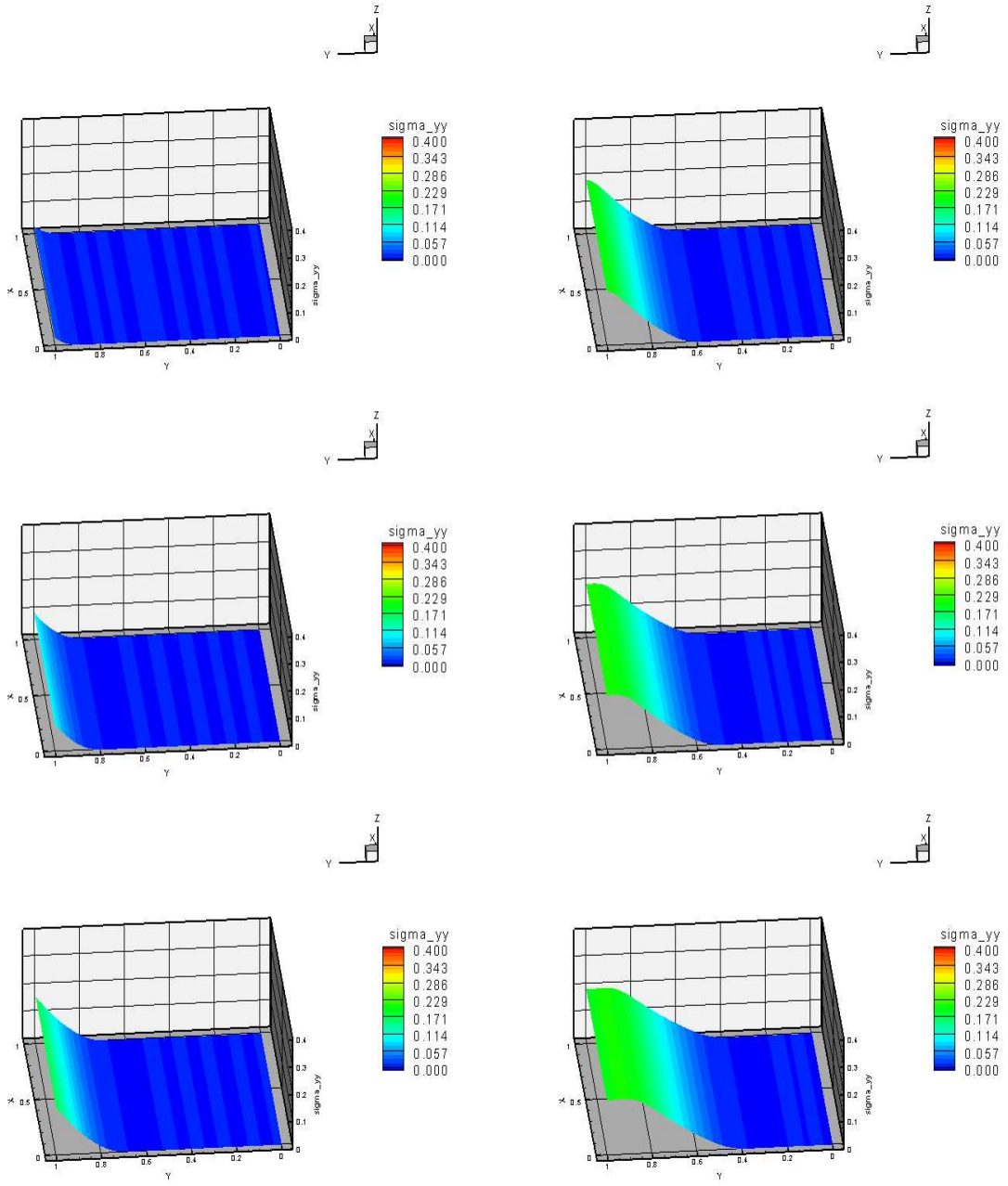

Figure 6.28: Model Problem 4, case (a_2) : $\nu = 0.0$ and $\sigma_{yy} = 0.2$: Evolution of σ_{yy} : Lower Convected Stress Rate - Time steps from 1^{st} to 6^{th}

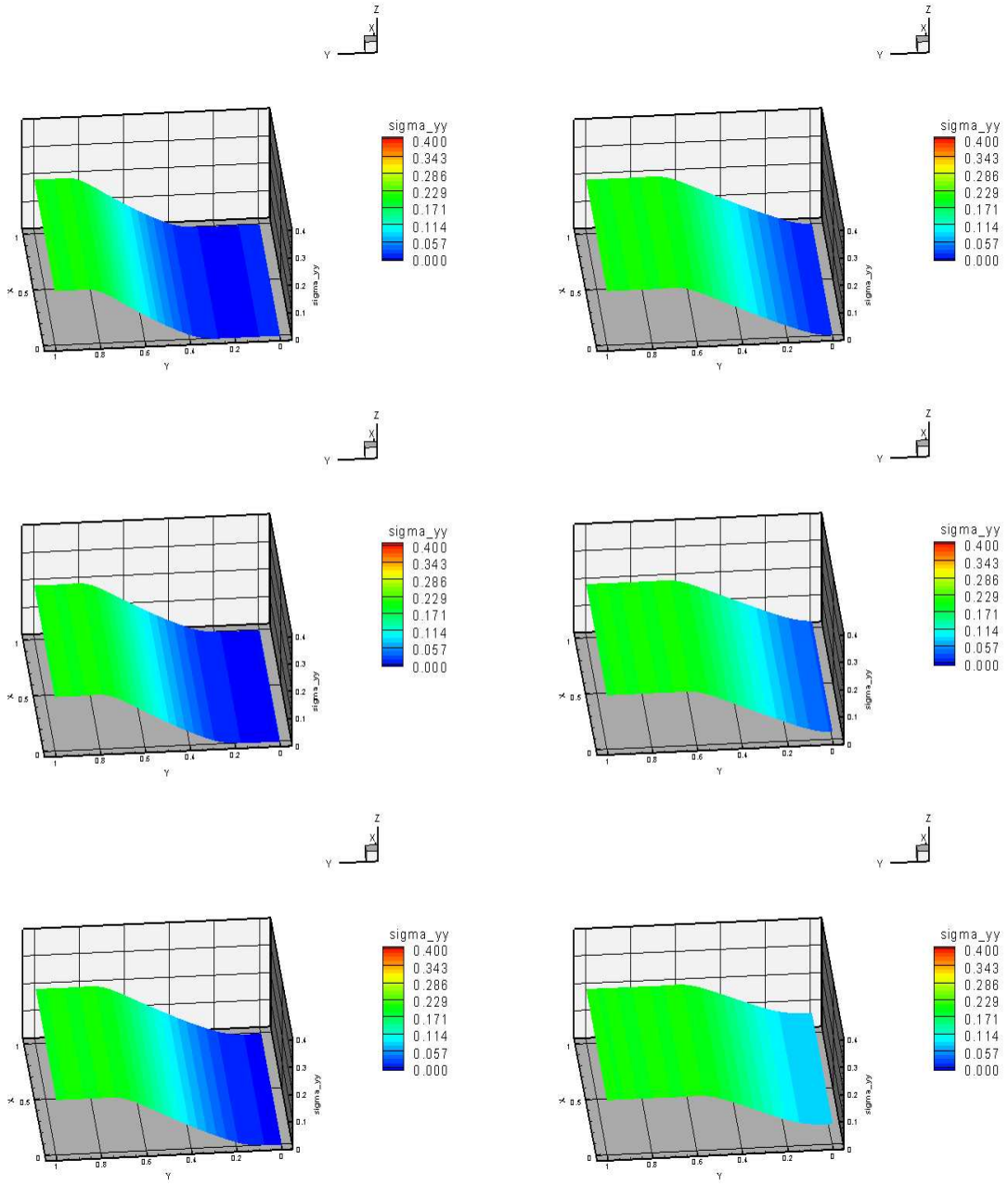

Figure 6.29: Model Problem 4, case (a_2) : $\nu = 0.0$ and $\sigma_{yy} = 0.2$: Evolution of σ_{yy} : Lower Convected Stress Rate - Time steps from 7^{th} to 12^{th}

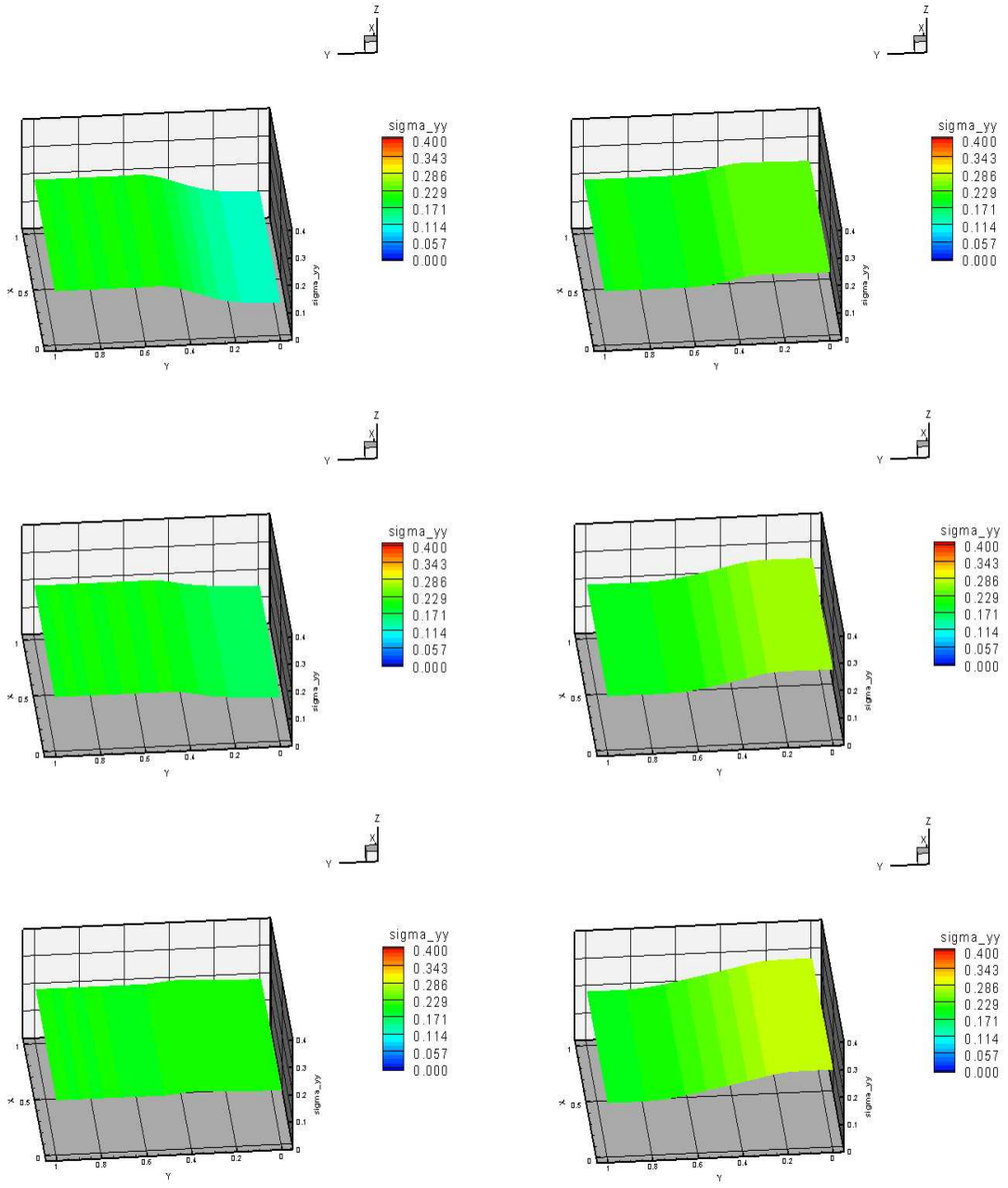

Figure 6.30: Model Problem 4, case (a_2) : $\nu = 0.0$ and $\sigma_{yy} = 0.2$: Evolution of σ_{yy} : Lower Convected Stress Rate - Time steps from 13^{th} to 18^{th}

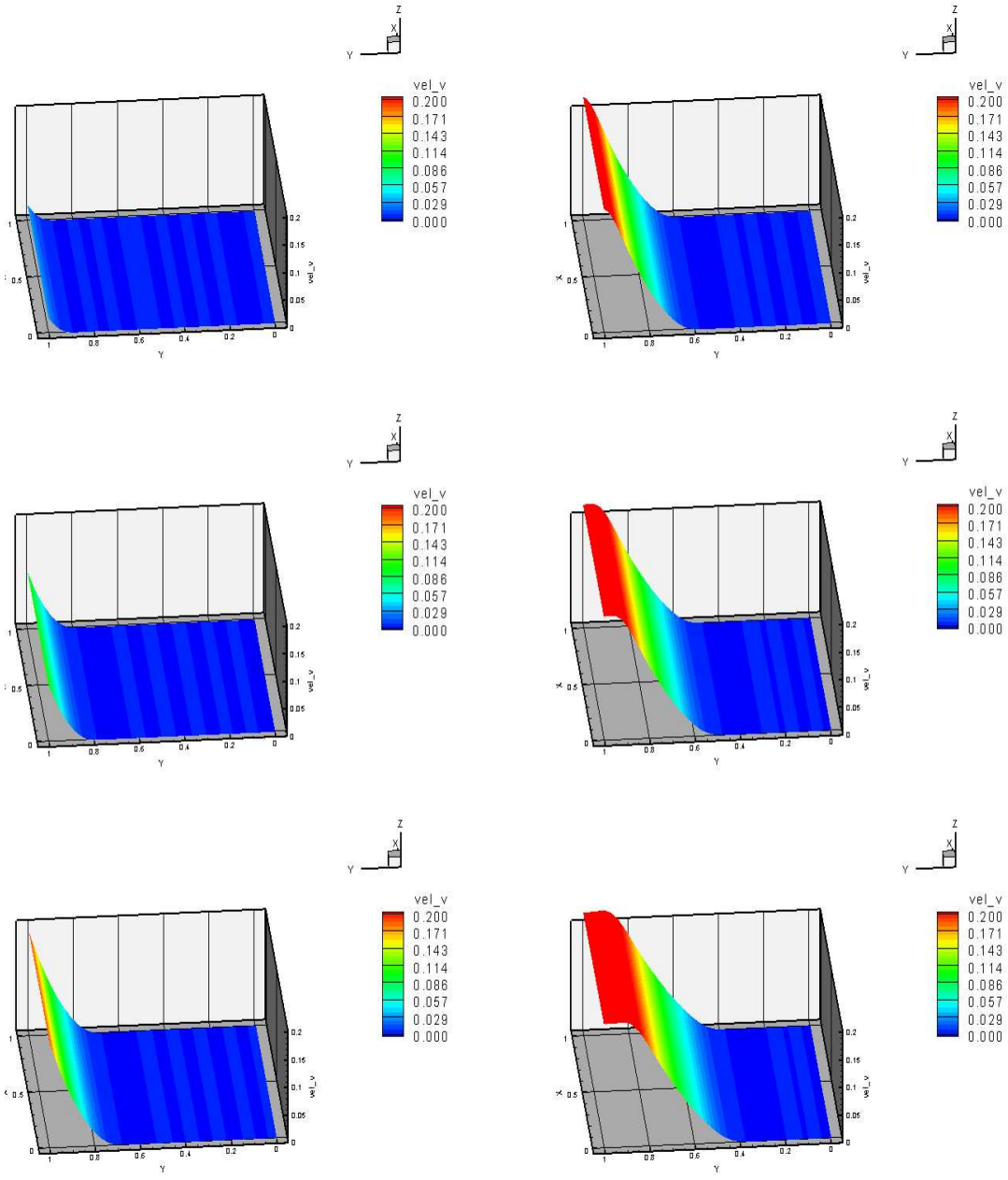

Figure 6.31: Model Problem 4, case (a_2) : $\nu = 0.0$ and $\sigma_{yy} = 0.2$: Evolution of v : Lower Convected Stress Rate - Time steps from 1^{st} to 6^{th}

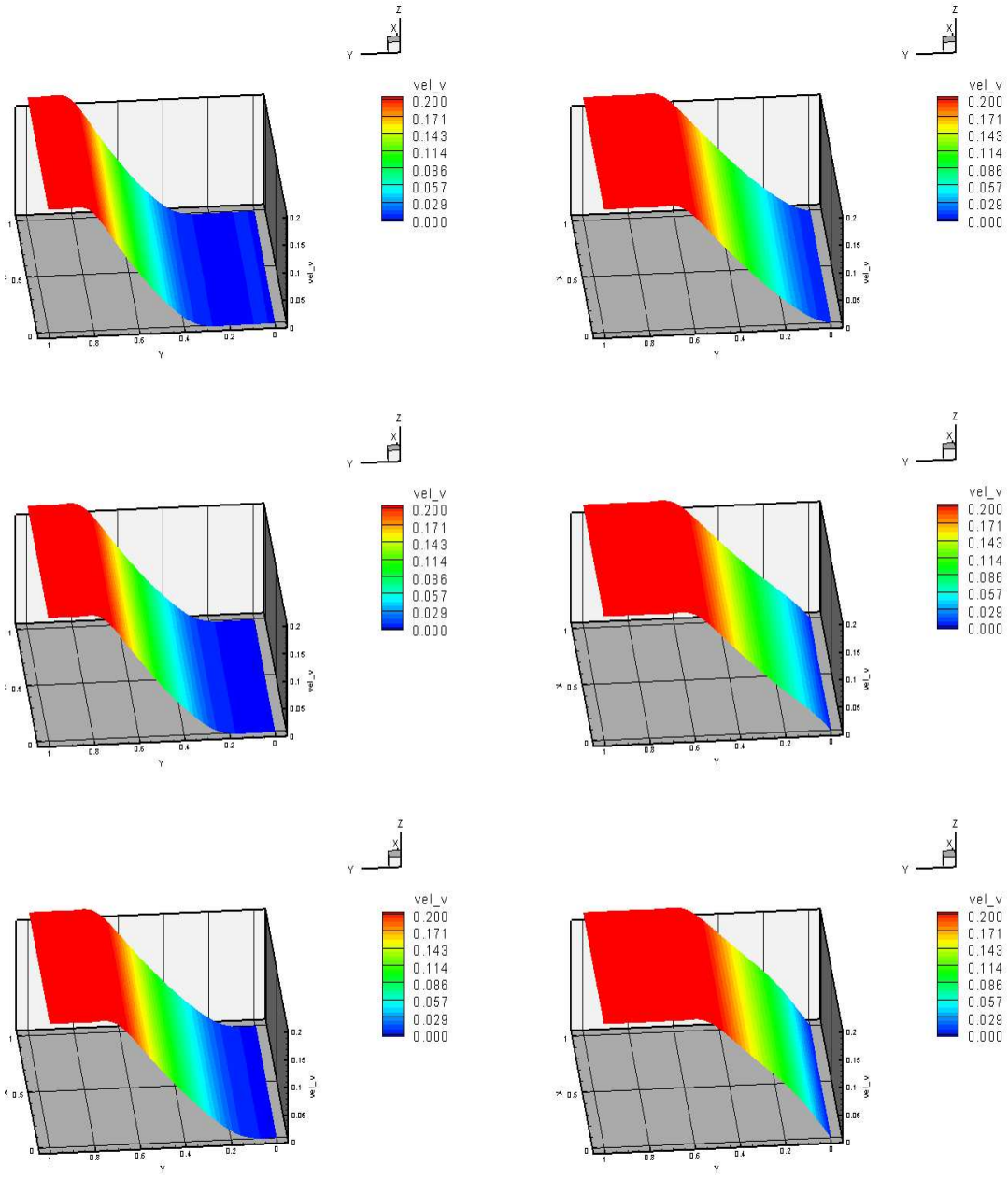

Figure 6.32: Model Problem 4, case (a_2) : $\nu = 0.0$ and $\sigma_{yy} = 0.2$: Evolution of v : Lower Convected Stress Rate - Time steps from 7^{th} to 12^{th}

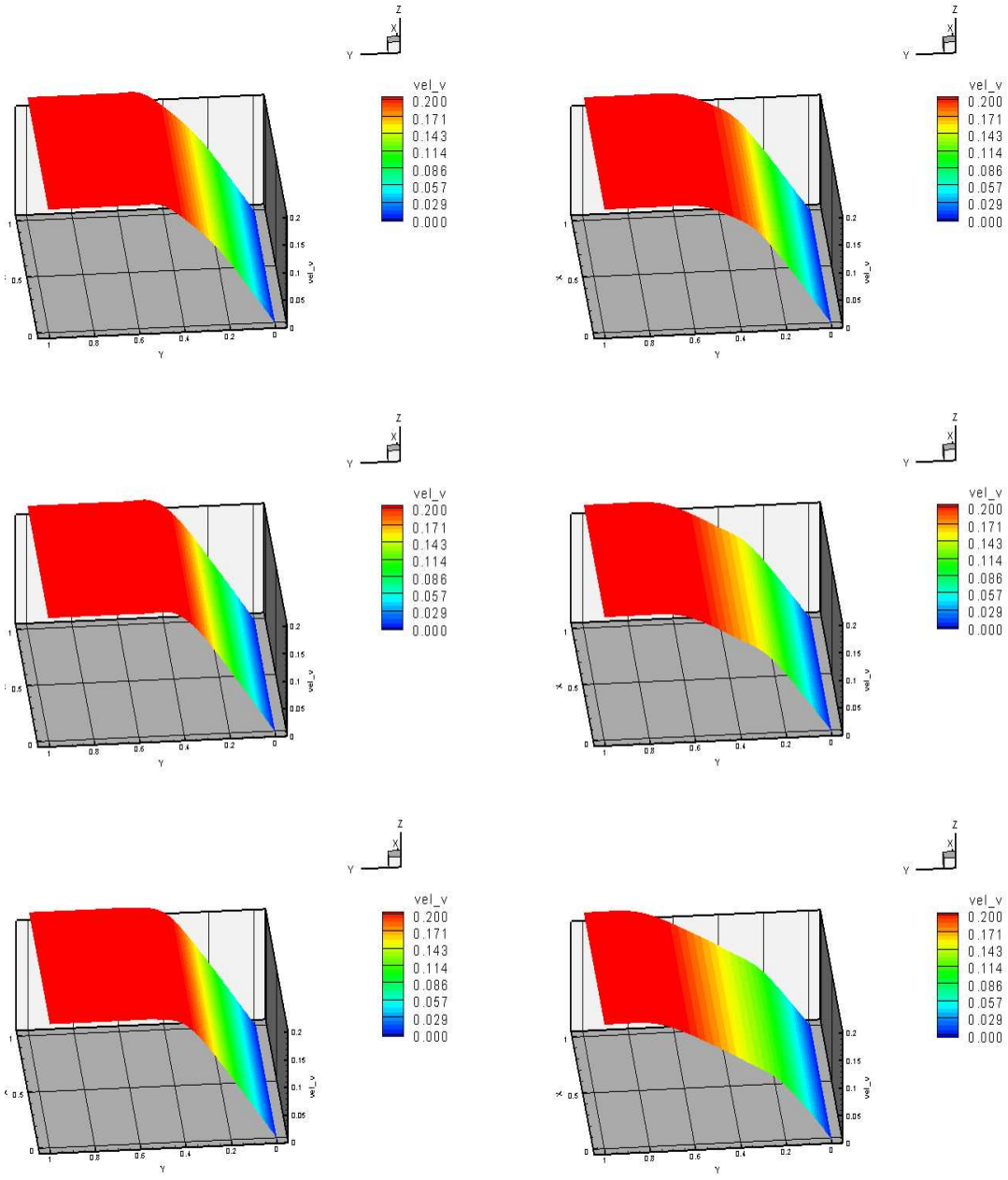

Figure 6.33: Model Problem 4, case (a_2) : $\nu = 0.0$ and $\sigma_{yy} = 0.2$: Evolution of v : Lower Convected Stress Rate - Time steps from 13^{th} to 18^{th}

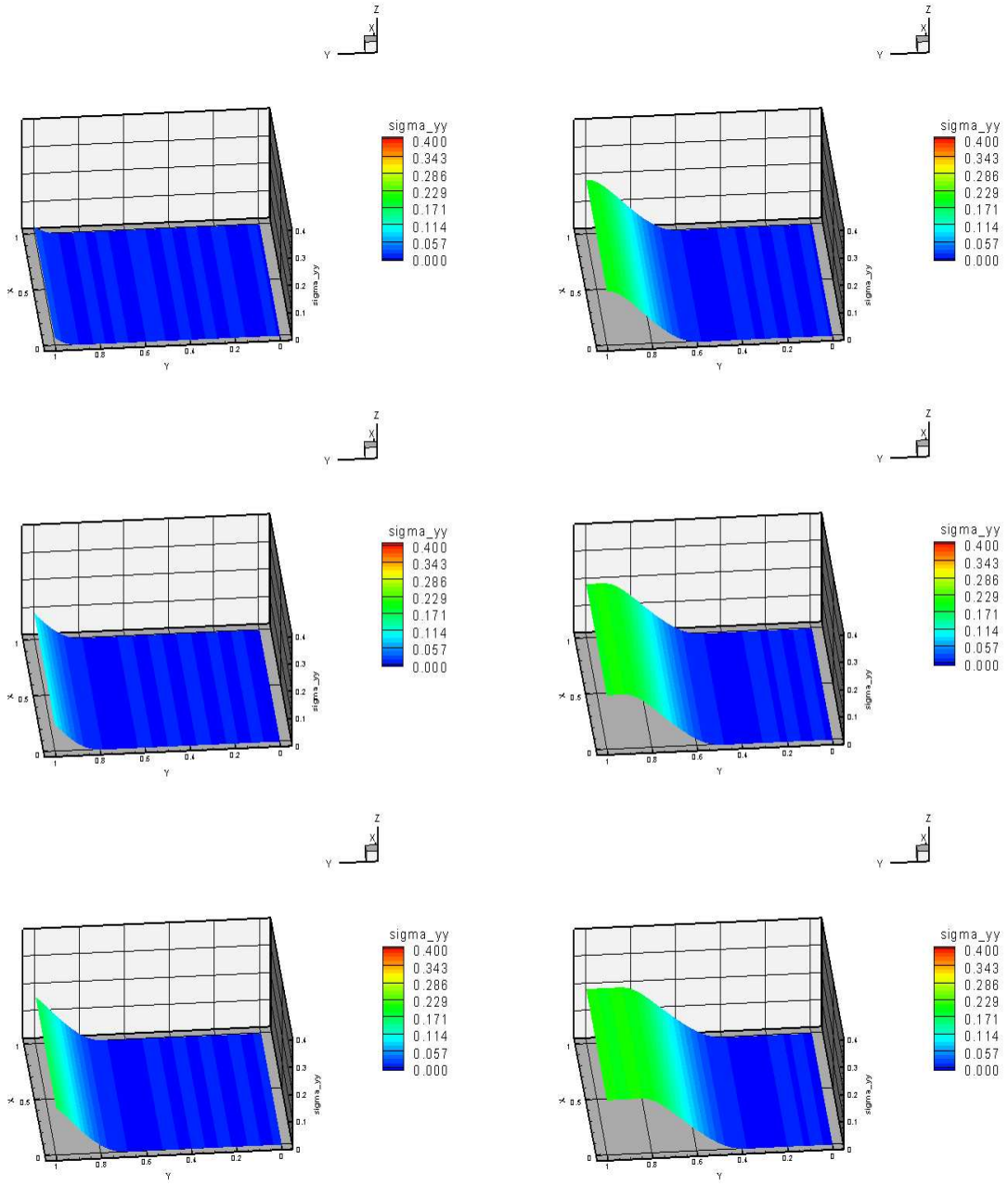

Figure 6.34: Model Problem 4, case (a_3) : $\nu = 0.0$ and $\sigma_{yy} = 0.2$: Evolution of σ_{yy} : Jaumann Stress Rate - Time steps from 1^{st} to 6^{th}

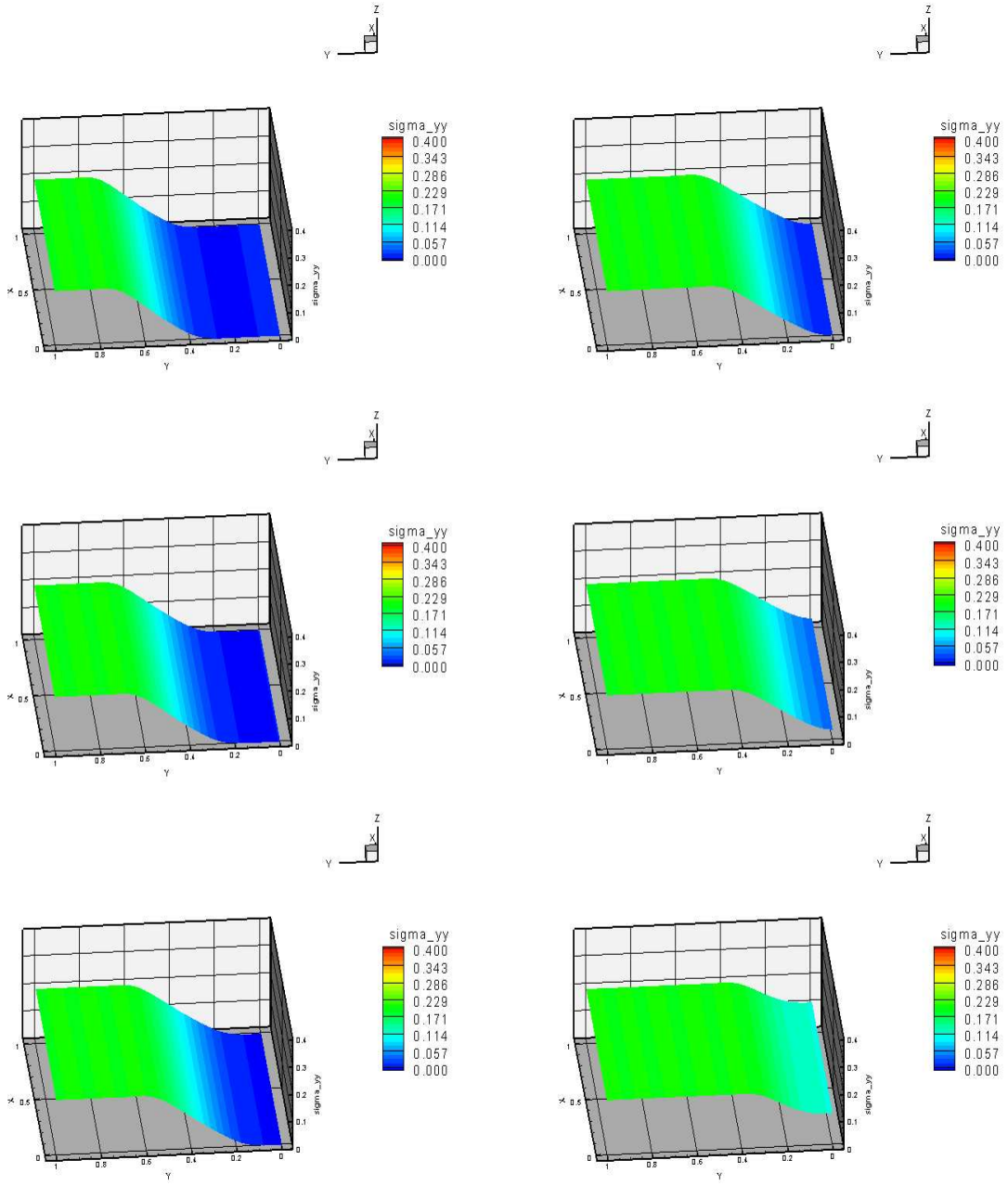

Figure 6.35: Model Problem 4, case (a_3) : $\nu = 0.0$ and $\sigma_{yy} = 0.2$: Evolution of σ_{yy} : Jaumann Stress Rate - Time steps from 7^{th} to 12^{th}

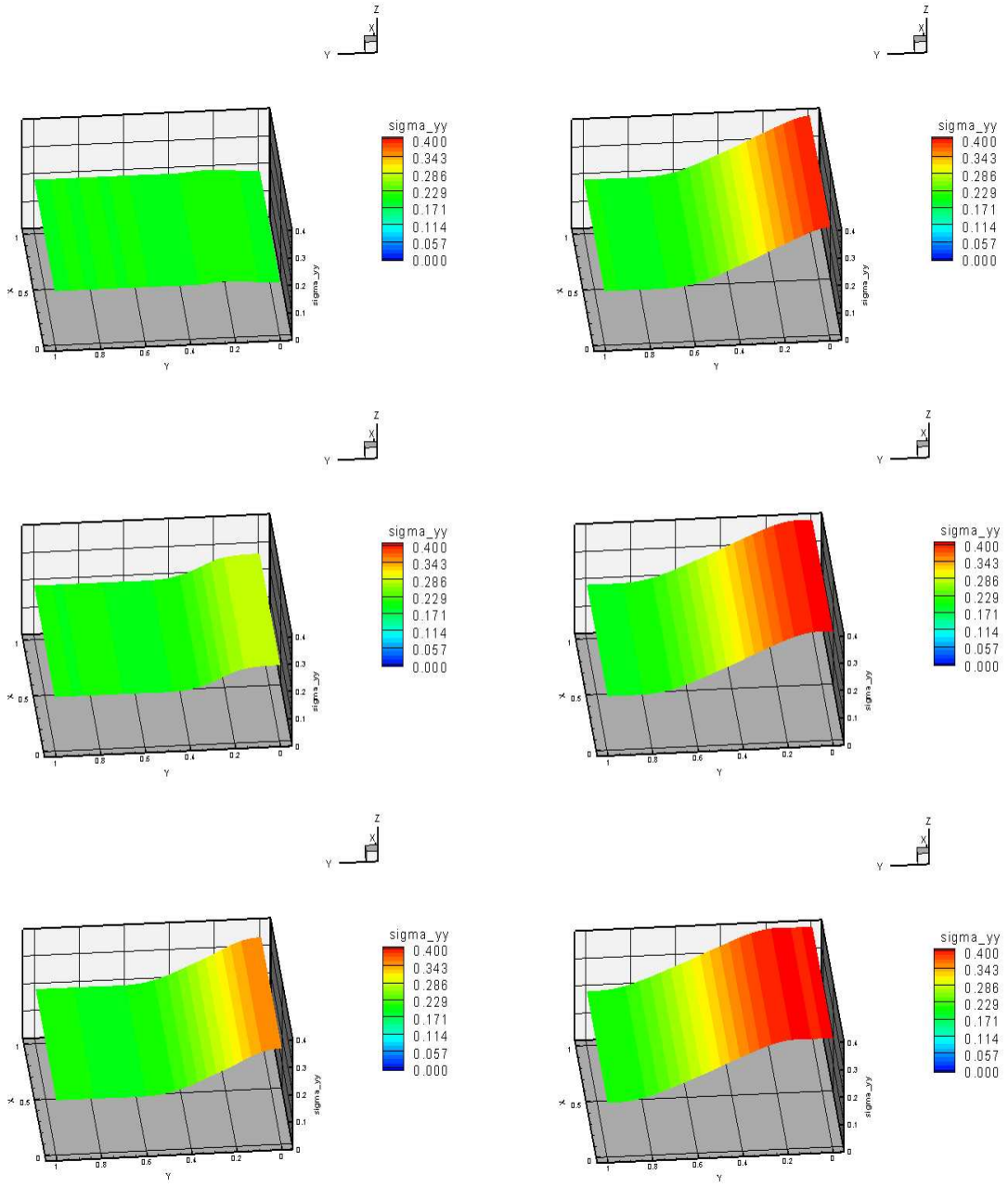

Figure 6.36: Model Problem 4, case (a_3) : $\nu = 0.0$ and $\sigma_{yy} = 0.2$: Evolution of σ_{yy} : Jaumann Stress Rate - Time steps from 13^{th} to 18^{th}

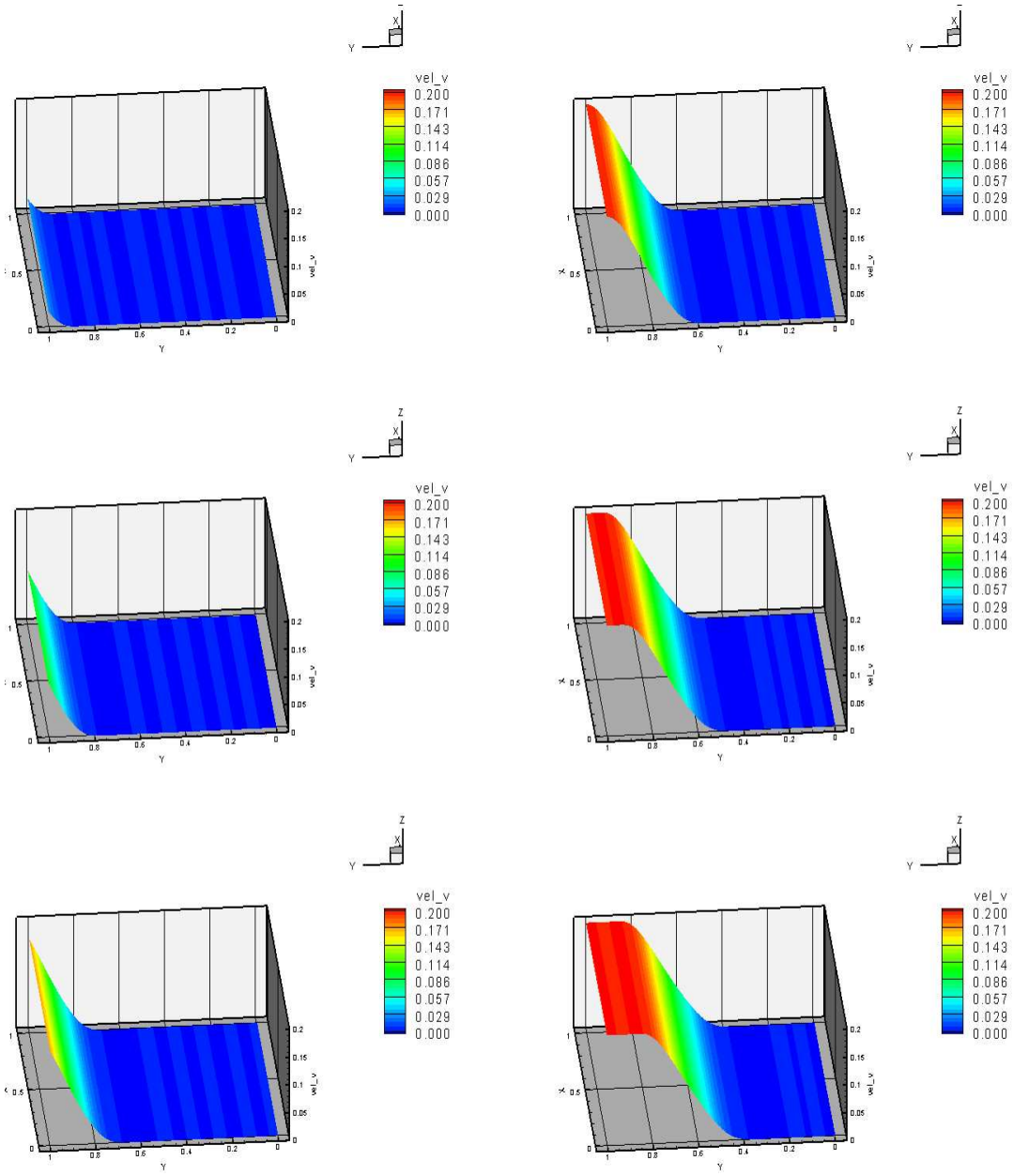

Figure 6.37: Model Problem 4, case (a_3) : $\nu = 0.0$ and $\sigma_{yy} = 0.2$: Evolution of v : Jaumann Stress Rate - Time steps from 1^{st} to 6^{th}

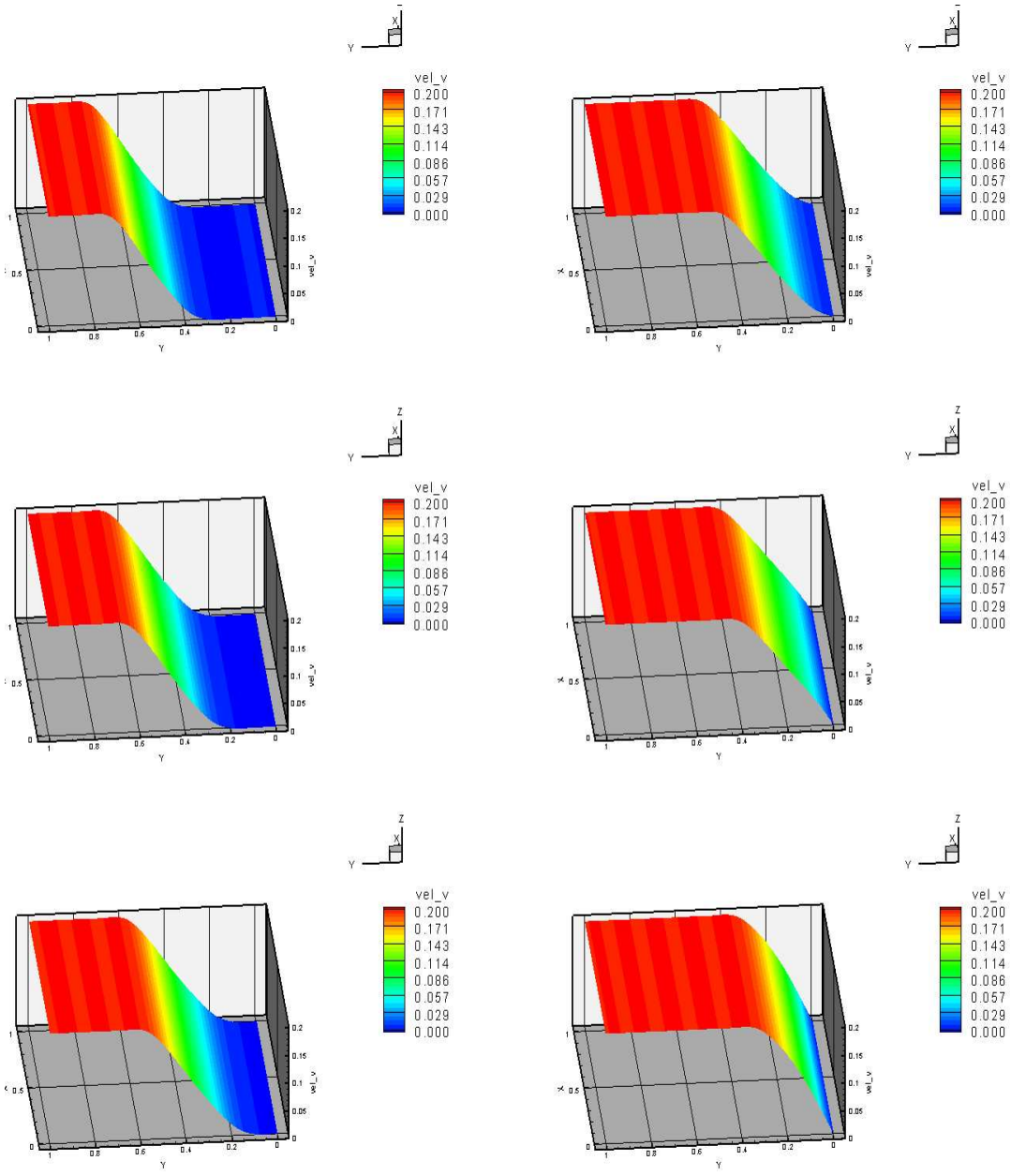

Figure 6.38: Model Problem 4, case (a_3) : $\nu = 0.0$ and $\sigma_{yy} = 0.2$: Evolution of v : Jaumann Stress Rate - Time steps from 7^{th} to 12^{th}

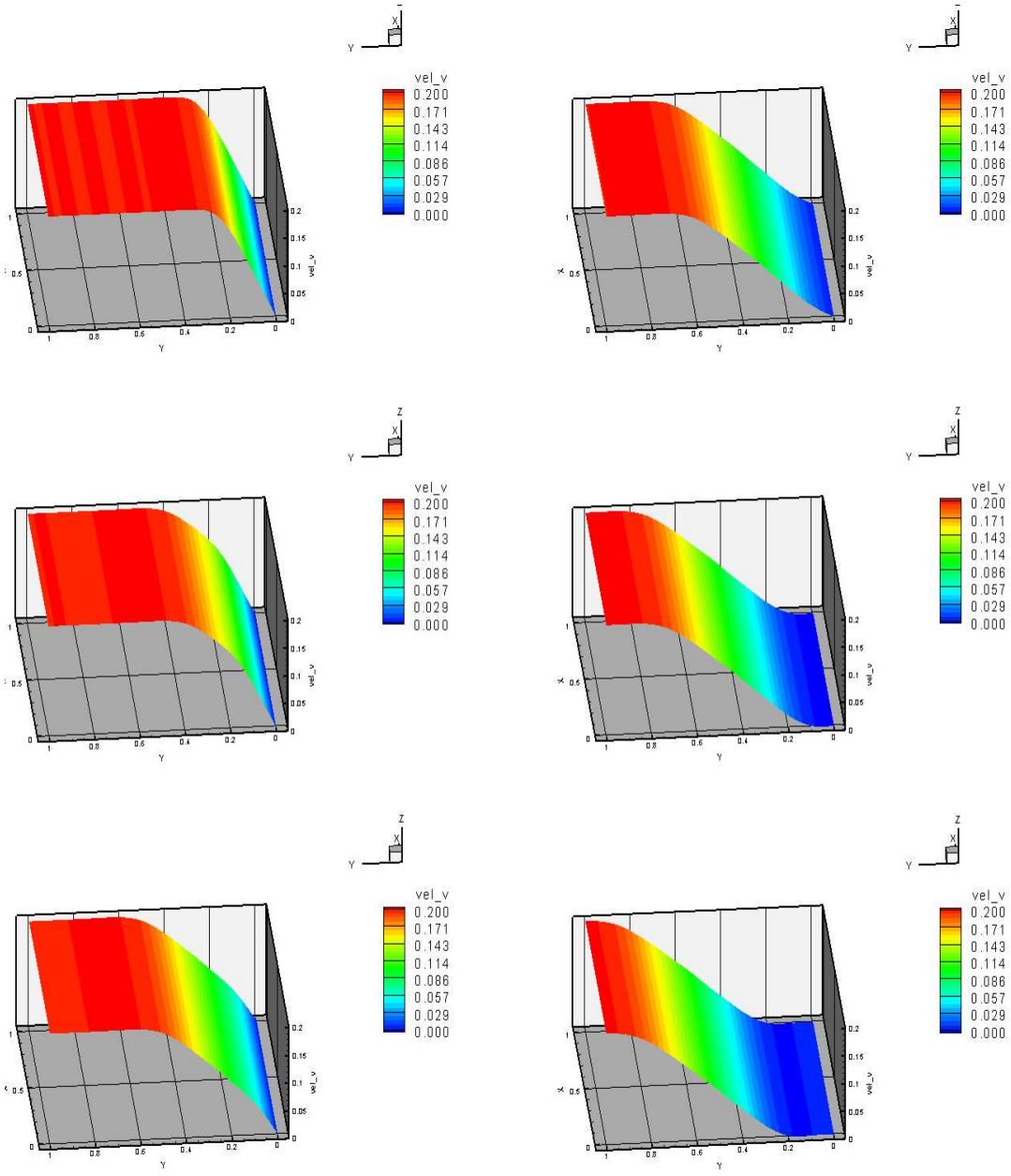

Figure 6.39: Model Problem 4, case (a_3) : $\nu = 0.0$ and $\sigma_{yy} = 0.2$: Evolution of v : Jaumann Stress Rate - Time steps from 13^{th} to 18^{th}

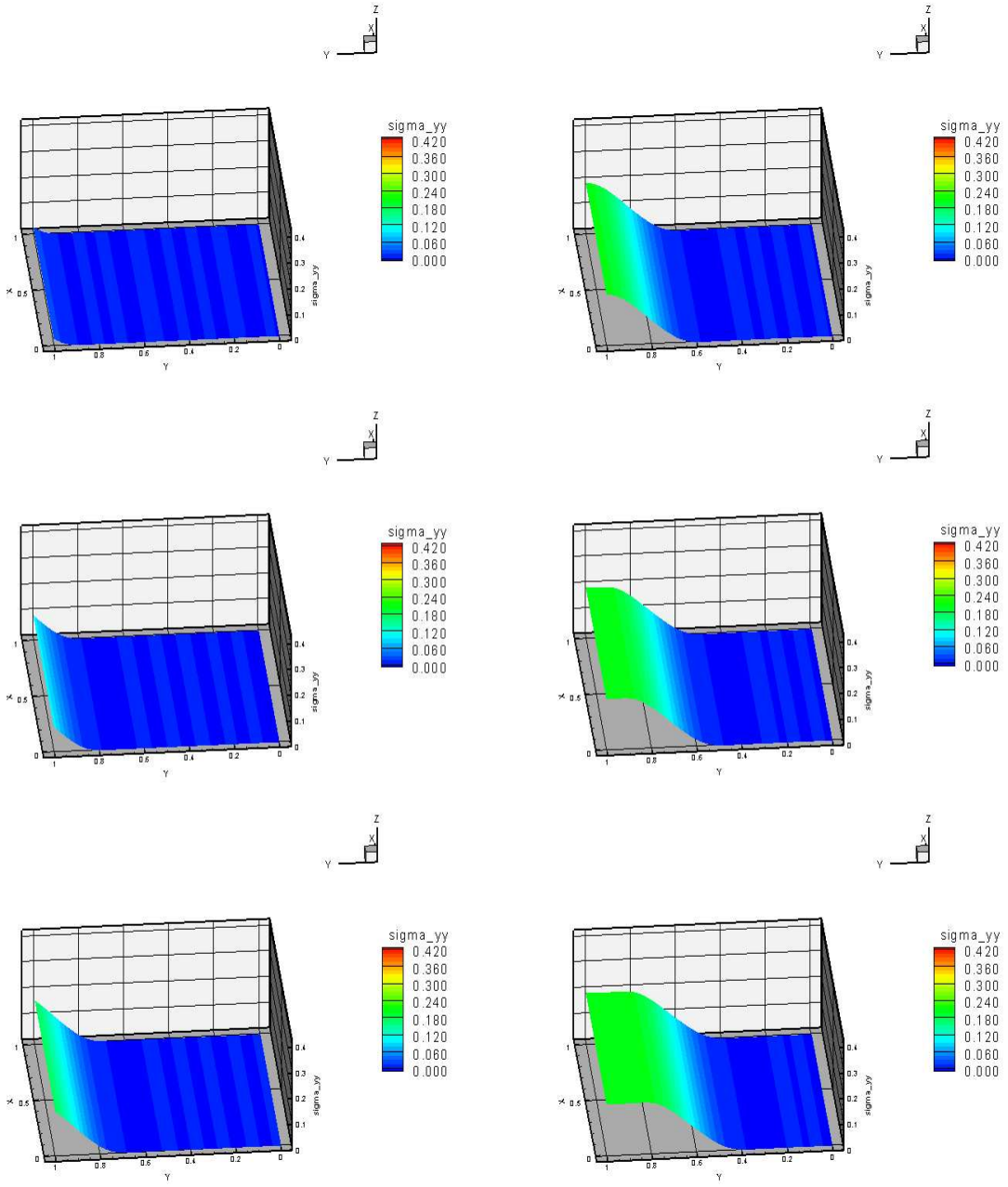

Figure 6.40: Model Problem 4, case (a_4) : $\nu = 0.0$ and $\sigma_{yy} = 0.2$: Evolution of σ_{yy} : Truesdell Stress Rate - Time steps from 1^{st} to 6^{th}

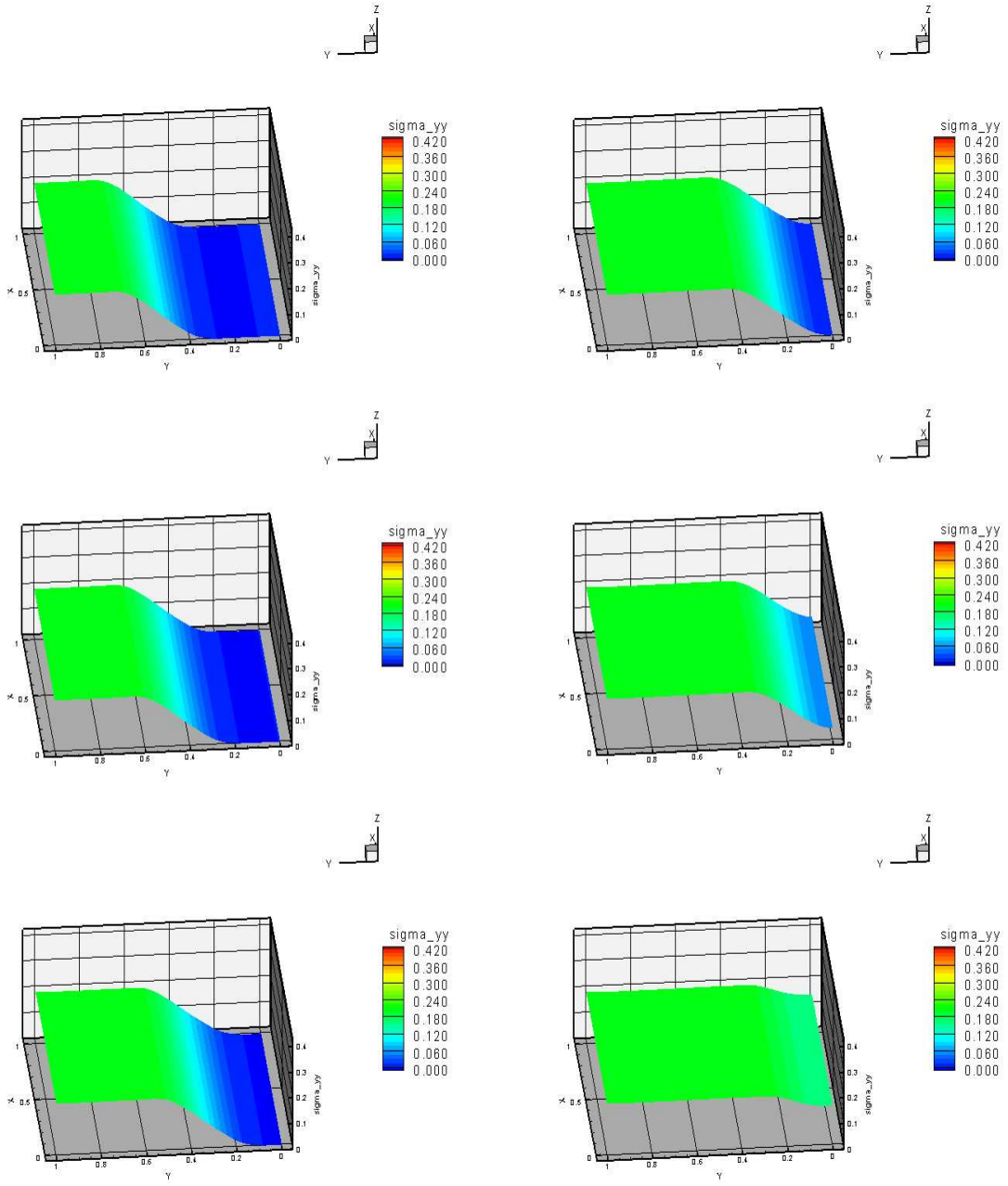

Figure 6.41: Model Problem 4, case (a_4) : $\nu = 0.0$ and $\sigma_{yy} = 0.2$: Evolution of σ_{yy} : Truesdell Stress Rate - Time steps from 7^{th} to 12^{th}

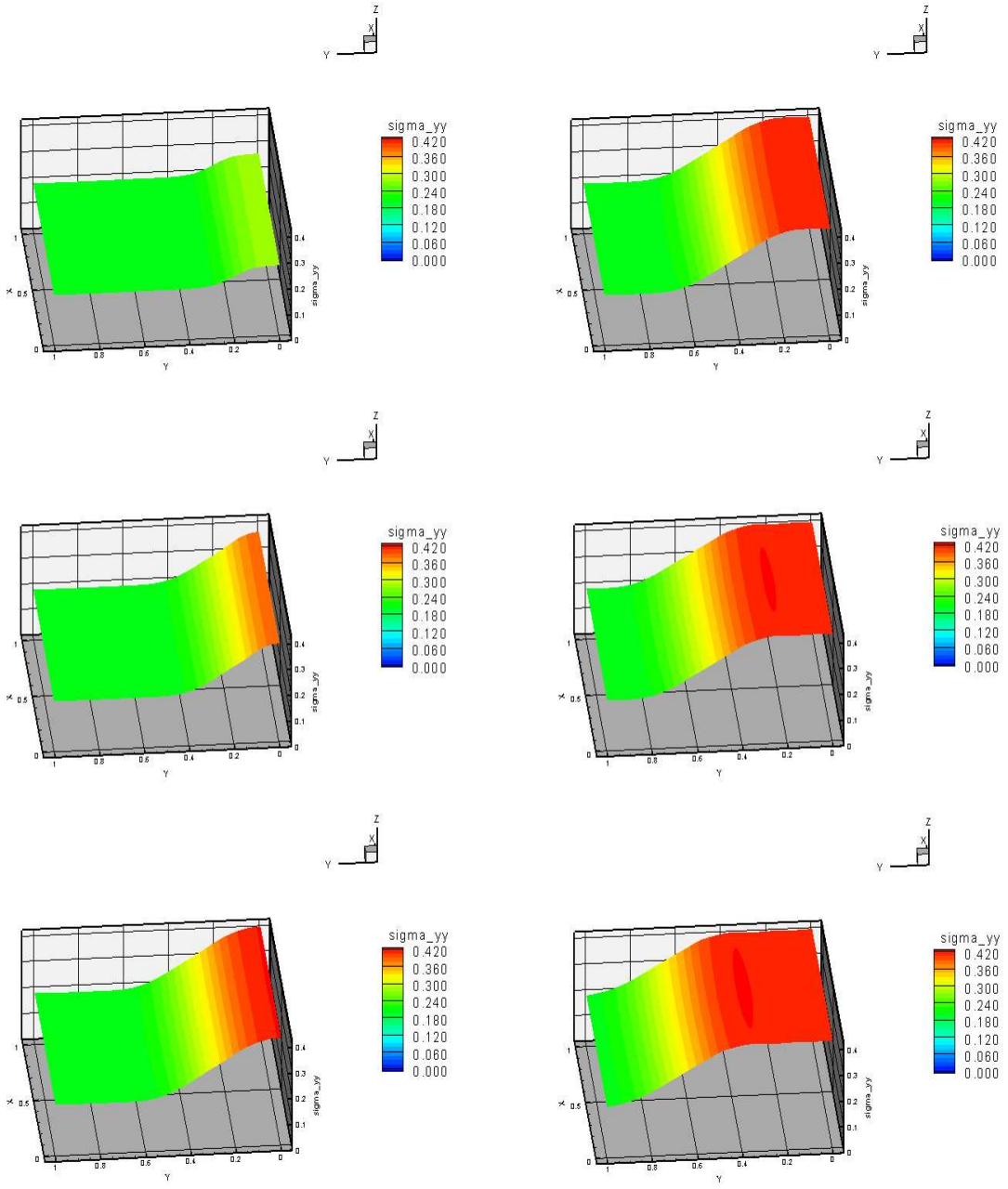

Figure 6.42: Model Problem 4, case (a_4) : $\nu = 0.0$ and $\sigma_{yy} = 0.2$: Evolution of σ_{yy} : Truesdell Stress Rate - Time steps from 13^{th} to 18^{th}

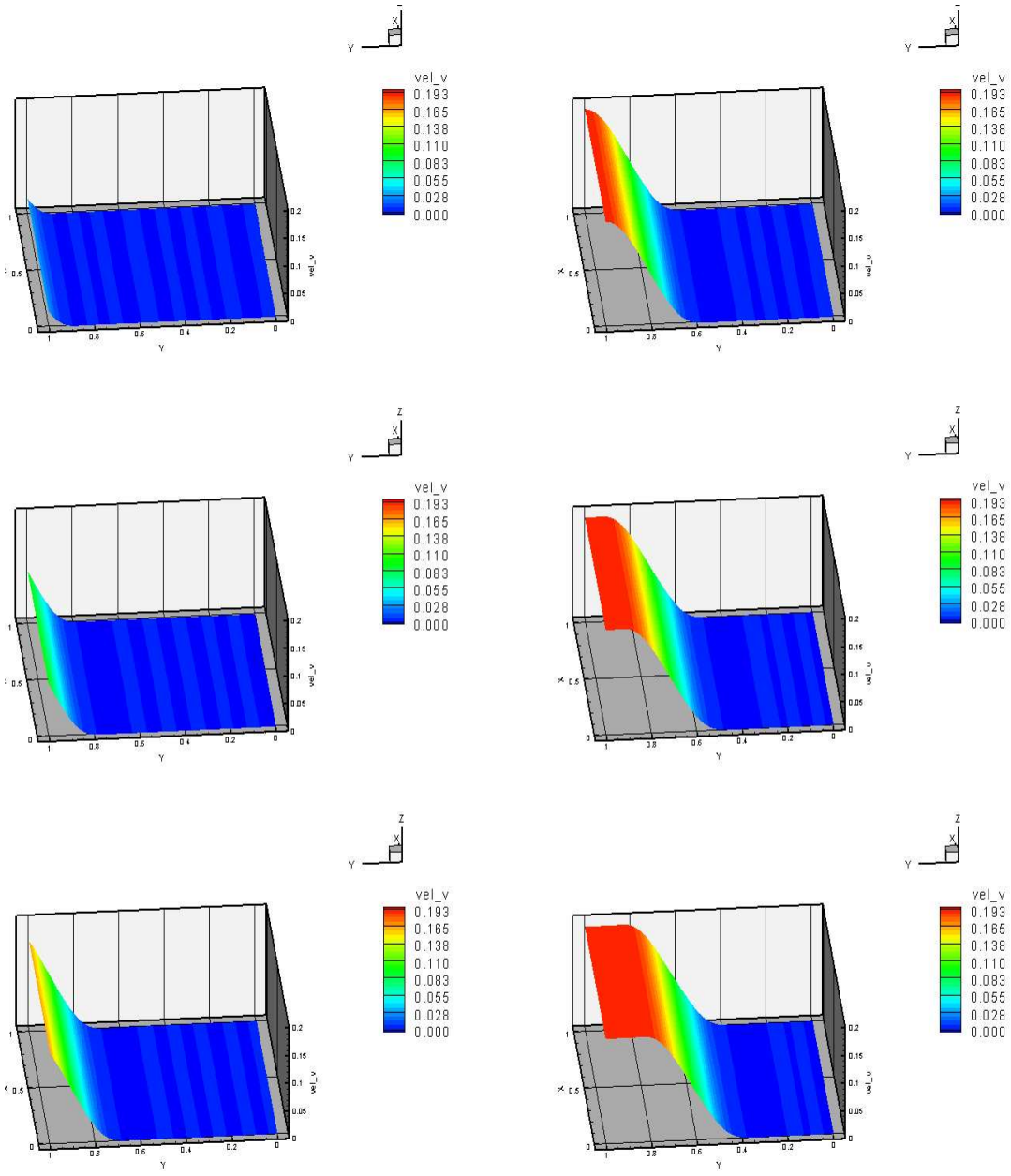

Figure 6.43: Model Problem 4, case (a_4) : $\nu = 0.0$ and $\sigma_{yy} = 0.2$: Evolution of v : Truesdell Stress Rate - Time steps from 1^{st} to 6^{th}

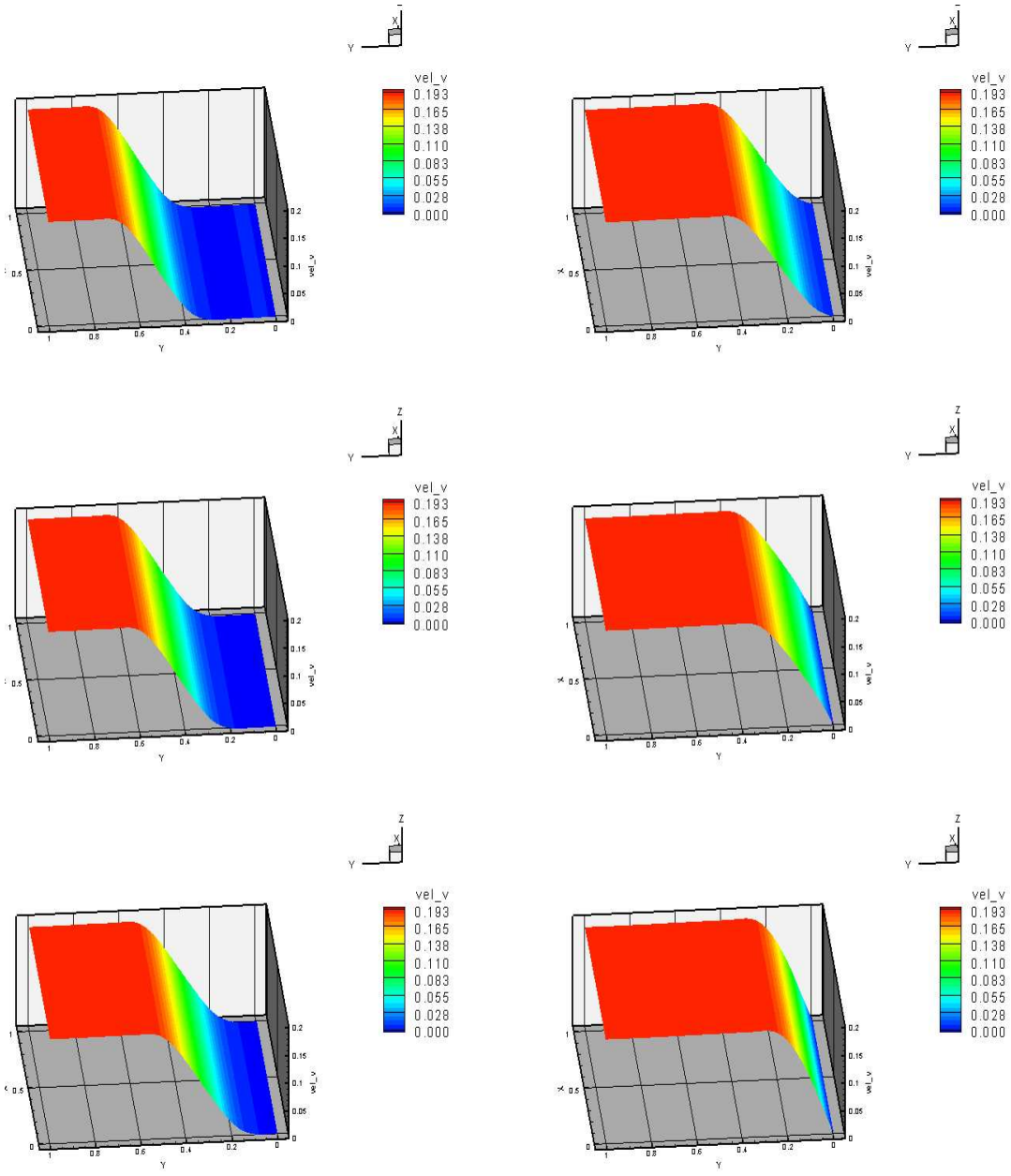

Figure 6.44: Model Problem 4, case (a_4) : $\nu = 0.0$ and $\sigma_{yy} = 0.2$: Evolution of v : Truesdell Stress Rate - Time steps from 7^{th} to 12^{th}

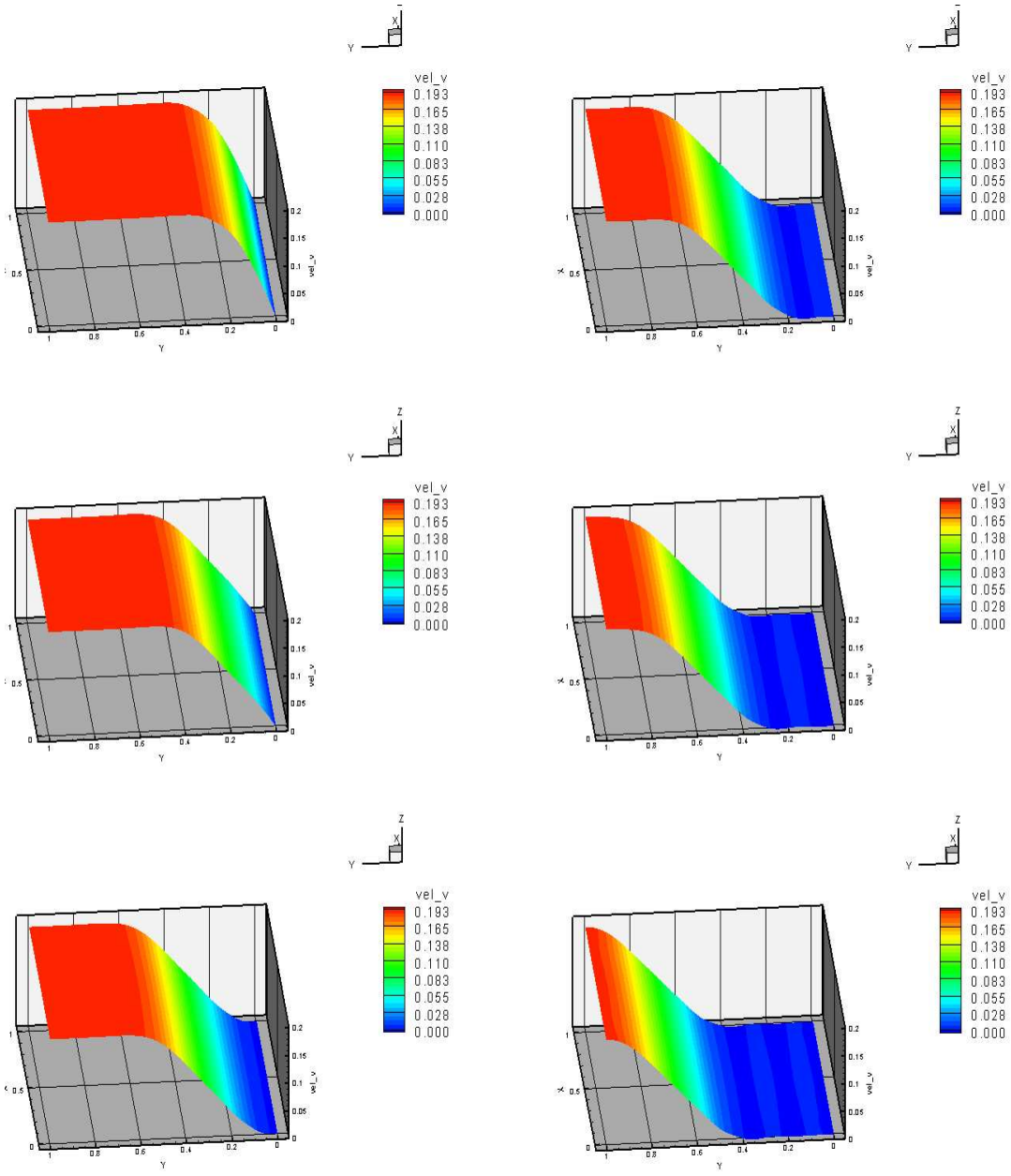

Figure 6.45: Model Problem 4, case (a_4) : $\nu = 0.0$ and $\sigma_{yy} = 0.2$: Evolution of v : Truesdell Stress Rate - Time steps from 13^{th} to 18^{th}

6.4.2 Case (b): Poisson's ratio, $\nu = 0.3$, and applied uniform tension $\sigma_{yy} = 0.01$

In this section we present numerical studies for the similar to model problem 4 (figure 6.21) with identical discretizations, p-levels and the orders of the approximation space except that the Poisson's ratio is 0.3. Based on the studies presented in case (a), we only consider upper Convected rate constitutive equations for this numerical study. For uniformly applied tension of $\sigma_{yy} = .01$, computed evolutions of σ_{yy}, σ_{xy}, σ_{xx}, v, and u are presented in the following figures.

Figures 6.46-6.48 : σ_{yy}

Figures 6.49-6.51 : σ_{xy}

Figures 6.52-6.54 : σ_{xx}

Figures 6.55-6.57 : v

Figures 6.58-6.60 : u

Evolution of σ_{yy} is a propagating front (with some shape change compared to ν=0.0). Upon reflections (figure 6.48), the complexities of the wave interactions and boundary effects are clearly observed. Symmetry of evolution about yz plane is some assurance of the validity of the evolution. In case of σ_{xy} we observe antisymmetric behavior whereas for σ_{xx} we observe symmetric behavior about yz plane (figures 6.49 - 6.51 and figures 6.52 - 6.54 respectively). Interaction of the stress wave with boundaries and the influence of the free boundaries is more clearly visible in case of the evolution of velocity v (figures 6.55 - 6.57). Symmetry of the evolution about yz plane is clearly seen. Velocity u is antisymmetric about yz plane as expected.

In all figures, the evolutions are smooth, reflections are simulated without any difficulty and the influence of the boundaries is clearly observed on the evolution.

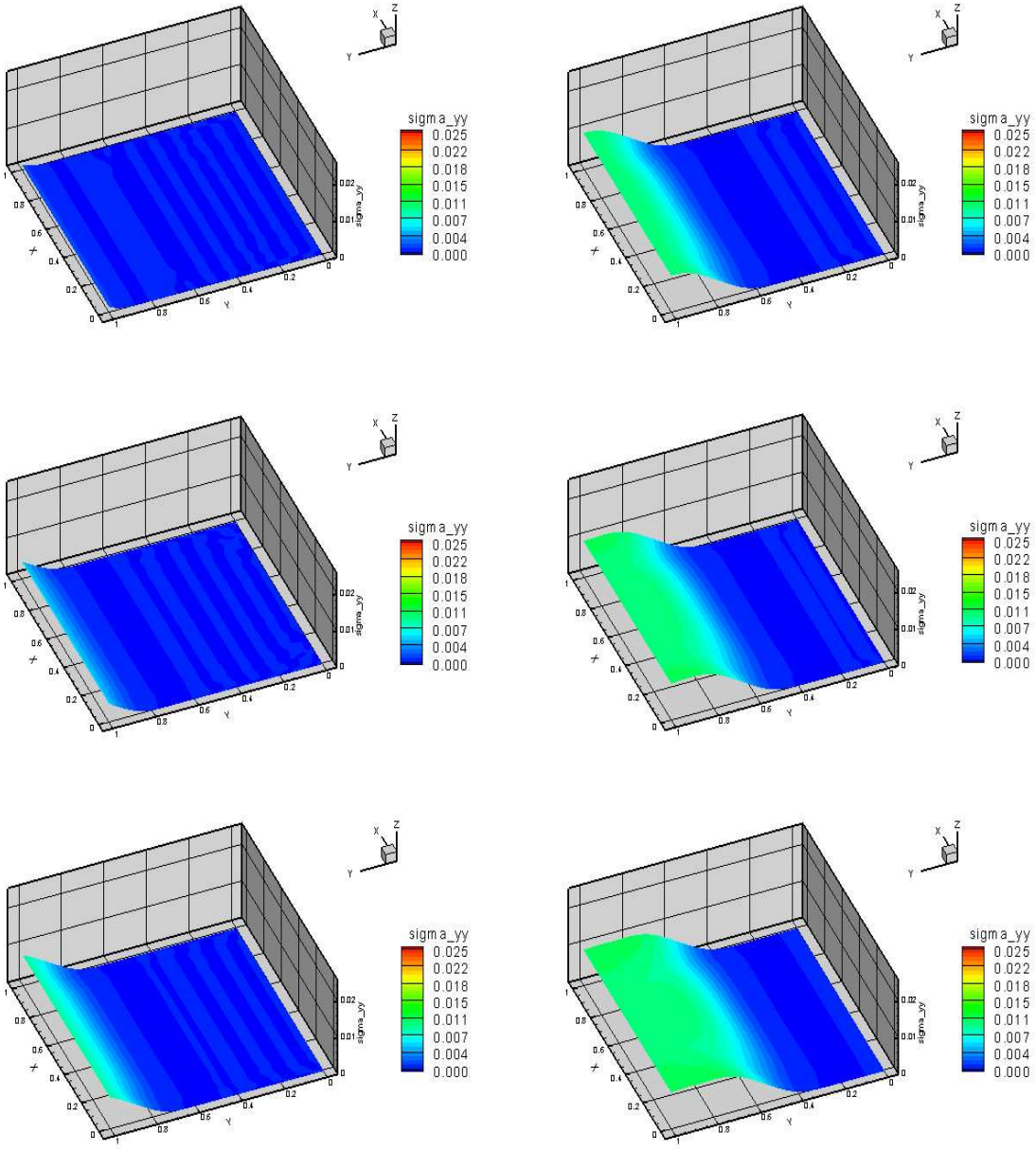

Figure 6.46: Model Problem 4, case (b) : $\nu = 0.3$ and $\sigma_{yy} = 0.01$: Evolution of σ_{yy} : Upper Convected Stress Rate - Time steps from 1^{st} to 6^{th}

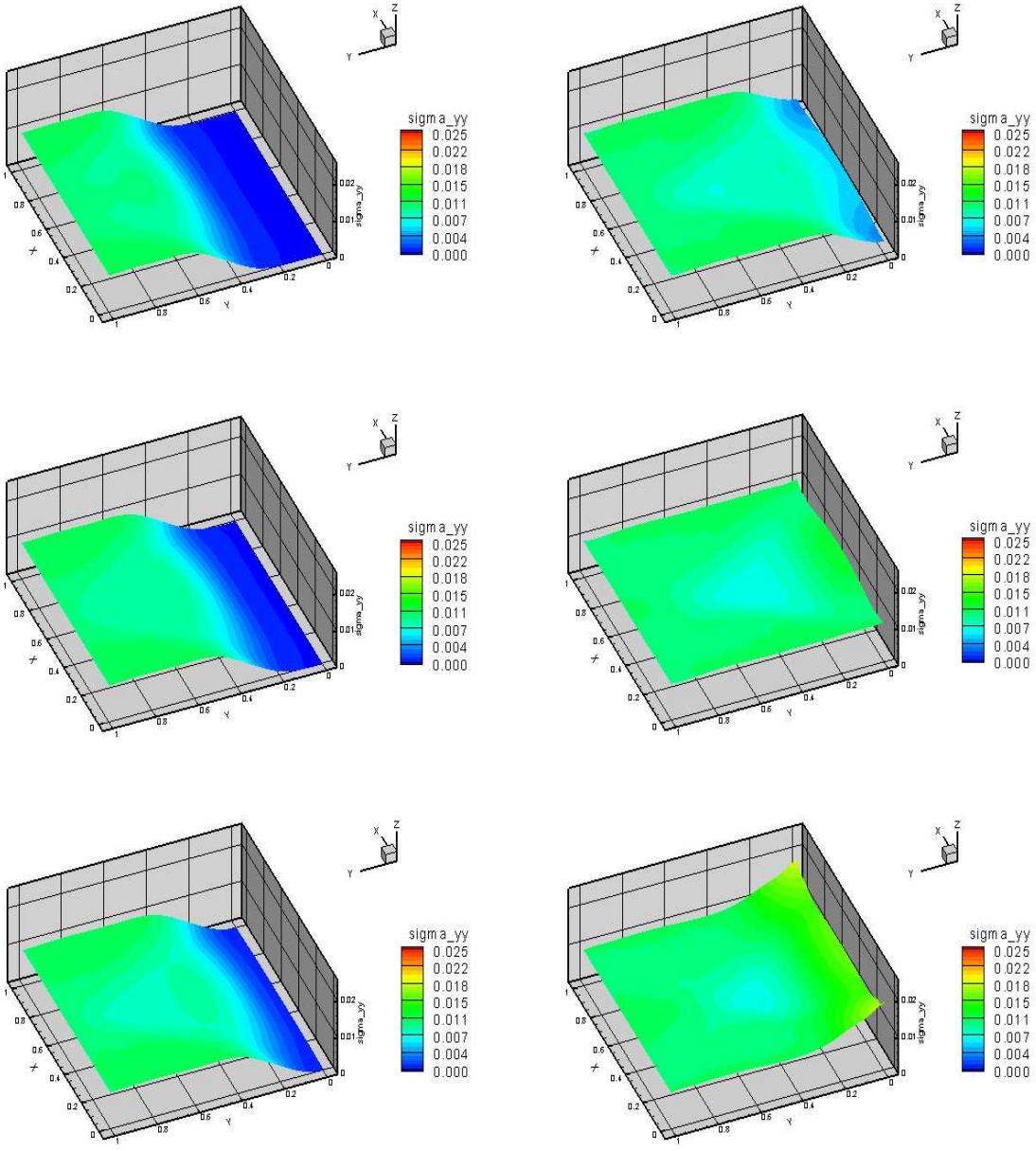

Figure 6.47: Model Problem 4, case (b) : $\nu = 0.3$ and $\sigma_{yy} = 0.01$: Evolution of σ_{yy} : Upper Convected Stress Rate - Time steps from 7^{th} to 12^{th}

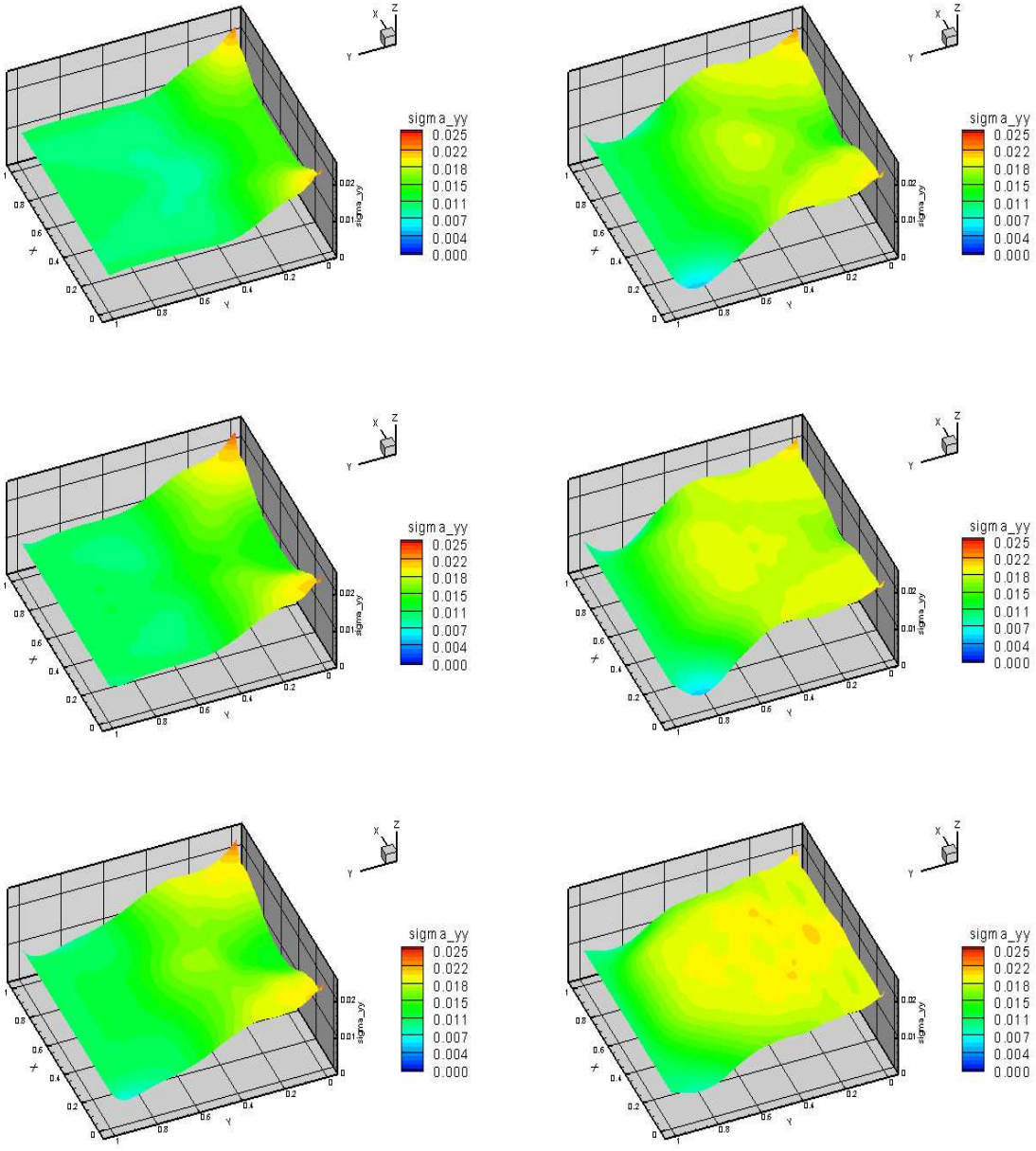

Figure 6.48: Model Problem 4, case (b) : $\nu = 0.3$ and $\sigma_{yy} = 0.01$: Evolution of σ_{yy} : Upper Convected Stress Rate - Time steps from 13^{th} to 18^{th}

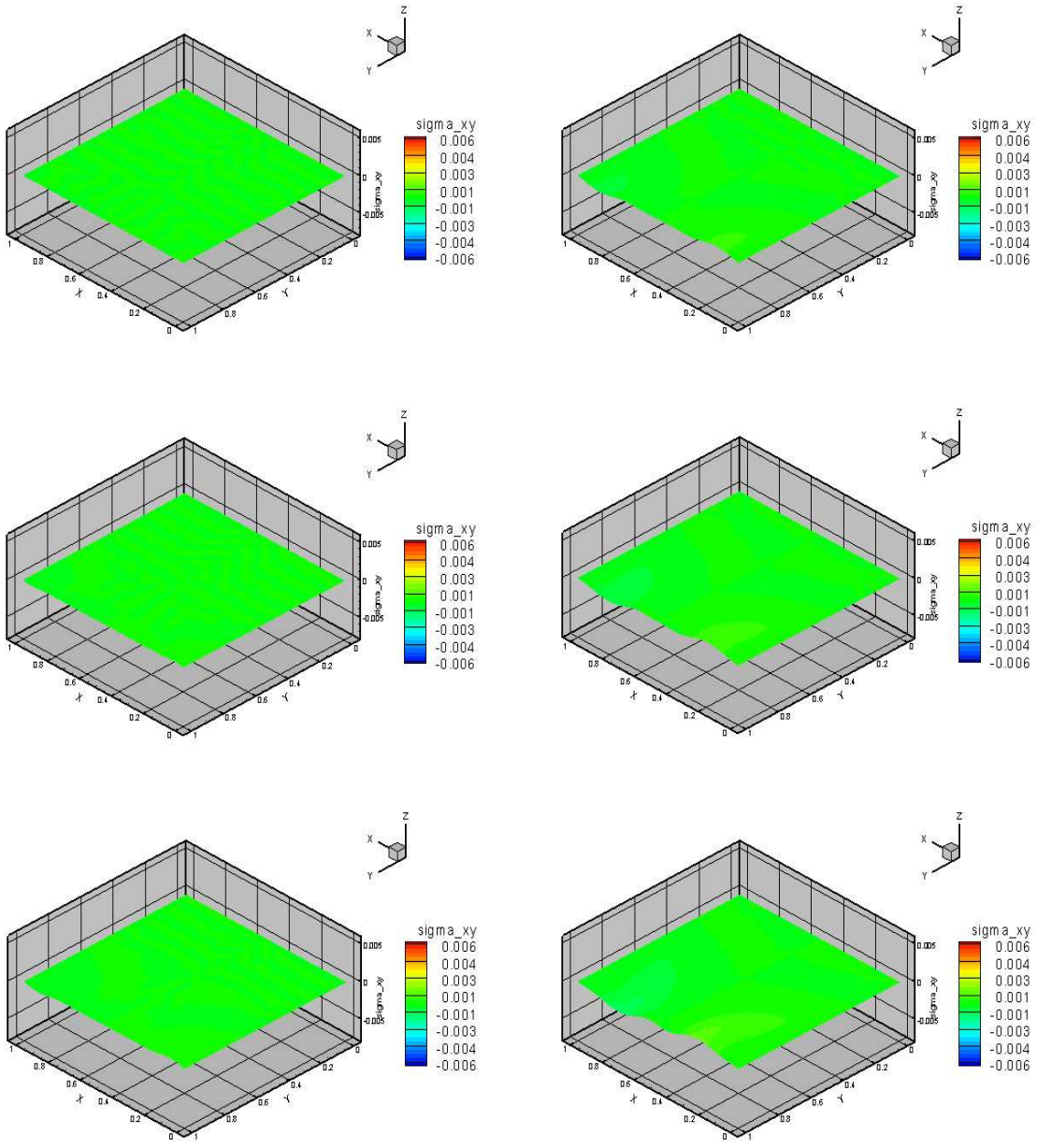

Figure 6.49: Model Problem 4, case (b) : $\nu = 0.3$ and $\sigma_{yy} = 0.01$: Evolution of σ_{xy} : Upper Convected Stress Rate - Time steps from 1^{st} to 6^{th}

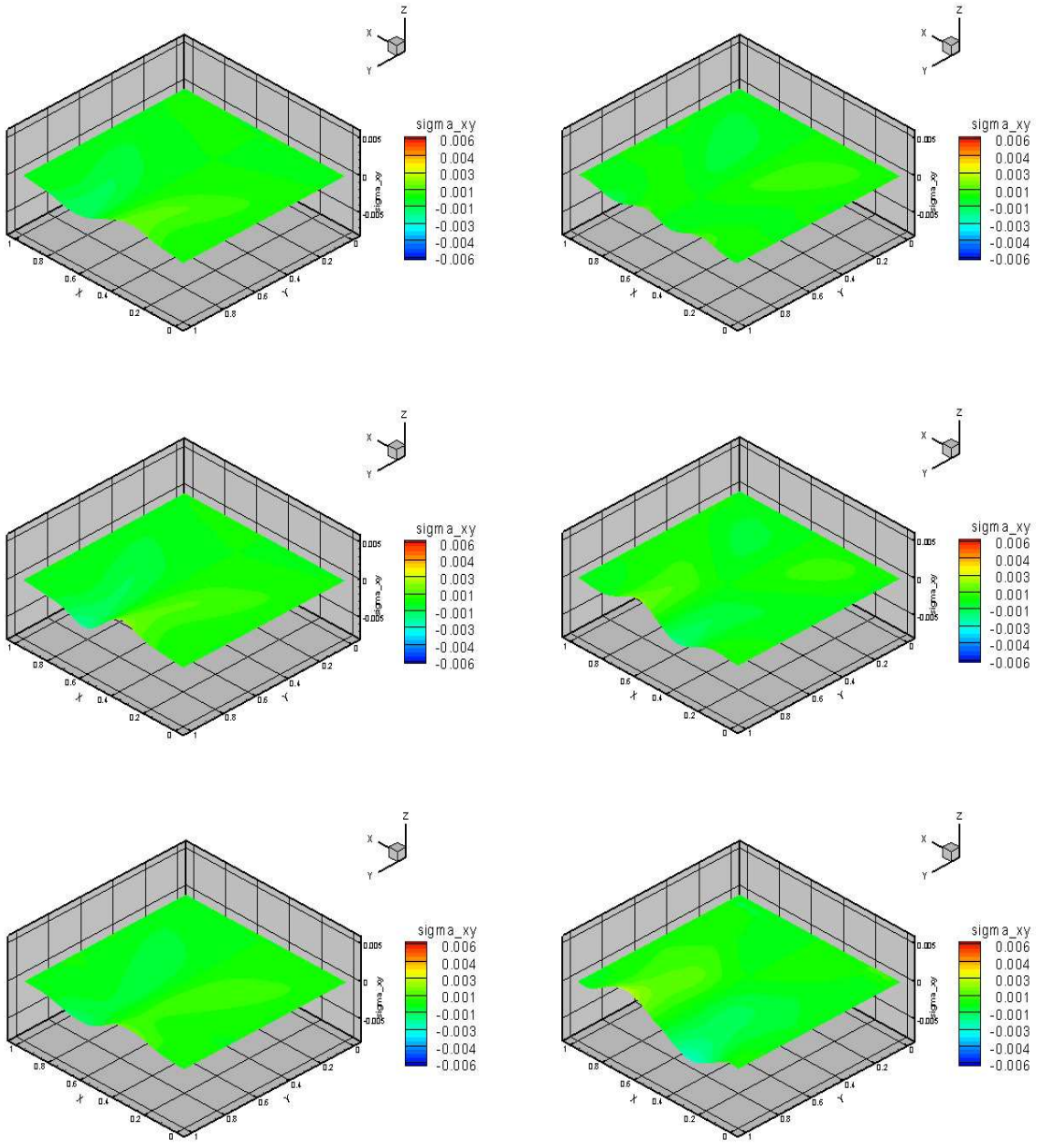

Figure 6.50: Model Problem 4, case (b) : $\nu = 0.3$ and $\sigma_{yy} = 0.01$: Evolution of σ_{xy} : Upper Convected Stress Rate - Time steps from 7^{th} to 12^{th}

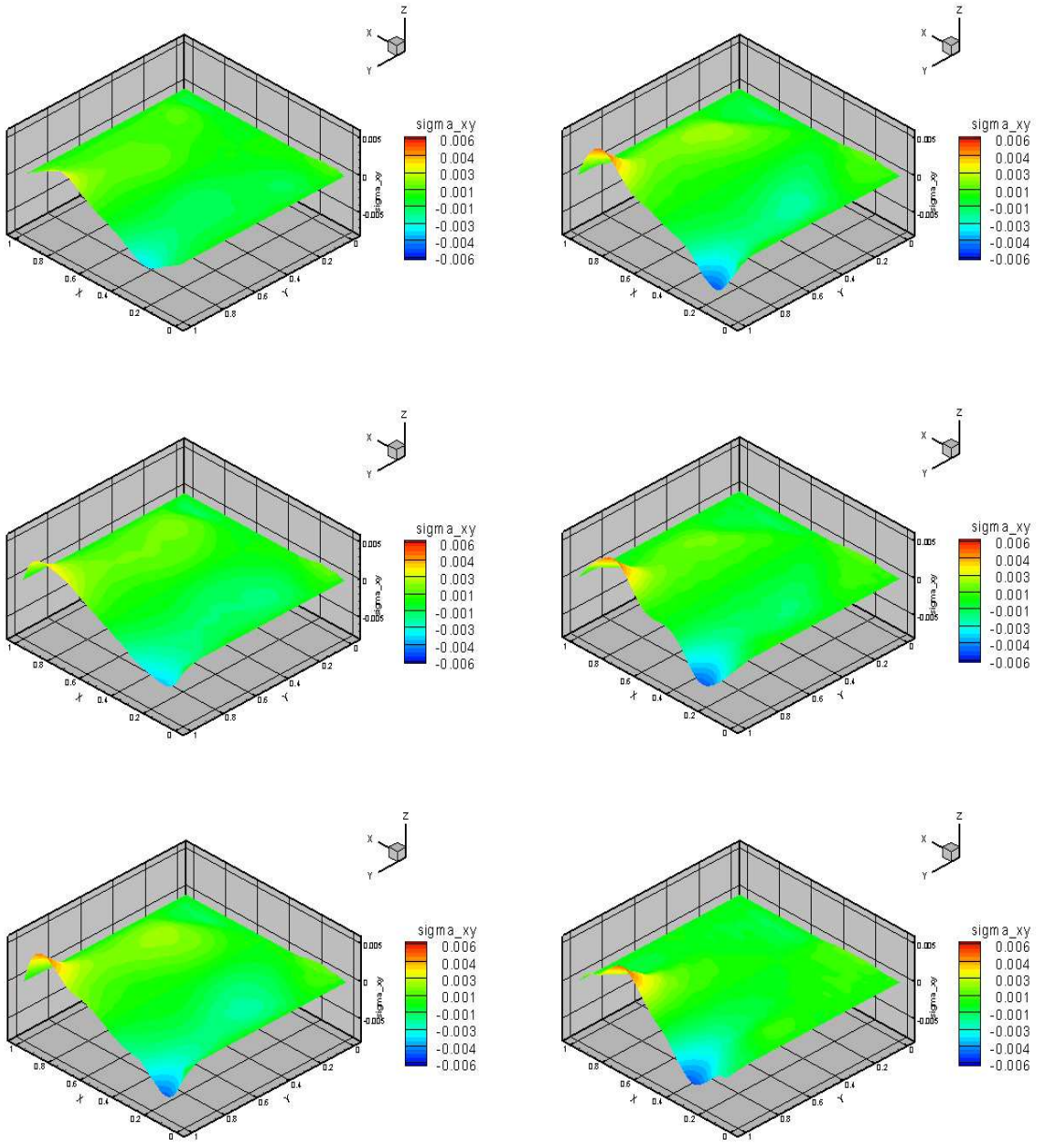

Figure 6.51: Model Problem 4, case (b) : $\nu = 0.3$ and $\sigma_{yy} = 0.01$: Evolution of σ_{xy} : Upper Convected Stress Rate - Time steps from 13^{th} to 18^{th}

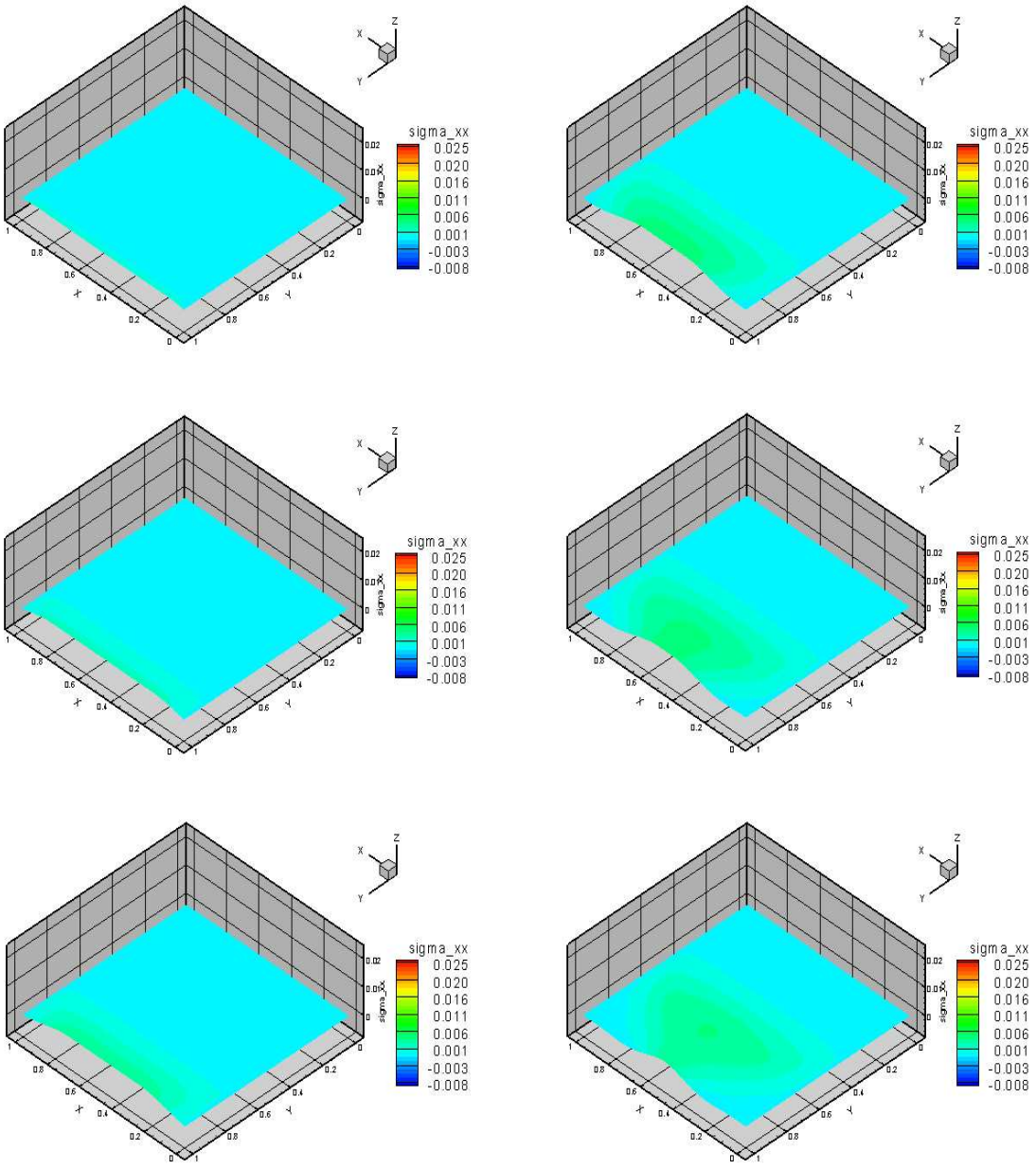

Figure 6.52: Model Problem 4, case (b) : $\nu = 0.3$ and $\sigma_{yy} = 0.01$: Evolution of σ_{xx} : Upper Convected Stress Rate - Time steps from 1^{st} to 6^{th}

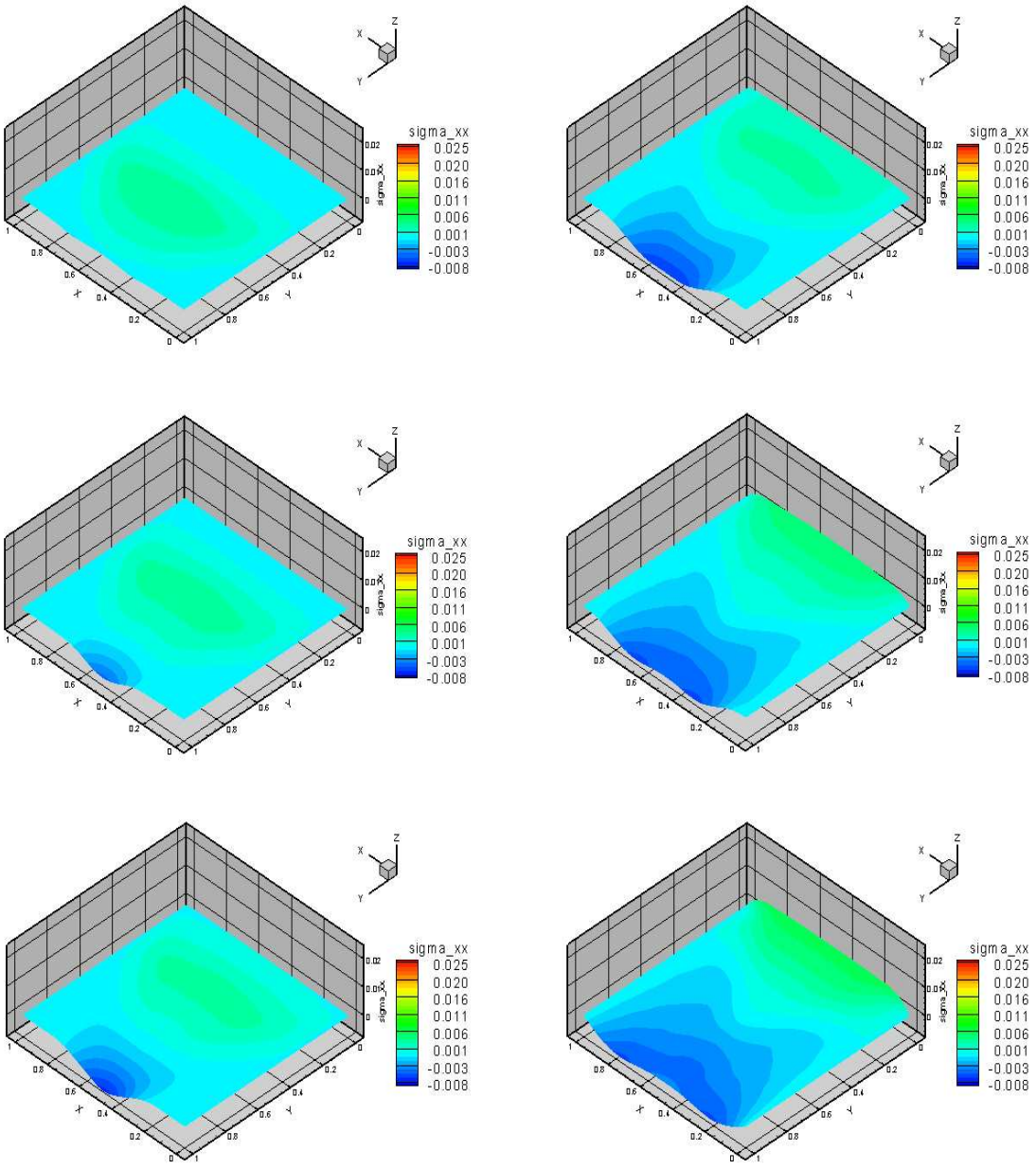

Figure 6.53: Model Problem 4, case (b) : $\nu = 0.3$ and $\sigma_{yy} = 0.01$: Evolution of σ_{xx} : Upper Convected Stress Rate - Time steps from 7^{th} to 12^{th}

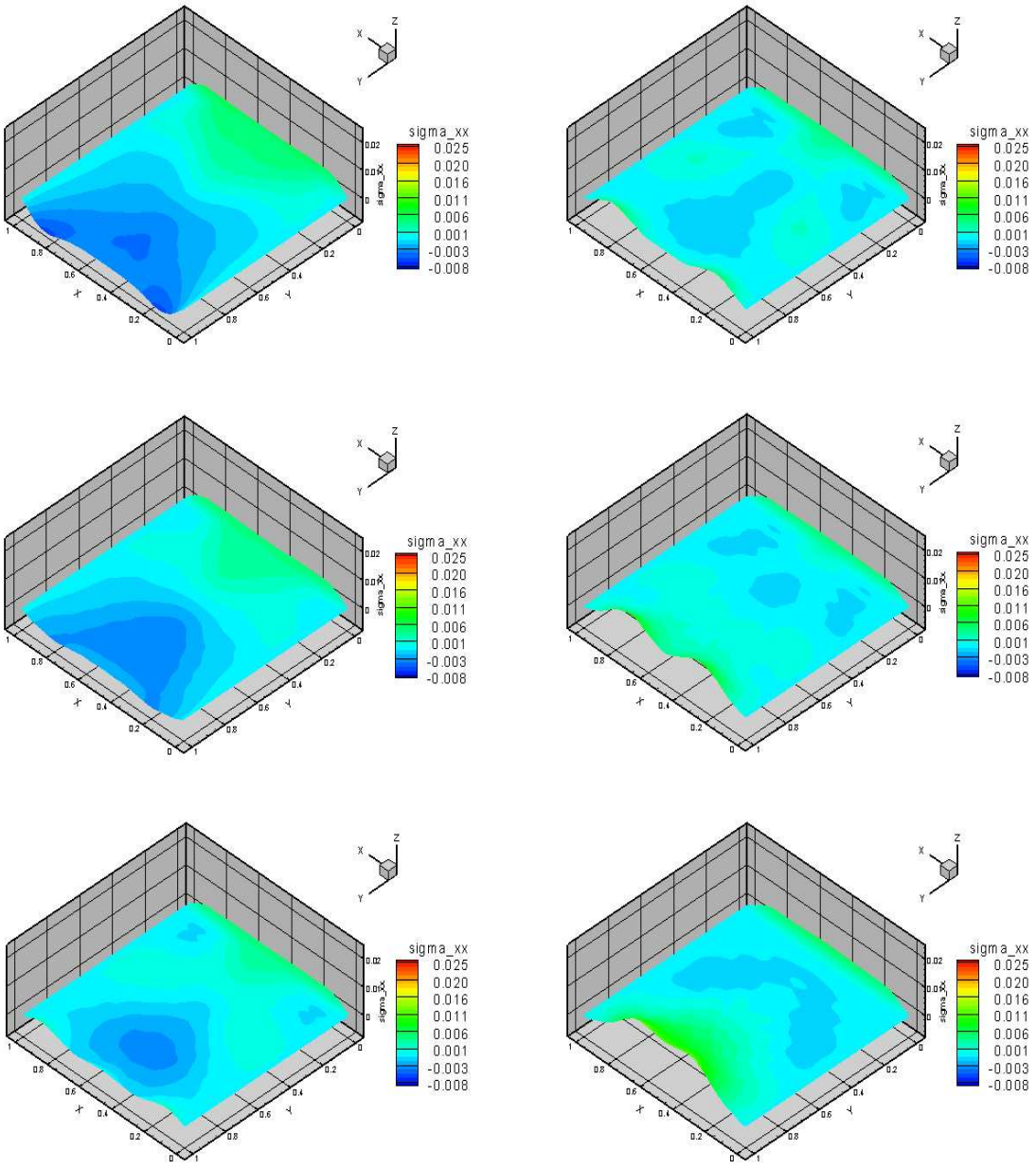

Figure 6.54: Model Problem 4, case (b) : $\nu = 0.3$ and $\sigma_{yy} = 0.01$: Evolution of σ_{xx} : Upper Convected Stress Rate - Time steps from 13^{th} to 18^{th}

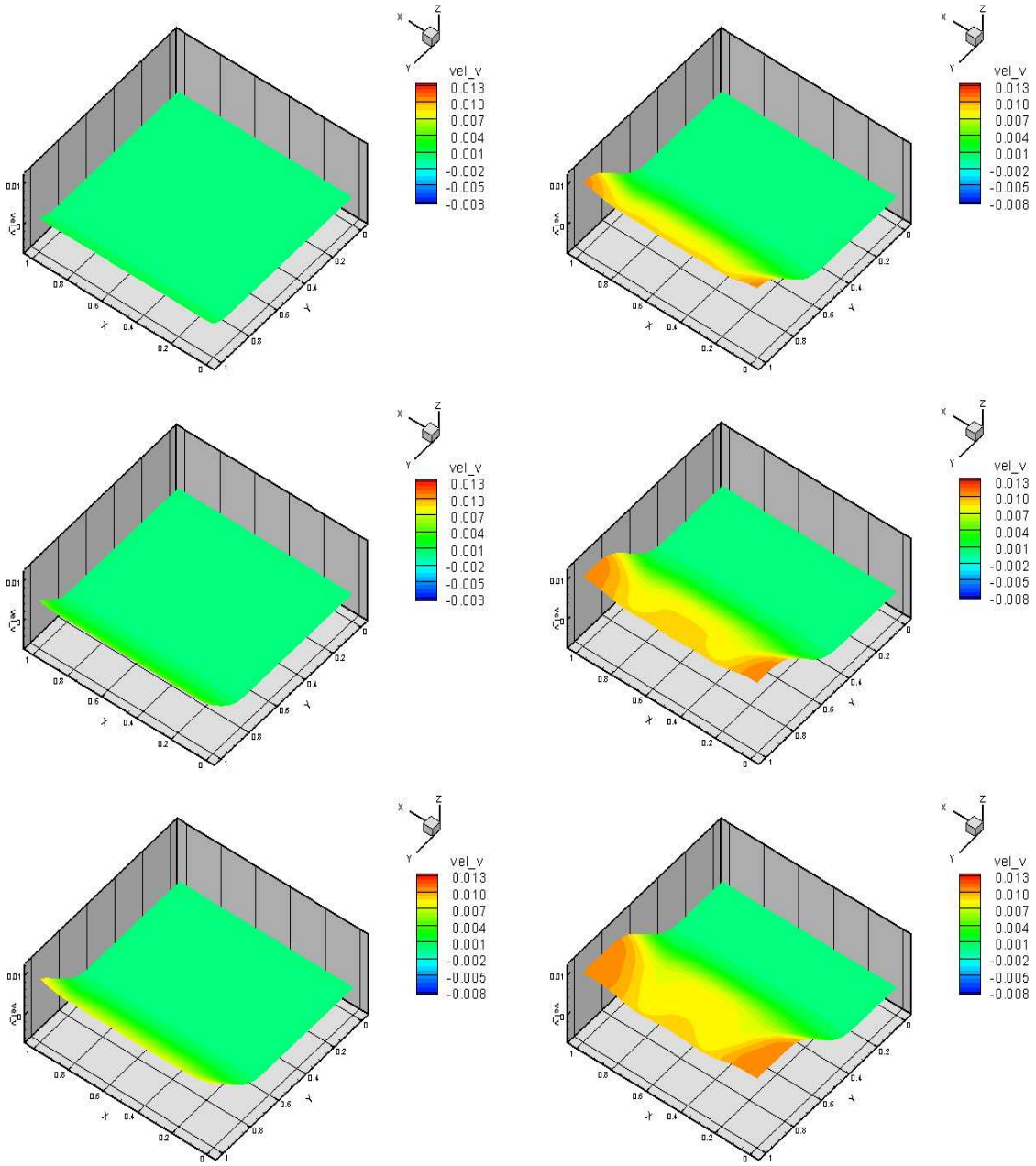

Figure 6.55: Model Problem 4, case (b) : $\nu = 0.3$ and $\sigma_{yy} = 0.01$: Evolution of v : Upper Convected Stress Rate - Time steps from 1^{st} to 6^{th}

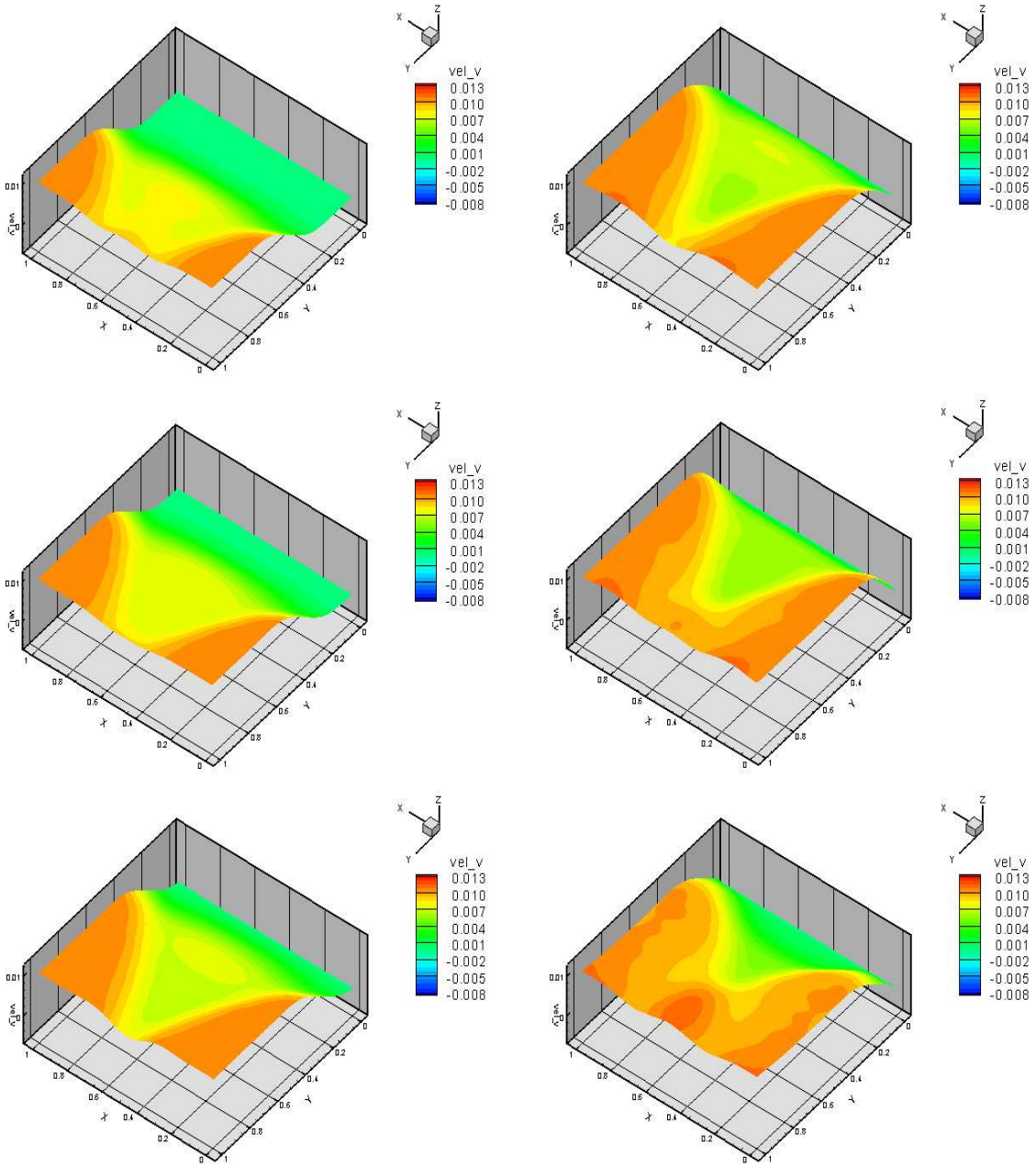

Figure 6.56: Model Problem 4, case (b) : $\nu = 0.3$ and $\sigma_{yy} = 0.01$: Evolution of v : Upper Convected Stress Rate - Time steps from 7^{th} to 12^{th}

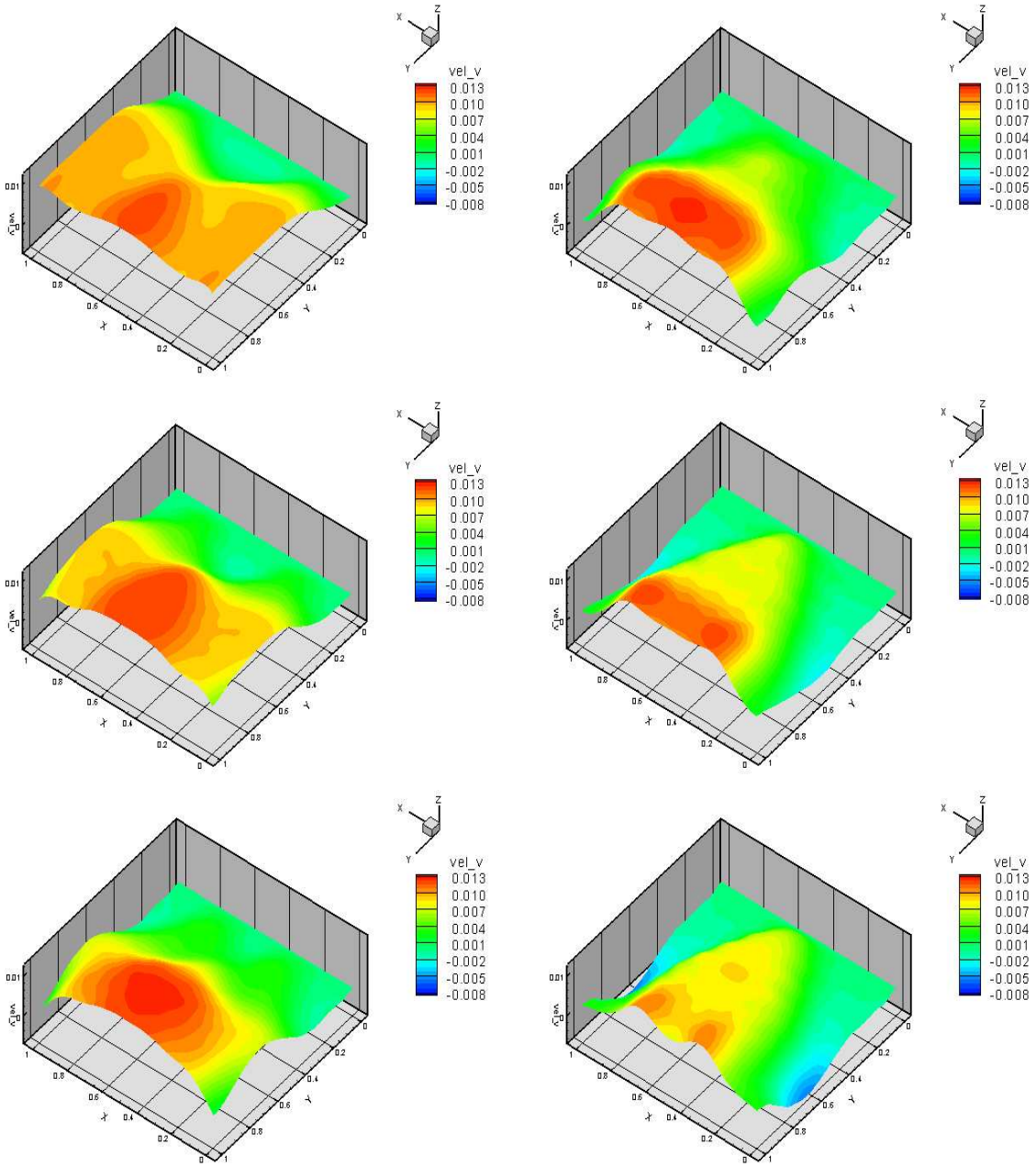

Figure 6.57: Model Problem 4, case (b) : $\nu = 0.3$ and $\sigma_{yy} = 0.01$: Evolution of v : Upper Convected Stress Rate - Time steps from 13^{th} to 18^{th}

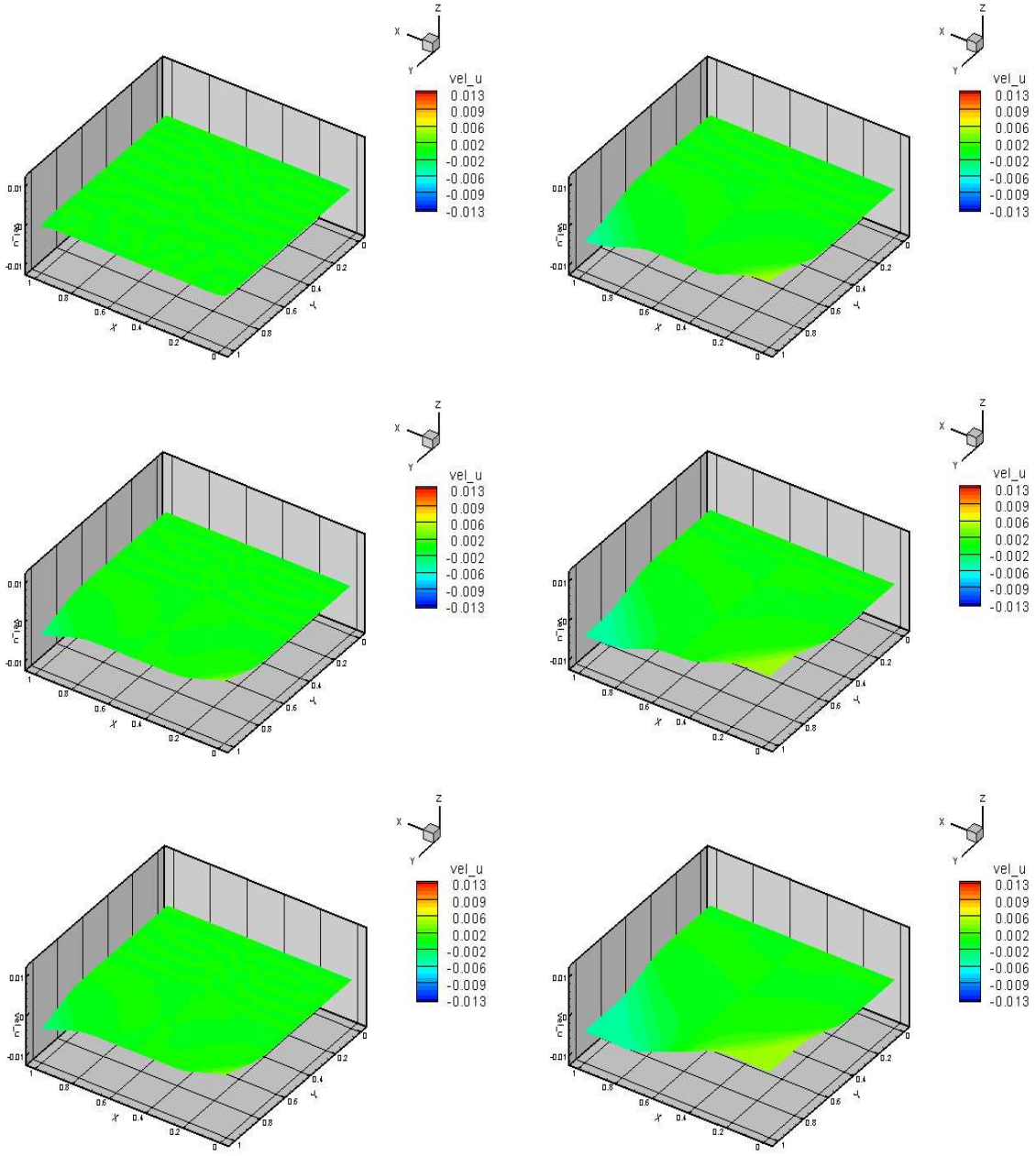

Figure 6.58: Model Problem 4, case (b) : $\nu = 0.3$ and $\sigma_{yy} = 0.01$: Evolution of u : Upper Convected Stress Rate - Time steps from 1^{st} to 6^{th}

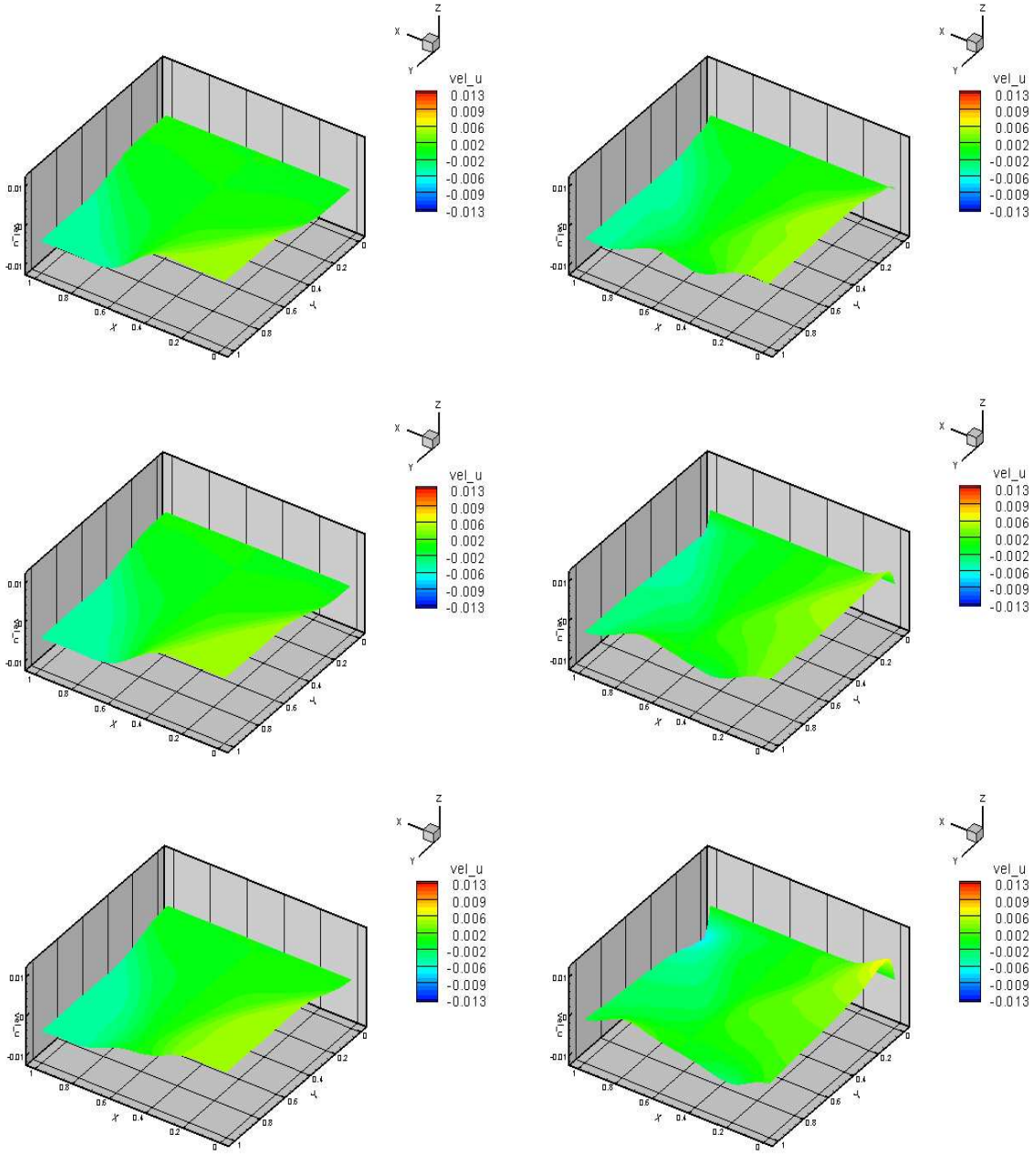

Figure 6.59: Model Problem 4, case (b) : $\nu = 0.3$ and $\sigma_{yy} = 0.01$: Evolution of u : Upper Convected Stress Rate - Time steps from 7^{th} to 12^{th}

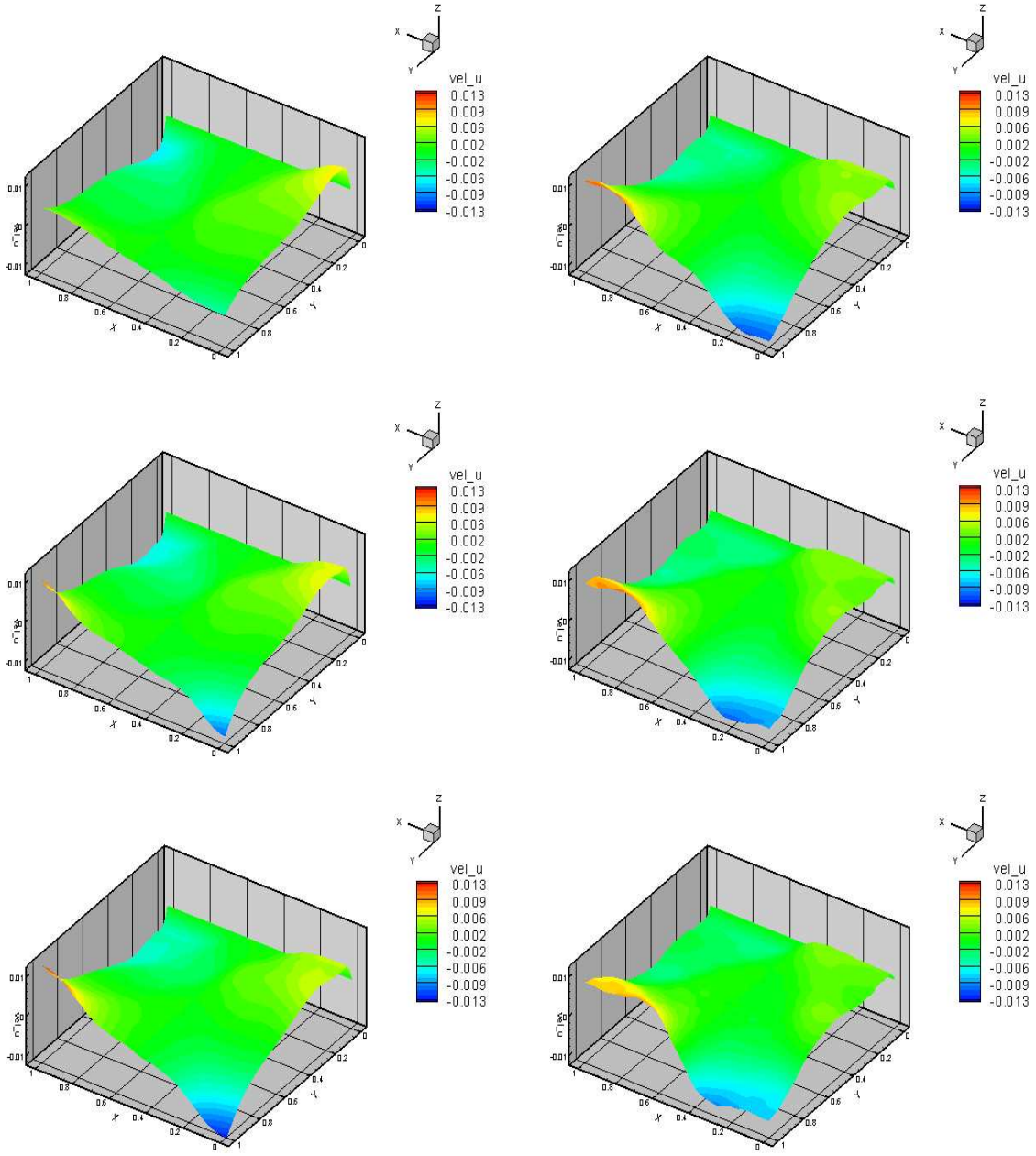

Figure 6.60: Model Problem 4, case (b) : $\nu = 0.3$ and $\sigma_{yy} = 0.01$: Evolution of u : Upper Convected Stress Rate - Time steps from 13^{th} to 18^{th}

6.5 Model Problem 5

In this study we consider the same model problem as in Section 6.4 but σ_{yy} is a parabolic distribution. All other details remain the same as in case of model problem 4. Figure 6.61 shows a schematic of the model problem, boundary conditions and the loading. Material properties, choices of reference quantities, dimensionless properties and the reference parameters are also shown in Figure 6.61.

In view of the studies presented in Section 6.3 and 6.4, we only consider upper Convected Constitutive rate equations in this study for the following two cases,

Case (a) : Poisson's ratio of 0.0

Case (b) : Poisson's ratio of 0.3

Choice of discretization, p-levels, orders of the space and time increment Δt are same as in case of model problem 4 (also see Figure 6.61). The objective of this study is to illustrate that a more complex loading may yield a complicated evolution but no difficulties are encountered in simulating it.

6.5.1 Case (a): Poisson's ratio $\nu = 0.0$

Figures 6.62-6.64 : σ_{yy}

Figures 6.65-6.67 : σ_{xy}

Figures 6.68-6.70 : σ_{xx}

Figures 6.71-6.73 : v

Figures 6.74-6.75 : u

Complexities in the wave formulations, propagation and specially upon reflection are quite clear from the results but no difficulties are encountered in their simulations. Symmetries of σ_{yy}, v, and σ_{xx} and antisymmetries of σ_{xy} and u about yz plane are clearly observed during the entire evolution. Even though ν=0.0, the effects transverse to yz plane are clearly observed.

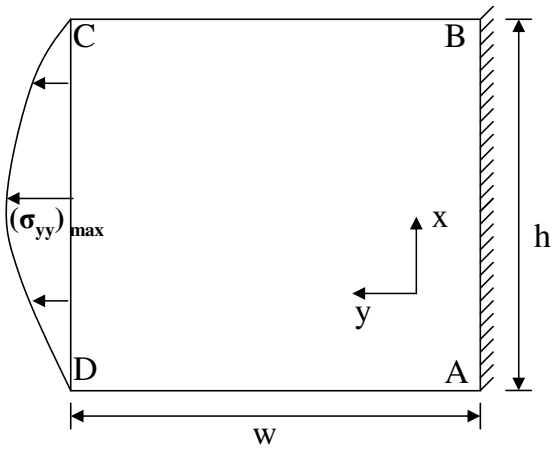

Boundary Conditions :

CD : $(\sigma_{yy})_{max} = 0.01$; applied stress

AD : $\sigma_{xx} = 0$; $\tau_{xy} = 0$; free surface

BC : $\sigma_{xx} = 0$; $\tau_{xy} = 0$; free surface

AB : $u = 0$; $v = 0$; $\tau_{xy} = 0$; fix end

Material Properties :

$$\hat{\rho} = 7860 \ \ kg/m^3$$

$$\hat{E} = 2 \times 10^{11} \ Pa$$

Dimensionless Properties :

$$h = 1 \quad ; \ w = 1 \quad ; \ \rho = 1$$

$$E = 1 \quad ; \ \nu = 0.3$$

Reference Properties :

$$\rho_0 = 7860 \ kg/m^3$$

$$E_0 = 2 \times 10^{11} \ Pa$$

$$u_0 = 5044.3 \ m/s$$

$$\tau_0 = 2 \times 10^{11} \ Pa$$

Figure 6.61: 2-D Elastic Wave Propagation, Model Problem 5 (parabolic load) : C^{11} with p-levels of 3 ; 10×10 uniform mesh ; $\Delta t = 0.1$

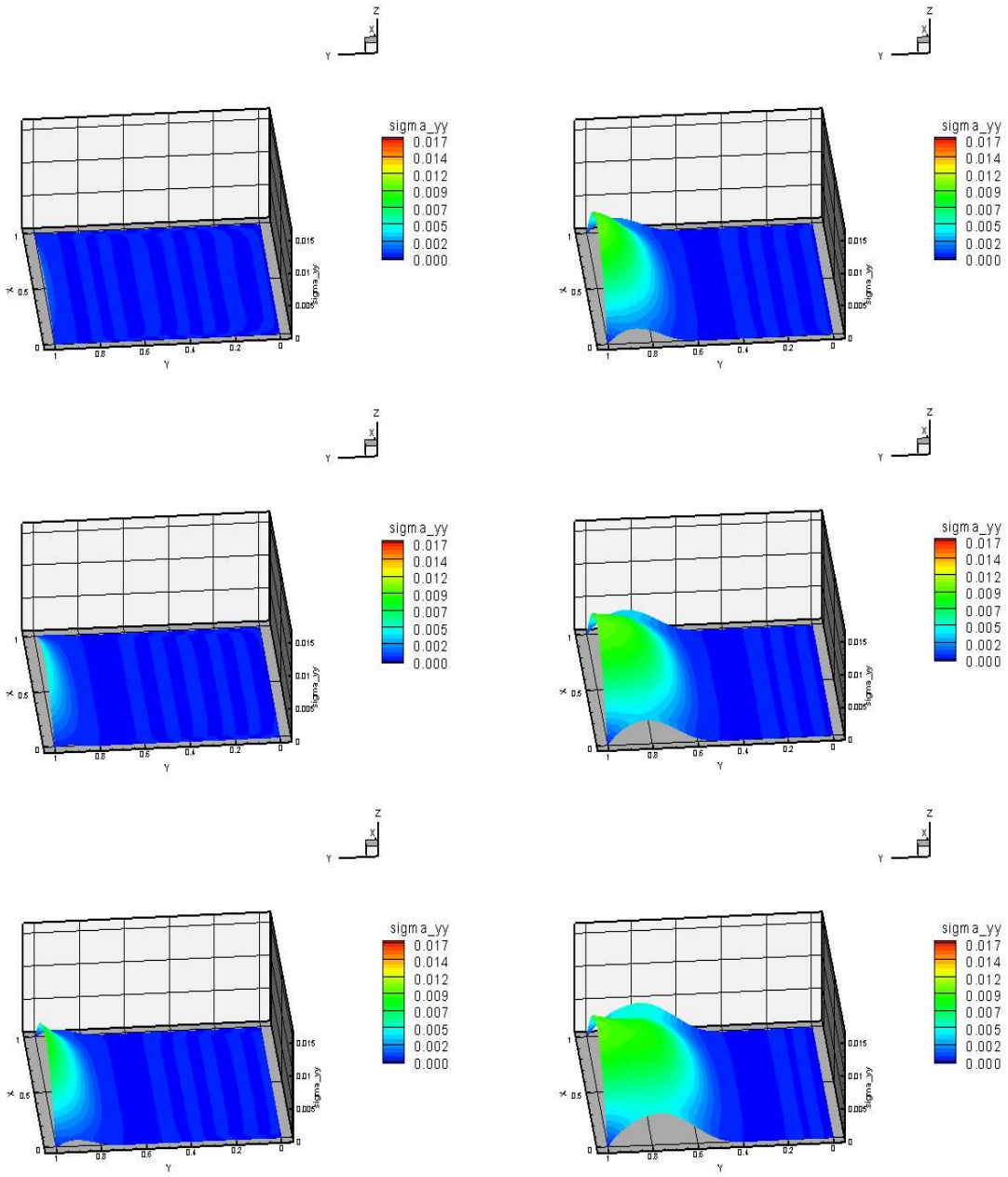

Figure 6.62: Model Problem 5, case (a) : $\nu = 0.0$ and $(\sigma_{yy})_{max} = 0.01$ (parabolic) : Evolution of σ_{yy} : Upper Convected Stress Rate - Time steps from 1^{st} to 6^{th}

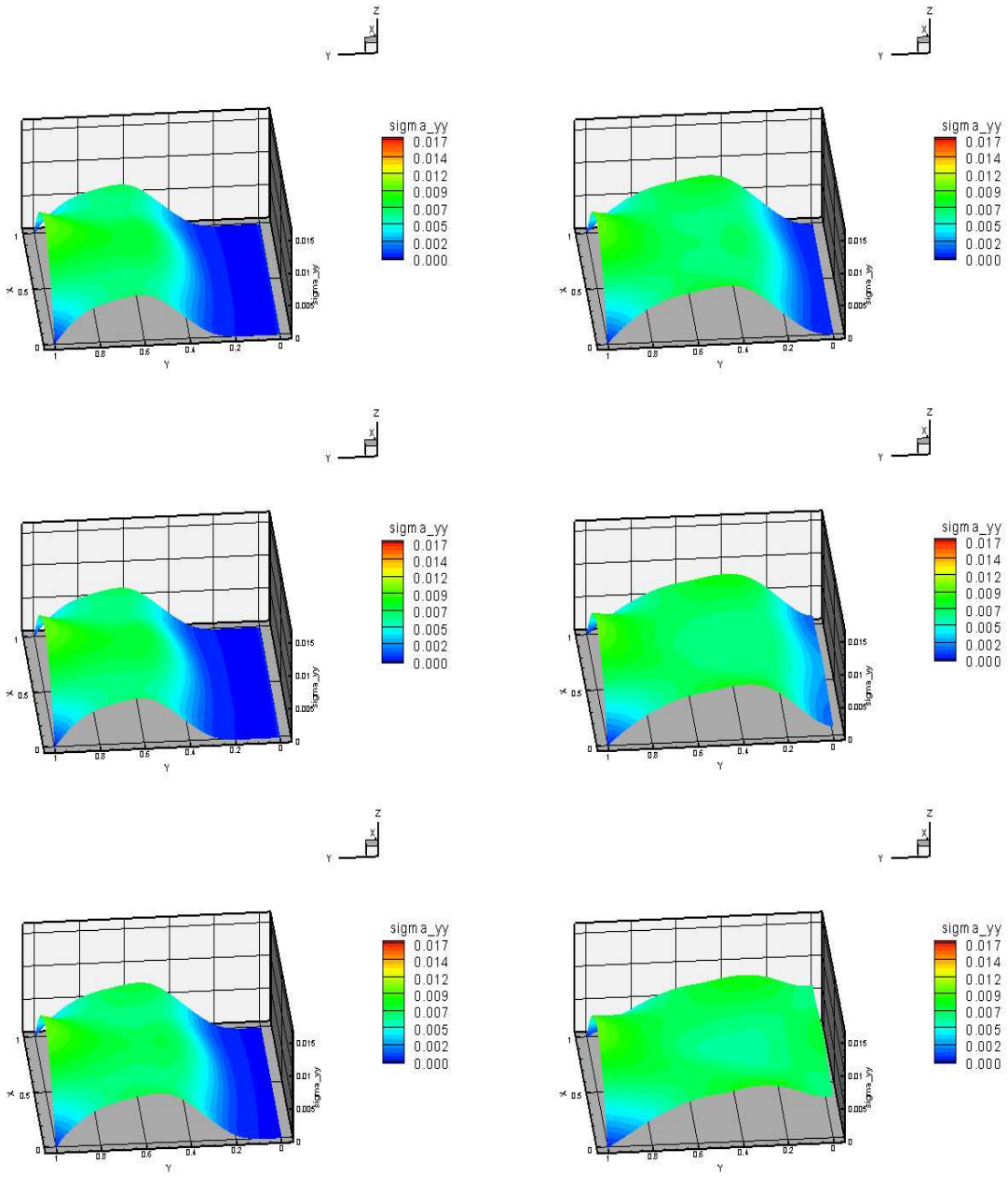

Figure 6.63: Model Problem 5, case (a) : $\nu = 0.0$ and $(\sigma_{yy})_{max} = 0.01$ (parabolic) : Evolution of σ_{yy} : Upper Convected Stress Rate - Time steps from 7^{th} to 12^{th}

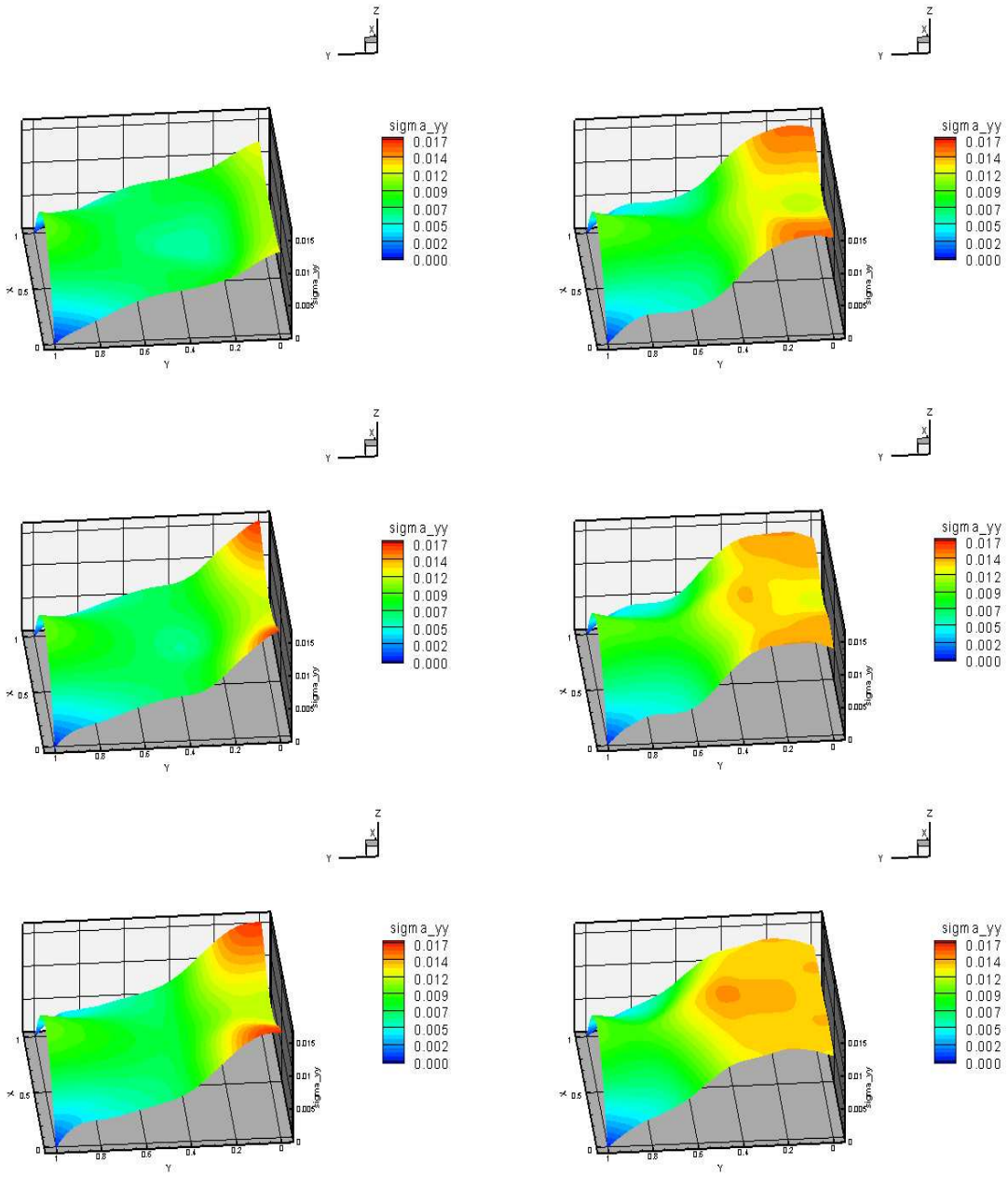

Figure 6.64: Model Problem 5, case (a) : $\nu = 0.0$ and $(\sigma_{yy})_{max} = 0.01$ (parabolic) : Evolution of σ_{yy} : Upper Convected Stress Rate - Time steps from 13^{th} to 18^{th}

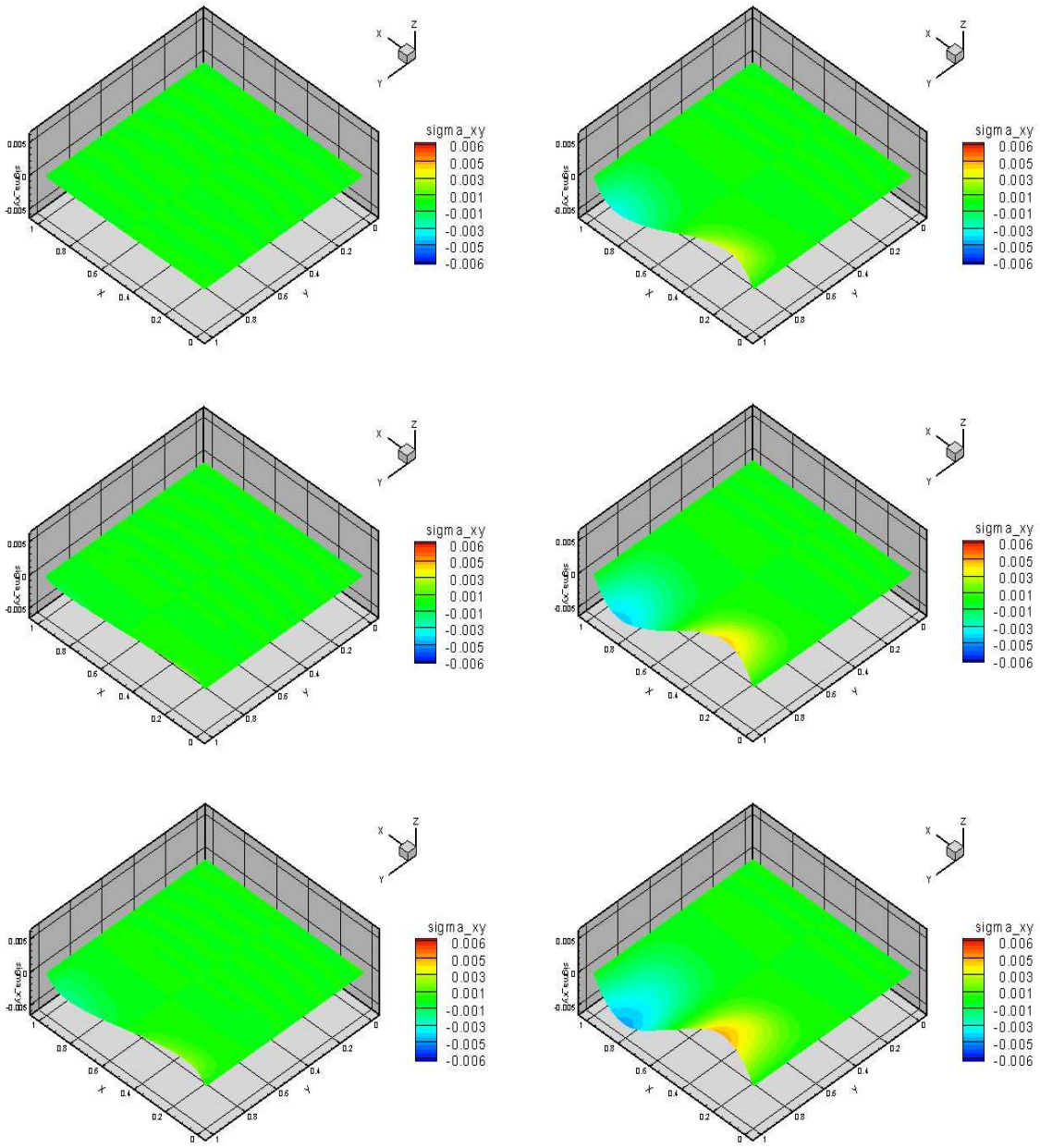

Figure 6.65: Model Problem 5, case (a) : $\nu = 0.0$ and $(\sigma_{yy})_{max} = 0.01$ (parabolic) : Evolution of σ_{xy} : Upper Convected Stress Rate - Time steps from 1^{st} to 6^{th}

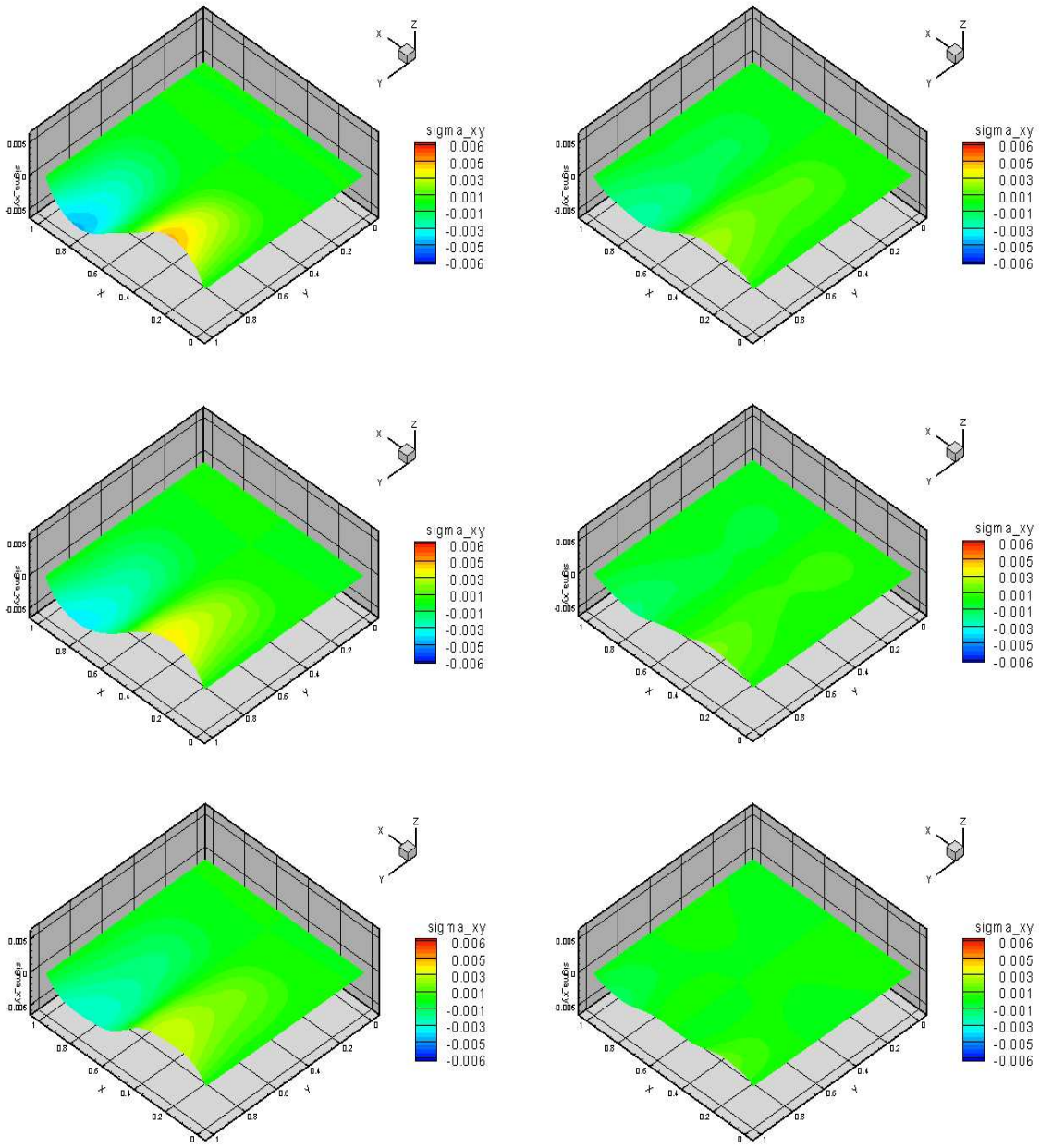

Figure 6.66: Model Problem 5, case (a) : $\nu = 0.0$ and $(\sigma_{yy})_{max} = 0.01$ (parabolic) : Evolution of σ_{xy} : Upper Convected Stress Rate - Time steps from 7^{th} to 12^{th}

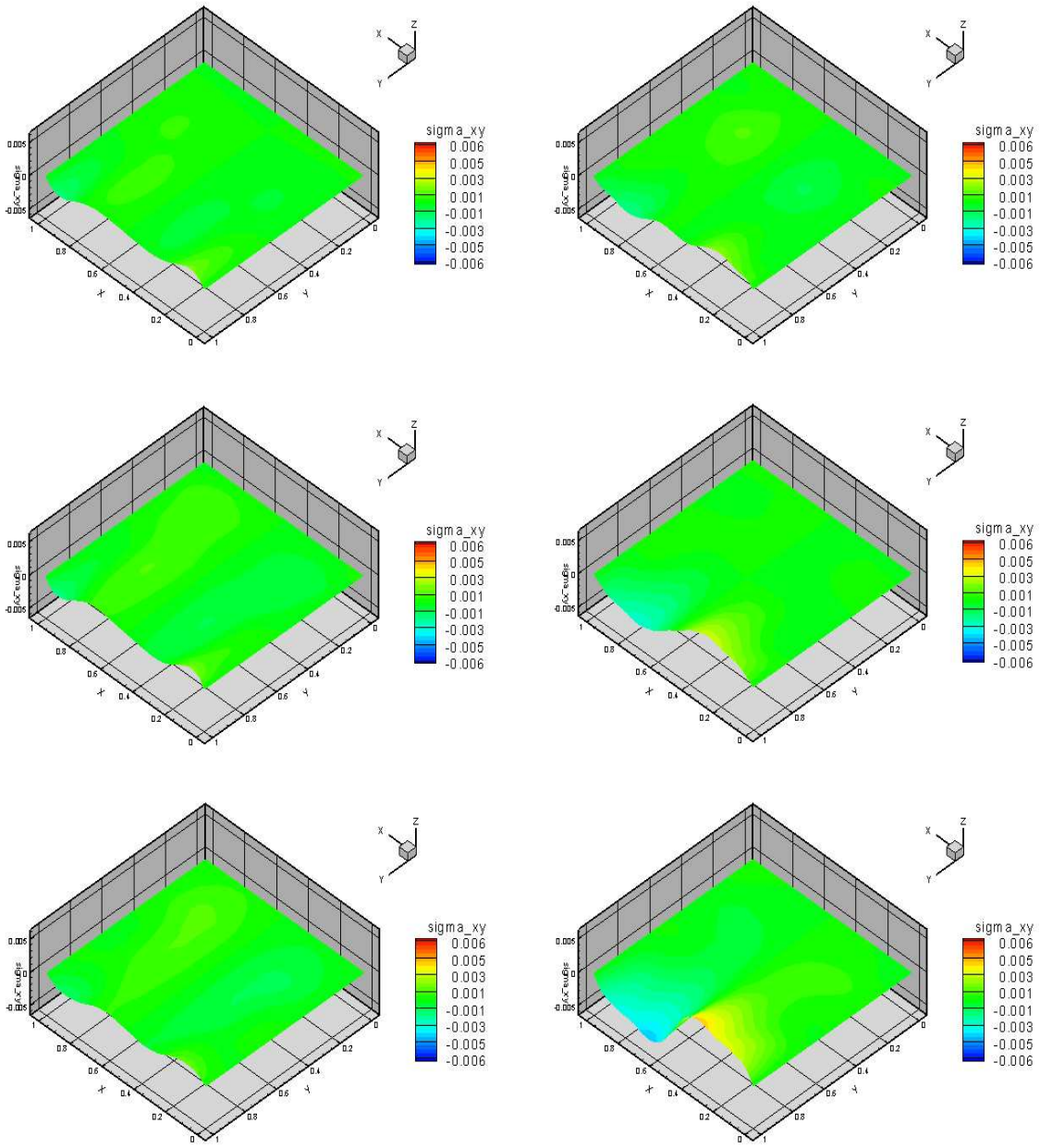

Figure 6.67: Model Problem 5, case (a) : $\nu = 0.0$ and $(\sigma_{yy})_{max} = 0.01$ (parabolic) : Evolution of σ_{xy} : Upper Convected Stress Rate - Time steps from 13^{th} to 18^{th}

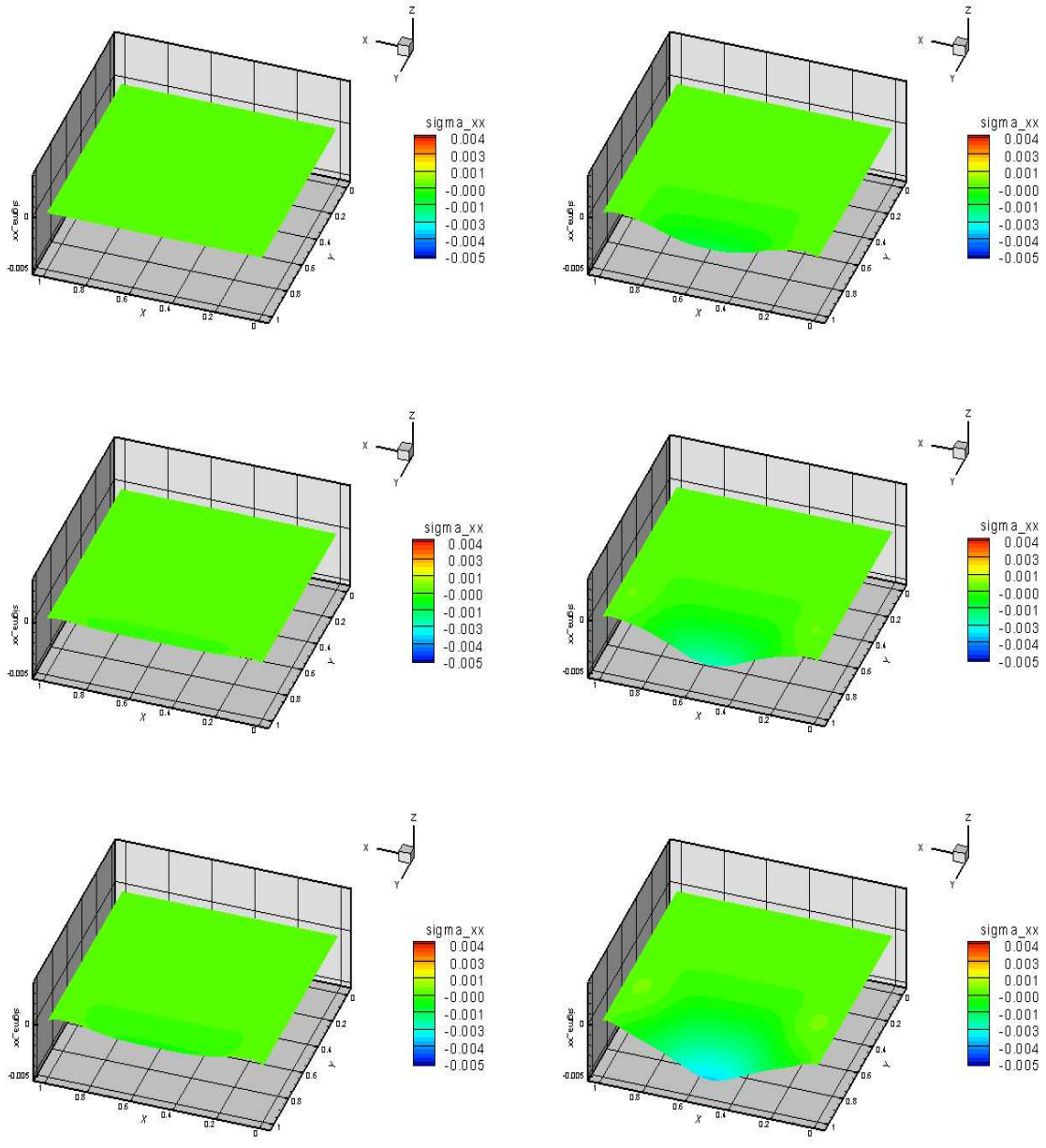

Figure 6.68: Model Problem 5, case (a) : $\nu = 0.0$ and $(\sigma_{yy})_{max} = 0.01$ (parabolic) : Evolution of σ_{xx} : Upper Convected Stress Rate - Time steps from 1^{st} to 6^{th}

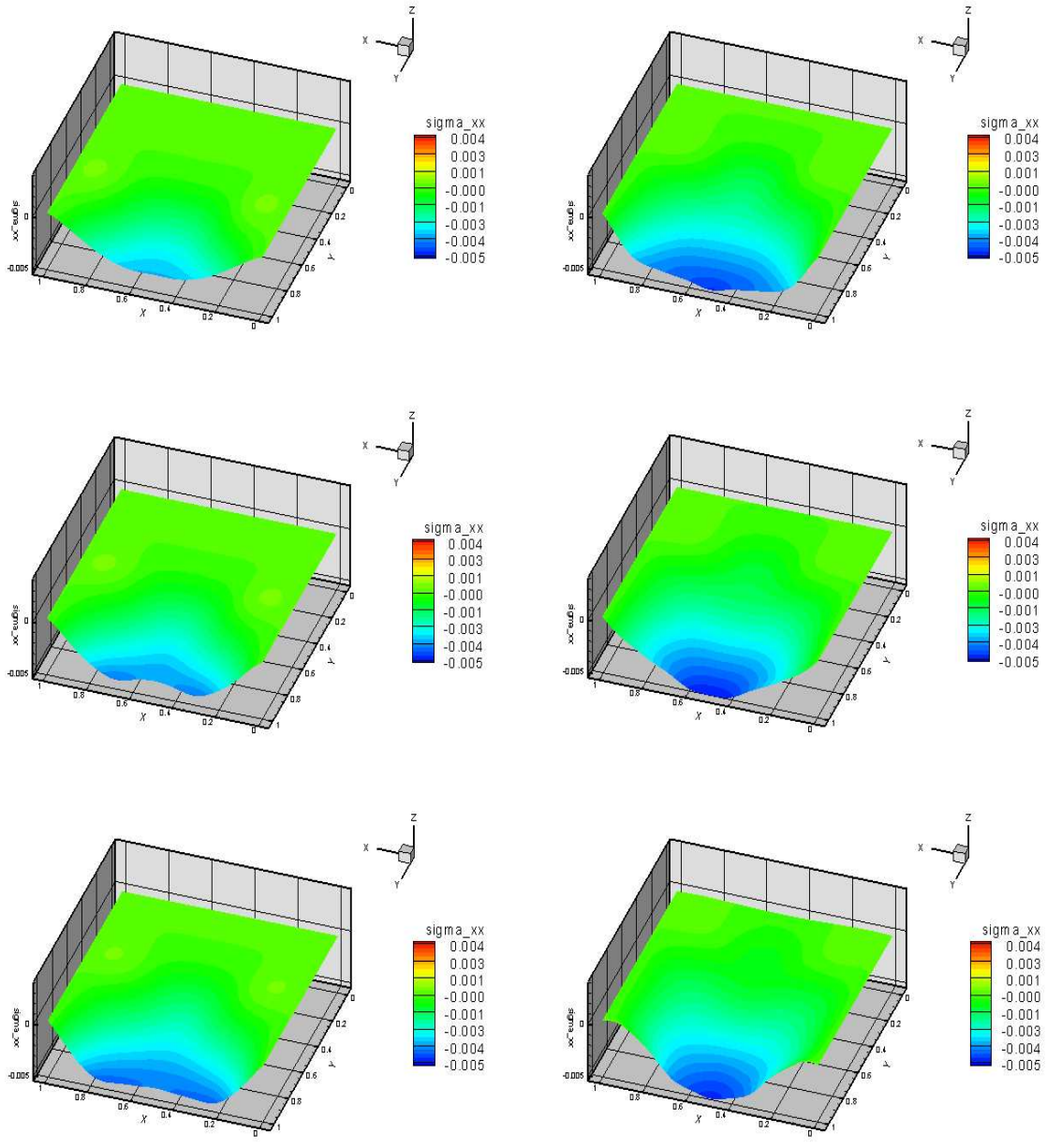

Figure 6.69: Model Problem 5, case (a) : $\nu = 0.0$ and $(\sigma_{yy})_{max} = 0.01$ (parabolic) : Evolution of σ_{xx} : Upper Convected Stress Rate - Time steps from 7^{th} to 12^{th}

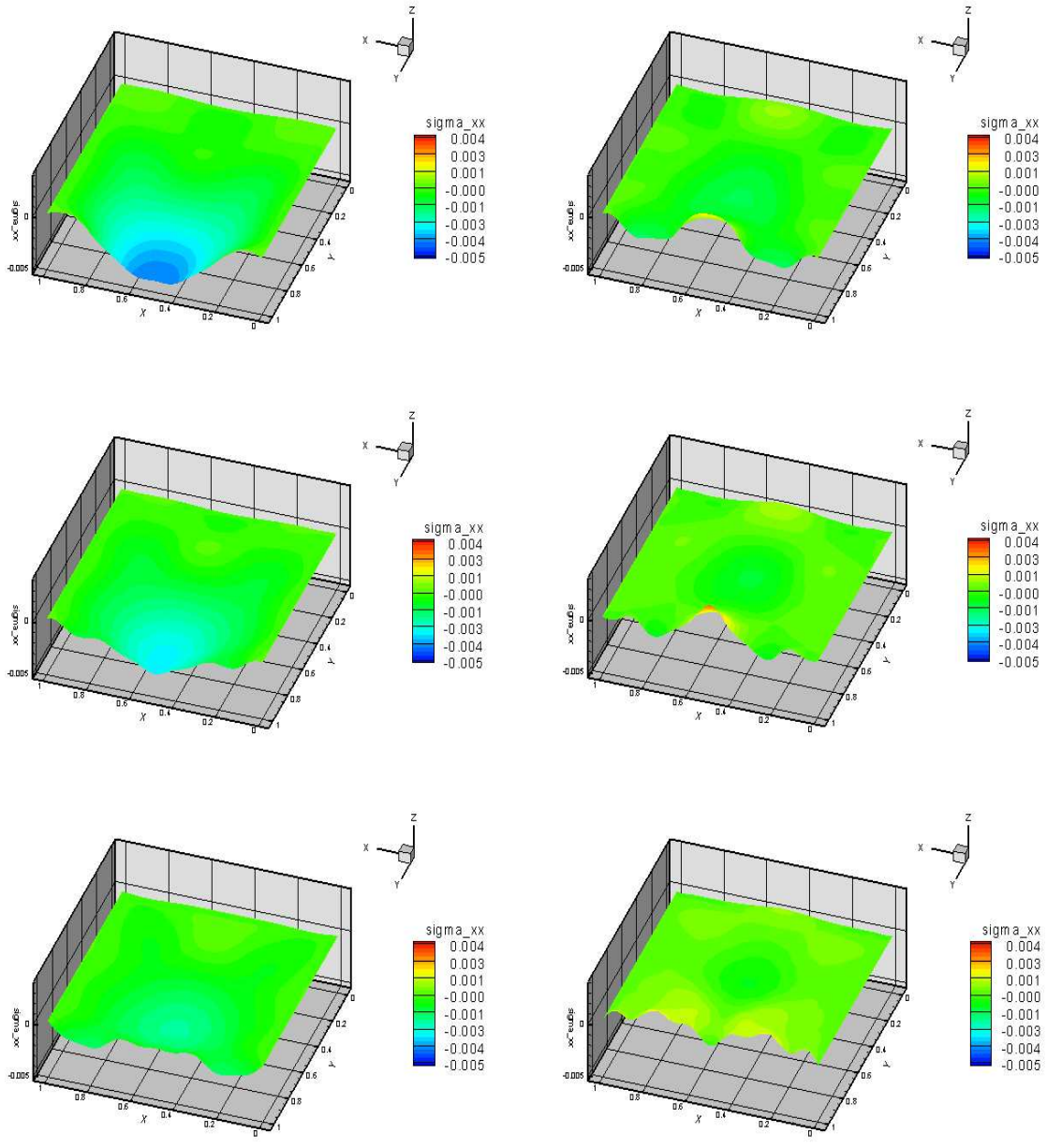

Figure 6.70: Model Problem 5, case (a) : $\nu = 0.0$ and $(\sigma_{yy})_{max} = 0.01$ (parabolic) : Evolution of σ_{xx} : Upper Convected Stress Rate - Time steps from 13^{th} to 18^{th}

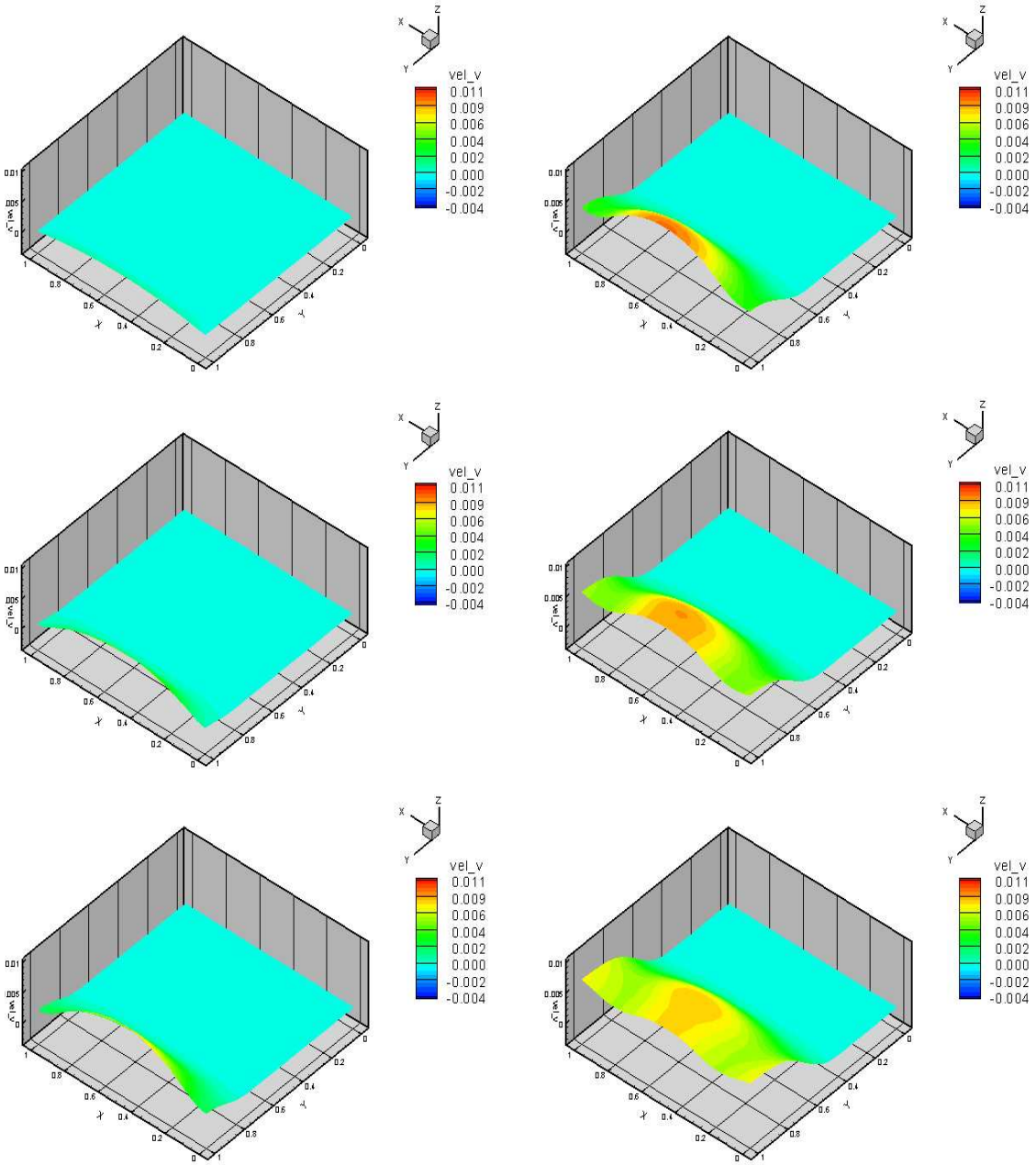

Figure 6.71: Model Problem 5, case (a) : $\nu = 0.0$ and $(\sigma_{yy})_{max} = 0.01$ (parabolic) : Evolution of v : Upper Convected Stress Rate - Time steps from 1^{st} to 6^{th}

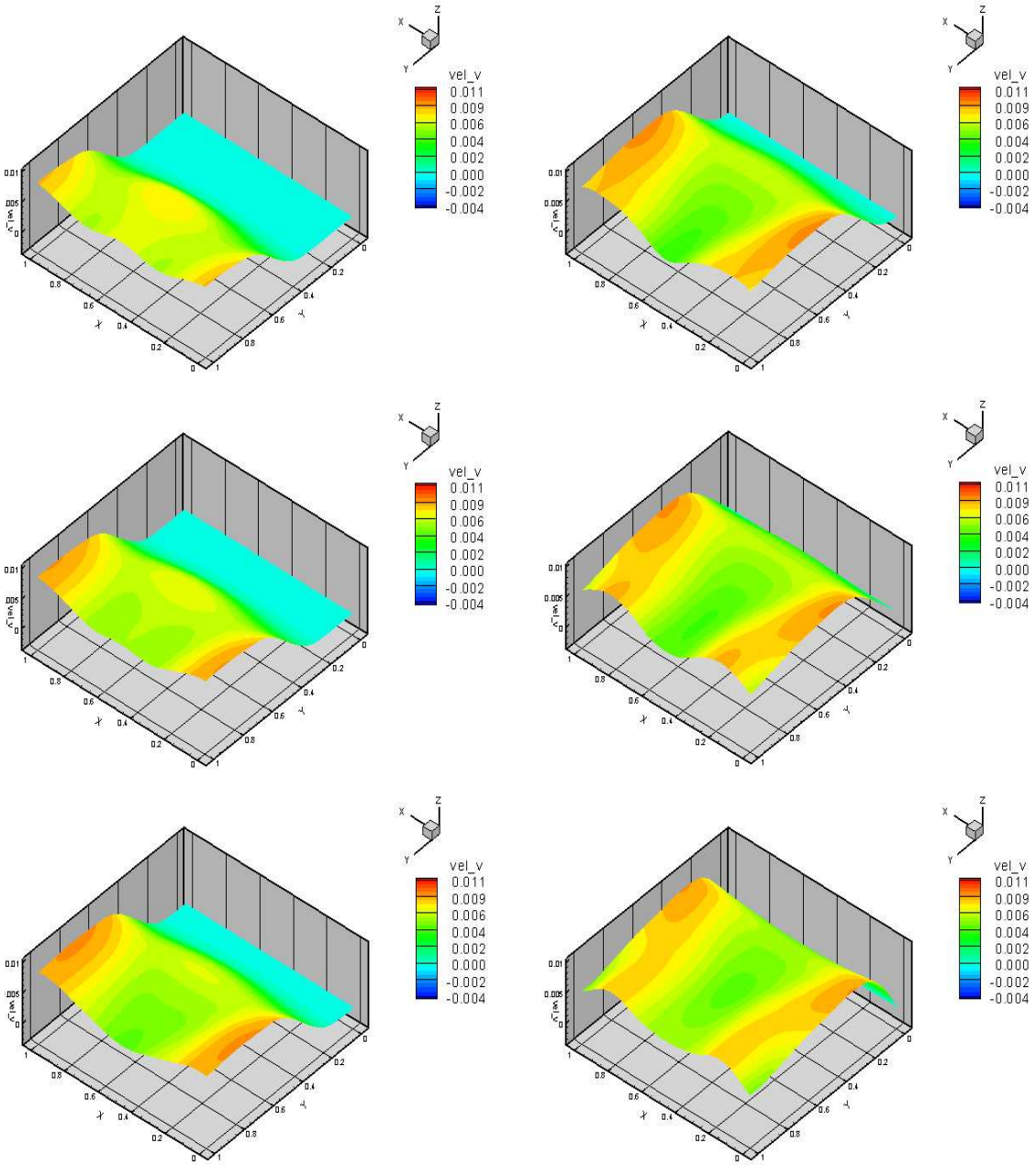

Figure 6.72: Model Problem 5, case (a) : $\nu = 0.0$ and $(\sigma_{yy})_{max} = 0.01$ (parabolic) : Evolution of v : Upper Convected Stress Rate - Time steps from 7^{th} to 12^{th}

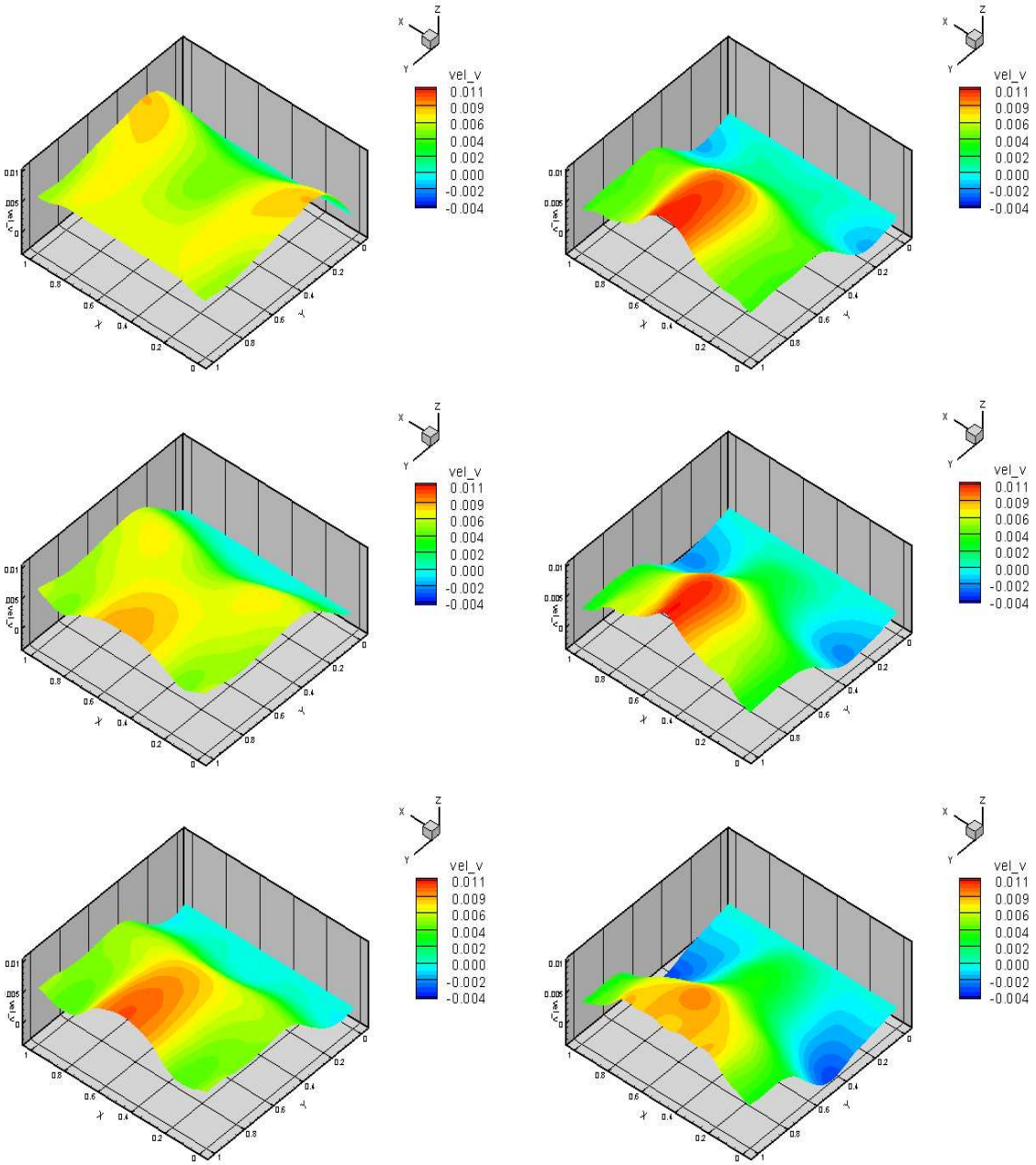

Figure 6.73: Model Problem 5, case (a) : $\nu = 0.0$ and $(\sigma_{yy})_{max} = 0.01$ (parabolic) : Evolution of v : Upper Convected Stress Rate - Time steps from 13^{th} to 18^{th}

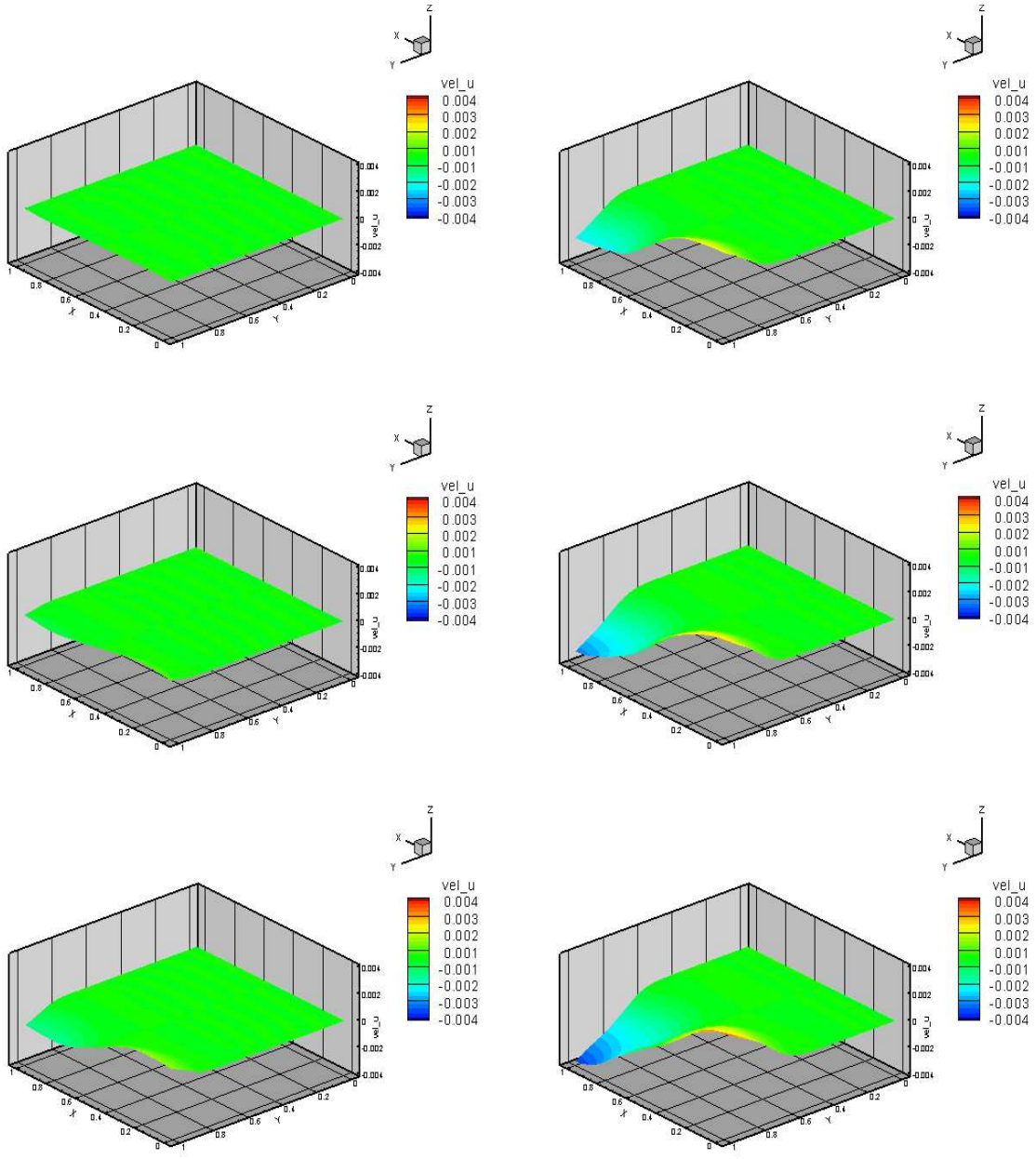

Figure 6.74: Model Problem 5, case (a) : $\nu = 0.0$ and $(\sigma_{yy})_{max} = 0.01$ (parabolic) : Evolution of u : Upper Convected Stress Rate - Time steps from 1^{st} to 6^{th}

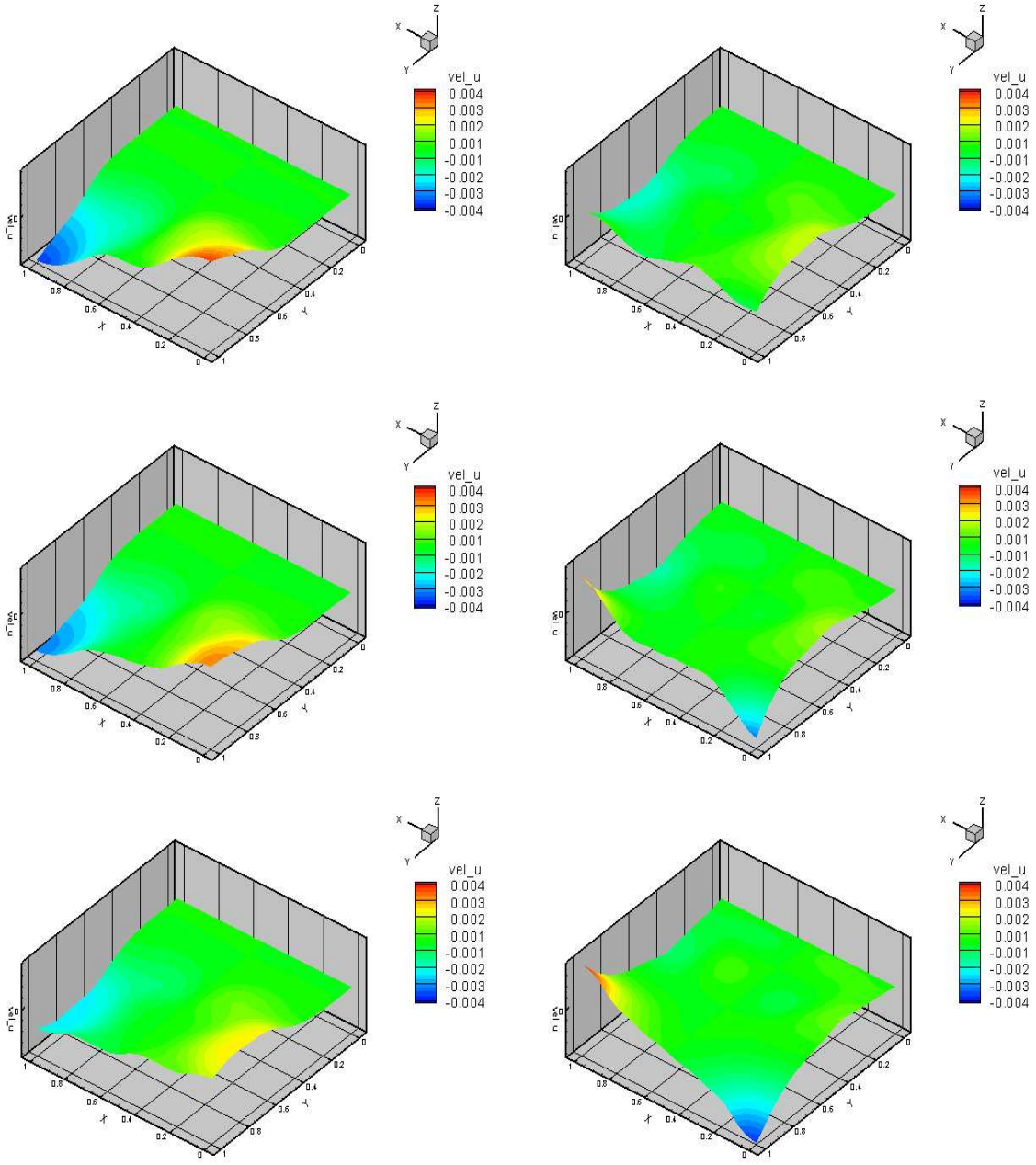

captionModel Problem 5, case (a) : $\nu = 0.0$ and $(\sigma_{yy})_{max} = 0.01$ (parabolic) : Evolution of u : Upper Convected Stress Rate - Time steps from 7^{th} to 12^{th}

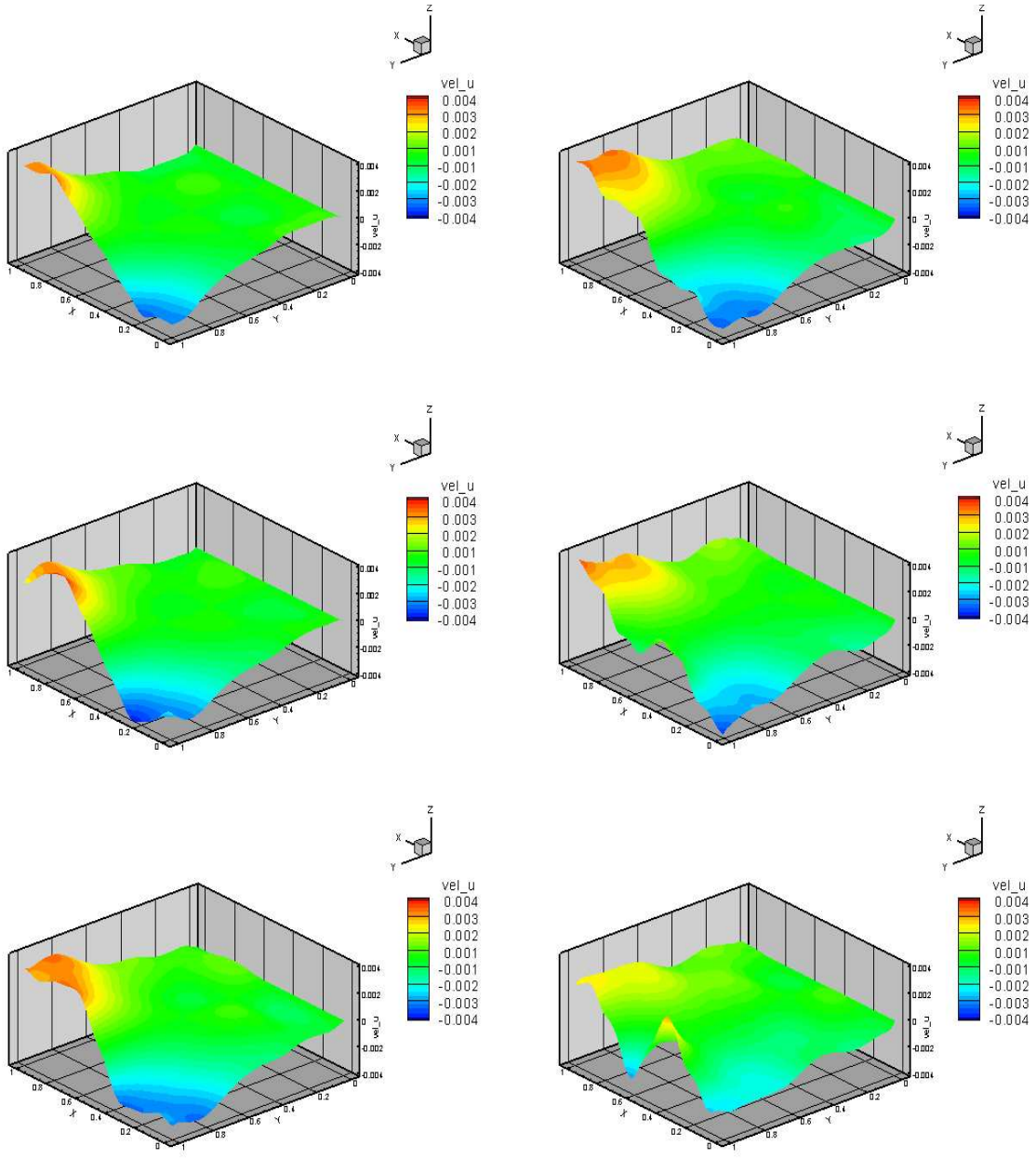

Figure 6.75: Model Problem 5, case (a) : $\nu = 0.0$ and $(\sigma_{yy})_{max} = 0.01$ (parabolic) : Evolution of u : Upper Convected Stress Rate - Time steps from 13^{th} to 18^{th}

6.5.2 Case (b): Poisson's ratio $\nu = 0.3$

The results of this study are summarized in the following figures.

Figures 6.76-6.78 : σ_{yy}

Figures 6.79-6.81 : σ_{xy}

Figures 6.82-6.84 : σ_{xx}

Figures 6.85-6.87 : v

Figures 6.88-6.90 : u

Due to non-zero Poisson's ratio, the waves, their evolutions, propagation and reflection is much more complicated compared to the case with ν=0.0 but are simulated without any difficulty. The effects transverse to yz plane are more significant in this case compared with ν=0.0. For example, σ_{xx} attains a maximum magnitude of 0.012 for ν=0.3 whereas for ν=0.0 the maximum magnitude of σ_{xx} is only 0.004. Similar behavior is observed for velocity u. We find that u_{max}=0.013 for ν=0.3 whereas for ν=0.0, u_{max} has a value of 0.004.

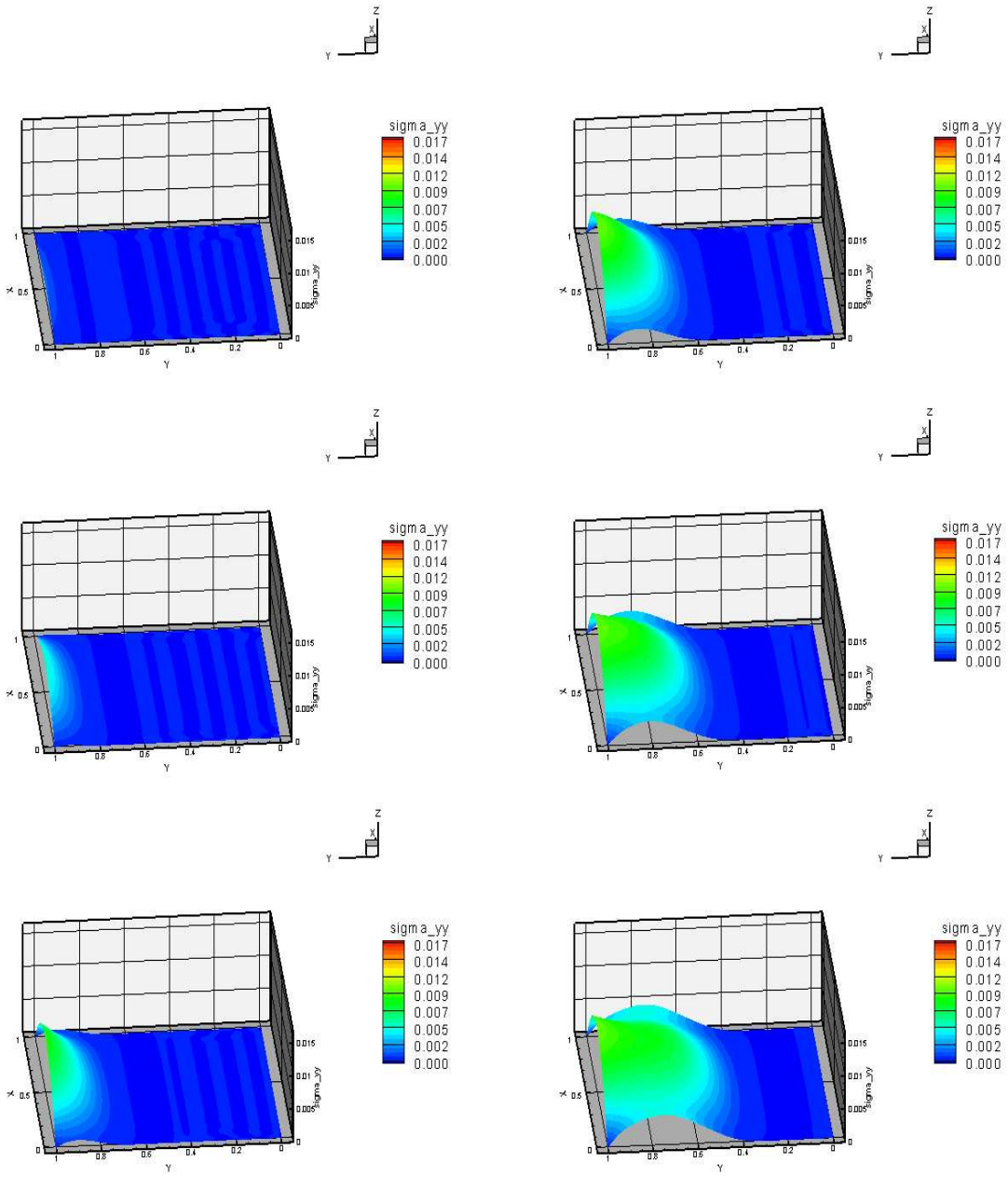

Figure 6.76: Model Problem 5, case (b) : $\nu = 0.3$ and $(\sigma_{yy})_{max} = 0.01$ (parabolic) : Evolution of σ_{yy} : Upper Convected Stress Rate - Time steps from 1^{st} to 6^{th}

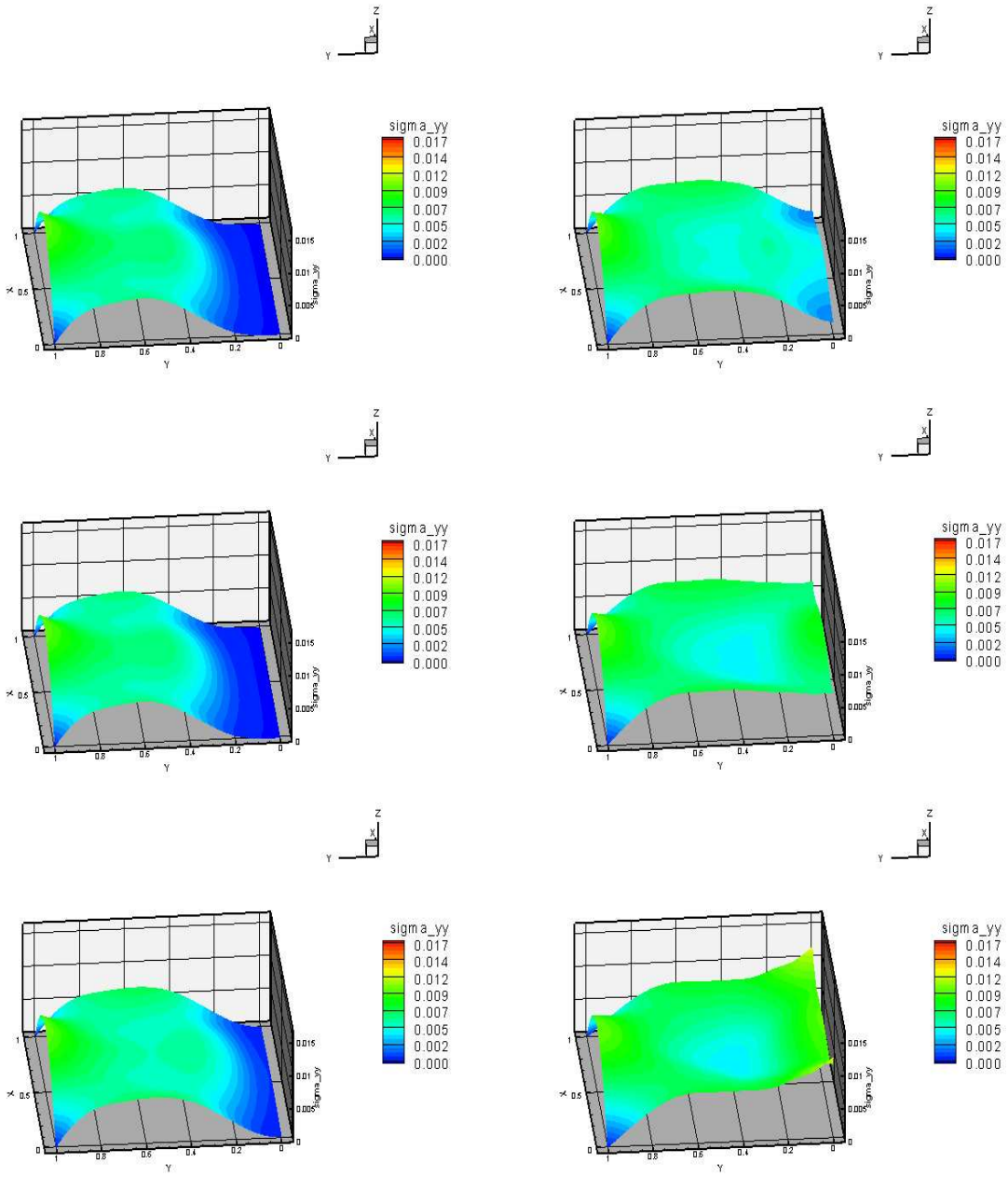

Figure 6.77: Model Problem 5, case (b) : $\nu = 0.3$ and $(\sigma_{yy})_{max} = 0.01$ (parabolic) : Evolution of σ_{yy} : Upper Convected Stress Rate - Time steps from 7^{th} to 12^{th}

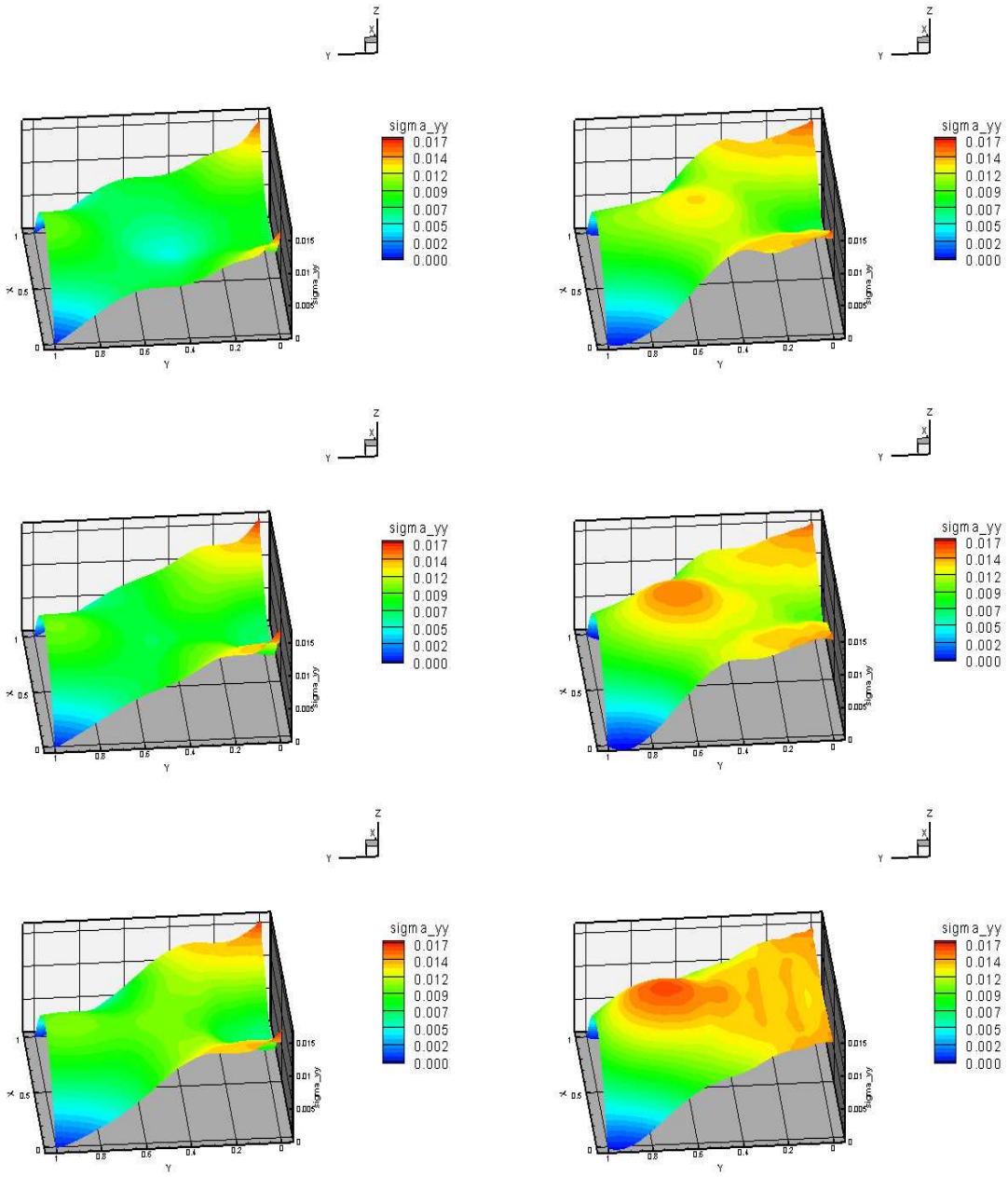

Figure 6.78: Model Problem 5, case (b) : $\nu = 0.3$ and $(\sigma_{yy})_{max} = 0.01$ (parabolic) : Evolution of σ_{yy} : Upper Convected Stress Rate - Time steps from 13^{th} to 18^{th}

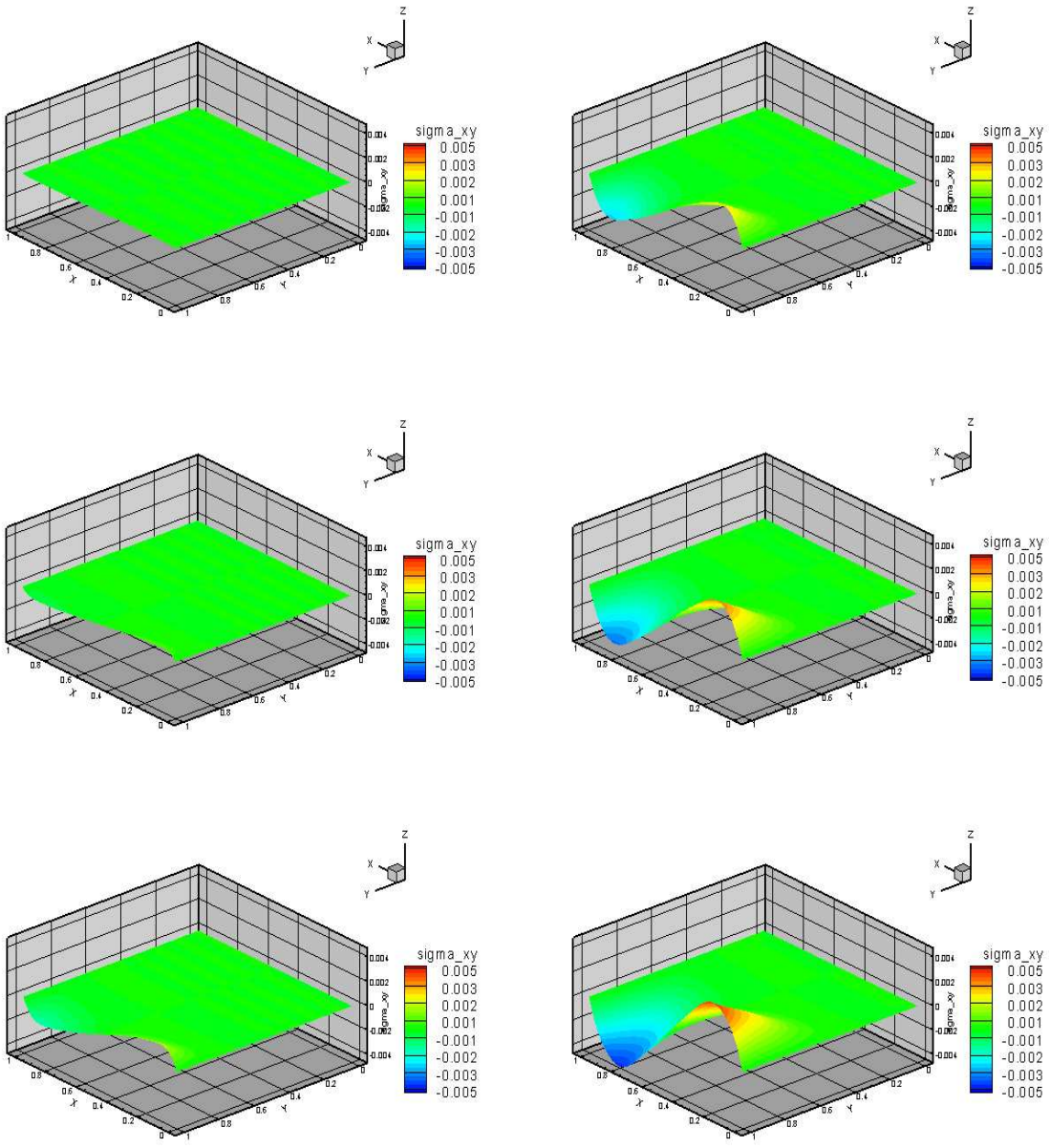

Figure 6.79: Model Problem 5, case (b) : $\nu = 0.3$ and $(\sigma_{yy})_{max} = 0.01$ (parabolic) : Evolution of σ_{xy} : Upper Convected Stress Rate - Time steps from 1^{st} to 6^{th}

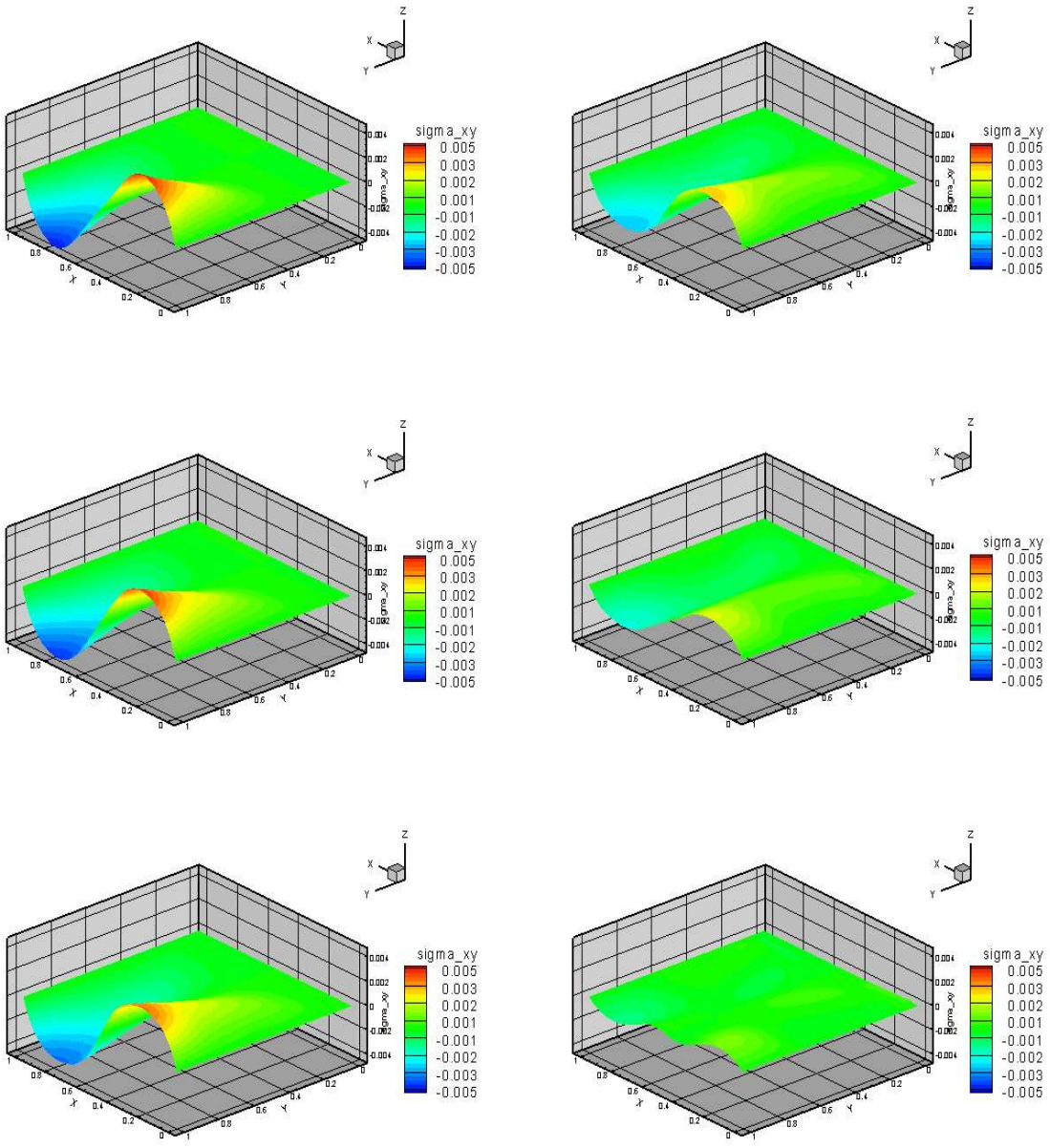

Figure 6.80: Model Problem 5, case (b) : $\nu = 0.3$ and $(\sigma_{yy})_{max} = 0.01$ (parabolic) : Evolution of σ_{xy} : Upper Convected Stress Rate - Time steps from 7^{th} to 12^{th}

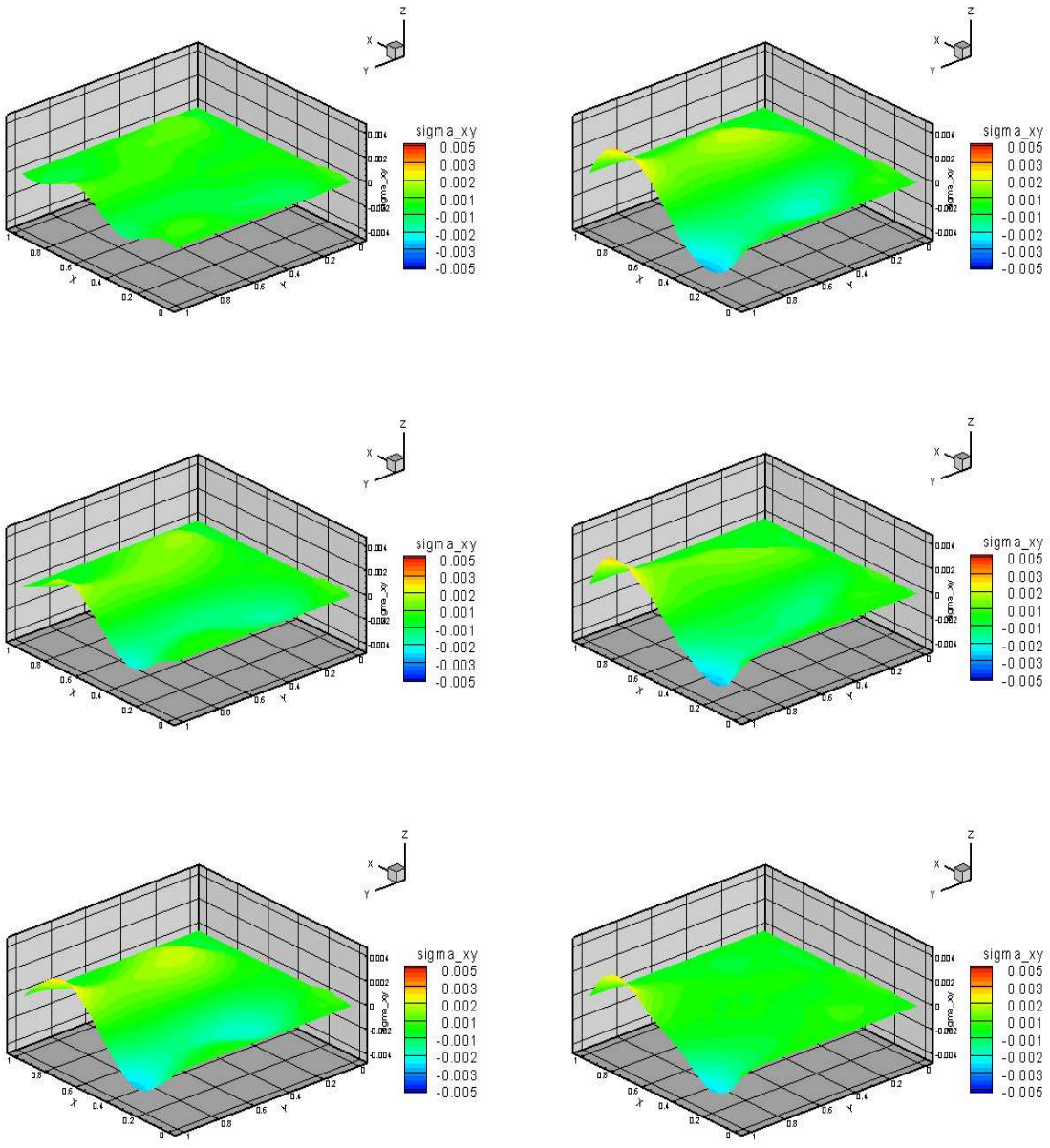

Figure 6.81: Model Problem 5, case (b) : $\nu = 0.3$ and $(\sigma_{yy})_{max} = 0.01$ (parabolic) : Evolution of σ_{xy} : Upper Convected Stress Rate - Time steps from 13^{th} to 18^{th}

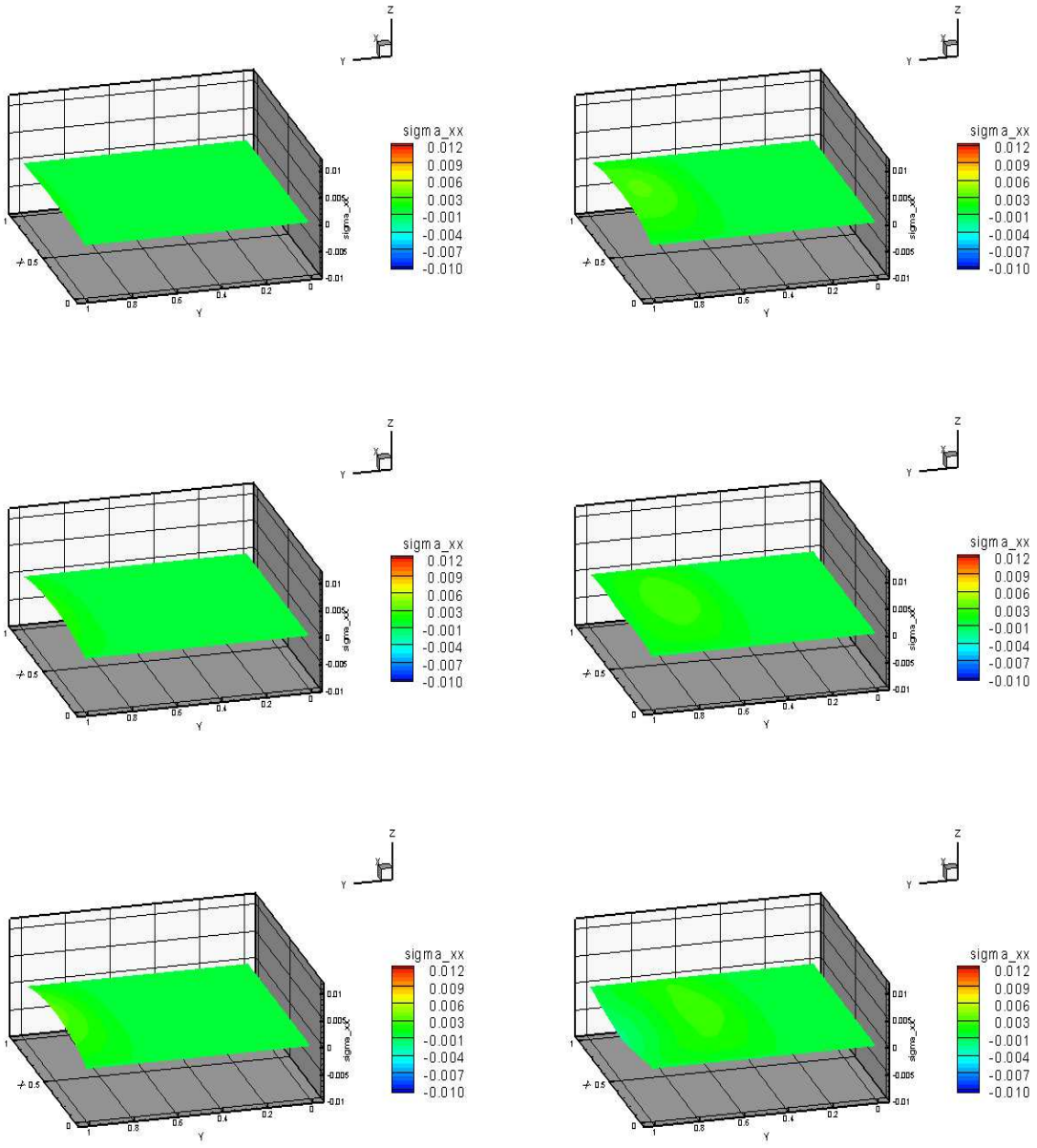

Figure 6.82: Model Problem 5, case (b) : $\nu = 0.3$ and $(\sigma_{yy})_{max} = 0.01$ (parabolic) : Evolution of σ_{xx} : Upper Convected Stress Rate - Time steps from 1^{st} to 6^{th}

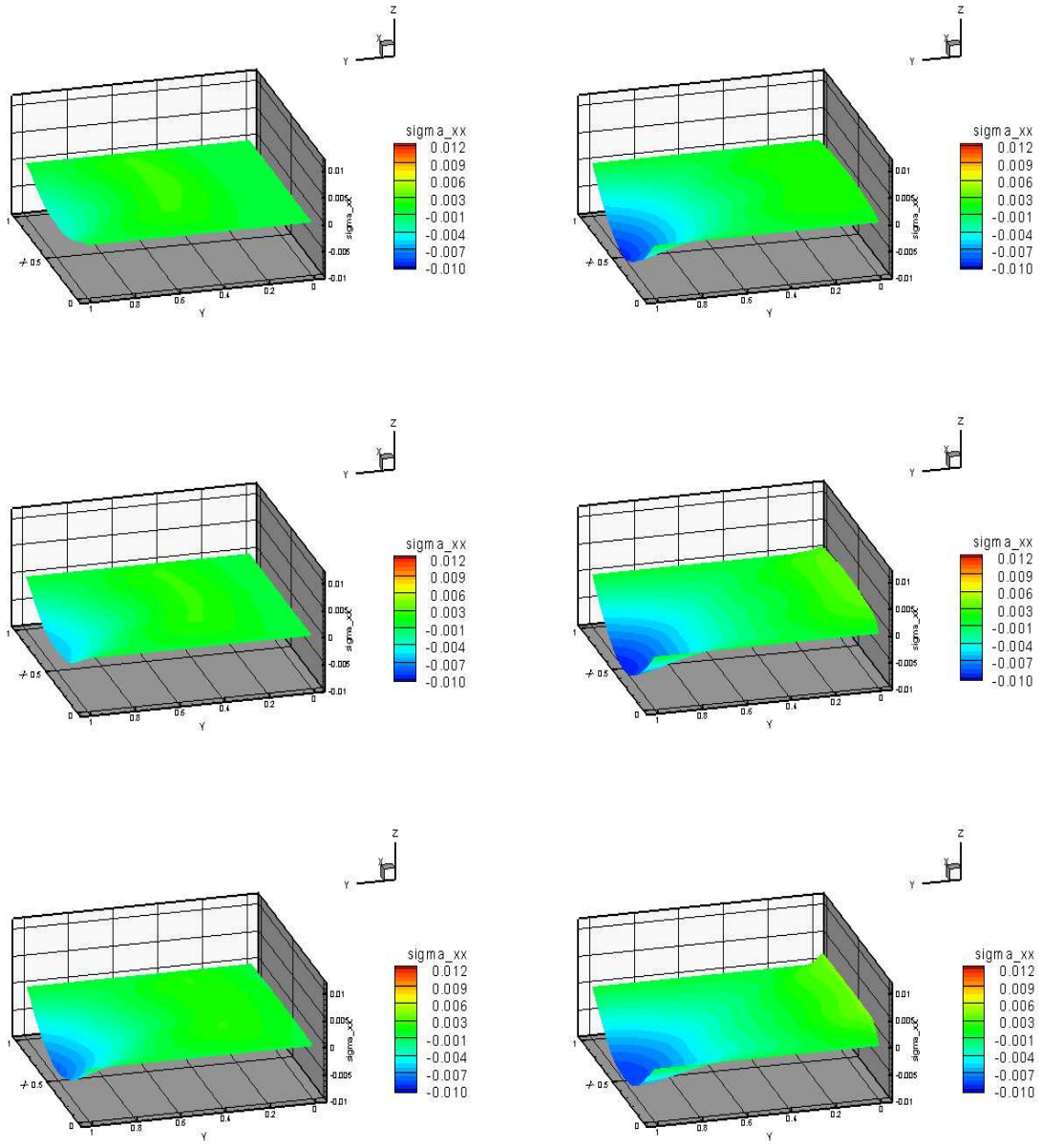

Figure 6.83: Model Problem 5, case (b) : $\nu = 0.3$ and $(\sigma_{yy})_{max} = 0.01$ (parabolic) : Evolution of σ_{xx} : Upper Convected Stress Rate - Time steps from 7^{th} to 12^{th}

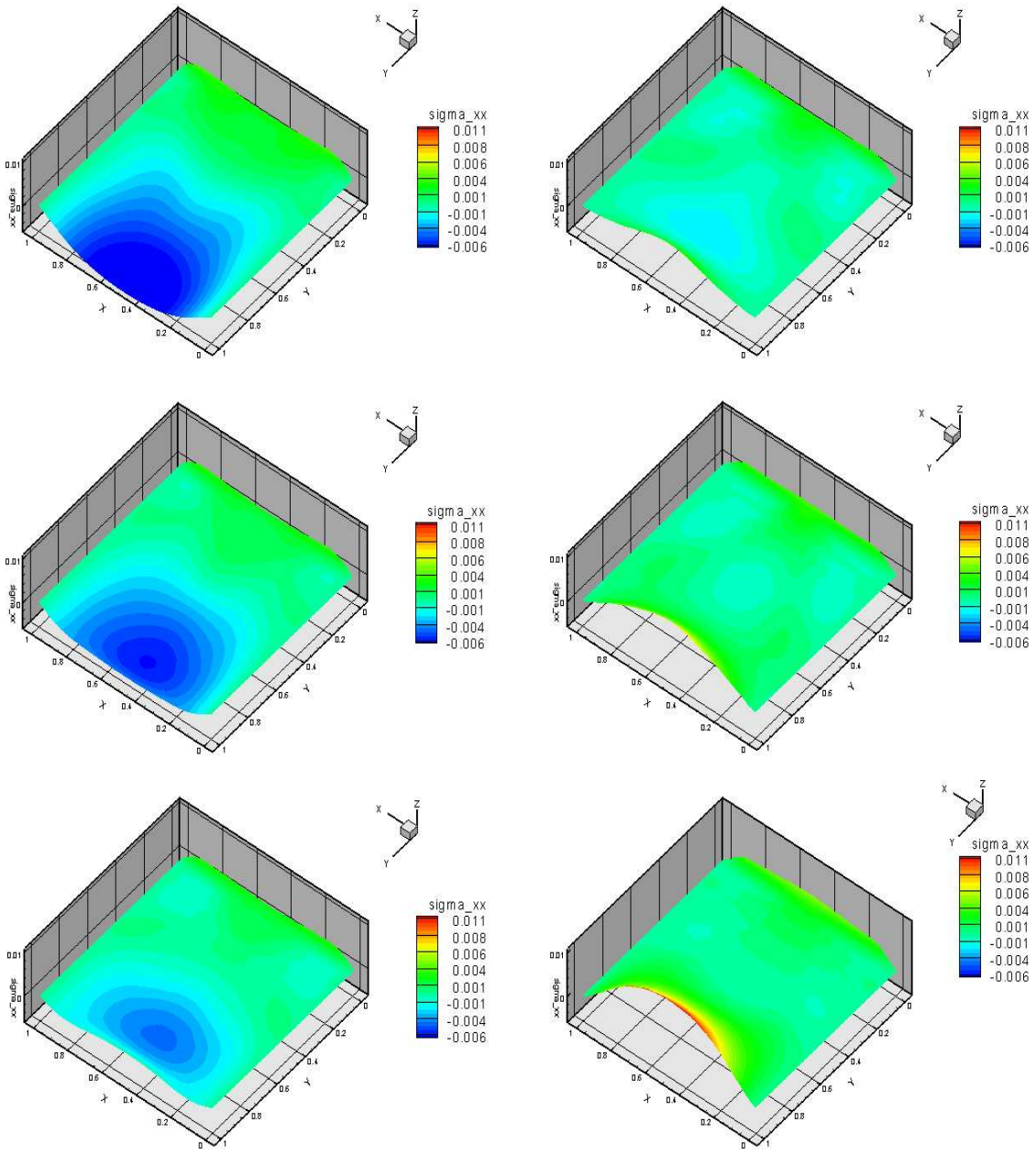

Figure 6.84: Model Problem 5, case (b) : $\nu = 0.3$ and $(\sigma_{yy})_{max} = 0.01$ (parabolic) : Evolution of σ_{xx} : Upper Convected Stress Rate - Time steps from 13^{th} to 18^{th}

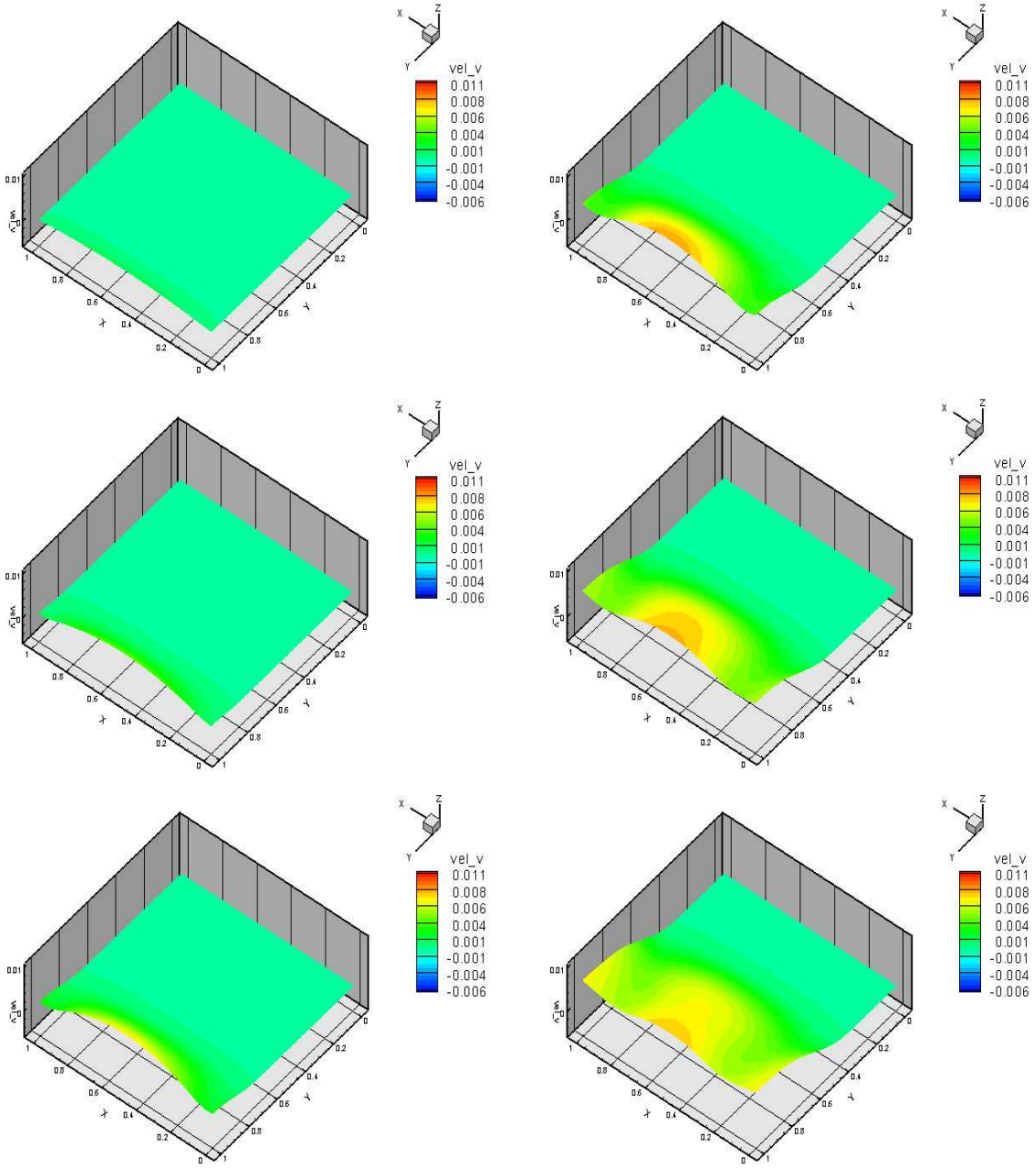

Figure 6.85: Model Problem 5, case (b) : $\nu = 0.3$ and $(\sigma_{yy})_{max} = 0.01$ (parabolic) : Evolution of v : Upper Convected Stress Rate - Time steps from 1^{st} to 6^{th}

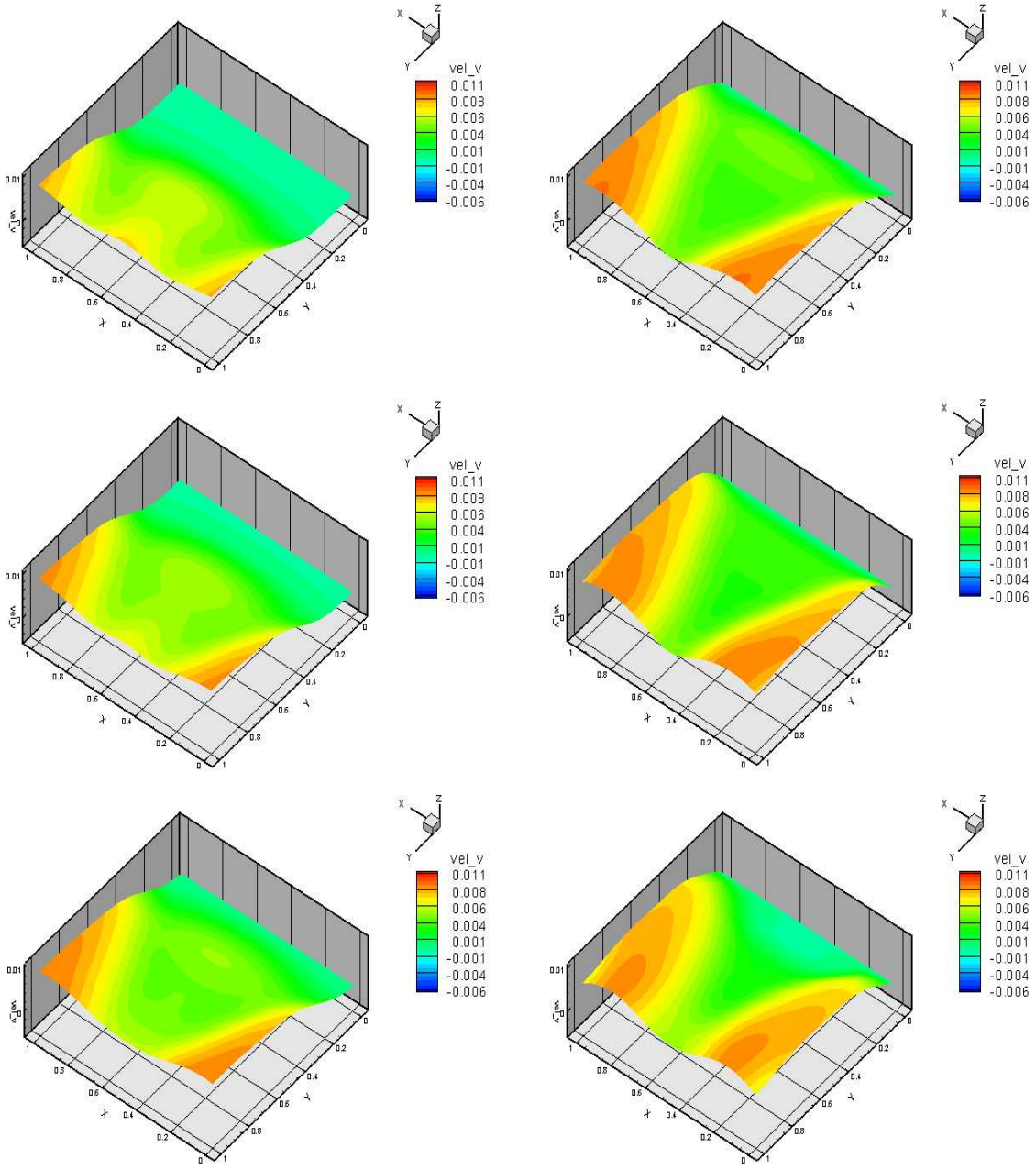

Figure 6.86: Model Problem 5, case (b) : $\nu = 0.3$ and $(\sigma_{yy})_{max} = 0.01$ (parabolic) : Evolution of v : Upper Convected Stress Rate - Time steps from 7^{th} to 12^{th}

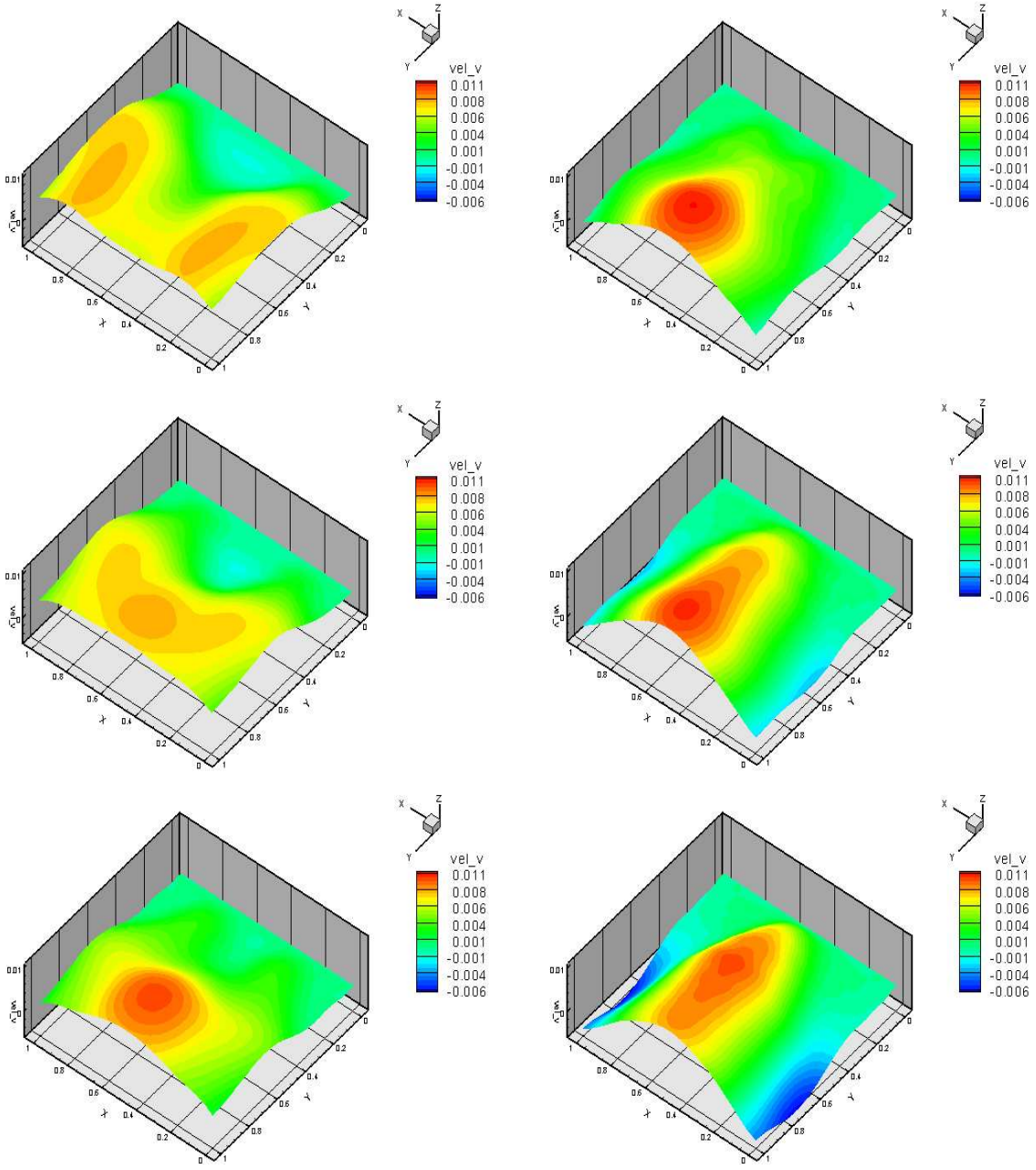

Figure 6.87: Model Problem 5, case (b) : $\nu = 0.3$ and $(\sigma_{yy})_{max} = 0.01$ (parabolic) : Evolution of v : Upper Convected Stress Rate - Time steps from 13^{th} to 18^{th}

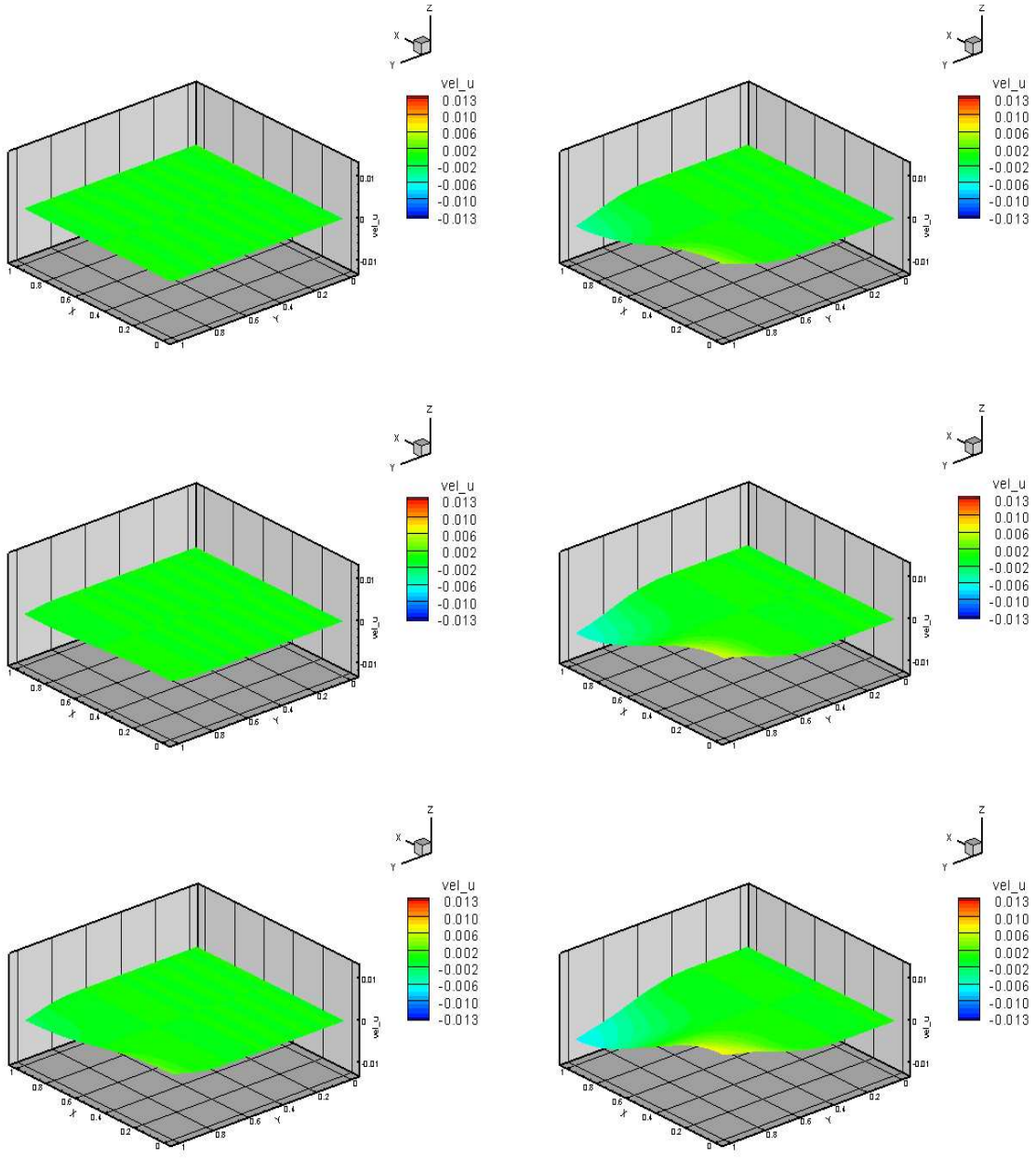

Figure 6.88: Model Problem 5, case (b) : $\nu = 0.3$ and $(\sigma_{yy})_{max} = 0.01$ (parabolic) : Evolution of u : Upper Convected Stress Rate - Time steps from 1^{st} to 6^{th}

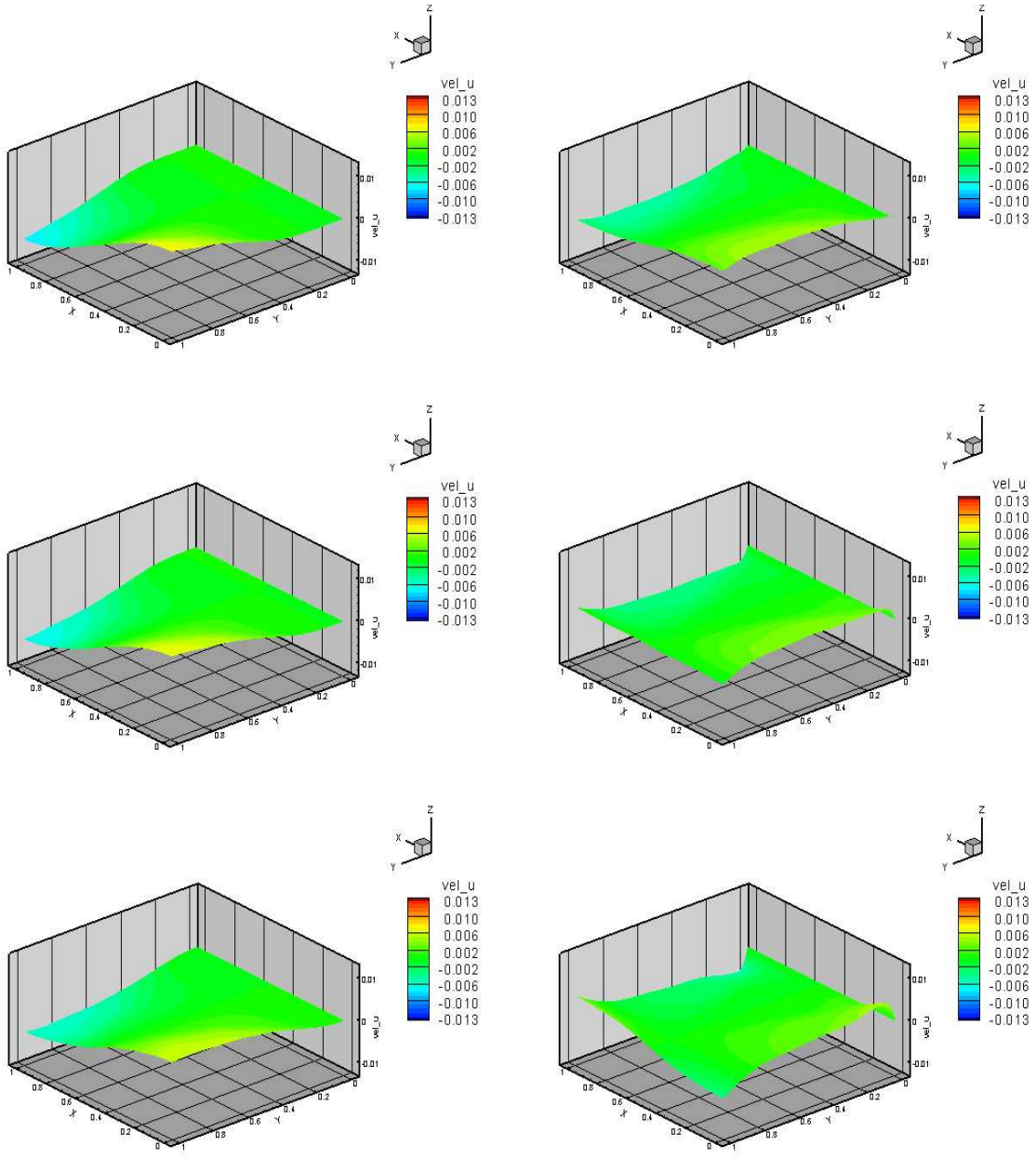

Figure 6.89: Model Problem 5, case (b) : $\nu = 0.3$ and $(\sigma_{yy})_{max} = 0.01$ (parabolic) : Evolution of u : Upper Convected Stress Rate - Time steps from 7^{th} to 12^{th}

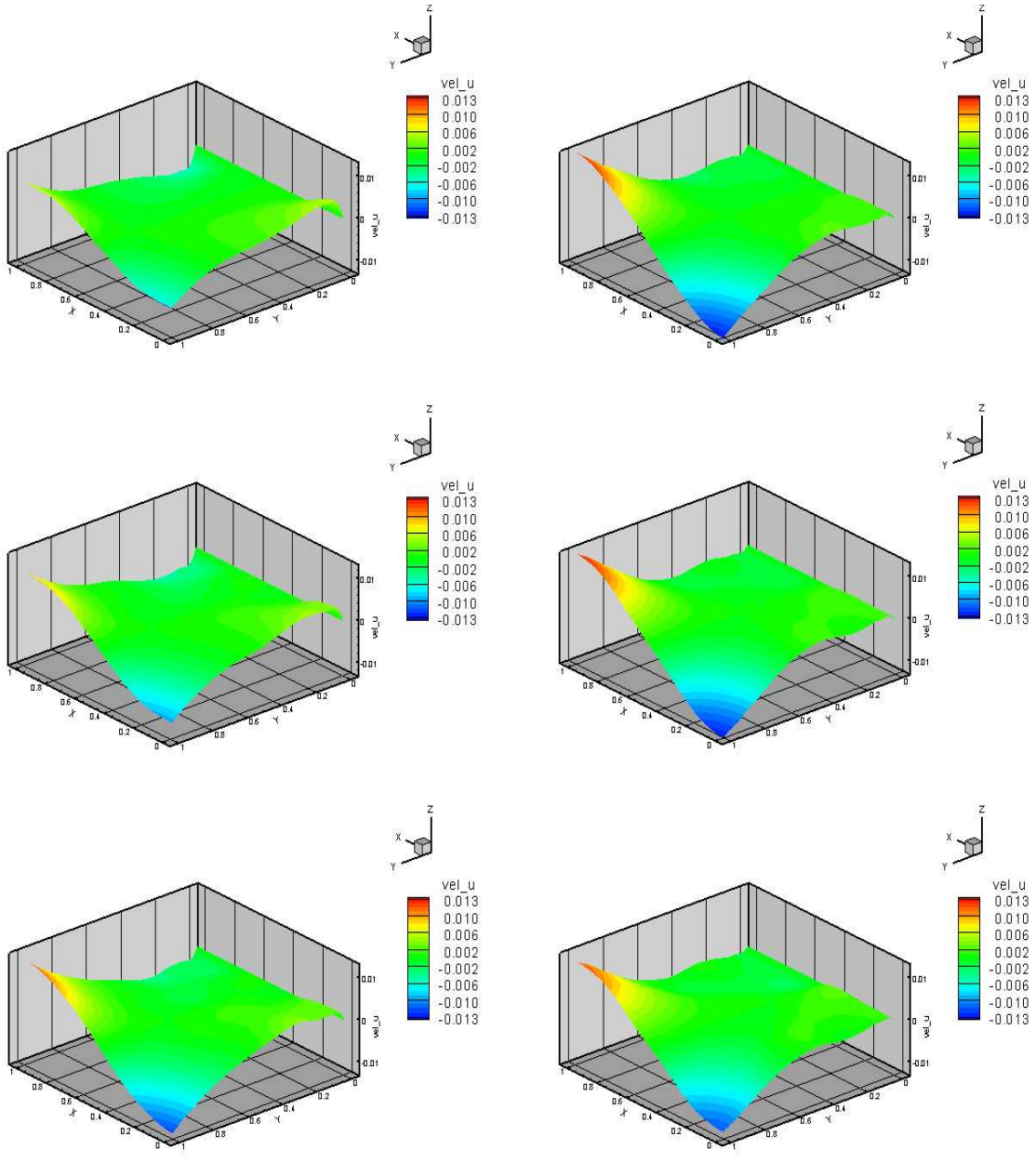

Figure 6.90: Model Problem 5, case (b) : $\nu = 0.3$ and $(\sigma_{yy})_{max} = 0.01$ (parabolic) : Evolution of u : Upper Convected Stress Rate - Time steps from 13^{th} to 18^{th}

6.6 General remarks (2-D model problems)

(1) Model problem 4 (uniform tension in y direction) clearly establishes that only upper Convected rate constitutive equations are able to preserve the wave shapes for higher amplitudes. All other rate equations exhibit significant deterioration in the wave forms at some point during the evolution after which the computations cease.

(2) In all numerical studies space-time least squares formulation for a space-time slab with time marching is used to compute the evolutions.

(3) The choices of local approximations of classes C^1 in space and time ensure the space-time integrals in Riemann sense.

(4) Symmetries or anti-symmetries of the results during the entire evolutions are preserved. In all cases evolutions are free of oscillations. $|g|_{max}$ is of the orders of $O(10^{-6})$ or lower for each space-time strip ensures that Newton's linear method with line search is satisfactory in finding a solution of the non-linear algebraic system. In most cases less than five iterations are required. The least squares functional ${}^nI$ for each space-time slab is of the order of $O(10^{-8})$ or lower. This ensures that GDEs are satisfied accurately in the pointwise sense (due to the space-time integrals being Riemann).

6.7 Summary

Investigation of the behavior of rate equilibrium equations in section 6.1 using 1-D elastic wave propagation problem shows that this formulation has many limitations. First of all, absence of inertial terms from the equilibrium equations inhibits correct simulation of dynamic processes. The 1-D convection diffusion equation is used to illustrate the shortcomings of the mathematical models derived using differentiated forms of the GDEs resulting from the conservation laws. Since the resulting GDEs require additional boundary condition(s) that may not be present in the physics of the problem, uniqueness of the solution from such models can not be guaranteed.

All other numerical studies employs GDEs resulting from the conservation laws in Eulerian description(chapter 2) and constitutive equations presented in chapter 3. In all the numerical studies, space-time least squares formulation for a space-time slab with time marching is used to compute the evolutions. The choices of local approximations of classes C^1 in space and time ensure the space-time integrals in Riemann sense. Based on section 4.3.2, if one chooses total stress $\bar{\sigma}_{ij}$ as a variable, incompressibility requirements warrants for continuity equations to be eliminated. This is due to fact that control volume in this model can experience motion, but it can not experience any change in size or shape (material particles remain intact). From 1-D stress wave propagation studies, we note that for small values of applied total stress ($(\sigma_{xx})_{max} = -0.01$ as compressive pulse over $2\Delta t$), all objective rate constitutive equations behave almost identically. The wave propagation and reflection processes are free of oscillation. If one continues to increase the magnitude of the applied stress, mathematical models employing different rate constitutive equations produces different numerical results. From the numerical studies, it is observed that only upper Convected rate constitutive equations preserve the wave during the evolution process where all the other rate constitutive equations (lower Convected, Jaumann and Truesdell) break down numerically at different values of time during the evolution for $(\sigma_{xx})_{max} = -0.1$ and $(\sigma_{xx})_{max} = -0.3$. Two dimensional studies are needed to further substantiate the behaviors of rate constitutive equations.

Square panel in plane strain is used as a model problem with $\nu = 0.0$. This model problem simulates 1-D stress wave propagation but in two-dimensional setting. Numerical studies show that,

(i) wave propagation and reflection processes are precisely simulated using formulations with different rate constitutive equations for small magnitudes of applied uniform tension, $\sigma_{yy} = 0.01$ (Appendix B).

(ii) For higher amplitudes of applied uniform tension, only upper Convected constitutive equations are able to preserve the wave shape whereas all the other rate constitutive equations show deterioration in the wave shape during the evolution.

Further studies using upper Convected rate constitutive equations are carried for different Poisson's ratio and non-uniformly applied stress. The wave propagation, reflections and interactions processes are more complex in this case than for $\nu = 0.0$ but no difficulties are encountered. Furthermore, symmetries and anti-symmetries of the solution are preserved throughout evolutions.

For all initial value problems (IVPs), Newton's linear method with line search is used for solving non-linear algebraic system of equations. Moreover the least square functional for each space-time strip or slab is of the order of $O(10^{-8})$ for studies carried out using maximum tension of $\sigma_{yy} = .01$ and is of the order of $O(10^{-6})$ for studies carried out using maximum tension of $\sigma_{yy} = .2$. This ensures that GDEs are satisfied accurately throughout the evolution.

Chapter 7

Summary, Conclusions and Future Work

The mathematical descriptions of the deforming solids are dominantly constructed using Lagrangian descriptions so that materials particles may be followed. The finite element formulation in solid mechanics is generally constructed using:

(i) either principle of virtual work in which case virtual work statement may be written directly without resorting to governing differential equations (GDEs)

(ii) or using GDEs of the mathematical models along with integral form based on Galerkin method with weak form.

Issues related to Lagrangian descriptions for large motion, finite strain are well known and have been documented in chapter 1. The Eulerian descriptions on the other hand are lucrative due to the fact that these descriptions avoid mesh distortion problems but bring in new problems of their own due to their inability to follow material particles.

The thrust in this work has been to present the most general and complete mathematical models for the deforming solids in both Lagrangian and Eulerian descriptions based on conservation laws. The mathematical models consider large motion, finite strain as well as compressibility. These models are also specialized for small deformation, small strain cases. The

Lagrangian descriptions employ displacements, stresses, temperature as variables in which the second Piola-Kirchhoff stresses and the Green's strains are conjugate pairs used in the development of constitutive equations. The stress and strain measures degenerate to Cauchy stress and linear strain in case of small motion, small strain. In Eulerian descriptions, velocities, Cauchy stresses, temperature and strain rates are quantities of choice in the development of the mathematical models. The choice of velocities in the conservation laws necessitates rate constitutive equations. The commonly used rate constitutive equations based on upper Convected, lower Convected, Jaumann, and Truesdell have been presented. The developments of the mathematical models in chapter 2 and the constitutive equations in chapter 3 are integrated in chapter 4 to to provide complete descriptions of the mathematical models that have closure. For compressible solid matter, the constitutive equations, equations of state and other thermodynamic relations such as specific heat, specific internal energy are also presented.

Details of mathematical model based on equilibrium rate equations are presented in section 4.4. It is demonstrated that such models are neither suitable for static nor dynamic applications. The absence of inertial terms precludes their use in time dependent processes. The main source of problem in this model is the use of differentiated form of conservation laws which require additional boundary conditions and/or initial conditions for the uniqueness of the solution. This additional information is generally not deducible from the physics. To substantiate this further, differentiated form of 1-D steady state convection diffusion problem has been used as a model problem. It is shown that for this model problem the numerical solutions are spurious or non-unique due to lack of additional boundary conditions. From these studies, it is concluded that differentiated form of the conservation equations as integral part of the mathematical model must be avoided. However, their use in simplifying the equations in the mathematical model is justified.

In chapter 5 brief summary of the hpk mathematical and computational framework [5–7] for initial value problems has been presented. Based on Surana et al. [38], the integral forms based on space-time least squares processes are utilized in formulating finite element processes for a space-time strip or slab for an increment of time. The space-time strip with marching is

used for computing evolutions in all cases.

A number of different numerical studies are presented to demonstrate various features, strengths and shortcomings. 1-D elastic wave propagation studies are presented using Eulerian description and the rate constitutive equations with incompressibility assumption. Numerical studies show that for lower values of applied stress (producing lower strain rates) all four objective rate constitutive equations produce almost identical behaviors of wave propagation and reflection. With increasing magnitude of the applied stress, only upper Convected rate constitutive equations preserve the wave shape during evolution. All other rate equations result in seizure of the computational processes. The results from Eulerian descriptions are in good agreement with those from Lagrangian descriptions. In all cases $|g|_{\max} \leq O(10^{-7})$ and least squares functional for each space-time strip of $O(10^{-8})$ or lower confirm convergence of the iterative solution procedure (Newton's linear method with line search) as well as accuracy of the computed solutions. Based on these studies, only upper Convected rate constitutive equations appear to have good performance for a wide range of strain rates.

Numerical studies are also presented for stress wave propagation in 2-D plane strain elasticity with Poisson's ratio $\nu = 0.0$ and $\nu = 0.3$ using a square panel subjected to uniform tension as well as parabolically varying stress. When $\nu = 0.0$, the simulation produce perfect 1-D elastic wave propagation behaviors that are in agreement with 1-D numerical studies. All four rate constitutive equations are investigated with findings exactly similar to 1-D elastic wave propagation. When Poisson's ratio is nonzero, the propagations, reflections and interactions are complex but no difficulties are encountered. Symmetries and antisymmetries of various quantities are observed precisely in the computed evolutions.

The work presented here is a comprehensive expose of mathematical models based on conservation laws, constitutive equations in Lagrangian and Eulerian descriptions. Numerical studies presented merely demonstrate the Eulerian descriptions to be meritorious of consideration with caution in the choice of rate constitutive equations. The findings regarding to rate constitutive equations are substantial from the view point that Jaumann constitutive equations are used almost exclusively [41, 42] in most solid mechanics applications which are shown to be

spurious as the strain rates increase.

This work needs to be continued in a rigorous fashion in order to bring it to maturity so that its application to real problems can be undertaken. The most immediate areas of research are: (i) investigation of level set for tracking material particles so that free boundaries, moving fronts, moving interfaces etc. can be simulated. (ii) investigation of second order elasticity for high strain rate applications. (iii) investigation of higher strain rates which are invariably accompanied by plasticity, hence, developments of elastoplastic constitutive models, first based on continuum flow plasticity and subsequently based on continuum endochronic theories are essential. (iv) a parallel development in Lagrangian descriptions which is essential to validate Eulerian simulations. (v) developing theoretical work that is essential to demonstrate the problems associated with the rate constitutive equations (lower Convected, Jaumann and Truesdell) as well as to demonstrate the validity of upper Convected constitutive model.

Bibliography

[1] T. Belytschko, W. K. Liu, and B. Moran. *Nonlinear finite elements for continua and structures*. Wiley New York, 2000.

[2] M. S. Gadala, M. A. Dokainish, and G. A. Oravas. Geometric and material nonlinearity problems: Lagrangian and updated lagrangian formulations. *Int.J.Nonlinear Mech.*, pages 277–293, 7th-11th July, 1980 1980.

[3] M. S. Gadala and G. Oravas. Consistent eulerian formulation of large deformation problems in statics and dynamics. *Int.J.Nonlinear Mech.*, 18(1):21–35, 1983.

[4] K. S. Surana and J. N. Reddy. k-version of finite element method: A new mathematical and computational framework for BVP and IVP. *AFRL, Air Force Office of Scientific Research*, Grant number: F49620-03-1-0298 and F49620-03-1-0201, 2007.

[5] K. S. Surana, A. R. Ahmadi, and J. N. Reddy. The K-version of finite element method for self-adjoint operators in BVP. *International Journal of Computational Engineering Science*, 3(2):155–218, 2002.

[6] K. S. Surana, A. R. Ahmadi, and J. N. Reddy. The k-Version Of Finite Element Method For Non-Self-Adjoint Operators In BVP. *International Journal of Computational Engineering Sciences*, 4(4):737–812, 2003.

[7] K. S. Surana, A. R. Ahmadi, and J. N. Reddy. k–version of Finite Element Method for Non-Linear Operators in BVP. *International Journal of Computational Engineering*, 5(1):133–207, 2004.

[8] C. Truesdell. *A First Course in Rational Continuum Mechanics*. Academic Press New York, 1977.

[9] J. N. Reddy. *An Introduction to Nonlinear Finite Element Analysis*. Oxford Univ Pr, 2004.

[10] M. A. Crisfield. *Non-Linear Finite Element Analysis of Solids and Structures: Advanced Topics*. John Wiley & Sons, Inc. New York, NY, USA, 1997.

[11] J. T. Oden. Numerical formulation of nonlinear elasticity problems. *J.Struct.Div.ASCE*, 93:235255, 1967.

[12] H. D. Hibbitt, P. V. Marcal, and J. R. Rice. *A Finite Element Formulation for Problems of Large Strain and Large Displacement*. Division of Engineering, Brown University, 1969.

[13] S. Nemat-Nasser and H. D. Shatoff. A consistent numerical method for the solution of nonlinear elasticity problems at finite strains. *SIAM Journal on Applied Mathematics*, 20(3):462–481, 1971.

[14] R. D. Wood and O. C. Zienkiewicz. Geometrically nonlinear finite element analysis of beams, frames, arches and axisymmetric shells. *Computers and Structures*, 7:725–735, 1977.

[15] A. T. Noel. *Spatial Formulation and Numerical Solution of Geometrically Nonlinear Problems in Finite Elasticity*. PhD thesis, Washington University, 1996.

[16] G. Horrigmoe and P. G. Bergan. Incremental variational principles and finite element models for nonlinear problems(in solid continuum mechanics). *Computer Methods in Applied Mechanics and Engineering*, 7:201–217, 1976.

[17] J. N. Reddy and P. R. Heyliger. A mixed updated lagrangian formulation for plane elastic problems. *ASTM J.Compos.Technol.Res.,*, 9(4):131–145, 1987.

[18] S. W. KEY. A finite element procedure for the large deformation dynamic response of axisymmetric solids. *Computer Methods in Applied Mechanics and Engineering*, 4:195–218, 1974.

[19] J. L. Swedlow. Character of the equations of elasto-plastic flow in three independent variables. *International Journal of Non-Linear Mechanics*, 3:325–336, 1968.

[20] J. R. Osias. Finite deformation of elasto-plastic solids. Technical report, National Aeronautics and Space Administration; For sale by the National Technical Information Service, 1973.

[21] J. R. Osias and J. L. Swedlow. Finite elasto-plastic deformation. i- theory and numerical examples. *International Journal of Solids and Structures*, 10:321–339, 1974.

[22] Y. K. Lee and J. L. Swedlow. Computation of shear bands using a new variational approach, i: theory and elementary examples. *International Journal for Numerical Methods in Engineering*, 20:409–421, 1984.

[23] Y. K. Lee and J. L. Swedlow. Computation of shear bands using a new variational approach. ii: Use of weight functions in a crack problem. *International Journal for Numerical Methods in Engineering*, 20(3):423–445, 1984.

[24] Y. K. Lee. Analysis of finite elastoplastic deformation using a new finite element method. *International Journal of Plasticity*, 6(5):521–549, 1990.

[25] A. H. P Siu and Y. K. Lee. A three dimensional least squares finite element technique for deformation analysis. *International Journal for Numerical Methods in Engineering*, 40(22):4159–4182, 1997.

[26] D. J. Benson. Computational methods in lagrangian and eulerian hydrocodes. *Computer Methods in Applied Mechanics and Engineering*, 99(2-3):235–394, 1992.

[27] D. J. Benson. An implicit multi-material eulerian formulation. *Int.J.Numer.Meth.Engng*, 48:475–499, 2000.

[28] S. N. Atluri. On constitutive relations at finite strain- hypo-elasticity and elasto-plasticity with isotropic or kinematic hardening. *Computer Methods in Applied Mechanics and Engineering*, 43:137–171, 1984.

[29] W. Prager. An elementary discussion of definitions of stress rate. *Quart.Appl.Math*, 18:403407, 1960.

[30] J. K. Dienes. On the analysis of rotation and stress rate in deforming bodies. *Acta Mechanica*, 32(4):217–232, 1979.

[31] H. Xiao, OT Bruhns, and A. Meyers. Logarithmic strain, logarithmic spin and logarithmic rate. *Acta Mechanica*, 124(1):89–105, 1997.

[32] H. Xiao, OT Bruhns, and A. Meyers. Hypo-elasticity model based upon the logarithmic stress rate. *Journal of Elasticity*, 47(1):51–68, 1997.

[33] A. S. Khan and S. Huang. *Continuum Theory of Plasticity*. Wiley-Interscience, 1995.

[34] R. W. Ogden. *Non-Linear Elastic Deformations*. Courier Dover Publications, 1997.

[35] K. S. Surana. *ME 840, Continuum Mechanics lecture notes*. The University of Kansas, Fall 2007.

[36] Y. K. Lee. A finite elastoplastic flow theory for porous media. *Int.J.Plast.*, 4(4):301–315, 1988.

[37] Y. K. Lee. Conditions for shear banding and material instability in finite elastoplastic deformation. *Int.J.Plast.*, 5(3):197–226, 1989.

[38] K. S. Surana, J. N. Reddy, and S. Allu. The k-Version of Finite Element Method for Initial Value Problems: Mathematical and Computational Framework. *International Journal for Computational Methods in Engineering Science and Mechanics*, 8(3):123–136, 2007.

[39] H. Xiao, O. T. Bruhns, and A. Meyers. Objective stress rates, cyclic deformation paths, and residual stress accumulation. *ZAMM Z.Angew.Math.Mech*, 1:13, 2006.

[40] A. Meyers, H. Xiao, and O. T. Bruhns. Choice of objective rate in single parameter hypoelastic deformation cycles. *Computers and Structures*, 84(17-18):1134–1140, 2006.

[41] LB Tran and HS Udaykumar. A particle-level set-based sharp interface cartesian grid method for impact, penetration, and void collapse. *Journal of Computational Physics*, 193(2):469–510, 2004.

[42] HS Udaykumar, R. Mittal, P. Rampunggoon, and A. Khanna. A sharp interface Cartesian grid method for simulating flows with complex moving boundaries. *Journal of Computational Physics*, 174(1):345–380, 2001.

Appendix A

Second Order Elasticity: $\left[D_S(\varepsilon)\right]$

Explicit form of $[D_s(\varepsilon)]$ in (3.58) is given in the following,

$$\begin{bmatrix} D_{s11}(\varepsilon) & D_{s12}(\varepsilon) & D_{s13}(\varepsilon) & D_{s14}(\varepsilon) & D_{s15}(\varepsilon) & D_{s16}(\varepsilon) \\ D_{s21}(\varepsilon) & D_{s22}(\varepsilon) & D_{s23}(\varepsilon) & D_{s24}(\varepsilon) & D_{s25}(\varepsilon) & D_{s26}(\varepsilon) \\ D_{s31}(\varepsilon) & D_{s32}(\varepsilon) & D_{s33}(\varepsilon) & D_{s34}(\varepsilon) & D_{s35}(\varepsilon) & D_{s36}(\varepsilon) \\ D_{s41}(\varepsilon) & D_{s42}(\varepsilon) & D_{s43}(\varepsilon) & D_{s44}(\varepsilon) & D_{s45}(\varepsilon) & D_{s46}(\varepsilon) \\ D_{s51}(\varepsilon) & D_{s52}(\varepsilon) & D_{s53}(\varepsilon) & D_{s54}(\varepsilon) & D_{s55}(\varepsilon) & D_{s56}(\varepsilon) \\ D_{s61}(\varepsilon) & D_{s62}(\varepsilon) & D_{s63}(\varepsilon) & D_{s64}(\varepsilon) & D_{s65}(\varepsilon) & D_{s66}(\varepsilon) \end{bmatrix} \tag{A.1}$$

where

$$D_{s11}(\varepsilon) = 3\varepsilon_{11}l_\varepsilon + 2\varepsilon_{22}(3l_\varepsilon + m_\varepsilon) + \varepsilon_{33}(6l_\varepsilon + 2m_\varepsilon) + \lambda_\varepsilon + 2\mu_\varepsilon$$

$$D_{s12}(\varepsilon) = \varepsilon_{22}(3l_\varepsilon + m_\varepsilon) + \varepsilon_{33}(6l_\varepsilon + 3m_\varepsilon + n_\varepsilon) + \lambda_\varepsilon$$

$$D_{s13}(\varepsilon) = \varepsilon_{33}(3l_\varepsilon + m_\varepsilon) + \lambda_\varepsilon$$

$$D_{s14}(\varepsilon) = -\gamma_{23}\left[\frac{m_\varepsilon}{2} + n_\varepsilon\right]$$

$$D_{s15}(\varepsilon) = -\gamma_{13}\frac{m_\varepsilon}{2}$$

$$D_{s16}(\varepsilon) = -\gamma_{12}\frac{m_\varepsilon}{2}$$

$$D_{s21}(\varepsilon) = \varepsilon_{11}(3l_\varepsilon + m_\varepsilon) + 2\varepsilon_{22}(3l_\varepsilon + m_\varepsilon) + \varepsilon_{33}(6l_\varepsilon + 3m_\varepsilon + n_\varepsilon) + \lambda_\varepsilon$$

$$D_{s22}(\varepsilon) = \varepsilon_{22}(3l_\varepsilon) + 2\varepsilon_{33}(3l_\varepsilon + m_\varepsilon) + \lambda_\varepsilon + 2\mu_\varepsilon$$

$$D_{s23}(\varepsilon) = \varepsilon_{33}(3l_\varepsilon + m_\varepsilon) + \lambda_\varepsilon$$

$$D_{s24}(\varepsilon) = -\gamma_{23}\frac{m_\varepsilon}{2}$$

$$D_{s25}(\varepsilon) = -\gamma_{13}\left[\frac{m_\varepsilon}{2} + n_\varepsilon\right]$$

$$D_{s26}(\varepsilon) = -\gamma_{12}\frac{m_\varepsilon}{2}$$

$$D_{s31}(\varepsilon) = \varepsilon_{11}(3l_\varepsilon + m_\varepsilon) + \varepsilon_{33}(6l_\varepsilon + 2m_\varepsilon) + \varepsilon_{22}(6l_\varepsilon + 3m_\varepsilon + n_\varepsilon) + \lambda_\varepsilon$$

$$D_{s32}(\varepsilon) = \varepsilon_{22}(3l_\varepsilon + m_\varepsilon) + \varepsilon_{33}(6l_\varepsilon + 2m_\varepsilon) + \lambda_\varepsilon$$

$$D_{s33}(\varepsilon) = \varepsilon_{33}(3l_\varepsilon) + \lambda_\varepsilon + 2\mu_\varepsilon$$

$$D_{s34}(\varepsilon) = -\gamma_{23}\frac{m_\varepsilon}{2}$$

$$D_{s35}(\varepsilon) = -\gamma_{13}\frac{m_\varepsilon}{2}$$

$$D_{s36}(\varepsilon) = -\gamma_{12}\left[\frac{m_\varepsilon}{2} + n_\varepsilon\right]$$

$$D_{s41}(\varepsilon) = 0$$

$$D_{s42}(\varepsilon) = 0$$

$$D_{s43}(\varepsilon) = 0$$

$$D_{s44}(\varepsilon) = -\varepsilon_{11}(m_\varepsilon + n_\varepsilon) - \varepsilon_{22}m_\varepsilon - \varepsilon_{33}m_\varepsilon + 2\mu_\varepsilon$$

$$D_{s45}(\varepsilon) = \gamma_{12}\frac{m_\varepsilon}{2}$$

$$D_{s46}(\varepsilon) = 0$$

$$D_{s51}(\varepsilon) = 0$$

$$D_{s52}(\varepsilon) = 0$$

$$D_{s53}(\varepsilon) = 0$$

$$D_{s54}(\varepsilon) = \gamma_{12}\frac{m_\varepsilon}{2}$$

$$D_{s55}(\varepsilon) = -\varepsilon_{11}m_\varepsilon - \varepsilon_{22}(m_\varepsilon + n_\varepsilon) - \varepsilon_{33}m_\varepsilon + 2\mu_\varepsilon$$

$$D_{s56}(\varepsilon) = 0$$

$$D_{s61}(\varepsilon) = 0$$

$$D_{s62}(\varepsilon) = 0$$

$$D_{s63}(\varepsilon) = 0$$

$$D_{s64}(\varepsilon) = \gamma_{13}\frac{m_\varepsilon}{2}$$

$$D_{s65}(\varepsilon) = 0$$

$$D_{s66}(\varepsilon) = -\varepsilon_{11}m_\varepsilon - \varepsilon_{22}m_\varepsilon - \varepsilon_{33}(m_\varepsilon + n_\varepsilon) + 2\mu_\varepsilon$$

Appendix B

2-D Elastic Wave Propagation, for uniform load of $\sigma_{yy} = 0.01$ with $\nu = 0.0$

The material properties, choice of reference quantities and the dimensional properties as well as dimensionless parameters are shown in figure B.1. For each space-time slab, time evolution is computed using $\Delta t = 0.1$ where the total $\sigma_{yy} = 0.01$ is applied in 4 increments of time in a continuous and differentiable manner. Figures B.2 - B.25 show evolution of σ_{yy} and v for rate constitutive equations of upper Convected, lower Convected, Jaumann, and Truesdell respectively. 2-D wave propagation and reflection processes are simulated correctly and all four rate constitutive equations produce the same behavior. At the reflection, the stress σ_{yy} doubles in magnitude and regains its amplitude upon further evolution. As expected σ_{xy}, σ_{xx}, and u are zero throughout the evolution. Newton's linear method with line search is used to solve non-linear algebraic system of equations where $|g|_{max}$ is of the orders of $O(10^{-6})$ or lower for each space-time strip. Moreover, the least squares functional ${}^{n}I$ is of the order of $O(10^{-8})$. This ensures the accuracy of the numerical simulations.

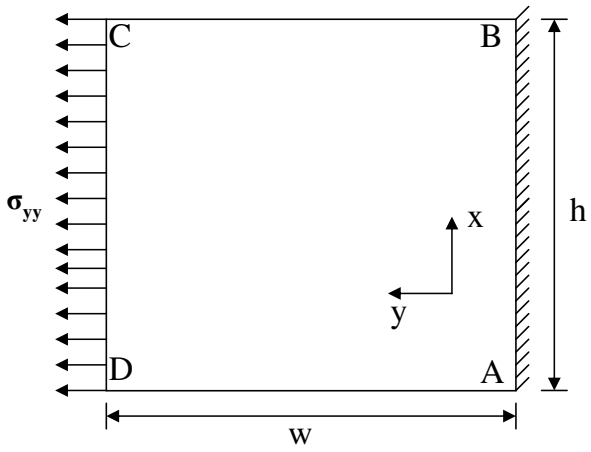

Boundary Conditions :

CD : σ_{yy}= 0.01 ; applied stress (uniform)

AD : σ_{xx}= 0 ; τ_{xy}= 0 ; free surface

BC : σ_{xx}= 0 ; τ_{xy} = 0 ; free surface

AB : u = 0 ; v = 0 ; τ_{xy}= 0 ; fix end

Material Properties :

$\hat{\rho} = 7860 \ \ \mathrm{kg/m^3}$

$\hat{E} = 2 \times 10^{11} \ \mathrm{Pa}$

Dimensionless Properties :

$h = 1 \quad ; \ w = 1 \quad ; \ \rho = 1$

$E = 1 \quad ; \ \nu = 0.3$

Reference Properties :

$\rho_0 = 7860 \ \mathrm{kg/m^3}$

$E_0 = 2 \times 10^{11} \ \mathrm{Pa}$

$u_0 = 5044.3 \ \mathrm{m/s}$

$\tau_0 = 2 \times 10^{11} \ \mathrm{Pa}$

Figure B.1: 2-D Elastic Wave Propagation, Model Problem 6 (uniform load) : C^{111} with p-levels of 3 ; 10×10 uniform mesh ; $\Delta t = 0.1$

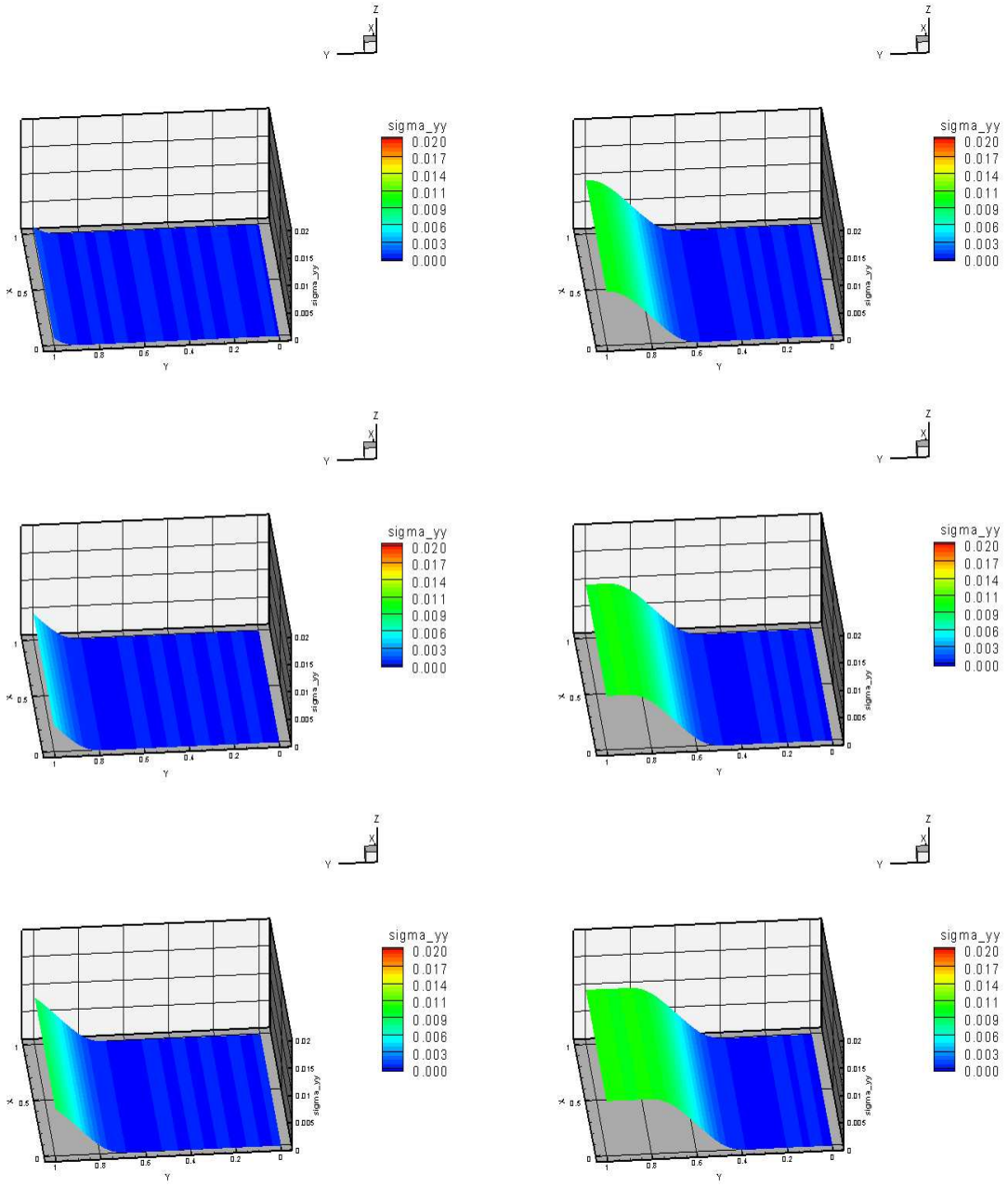

Figure B.2: Model Problem 6 : $\nu = 0.0$ and $\sigma_{yy} = 0.01$: Evolution of σ_{yy} : Upper Convected Stress Rate - Time steps from 1^{st} to 6^{th}

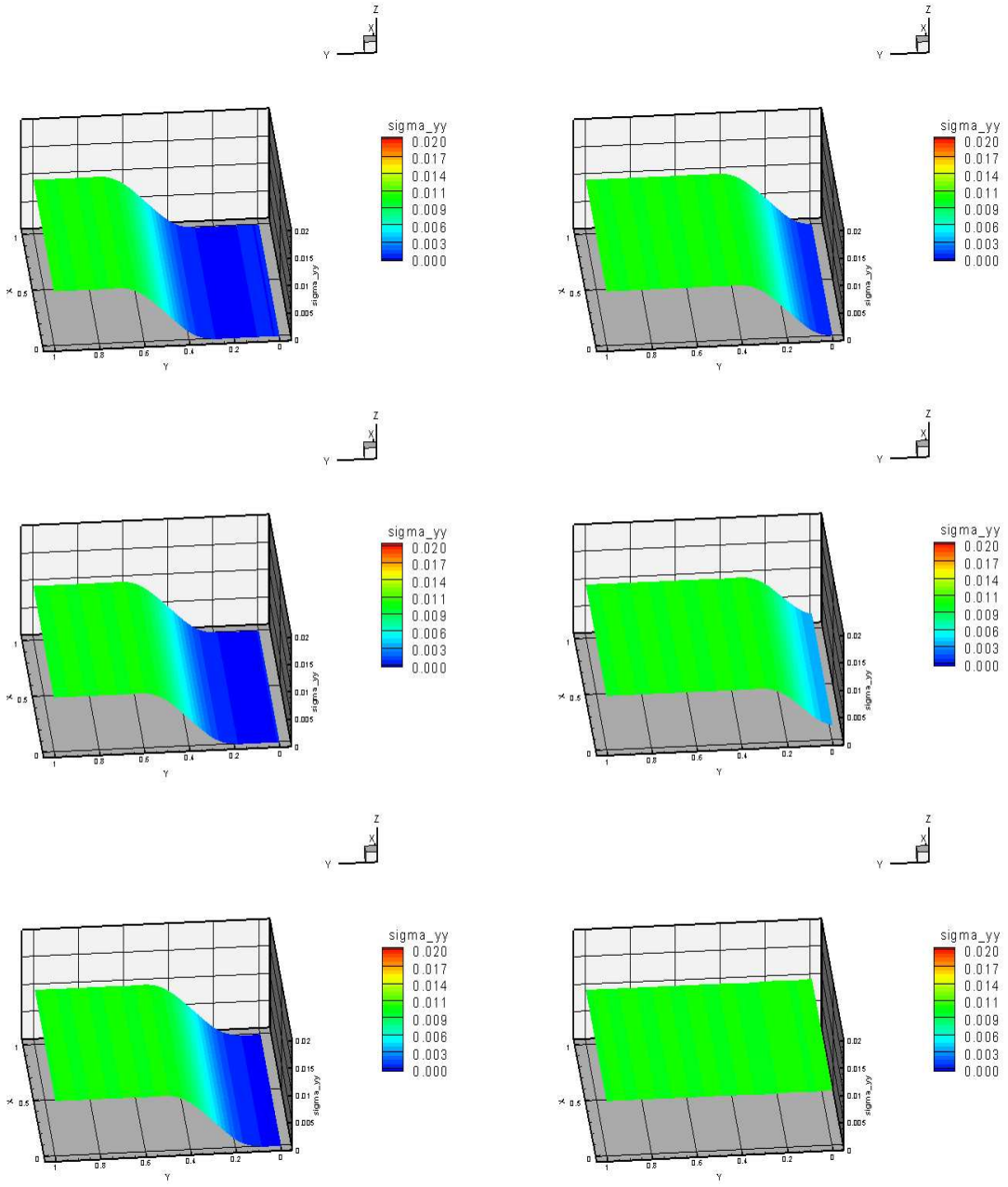

Figure B.3: Model Problem 6 : $\nu = 0.0$ and $\sigma_{yy} = 0.01$: Evolution of σ_{yy} : Upper Convected Stress Rate - Time steps from 7^{th} to 12^{th}

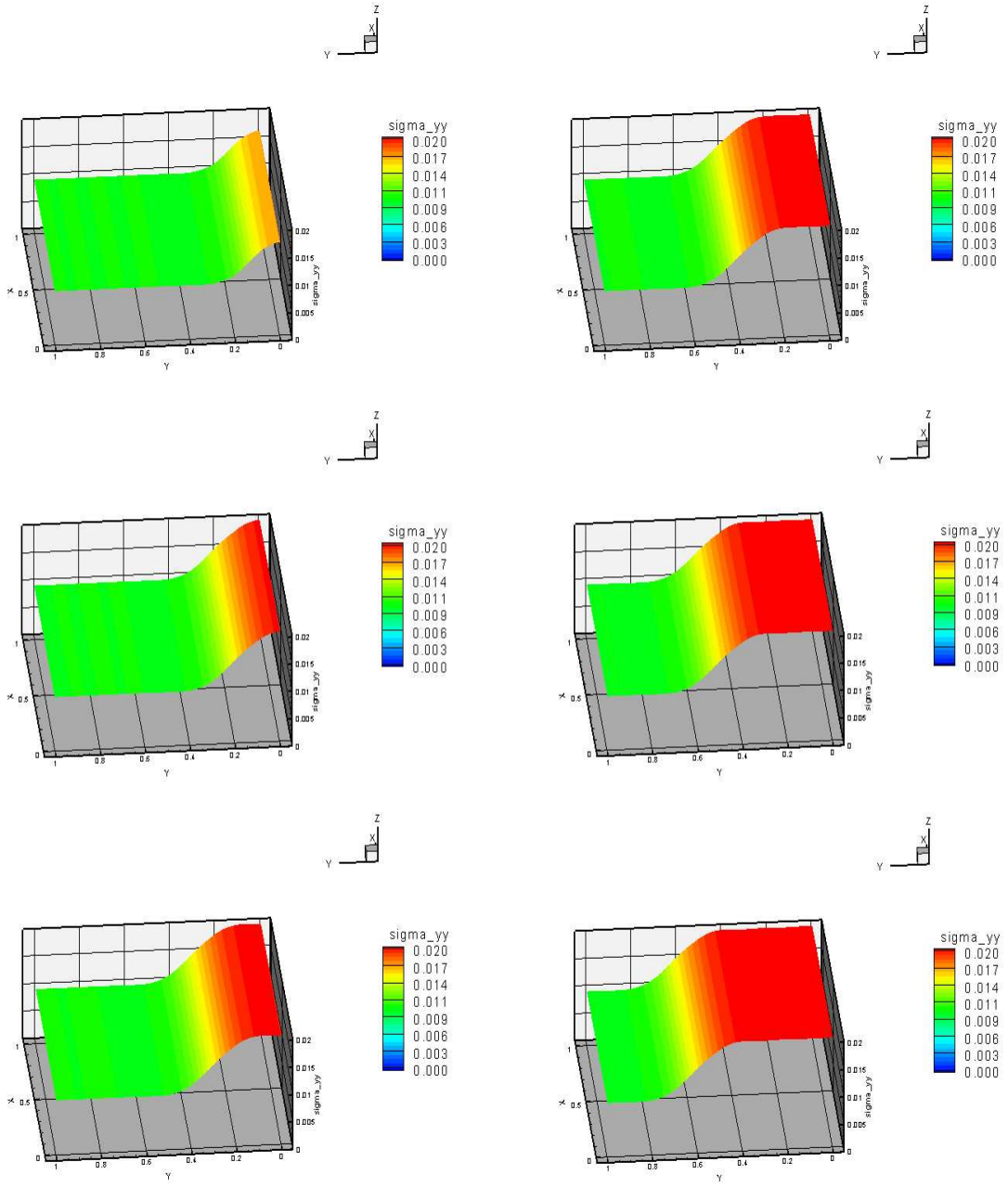

Figure B.4: Model Problem 6 : $\nu = 0.0$ and $\sigma_{yy} = 0.01$: Evolution of σ_{yy} : Upper Convected Stress Rate - Time steps from 13^{th} to 18^{th}

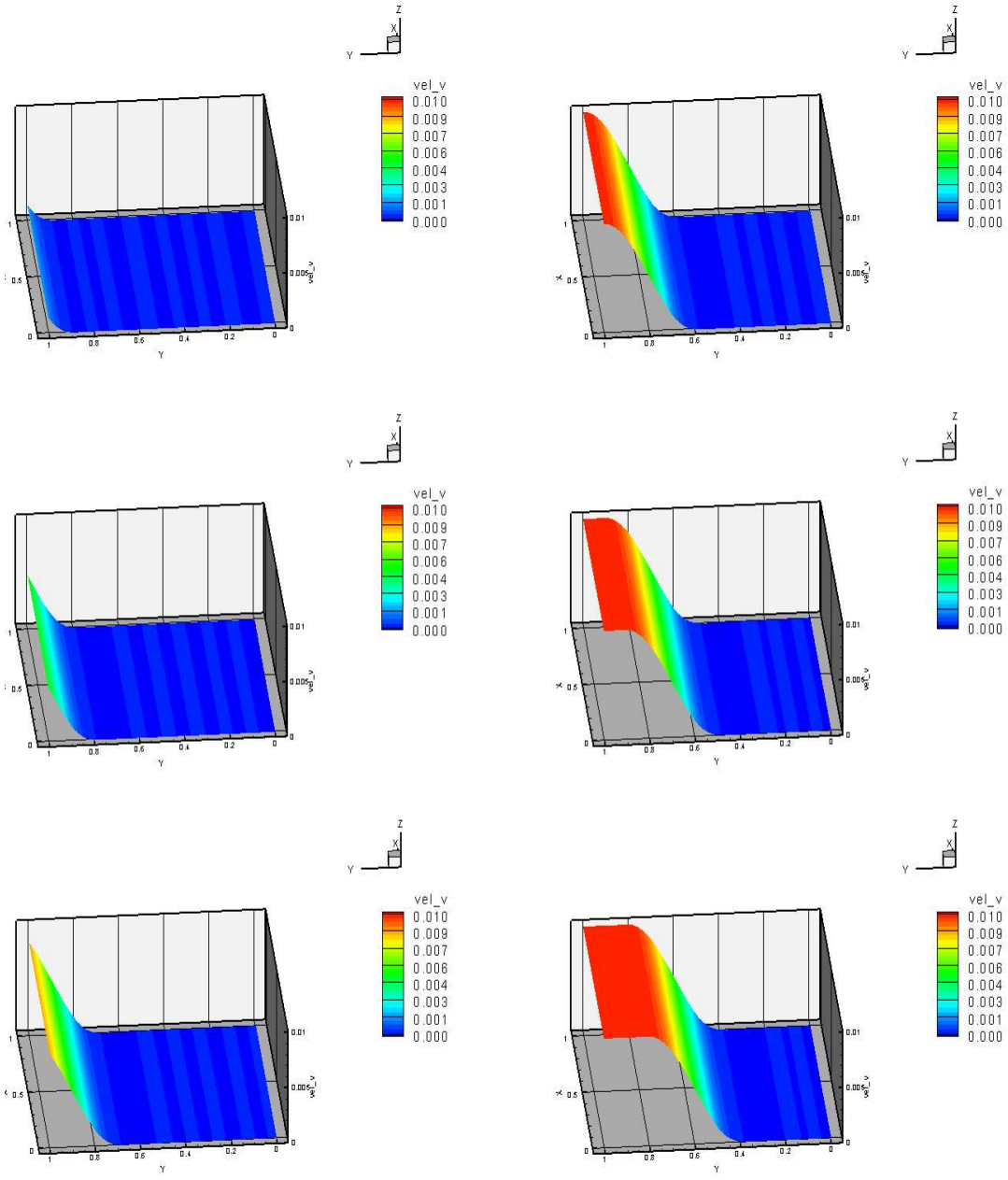

Figure B.5: Model Problem 6 : $\nu = 0.0$ and $\sigma_{yy} = 0.01$: Evolution of v : Upper Convected Stress Rate - Time steps from 1^{st} to 6^{th}

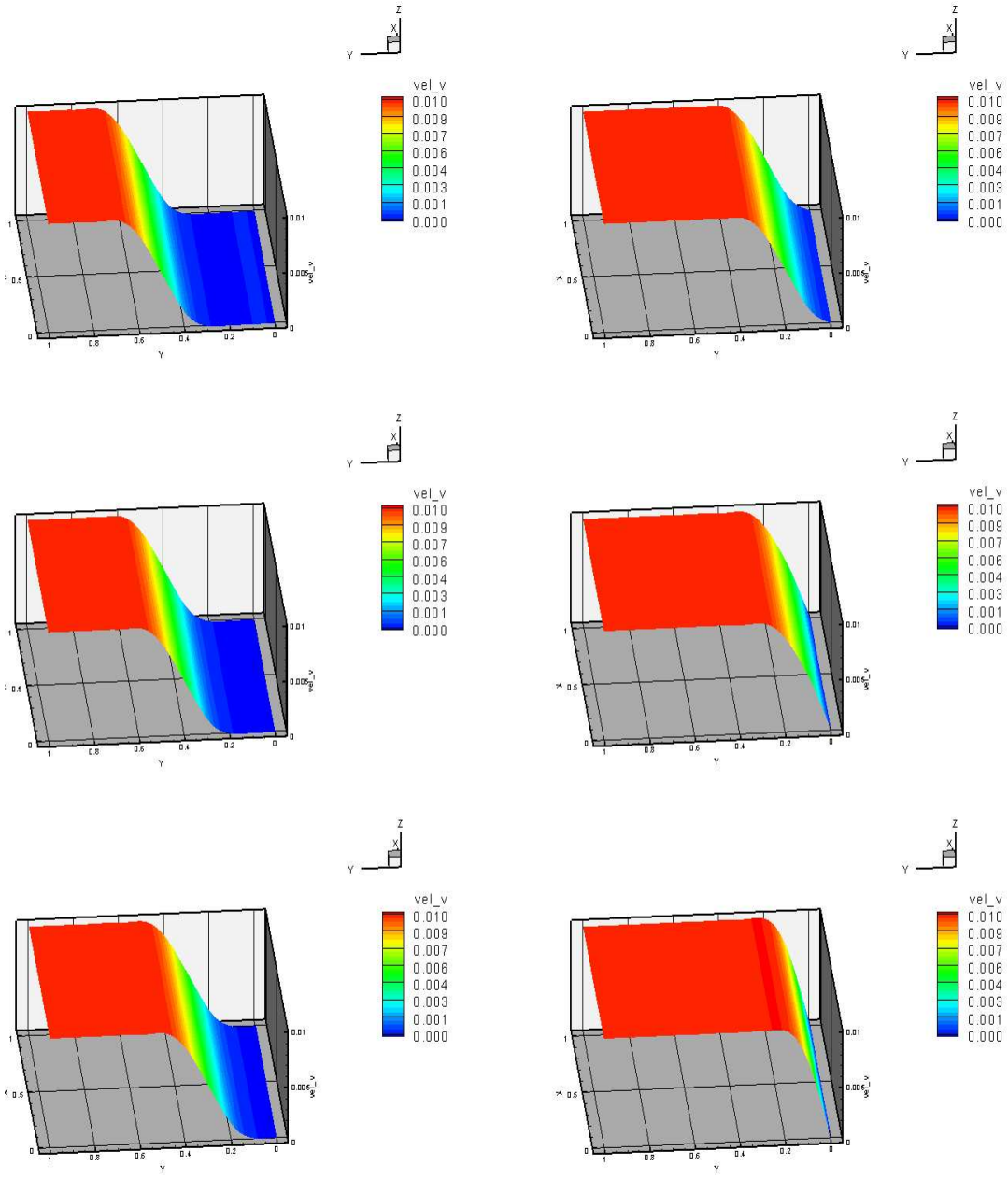

Figure B.6: Model Problem 6 : $\nu = 0.0$ and $\sigma_{yy} = 0.01$: Evolution of v : Upper Convected Stress Rate - Time steps from 7^{th} to 12^{th}

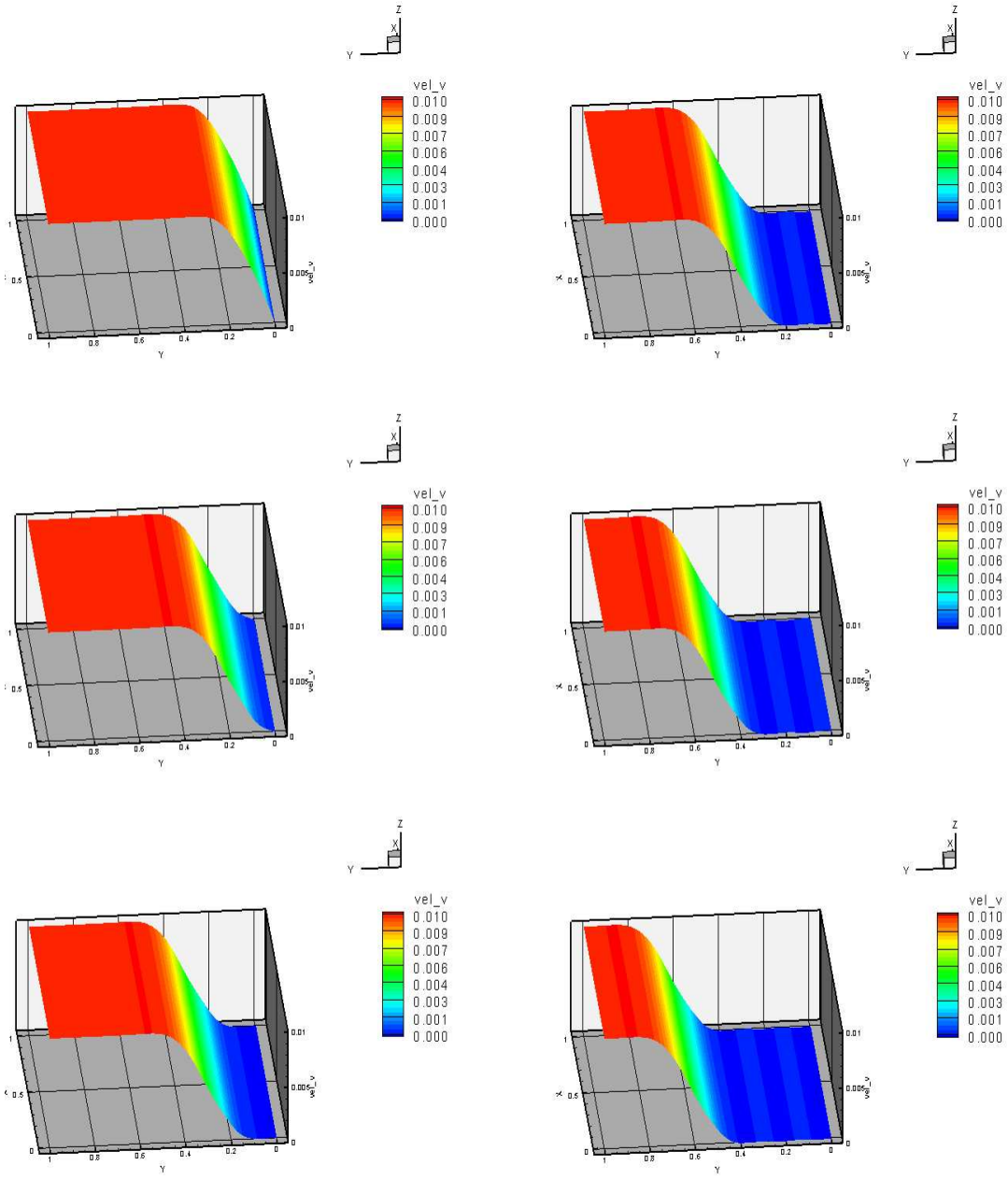

Figure B.7: Model Problem 6 : $\nu = 0.0$ and $\sigma_{yy} = 0.01$: Evolution of v : Upper Convected Stress Rate - Time steps from 13^{th} to 18^{th}

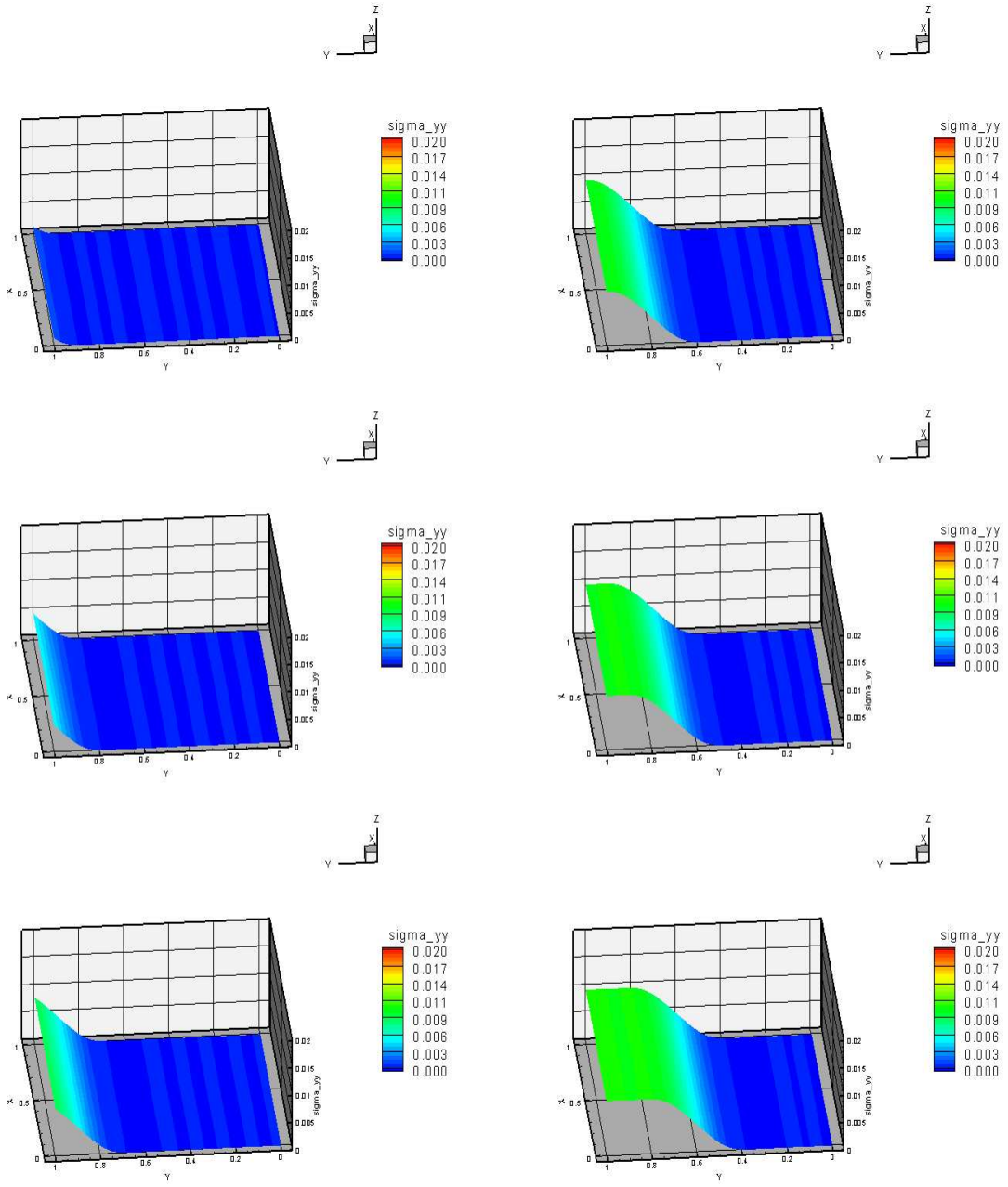

Figure B.8: Model Problem 6 : $\nu = 0.0$ and $\sigma_{yy} = 0.01$: Evolution of σ_{yy} : Lower Convected Stress Rate - Time steps from 1^{st} to 6^{th}

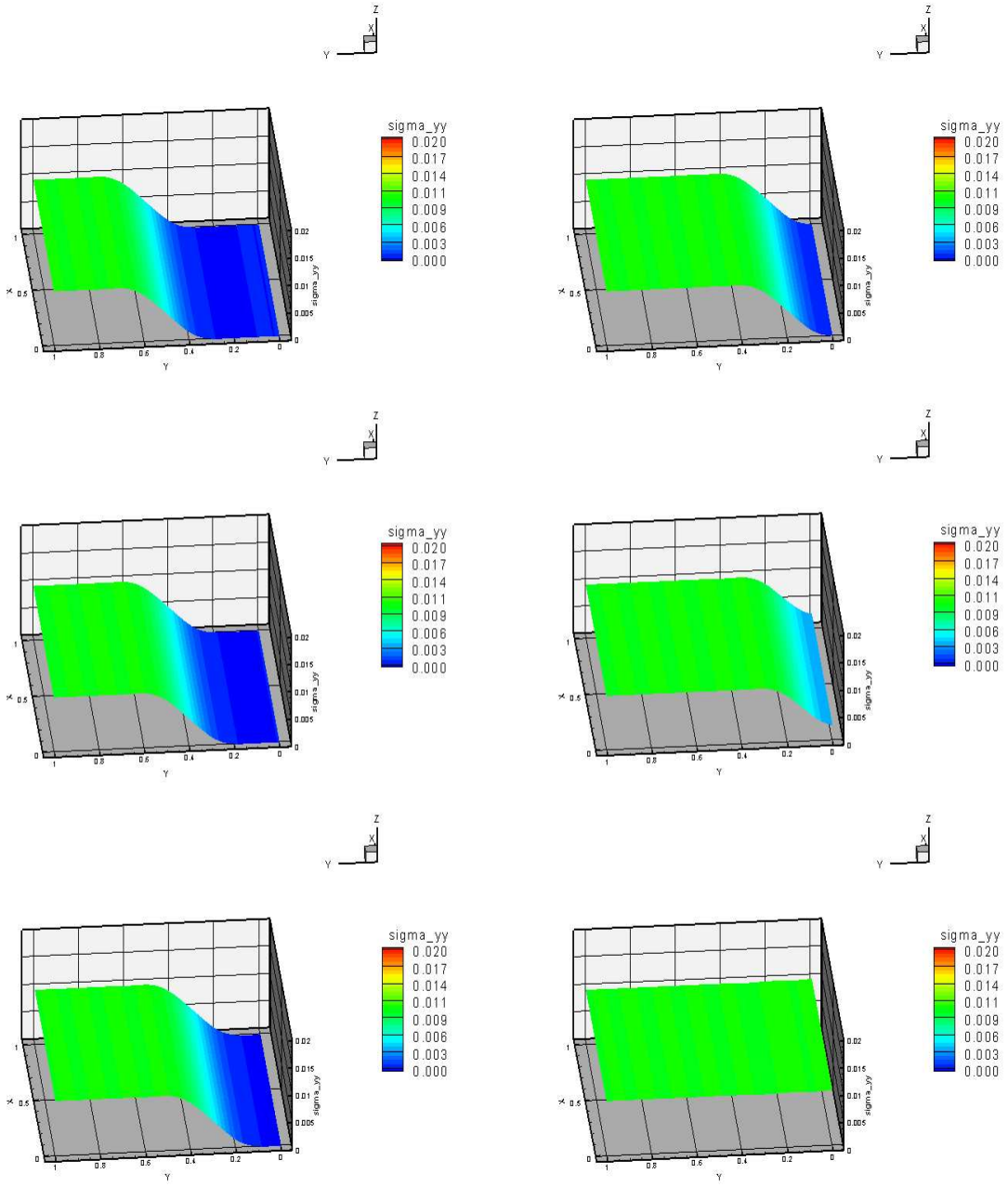

Figure B.9: Model Problem 6 : $\nu = 0.0$ and $\sigma_{yy} = 0.01$: Evolution of σ_{yy} : Lower Convected Stress Rate - Time steps from 7^{th} to 12^{th}

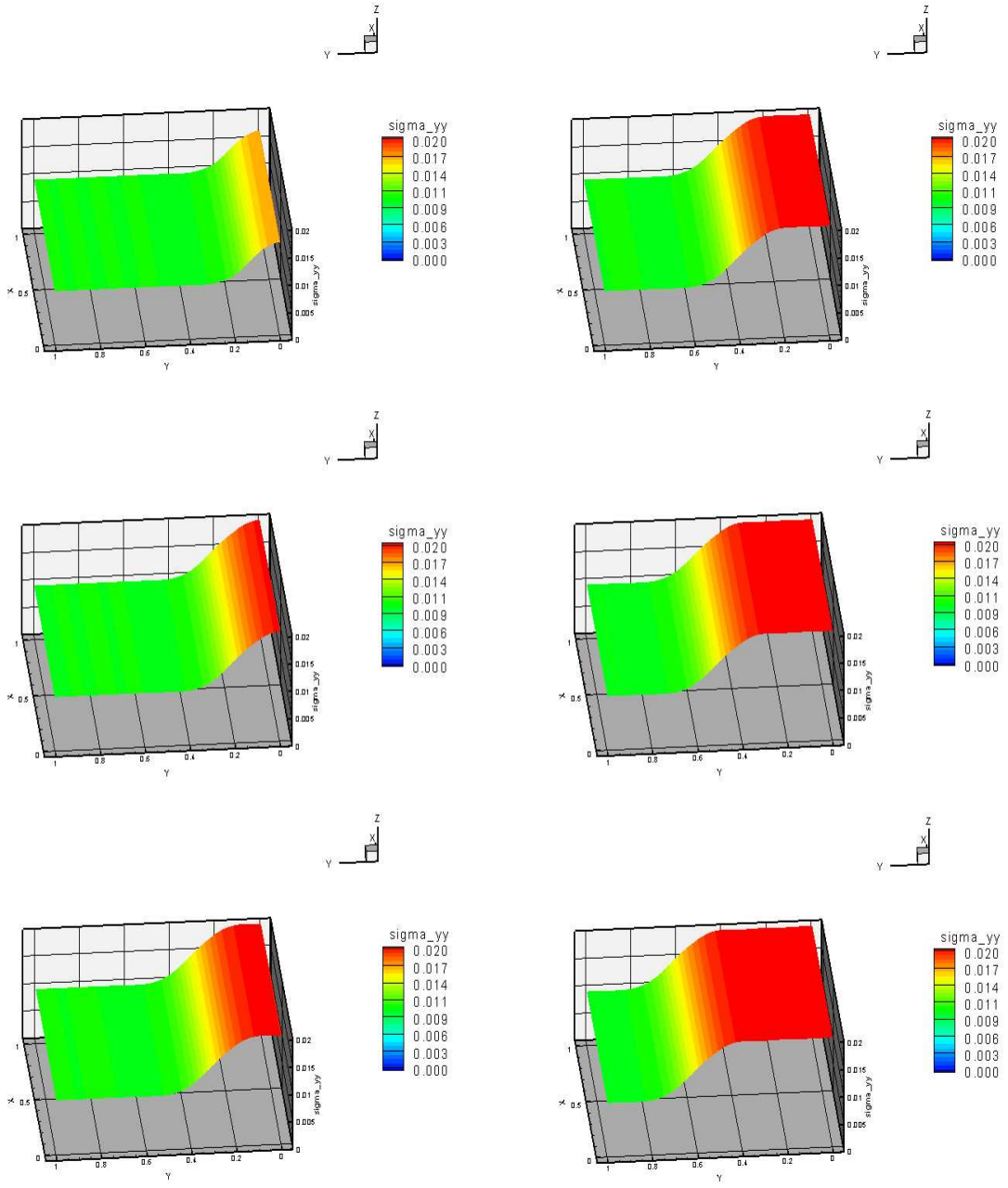

Figure B.10: Model Problem 6 : $\nu = 0.0$ and $\sigma_{yy} = 0.01$: Evolution of σ_{yy} : Lower Convected Stress Rate - Time steps from 13^{th} to 18^{th}

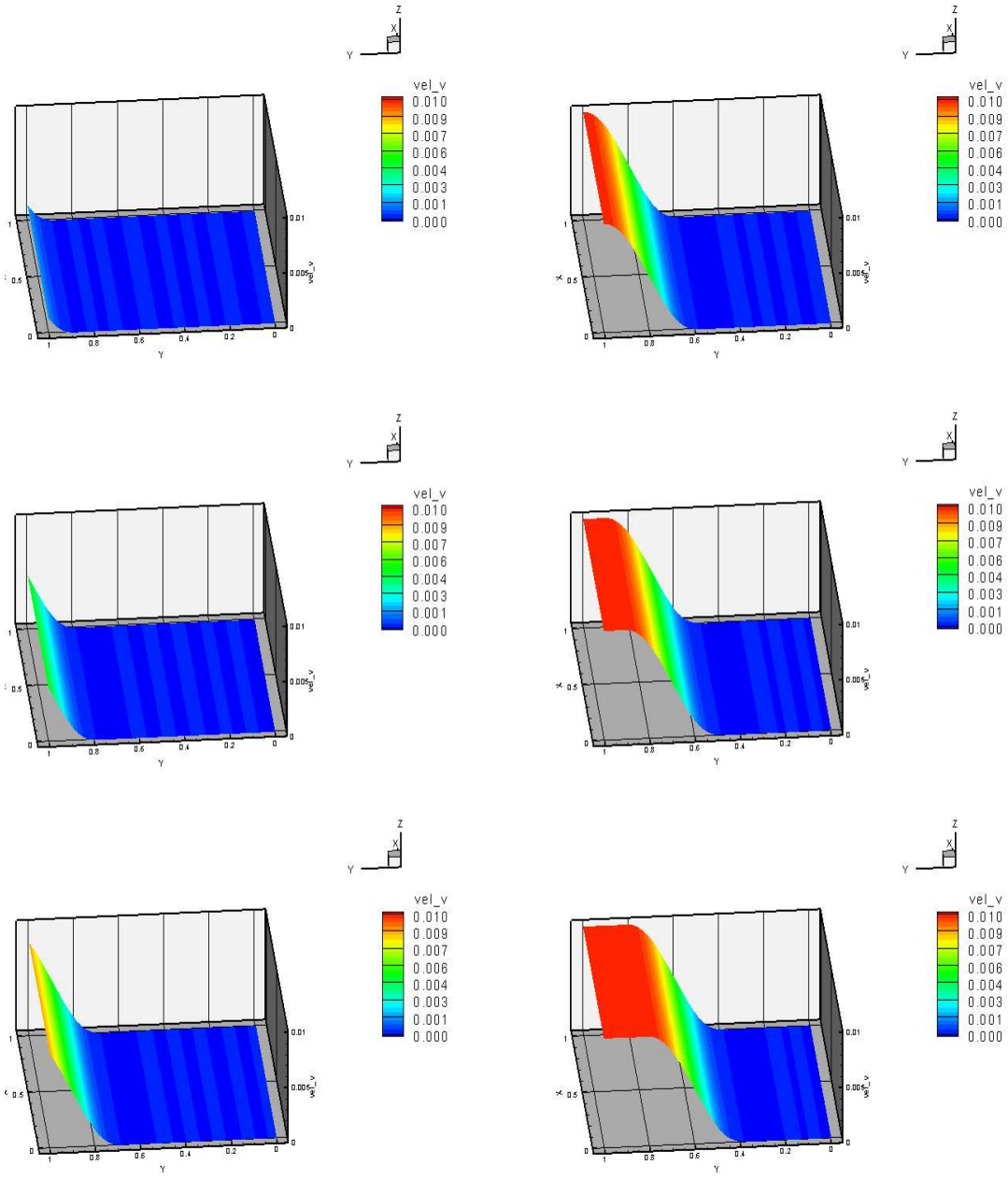

Figure B.11: Model Problem 6 : $\nu = 0.0$ and $\sigma_{yy} = 0.01$: Evolution of v : Lower Convected Stress Rate - Time steps from 1^{st} to 6^{th}

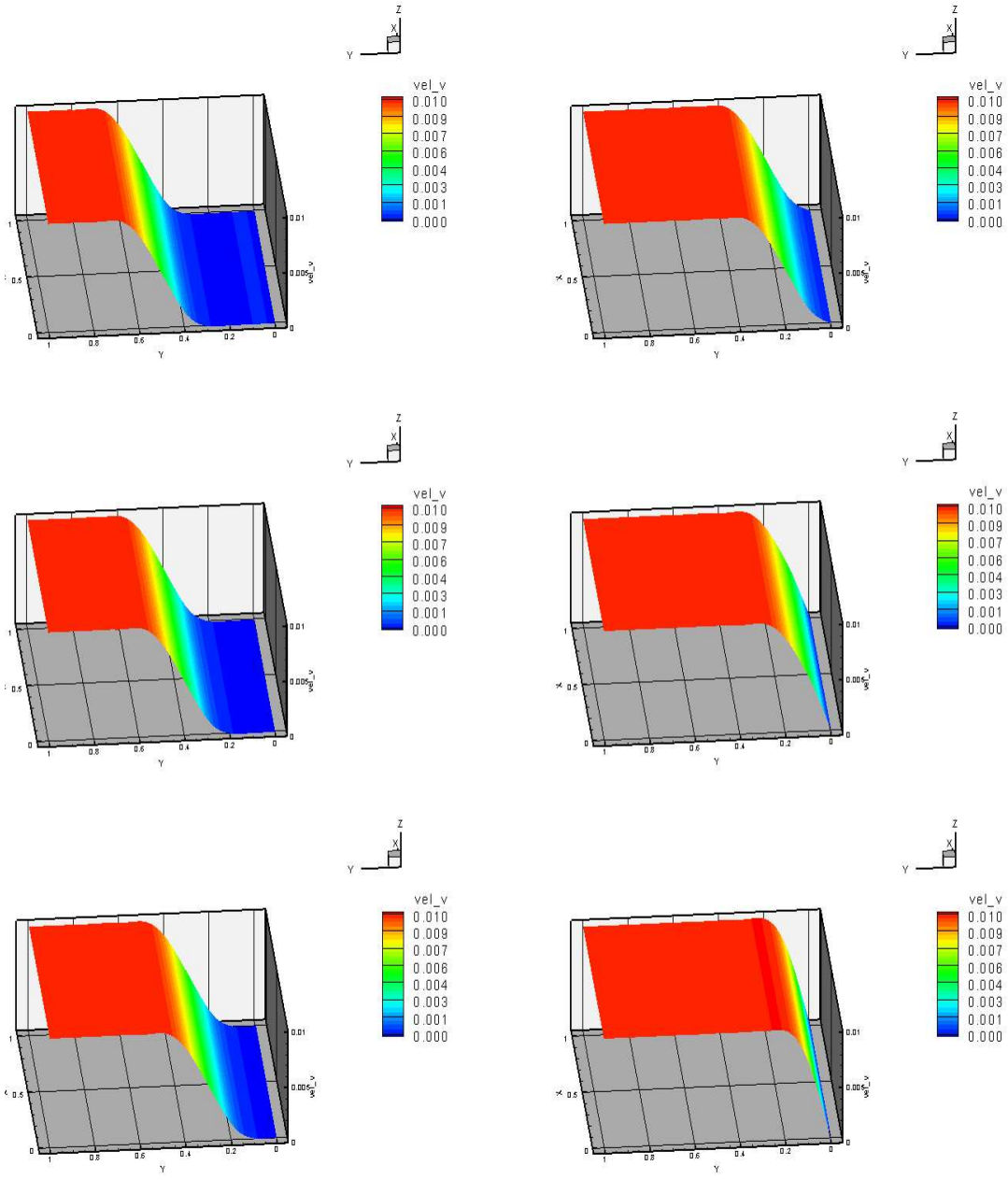

Figure B.12: Model Problem 6 : $\nu = 0.0$ and $\sigma_{yy} = 0.01$: Evolution of v : Lower Convected Stress Rate - Time steps from 7^{th} to 12^{th}

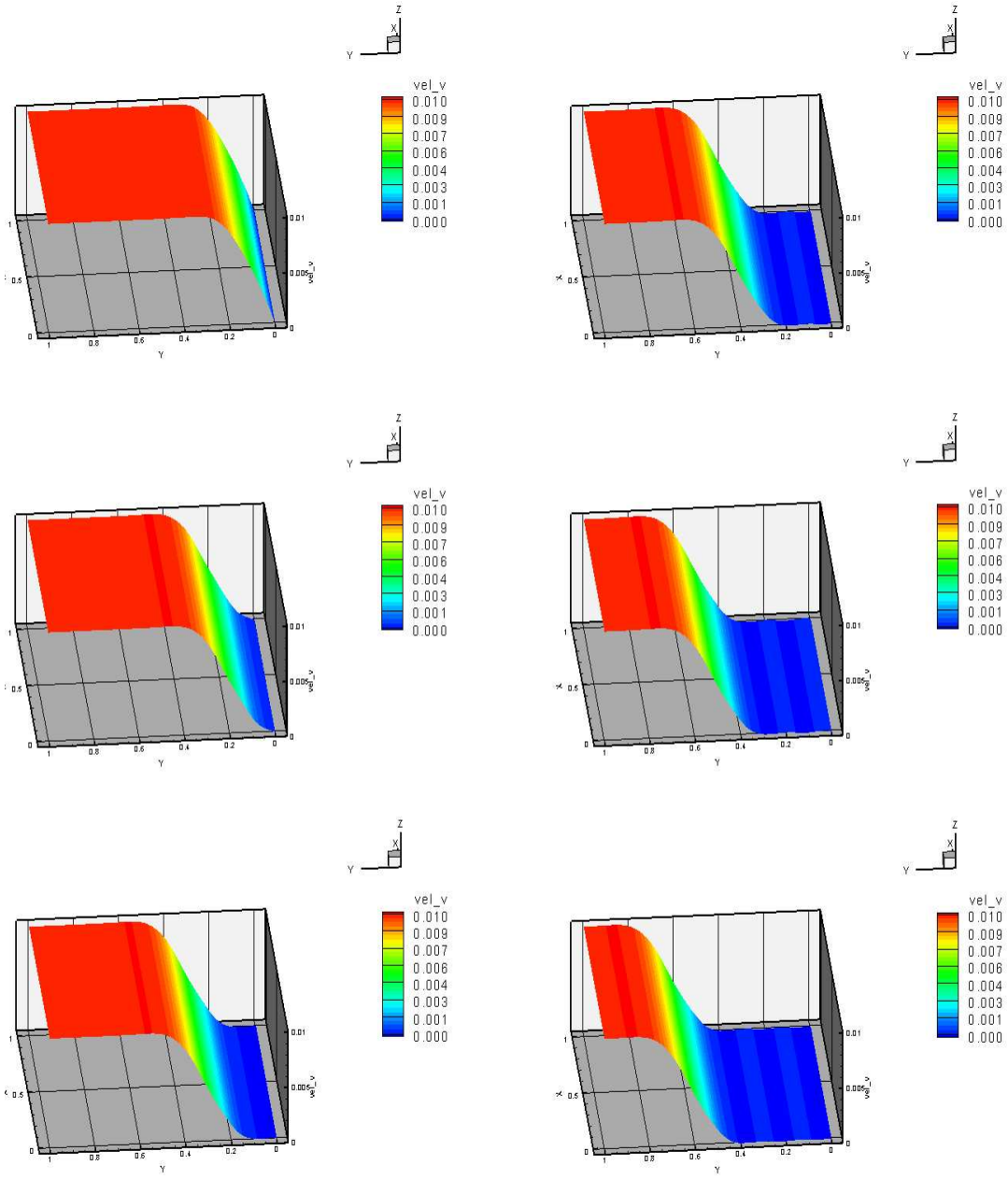

Figure B.13: Model Problem 6 : $\nu = 0.0$ and $\sigma_{yy} = 0.01$: Evolution of v : Lower Convected Stress Rate - Time steps from 13^{th} to 18^{th}

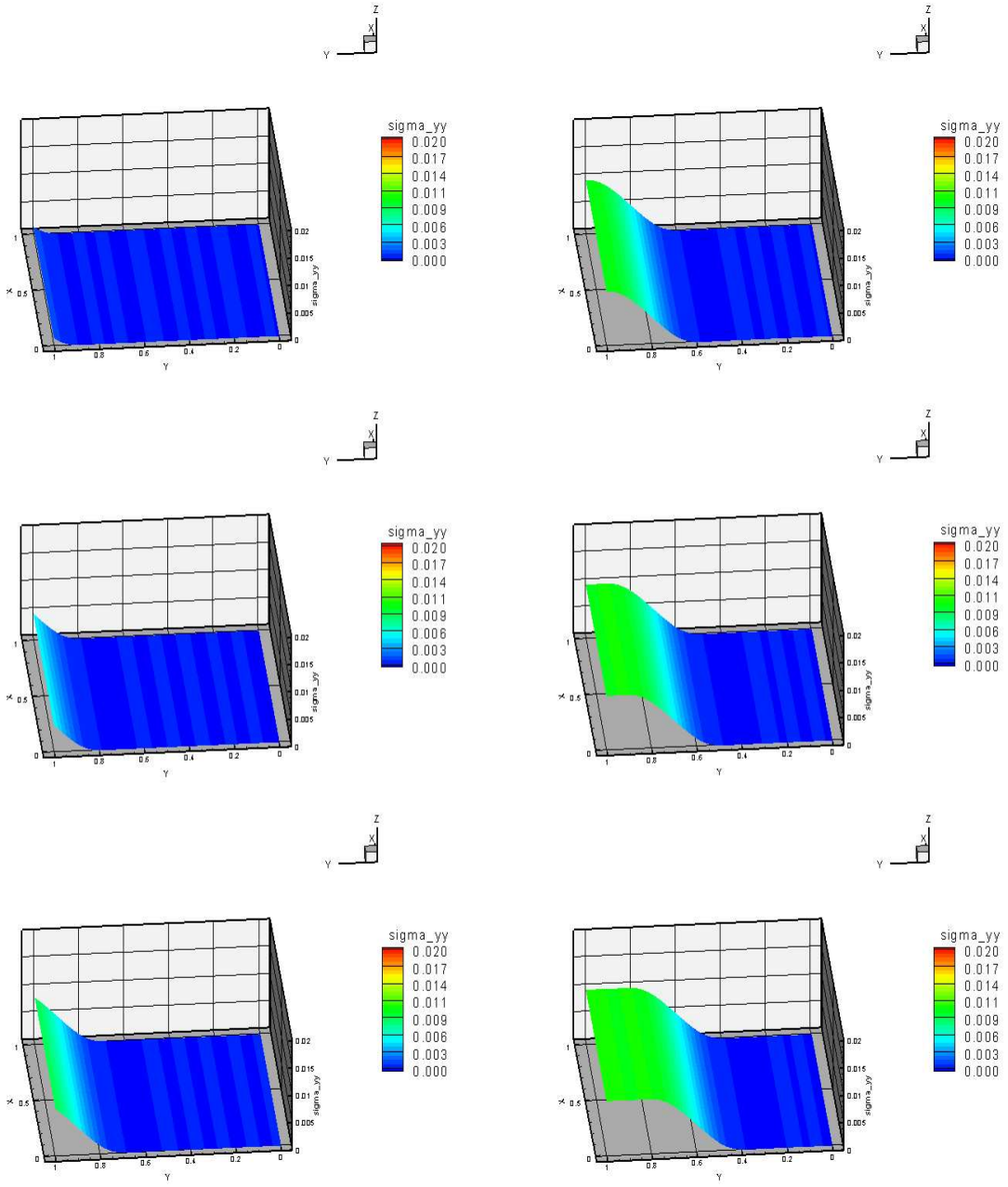

Figure B.14: Model Problem 6 : $\nu = 0.0$ and $\sigma_{yy} = 0.01$: Evolution of σ_{yy} : Jaumann Stress Rate - Time steps from 1^{st} to 6^{th}

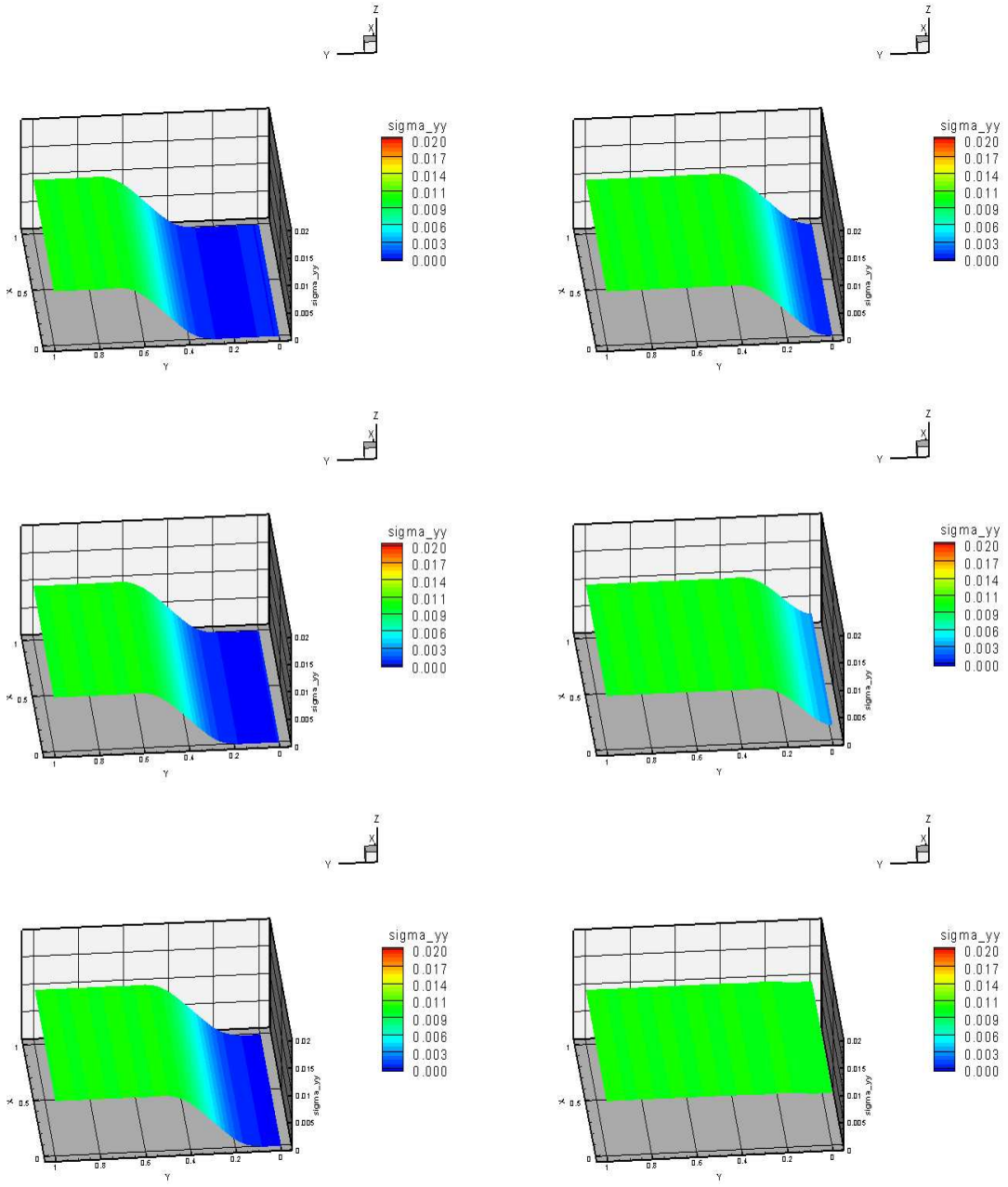

Figure B.15: Model Problem 6 : $\nu = 0.0$ and $\sigma_{yy} = 0.01$: Evolution of σ_{yy} : Jaumann Stress Rate - Time steps from 7^{th} to 12^{th}

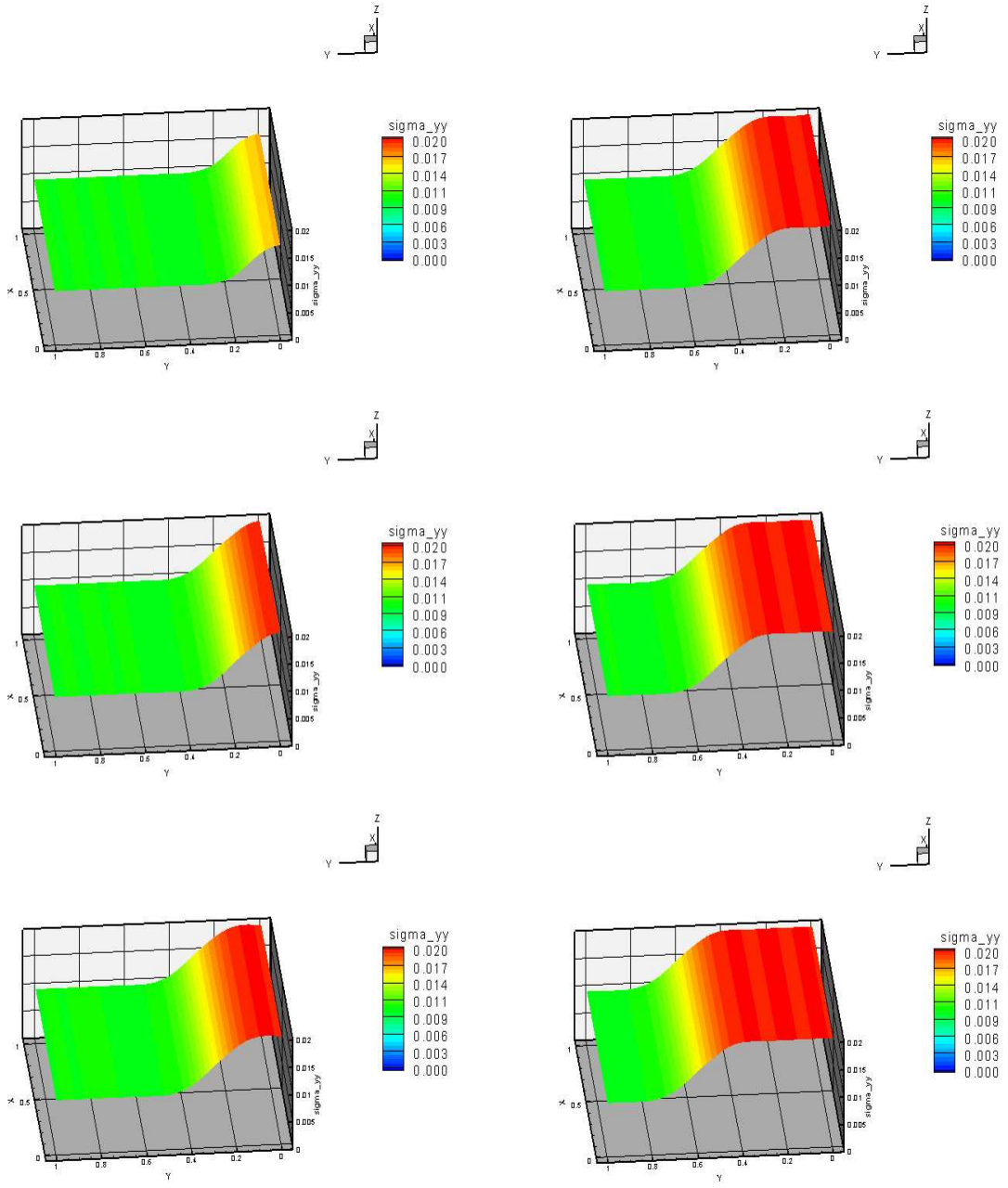

Figure B.16: Model Problem 6 : $\nu = 0.0$ and $\sigma_{yy} = 0.01$: Evolution of σ_{yy} : Jaumann Stress Rate - Time steps from 13^{th} to 18^{th}

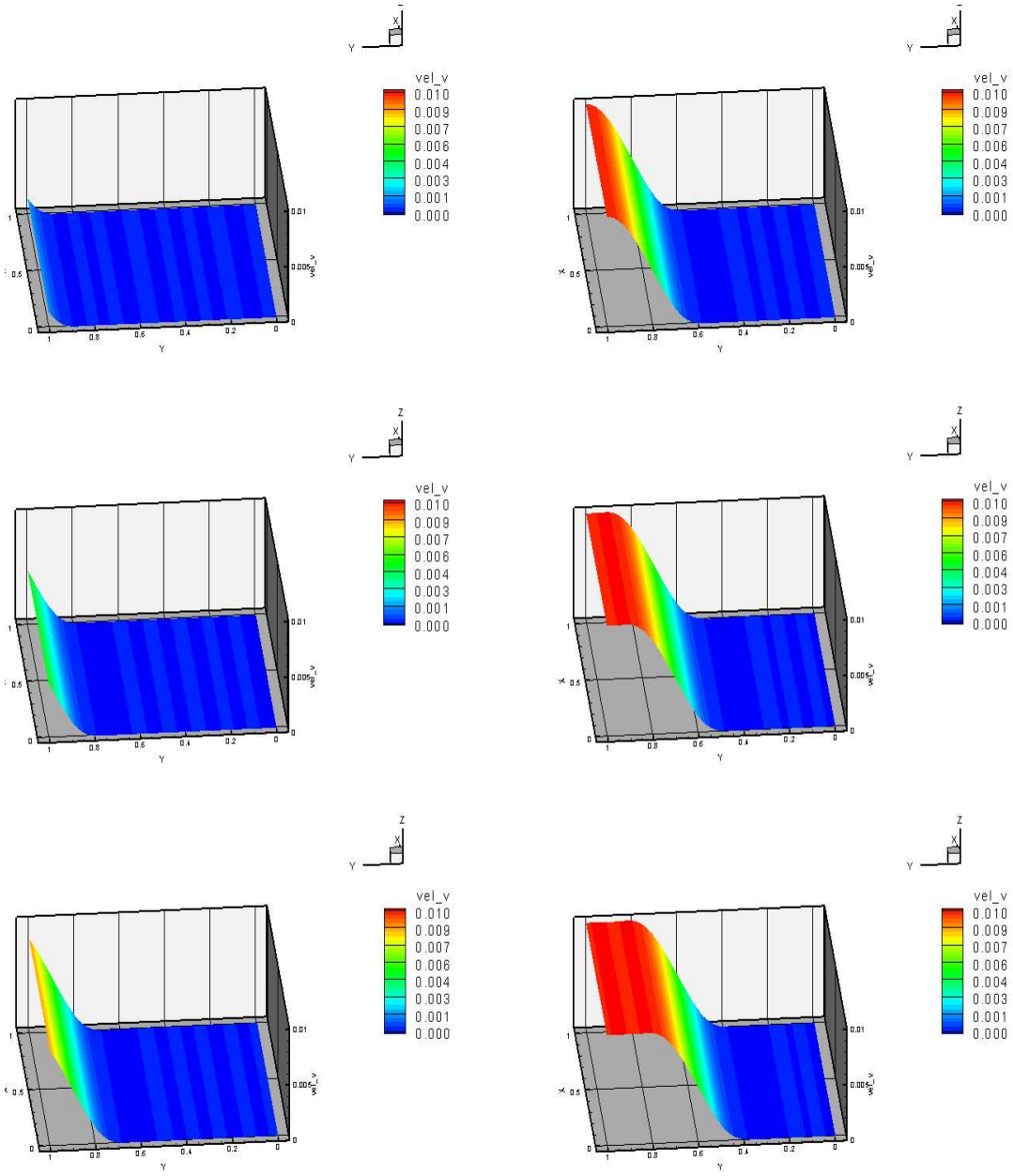

Figure B.17: Model Problem 6 : $\nu = 0.0$ and $\sigma_{yy} = 0.01$: Evolution of v : Jaumann Stress Rate - Time steps from 1^{st} to 6^{th}

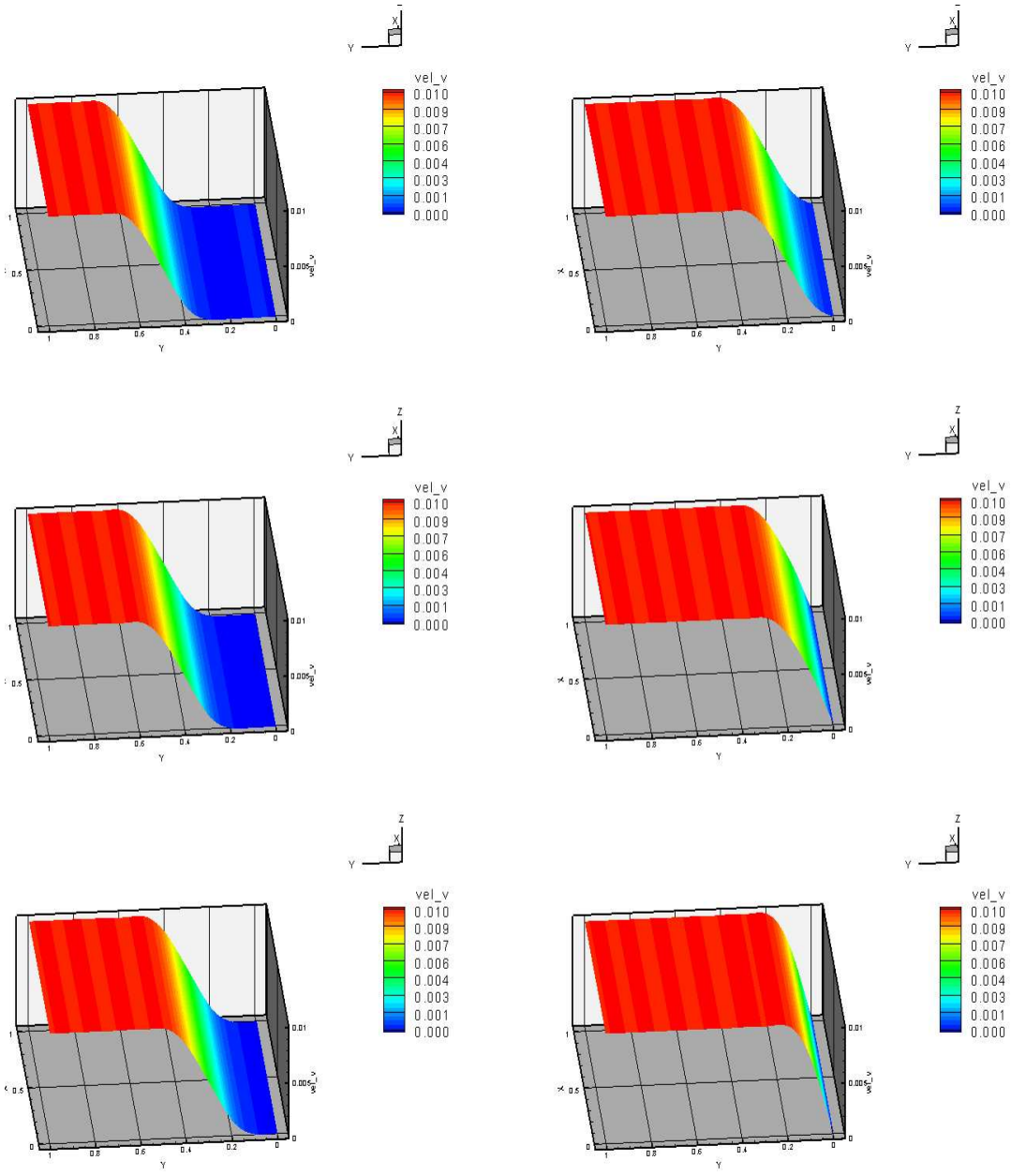

Figure B.18: Model Problem 6 : $\nu = 0.0$ and $\sigma_{yy} = 0.01$: Evolution of v : Jaumann Stress Rate - Time steps from 7^{th} to 12^{th}

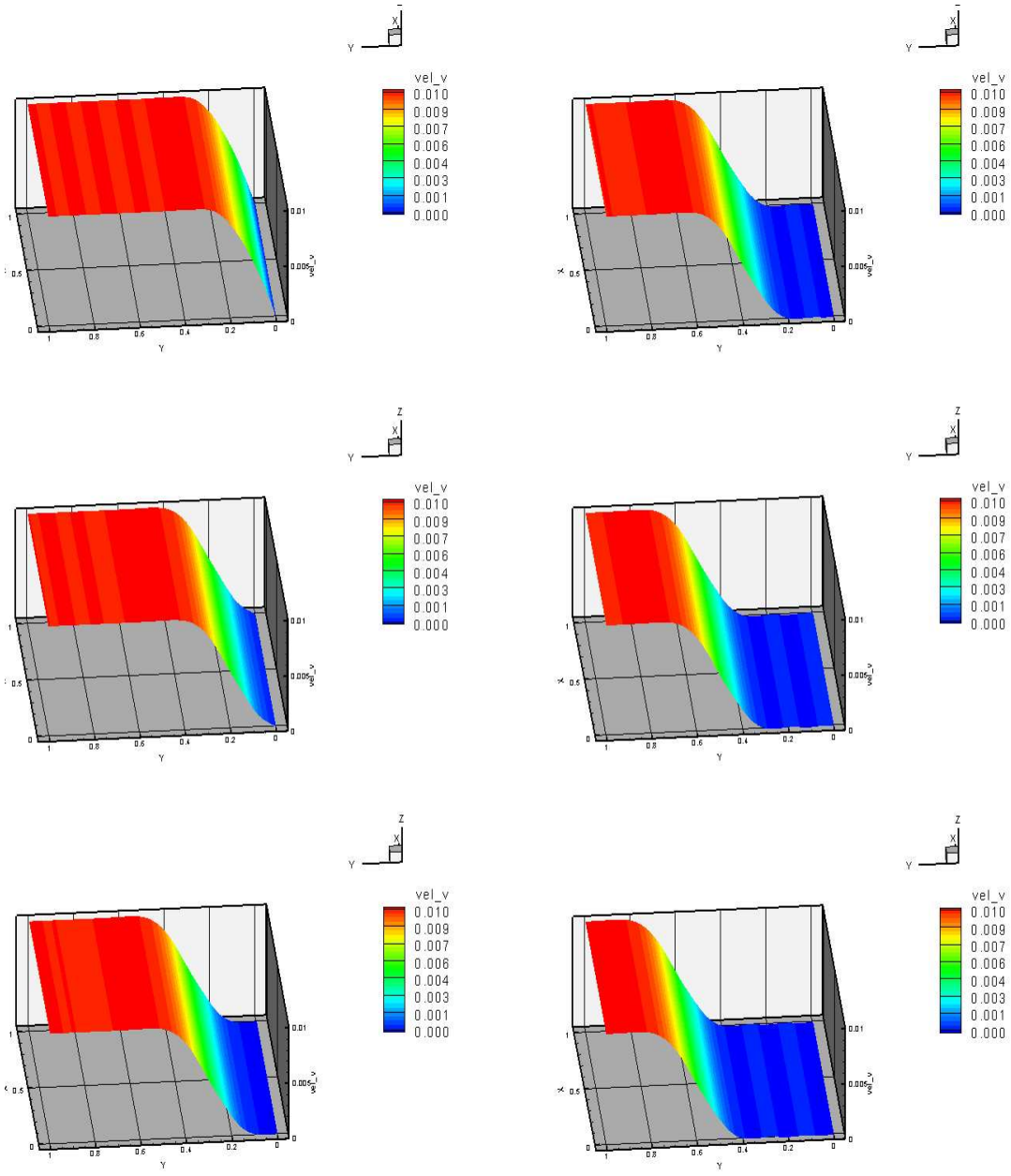

Figure B.19: Model Problem 6 : $\nu = 0.0$ and $\sigma_{yy} = 0.01$: Evolution of v : Jaumann Stress Rate - Time steps from 13^{th} to 18^{th}

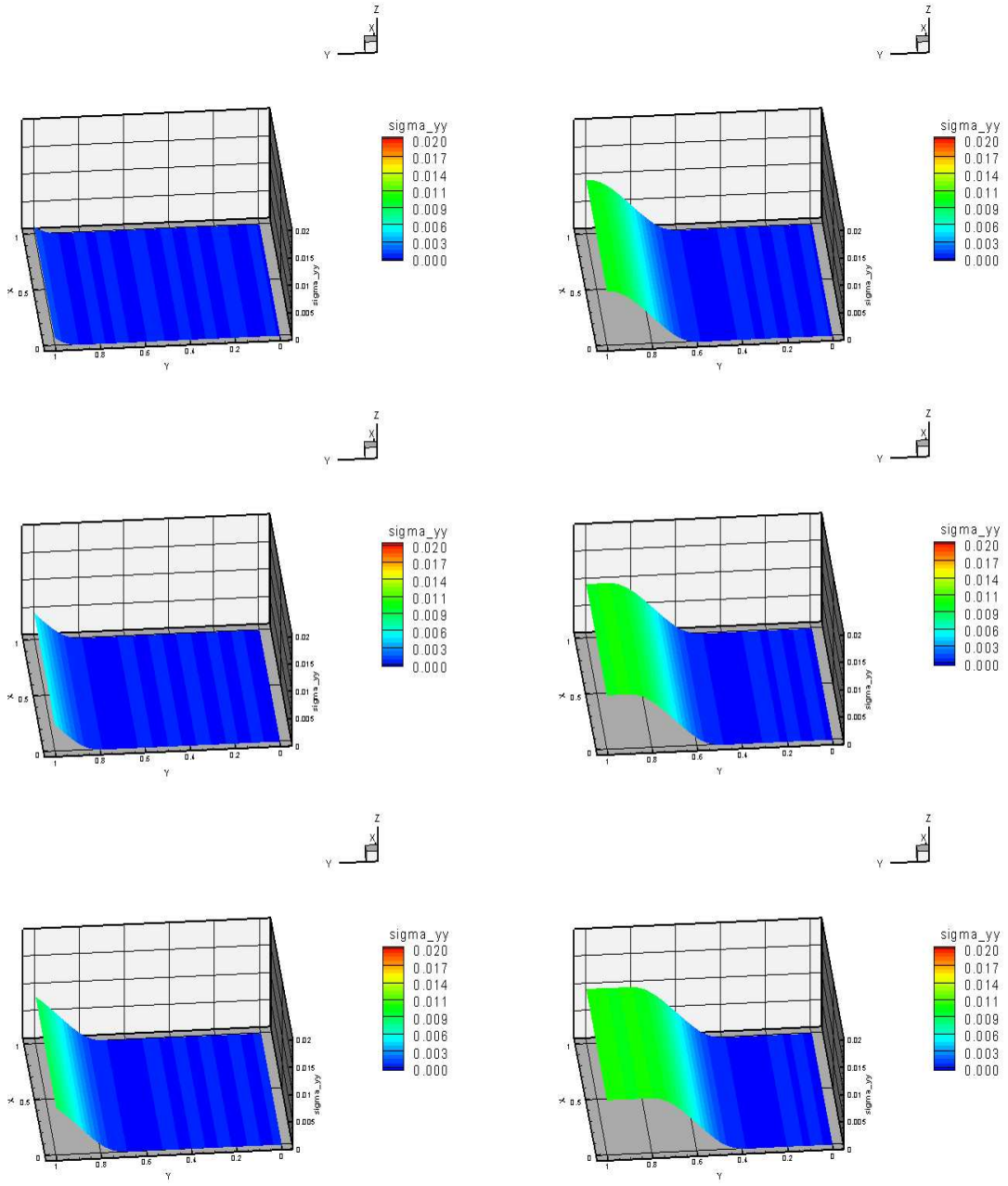

Figure B.20: Model Problem 6 : $\nu = 0.0$ and $\sigma_{yy} = 0.01$: Evolution of σ_{yy} : Truesdell Stress Rate - Time steps from 1^{st} to 6^{th}

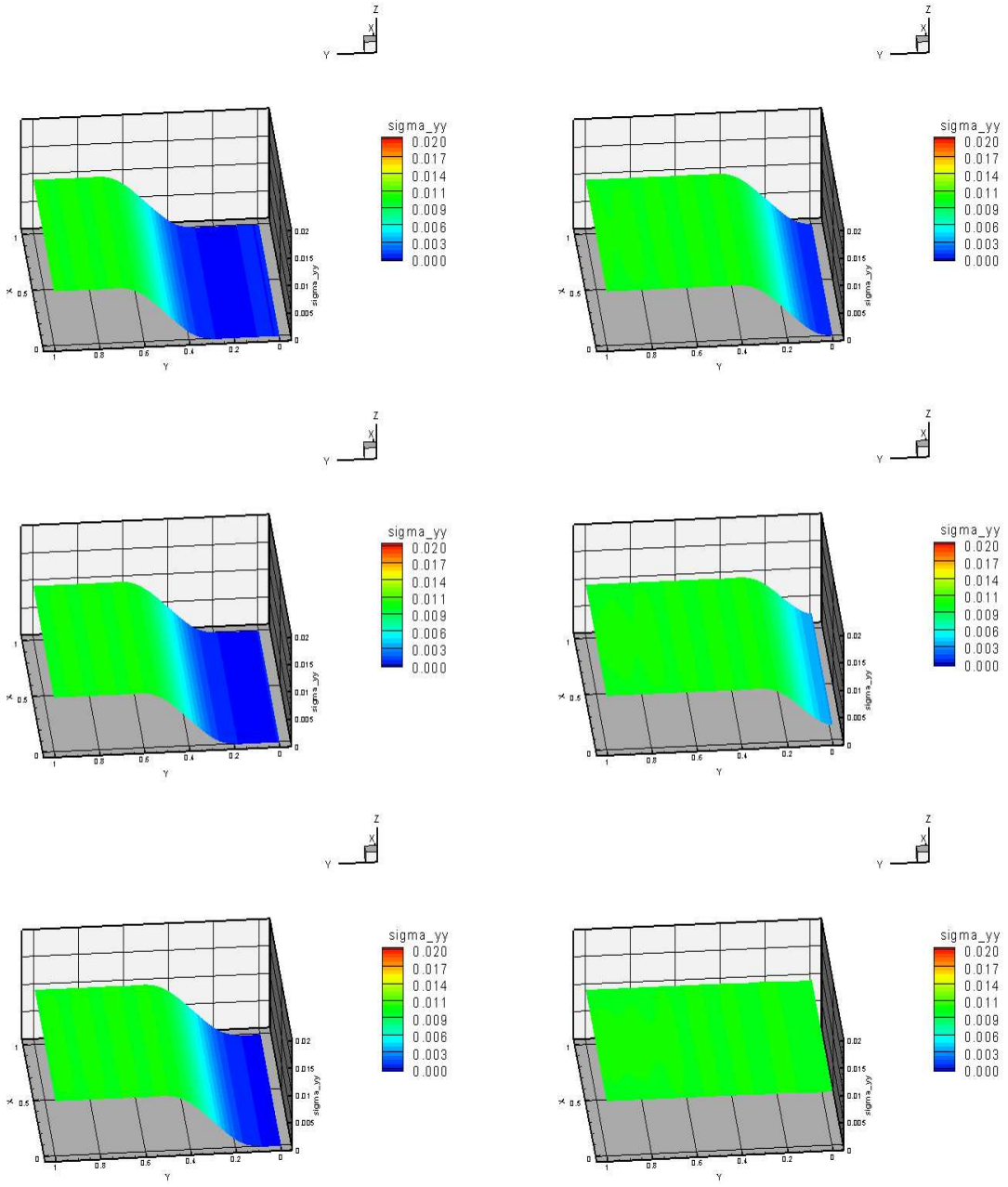

Figure B.21: Model Problem 6 : $\nu = 0.0$ and $\sigma_{yy} = 0.01$: Evolution of σ_{yy} : Truesdell Stress Rate - Time steps from 7^{th} to 12^{th}

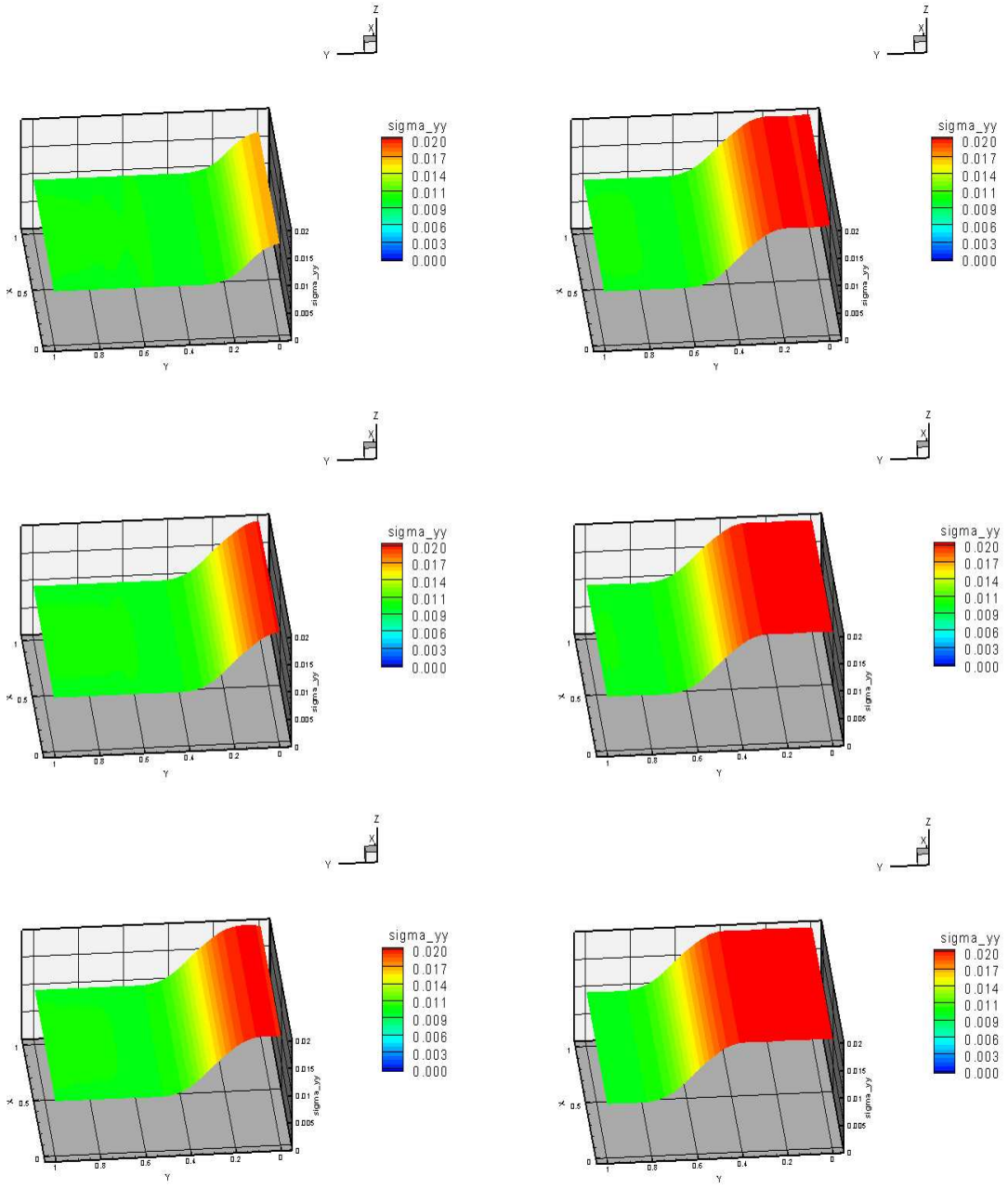

Figure B.22: Model Problem 6 : $\nu = 0.0$ and $\sigma_{yy} = 0.01$: Evolution of σ_{yy} : Truesdell Stress Rate - Time steps from 13^{th} to 18^{th}

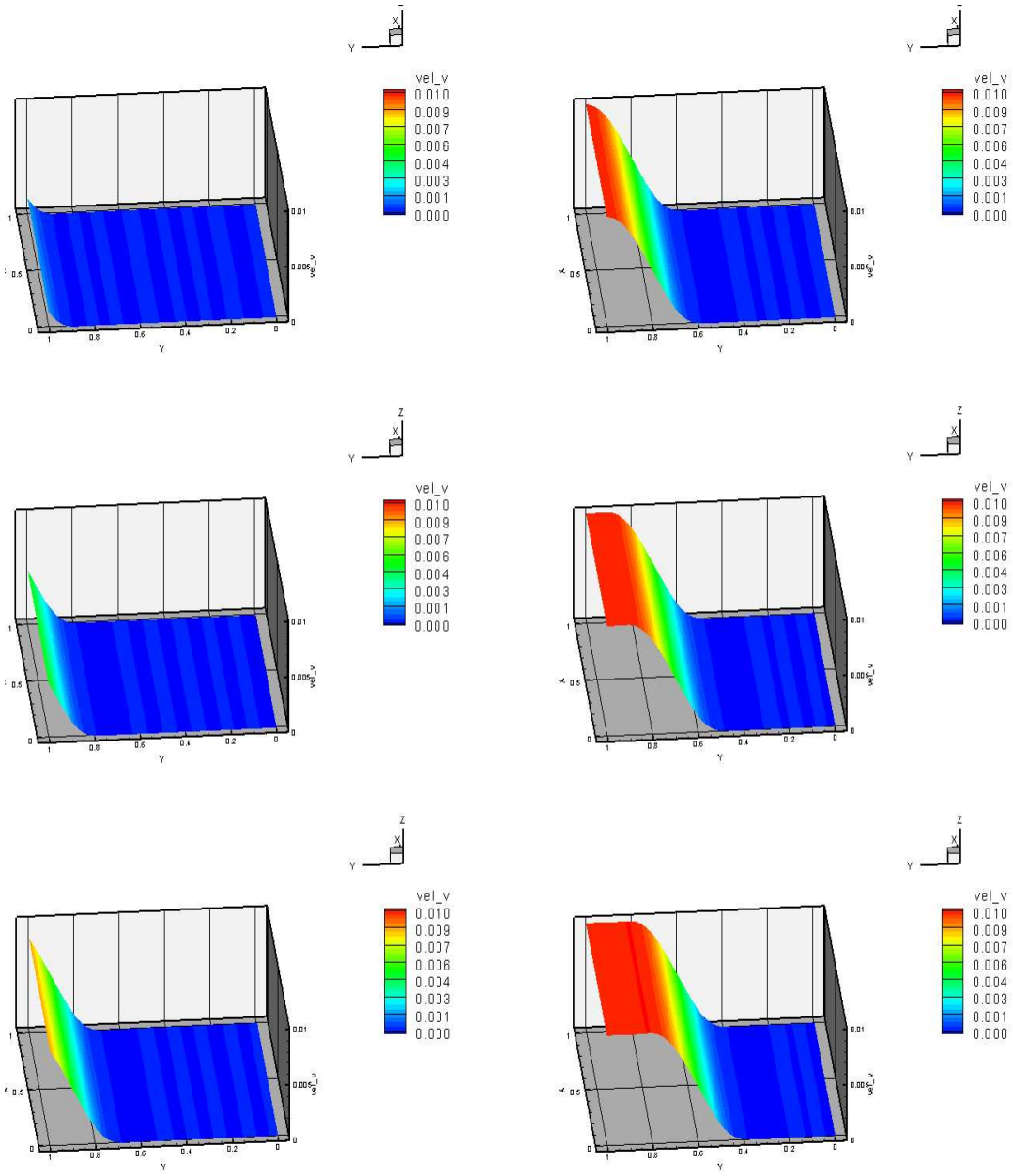

Figure B.23: Model Problem 6 : $\nu = 0.0$ and $\sigma_{yy} = 0.01$: Evolution of v : Truesdell Stress Rate - Time steps from 1^{st} to 6^{th}

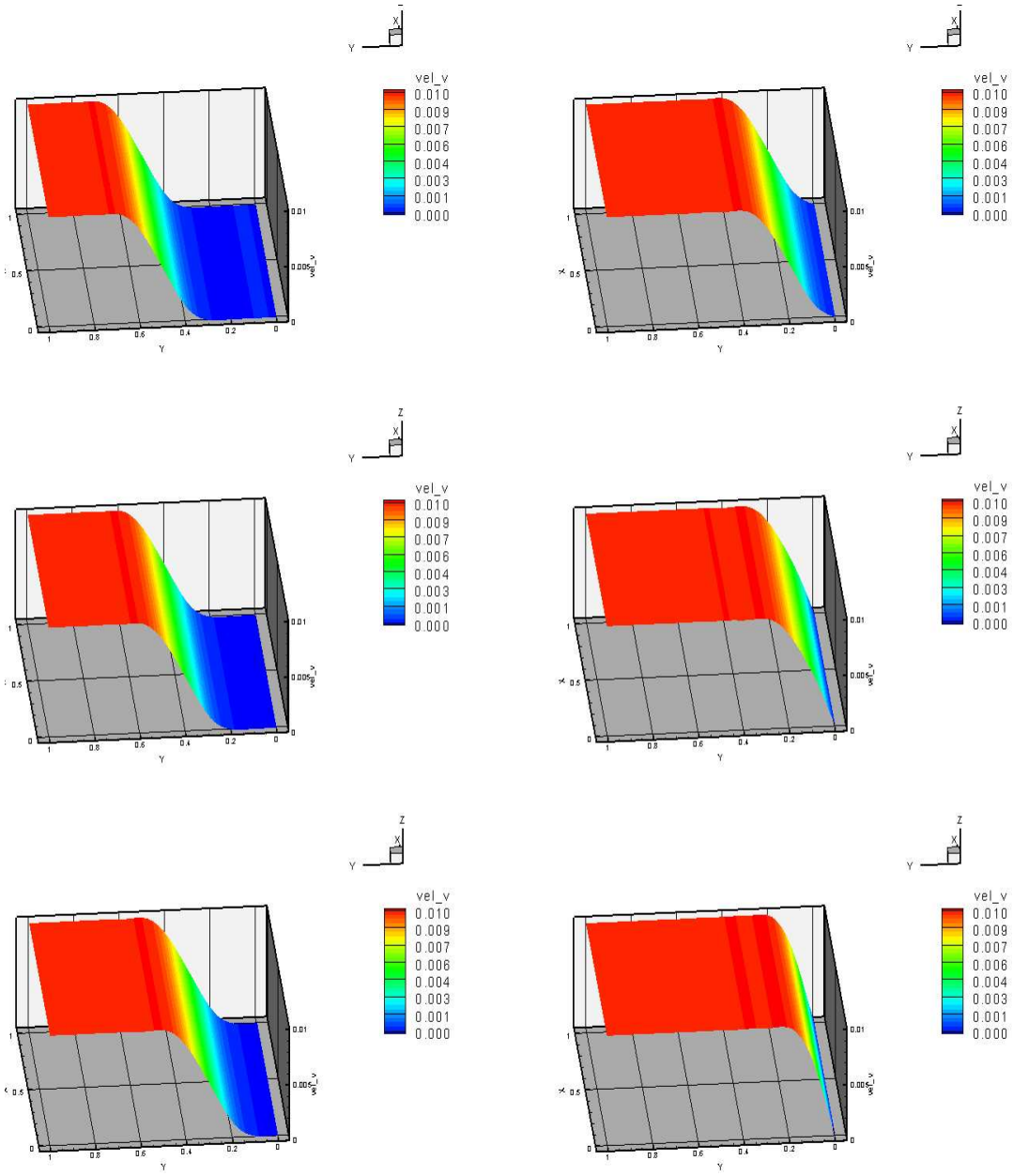

Figure B.24: Model Problem 6 : $\nu = 0.0$ and $\sigma_{yy} = 0.01$: Evolution of v : Truesdell Stress Rate - Time steps from 7^{th} to 12^{th}

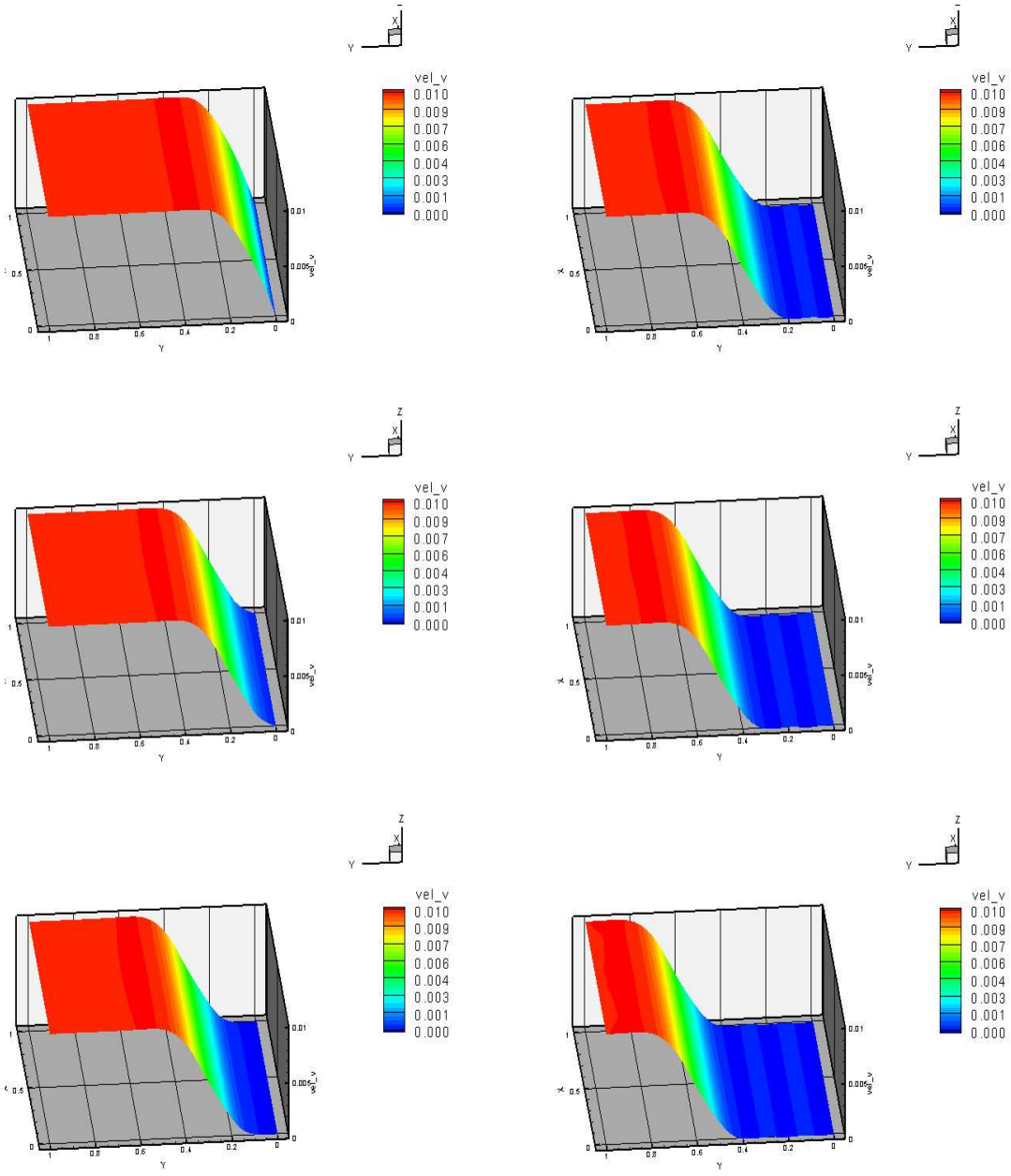

Figure B.25: Model Problem 6 : $\nu = 0.0$ and $\sigma_{yy} = 0.01$: Evolution of v : Truesdell Stress Rate - Time steps from 13^{th} to 18^{th}